BioMed Research International

Microbial Diversity for Biotechnology 2014

Guest Editors: George Tsiamis, Ameur Cherif, Dimitrios Karpouzas, and Spyridon Ntougias

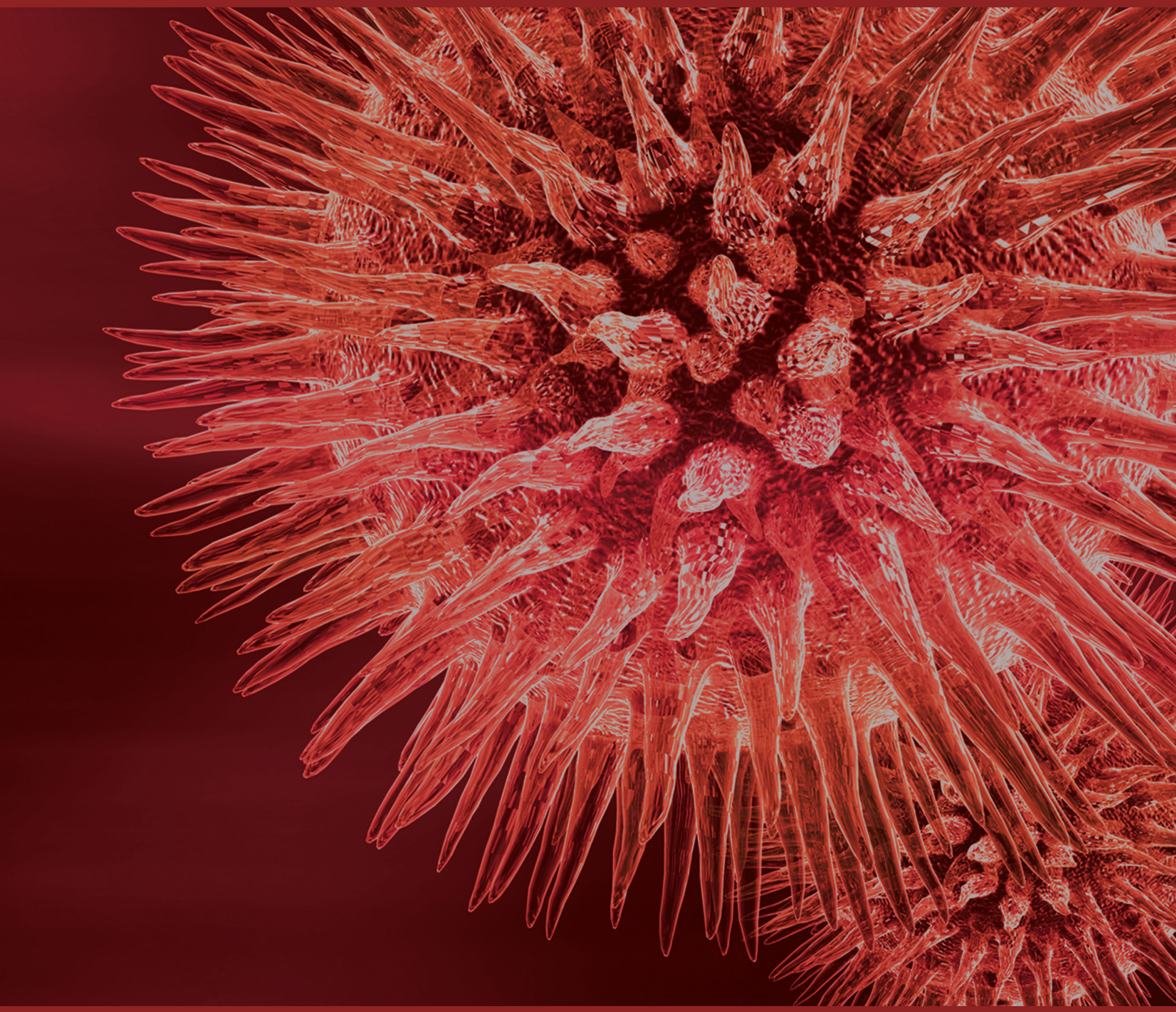

Microbial Diversity for Biotechnology 2014

BioMed Research International

Microbial Diversity for Biotechnology 2014

Guest Editors: George Tsiamis, Ameur Cherif,
Dimitrios Karpouzas, and Spyridon Ntougias

Contents

Hindawi Publishing Corporation
BioMed Research International
Volume 2015, Article ID 604264, 2 pages
http://dx.doi.org/10.1155/2015/604264

Editorial

Microbial Diversity for Biotechnology 2014

George Tsiamis,[1] Ameur Cherif,[2] Dimitrios Karpouzas,[3] and Spyridon Ntougias[4]

[1]*Department of Environmental and Natural Resources Management, University of Patras, 2 Seferi Street, 30100 Agrinio, Greece*
[2]*LR11-ES31, Biotechnology and Bio-Geo Resources Valorization, ISBST, BiotechPole Sidi Thabet, University of Manouba, 2020 Ariana, Tunisia*
[3]*Department of Biochemistry and Biotechnology, University of Thessaly, Ploutonos 26 and Aiolou Street, 41221 Larisa, Greece*
[4]*Department of Environmental Engineering, Democritus University of Thrace, Vasilissis Sofias 12, 67100 Xanthi, Greece*

Correspondence should be addressed to George Tsiamis; gtsiamis@upatras.gr

Received 28 May 2015; Accepted 28 May 2015

The focus of this special issue is the characterization of the microbial diversity and the development of potential biotechnological applications. Despite the great importance of microbes, only a small fraction has been able to be cultivated in the laboratory. It is now clear that molecular techniques have played a significant role in the detection and unravelling of the enormous microbial diversity. Omic technologies like genomics, metagenomics, and single cell genomics enabled the characterization of a vast and unexplored portion of the microbial diversity.

Human life and microbes are highly coupled since key biogeochemical cycles like carbon, nitrogen, and sulfur are microbially dependent. Even the photosynthetic capacity on Earth is microbial dependent and not plant based. In humans, the gut symbionts assist in food digestion, toxin breakdown, and boosting the immune system. In an attempt to understand the unculturable fraction programs like the Earth Microbiome Project (EMP), the International Census of Marine Microbes, and the Human Microbiome Project have been launched. The next step is to use this boundless and fascinating resource for the discovery of new genes and enzymes for use in biotechnology.

This special issue includes nine research articles describing the microbial diversity and the deployment of new technologies that can lead to prospective biotechnological applications.

D. H. Green et al. studied the bacterial diversity associated with the coccolithophorid algae *Emiliania huxleyi* and *Coccolithus pelagicus* f. *braarudii*. Coccolithophores make significant contributions to oceanic carbon cycling and atmospheric CO_2 regulation, but despite their importance the bacterial diversity associated with these algae has not been explored from ecological or biotechnological point of view. Culture-dependent and independent analyses indicated that the bacterial diversity was spread across five phyla. *Alphaproteobacteria*, *Gammaproteobacteria*, and *Bacteroidetes* were the most dominant, followed by *Actinobacteria* and *Acidobacteria*.

G. Merlino et al. present the characterization of the bacterial community developed in anaerobic microcosms after biostimulation with lactate from a groundwater polluted with 1,2-dichloroethane (1,2-DCA). Molecular approaches targeting conserved regions of known reductive dehalogenase genes identified four novel variants that have been associated with the reductive dechlorination of 1,2-DCA.

H. Lin et al. examined the microbial community structure and pathogen occurrence in urban faucet biofilms in South China using microstructure analysis and 454 pyrosequencing. *Proteobacteria* were found to be the most predominant group in all biofilms samples. Interestingly, some potential pathogens (e.g., *Legionellales* and *Enterobacteriales*) and corrosive microorganisms were also found in these biofilms.

H. Xu et al. examined the heterologous expression of cellulases in *Thermotoga* sp. isolated from *Caldicellulosiruptor saccharolyticus*. Although the vectors were lost from the *Thermotoga* strain after three consecutive transfers, all three recombinant enzymes were successfully expressed rendering the host with increased endo- and/or exoglucanase activities. This work demonstrated the feasibility of genetically engineering *Thermotoga* spp. for efficient cellulose utilization.

E. G. Di Domenico et al. explored the anaerobic digestate as feed in H-type MFC reactors: one with a graphite anode preconditioned with *Geobacter sulfurreducens* and the other with an unconditioned graphite anode. Their results indicated that MFCs can be used to recover anammox bacteria from natural sources. This opens the possibility of using anaerobic digester for the simultaneous nitrogen removal and electricity generation.

G. A. Silva-Castro et al. studied the precipitation of calcium carbonate and calcium sulphate by isolating bacteria from seawater and real brine. *Bacillus* and *Virgibacillus* strains were able to form calcium carbonate minerals, which precipitated as calcite and aragonite crystals. Further characterization of these bacterial strains is of great importance for the bioremediation of CO_2 and calcium capture in certain environments.

A. Krasowska et al. isolated and characterized at molecular level the bacteriophages of *Bacillus subtilis*. The studied phages were from the Myoviridae and the Siphoviridae family. The host range, pH and temperature resistance, adsorption rate, latent time, and phage burst size were determined. These findings can be used in industry since *Bacillus* spp. are very persistent strains.

M. Nampally et al. searched for novel chitin and chitosan modifying enzymes isolated from soil microorganisms with more than ten years of history of chitin and chitosan exposure. After screening for chitinase and chitosanase isoenzymes, eight bacterial strains and twenty fungal isolates were found to be chitinolytic and/or chitosanolytic.

R. A. Amer et al. examined the physical, chemical, and microbiological features of hydrocarbon and heavy metals contaminated sediments collected at El-Max Bay (Egypt). Following a culture-dependent approach fifty bacterial strains were isolated and were identified as hydrocarbon-degrading bacteria involved in different stages of biodegradation. The El-Max sediment represents a promising reservoir of novel bacterial strains adapted to high hydrocarbon contamination loads.

These papers highlight the importance of the study and characterization of the hidden microbial diversity and the vast potential that exists in order to transform this basic knowledge to applied knowledge with the assistance of biotechnology. New developments in the field of omic approaches will certainly propel our ability to understand and further exploit microbial diversity. In this regard, these papers provide a glimpse into the future of this field.

Acknowledgments

We would like to extend our appreciation to all authors of the submitted papers. We would also like to thank the expert reviewers who participated in the reviewing process.

George Tsiamis
Ameur Cherif
Dimitrios Karpouzas
Spyridon Ntougias

Hindawi Publishing Corporation
BioMed Research International
Volume 2015, Article ID 351014, 10 pages
http://dx.doi.org/10.1155/2015/351014

Research Article

Development of Electroactive and Anaerobic Ammonium-Oxidizing (Anammox) Biofilms from Digestate in Microbial Fuel Cells

Enea Gino Di Domenico,[1] Gianluca Petroni,[1,2] Daniele Mancini,[3] Alberto Geri,[2] Luca Di Palma,[3] and Fiorentina Ascenzioni[1]

[1]*Pasteur Institute-Cenci Bolognetti Foundation, Department of Biology and Biotechnology "C. Darwin", Sapienza University of Rome, 00185 Rome, Italy*
[2]*Astronautic Electric and Energetic Engineering Department, Sapienza University of Rome, 00184 Rome, Italy*
[3]*Department of Chemical Engineering Materials Environment, Sapienza University of Rome, 00184 Rome, Italy*

Correspondence should be addressed to Enea Gino Di Domenico; enea.didomenico@uniroma1.it

Received 3 October 2014; Revised 30 December 2014; Accepted 31 December 2014

Academic Editor: Dimitrios Karpouzas

Microbial Fuel cells (MFCs) have been proposed for nutrient removal and energy recovery from different wastes. In this study the anaerobic digestate was used to feed H-type MFC reactors, one with a graphite anode preconditioned with *Geobacter sulfurreducens* and the other with an unconditioned graphite anode. The data demonstrate that the digestate acts as a carbon source, and even in the absence of anode preconditioning, electroactive bacteria colonise the anodic chamber, producing a maximum power density of 172.2 mW/m^2. The carbon content was also reduced by up to 60%, while anaerobic ammonium oxidation (anammox) bacteria, which were found in the anodic compartment of the reactors, contributed to nitrogen removal from the digestate. Overall, these results demonstrate that MFCs can be used to recover anammox bacteria from natural sources, and it may represent a promising bioremediation unit in anaerobic digestor plants for the simultaneous nitrogen removal and electricity generation using digestate as substrate.

1. Introduction

Anaerobic digestion (AD) of organic waste and/or animal manure is considered a key technology that meets the production of renewable energy with greenhouse gas mitigation. AD is accomplished through a series of complex microorganisms-driven reactions breaking down organic substances into CO_2 and volatile fatty acids (acidogenesis) that are then converted to biogas (methanogenesis). The remaining fraction in the digester is a nutrient-rich sludge, the digestate. Although transformation of nitrogen compounds occurs in AD, the nitrogen content remains high in the digestate making this by-product suitable to be used as fertilizer. However, accumulation of biogas plants in small agriculture area or regions of intensive dairy cattle farming may lead to an oversupply of digestate. Indeed, digestate-based fertilization, when exceeding the need of crops, contributes to eutrophication of land and water bodies [1, 2].

One of the most promising techniques to reduce nitrogen content from ammonia-rich wastewaters is the anaerobic ammonium oxidation (ANAMMOX). Nitrogen removal under anaerobic conditions is driven by a group of anammox bacteria, which are affiliated to the order *Brocadiales*, within the phylum of *Planctomycetes* [3]. The advantages of the anammox process, over the conventional method of nitrification and denitrification, include the lower oxygen demand and the absence of external carbon sources requirements. However, a critical aspect limiting the application of this process in large bioreactors is the requirement of long start-up periods caused by the slow growth rate (doubling time approximately 1-2 weeks) of the anammox bacteria and by

the absence of conventional microbiological techniques for their cultivation [4]. Several methods have been proposed to obtain enrichment of anammox bacteria [4–9]; however, cultivation still poses a serious challenge.

Nitrogen removal from wastewater has been studied in microbial fuel cells (MFCs), electrochemical devices that catalyse the conversion of chemical oxygen demand into electricity through the metabolic activity of microorganisms [10]. Typically in the anodic chamber, microorganisms oxidize the organic matter and the electrons are donated to the anode. These electrons are subsequently transferred, through an electric circuit, to the cathode electrode where they reduce terminal electron acceptors.

Several bacteria have naturally evolved strategies to transfer electrons outside the cell surface and this feature has allowed the use of these microorganisms in MFCs. The main quality of electroactive bacteria in the MFC system is the ability to transfer electrons from the microbial cell to an electrode instead of the natural redox partner [11]. Different microorganisms, either gram-positive or gram-negative, can exchange electrons with electrodes and this is accomplished by different mechanisms: reduction of self-produced soluble shuttles; short-range electron transfer through membrane-bound redox-active proteins (i.e., c-type cytochrome); long-range electron transfer mediated by a special class of conductive pili, the nanowires [12]. In most cases, bacteria may use more than one mechanism. For example, in *Shewanella oneidensis* the electrons may hop from the cell-surface *c*-type cytochrome, which is part of a multiprotein complex that transferred the electrons from the periplasm to the cell surface, to an external acceptor directly or via a flavin produced by the cell itself. *Geobacter sulfurreducens* has many c-type cytochromes exposed to the cell surface among which OmcZ appears to be the key element for electron transfer. Additionally, the conductive pili ensure the long-range electron transfer between the typical multilayer *G. sulfurreducens* biofilms and the electrodes. *G. sulfurreducens* current production is mediated by biofilms with a two-phase process in which long-range electron transport occurs along the conductive pili network and OmcZ facilitates electron transfer from those cells closer to the electrode surface [12]. However, when MFCs are inoculated with a mixed culture, bacterial community analysis of the anodic biofilms revealed a great diversity in electroactive bacteria, regardless of the substrate type. This finding suggests a potential existence of other unknown species contributing to electricity generation through a variety of ways beyond the accepted *Geobacter* or *Shewanella* species [13].

In addition to electricity production, the microbial metabolism can be used to produce valuable products or to remove unwanted compounds [14]. Accordingly, in the development of MFC, nitrogen removal has been considered as an added endpoint. Nitrate reduction at the cathode of MFC has been demonstrated by different experimental approaches including the use of a potentiostat-poised half-cell in which nitrogen was completely reduced to N_2 gas in the absence of any organic substance (electron donors) [15]. More recently, a variety of denitrifying MFC reactors have been designed: two-chamber MFC reactors including both nitrification and denitrification steps at the cathode were obtained by aerated cathode chamber [16] or by preaerated cathode influent [17, 18]. Single-chamber MFC, with the cathode exposed to air (air-cathode), and two-chamber MFC, with ferricyanide catholyte were also tested for ammonia removal from swine wastewater [19, 20]. In both reactors electricity generations and high levels of ammonium removal were achieved; however, ammonia volatilization and/or diffusion through the cation exchange membrane connecting the anode and cathode chambers accounts for most of the nitrogen reduction [20]. More recently, single-chamber MFC reactors with PTFE (polytetrafluoroethylene) coated cathode, which reduces ammonia diffusion, and preenriched nitrifying biofilms were shown to remove up to 96% ammonia from a synthetic feeding medium [21]. Ammonia and COD removal rates by single-chamber MFC were significantly improved by doubling the gas diffusion area [22].

In this study we investigated the possibility of biological ammonia removal with current generation in MFC reactors from digestate. This was accomplished by feeding MFC reactors in batch mode with anaerobic digestate from agricultural by-products and cow manure. The reactors were H-type MFCs with a sterile graphite anode (MFC-U) and with a *G. sulfurreducens* preconditioned anode (MFC-C). *G. sulfurreducens* preconditioning was included as a control because of the well-known ability of this bacterium to convert organic matter into electricity in MFC devices [23]. Electrical and chemical performances of both cells were investigated. Additionally, the presence of anammox bacteria in the digestate and their establishment in the MFC conditions had been assessed by molecular methods. Our results demonstrate that MFC reactors allow the development of digestate-derived biofilms that contribute to the simultaneous generation of electricity and nitrogen removal from the digestate. However, since the substrate influences the bacterial diversity in the anode biofilm additional studies are needed to compare different types of digestate as well as to better understand the physical and biological mechanisms that can affect MFC performances in full-scale application systems.

2. Materials and Methods

2.1. Feed and Inoculum. The digestate was the effluent of an anaerobic digestion plant treating agricultural wastes and cow manure (Azienda Agricola Bruni, Sutri, VT, Italy). It was representative of a typical effluent of this kind of power plant in Italy [24]. The liquid phase of the digestate (pH = 7.98, Total Kjeldahl Nitrogen (TKN) = 4.9 g/L of N, total COD = 22.4 g/L), used for the experiments, was obtained by sieving the granules with a mesh of 2.36 mm pore size. Aliquots of 1 L were stored at 4°C and used during the first one-month feeding, frozen aliquots were used from the second month on.

2.2. Reactor Configuration and Operation. All experiments were performed using H-type MFC. The MFCs were done by two glass bottles (250 mL each) connected by a glass tube and a Nafion 117 proton exchange membrane (Sigma, UK) 7 cm^2 in area, held by a clamp. Graphite electrodes (2.5 cm × 5 cm × 0.05 cm Goodfellow Cambridge Ltd, UK) were

positioned 4 cm far from either side of the membrane. Each chamber was filled to 200 mL with feed solution in the anode and potassium phosphate buffer (100 mM pH 7.5) containing 50 mM $K_3Fe(CN)_6$ in the cathode. Anodic chambers were flushed with N_2 gas to maintain anaerobic conditions. MFCs operated at constant temperature of 30°C in batch mode with a fixed external resistance, R_{ext}, of 180 Ω. In the anodic chamber 150 mL of medium was replaced every 7 days leaving 50 mL of anolyte with each substitution. 200 mL of catholyte was replaced weekly. Feed solution (digestate-based feeding) was 1 : 10 digestate to medium; medium contained (per liter) KCl, 0.1 g; NH_4Cl, 1.5 g; NaH_2PO_4, 0.6 g; $NaHCO_3$, 2.5 g; Na-acetate, 0.82 g; vitamin solution 10 mL (Sigma-Aldrich), trace element solution, 10 mL [25]. Two MFC reactors operated under the same condition and configuration except the anode: MFC-U was assembled with a sterile anode; MFC-C was assembled with a precolonized *G. sulfurreducens* bioanode. *G. sulfurreducens* bioanode was obtained by a H-type MFC inoculated with *G. sulfurreducens* pure cultures. *G. sulfurreducens* was obtained from the German Collection of Microorganisms and Cell Cultures (DSMZ, Braunschweig, Germany).

2.3. Electrochemical Measurements. Open circuit voltage (OCV) and closed circuit voltage (CCV) across the external resistance (R_{ext} = 180 Ω) were monitored at 30 min intervals using a multichannel potentiostat/galvanostat VSP (Biologic Sas) connected to a personal computer. Current (I) was measured using the same instrument in a chronoamperometric mode, and Coulombic Efficiency (CE) was calculated as

$$\mathrm{CE}\,(\%) = 100 \cdot \frac{C_p}{C_{\mathrm{th}}}, \tag{1}$$

where C_p was the total electric charge calculated by integrating the current over time and C_{th} was the theoretical amount of electric charge available based on the total COD removal in the MFC section of the reactor [26].

Power, calculated as

$$P = \mathrm{CCV} \times I = R_{ext} \times I^2 = \frac{\mathrm{CCV}^2}{R_{ext}}, \tag{2}$$

was normalized with respect to both the projected surface area of the cathode (power density) and the volume of the liquid media (volumetric power density). MFC internal resistance was estimated using both maximum power transfer theorem (varying the external load by a resistance box ranging from 0 Ω, that is, the short circuit condition, up to 4 kΩ. The internal resistance value coincides with the value of the external resistance that maximizes load power consumption) and drawing typical polarization curves (by using the VSP instrument).

2.4. Chemical Analyses. The pH was measured using a GPL 42 instrument (Crison). The dissolved oxygen was measured with a 913 OXY oximeter (Mettler-Toledo). The total COD was determined by acid digestion and dichromate titration, according to standard methods (APHA, AWWA, and WEF, 2005). In order to evaluate the TKN, sample was heated at 400°C after mixing with 98% sulphuric acid and K_2SO_4. The obtained solution was cooled, blended with NaOH, and distilled using the Kjeldahl method. The amount of nitrogen into the distilled solution was determined by spectrophotometry with the Nessler reagent, using a T80+ UV/Vis spectrometer (PG Instruments, Ltd). Nitrites and nitrates were determined by ion chromatography, using a DX 120 instrument (Dionex).

2.5. Microbial Community Analysis

2.5.1. DNA Extraction and PCR Amplification. At the end of the experimental procedure (day 49) the graphite anode was cut into three sections. The surface of each slide covered by the anodic biofilm was scraped and placed in sterile 50 mM PBS; at the same time samples from the digestate and from different pure bacterial cultures were collected. Total DNA was extracted using the QIAamp DNA stool Mini-Kit (Qiagen Inc., Valencia, CA, USA) according to the manufacturer's instructions.

PCR amplification was carried out using the following primers: P0 and P6 for the bacterial 16S rRNA gene [27]; Geo587F/Geo978R targeting *G. sulfurreducens* and other closely related *Geobacter* [28]; amoA-1F/amoA2R targeting the AmoA gene that codifies ammonia monooxygenase (AMO) of ammonia oxidizing bacteria [29]; Brod541F-Brod1260R targeting the 16S rRNA gene specific for anammox bacteria [30]; and AnnirS379F-AnnirS821R targeting nitrite reductase gene of the anammox bacteria [31].

Real-time PCR was used to determine the relative abundance of the 16S rRNA gene of anammox bacteria in the MFC cultures with respect to digestate. First, the relative abundance of the anammox 16S rRNA gene with respect to total 16S rRNA gene (ΔCt) was determined for each sample (digestate, MFC-C and MFC-U); next the relative quantification (RQ) of the anammox gene in the MFC-C and MFC-U with respect to the digestate was calculated using the delta delta Ct method ($2^{-\Delta\Delta Ct}$). SYBR Green real-time PCR assays were performed using the following primer sets: anammox 16S rRNA gene, AMX818F-AMX1066R described in Tsushima et al. 2007 [32]; universal 16S rRNA gene, U16SRT-F-U16SRT-R, designed in the consensus sequence of bacterial 16S rRNA gene [33]. All primer sets were tested for sensitivity, optimal annealing, temperature, and primer efficiency with proper positive and negative controls. The positive control for the anammox 16S rRNA gene amplification was a plasmid containing the sequence of the anammox 16S rRNA gene obtained in this study.

2.5.2. Cloning and Sequencing of the 16S rRNA Gene. Brod541F-Brod1260R primers were used to amplify the 16S rRNA gene of the anammox bacteria. PCR products were purified from preparative agarose gels and cloned in the TOPO TA cloning kit (Invitrogen) for sequencing. The 16S rRNA gene sequences were compared for similarities to DNA sequences in the NCBI databases by BLAST. The phylogenetic tree was obtained using the multiple alignment program for amino acid or nucleotide sequences (MAFFT

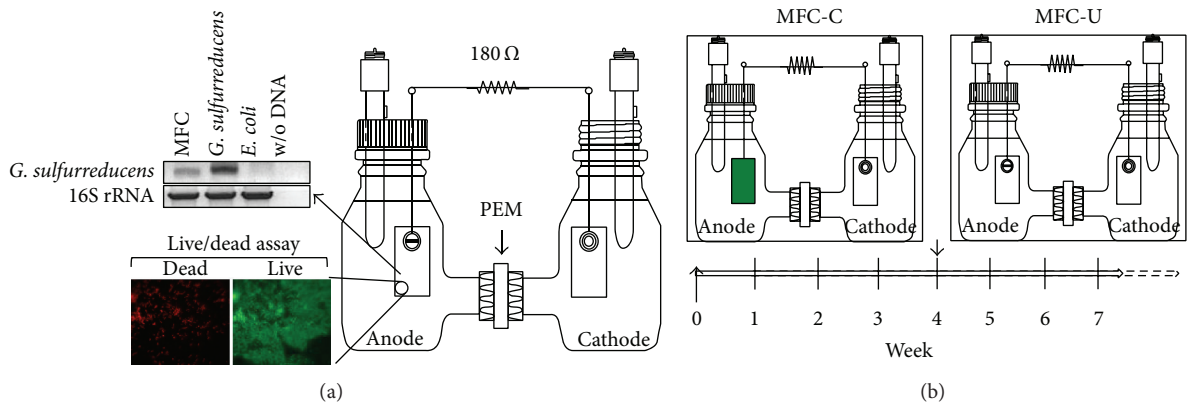

Figure 1: Schematic representation of the MFC-C and MFC-U reactors and the start-up phase. (a) H-type MFC inoculated with *G. sulfurreducens* and fed with synthetic medium containing acetate; after one-month operation small pieces of the anode were cut out and bacterial biofilm was visualized by the live-dead assay. Additionally, DNA samples were obtained from biofilm and amplified with universal or *G. sulfurreducens* 16S rRNA primers. *E. coli* and *G. sulfurreducens* DNAs were used as controls. (b) MFC-C was assembled with the anode from the reactor in panel (a); MFC-U was assembled with a sterile anode. Both reactors were operated under the same conditions and fed with digestate medium once a week. The arrowhead marks the transition from inactive to active MFC-U reactor.

version 7). The sequences were deposited in the European Nucleotide Archive (ENA) with accession numbers LN714795-LN714796.

2.5.3. Biofilm Imaging. Anodic biofilm samples were collected from each reactor by slicing 1 cm^2 carbon anode with sterilized scissors in an anaerobic chamber. Samples were stained using the LIVE/DEAD BacLight kit (Invitrogen), according to supplier specifications and examined with Apotome Fluorescence Microscope (Carl Zeiss International). Data were collected and analysed with the Axiovision 4.8 software. Samples for SEM analysis were fixed in 2.5% glutaraldehyde (Sigma-Aldrich) in PBS solution (0.1 M, pH = 7.4) for 3 hours at 4°C, washed three times in the same buffer (10 min each), and then postfixed with osmium tetroxide solution (1% in 0.1 M phosphate buffer, pH = 7.2). After rinsing in phosphate buffer, the samples were dehydrated in a series of graded ethanol and air-dried. All samples were coated with a 10 nm thick gold film. Coated samples were examined using an electron acceleration voltage of 20 keV, in both the secondary and the backscattered electron modes using a LEO 1450 VP microscope.

3. Results and Discussion

3.1. Start-Up of the MFC Reactor Fed with Digestate. In order to determine whether the resident microbial community of the digestate can convert organic matter into electricity while reducing nitrogen content we set up H-type MFCs with the two-chamber separated by proton exchange membranes (Figure 1). The first reactor (MFC-U) was assembled with a sterile anode whereas the second one (MFC-C) was assembled with a preconditioned *G. sulfurreducens* biofilm on the anode (Figure 1(b)). The latter was obtained from an MFC operated with *G. sulfurreducens* pure culture and synthetic feeding (Figure 1(a)). Both MFC-U and MFC-C were fed with a digestate-based medium as reported in materials and

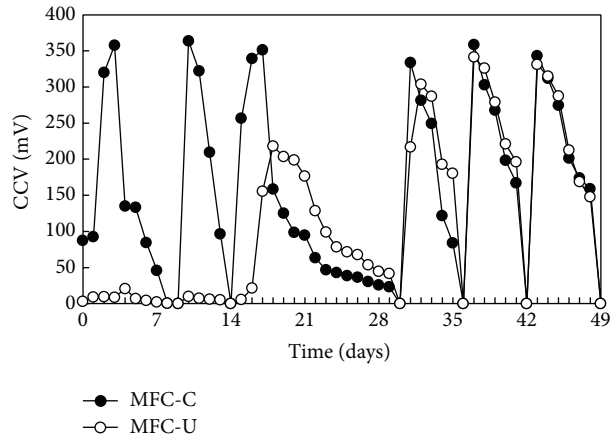

Figure 2: Voltage generation with digestate-feeding in MFC-C and MFC-U. Time 0 was the third week of operation.

methods. The initial digestate was diluted in order to obtain more favourable conditions for the growth of the resident bacteria and to reduce the introduction of toxic compounds that may inhibit bacterial activity [34–36]. During the first month the reactors behaved differently: MFC-U did not reveal any cell voltage while MFC-C showed a rapid CCV increase after feeding (Figure 2). In the MFC-C, after each feed solution replacement, CCV increased reaching similar values as in the previous cycle. Additionally, the rapid increase of CCV observed following feeding strongly suggested that it was due to the activity of the anode-associated biofilm. In the first three weeks, after reaching the peak, the CCV decreased with a different rate, whereas from day 28 to the end of operation the CCV cycles were more homogeneous. This may be due to the presence of an evolving bacterial population in the anodic chamber that reached the equilibrium after 3-4 weeks of operation.

After the fourth refeeding the MFC-U showed an increase of the CCV to about half of that recorded in MFC-C and a subsequent decrease that appeared somewhat slower than that in the MFC-C. To synchronize the two reactors, the fifth feeding was postponed by one week, after which weekly feeding was restored. As expected, from day 28 on the MFC-U and MFC-C cycled similarly showed a rapid increase of CCV after feeding and subsequent decrease in the following 5-6 days.

After the start-up period MFC-C reached a reproducible maximum power (computed by (2)) of 0.6 mW (i.e., 240 mW/m^2) at 346.8 mV, similarly MFC-U reached a maximum power transfer of 0.4 mW (i.e., 172.2 mW/m^2) at 359.4 mV. The time to achieve the maximum cell voltage after feeding (16–18 hr) was longer than that reported for MFC reactors fed with acetate [13] but similar to that obtained with slaughterhouse wastewater-fed reactors [13]. The substrate type influences the MFC performance, not only in terms of bacterial community but also in the maximum power and Coulombic Efficiency. Therefore, the time required to achieve the maximum cell voltage observed in our MFC systems is in accordance with the composition of the digestate-like medium supplemented with acetate.

It has been reported that methanogens, by competing with electroactive bacteria for substrates, can reduce the performance of MFCs [37]. Nonetheless, in both reactors we did not detect CH_4 production, neither in the start-up period nor during operation regime, suggesting that methanogenesis did not take place in the MFCs or it was very low. Since the digestate was collected in the final stage of biogas production it may be that methanogenesis was exhausted although we cannot exclude that digestate-based medium in MFC conditions outcompeted methanogens while favoring colonization of electrogenic bacteria.

3.2. Electrochemical Performance. Maximum power transfer curves (Figure 3(a)) and polarization curves (Figures 3(b) and 3(c)) for both the MFCs were carried out in correspondence of CCV peak values at the sixth batch cycle when the reactors reached stable performances. The maximum power density was determined by varying the external resistance over a range of 0–4000 Ω and recording the voltage (Figure 3(a)).

The maximum power generation reached a peak value of 0.60 mW for the MFC-C and 0.43 mW for the MFC-U when the applied external resistance matched the internal resistance of the system at 200 and 300 Ω for the MFC-C and MFC-U, respectively.

The higher maximum power density and the reduced ohmic resistance of the MFC-C with respect to MFC-U might be ascribed to the *G. sulfurreducens* anode preconditioning. Conversely, in the MFC-U the digestate-resident microbial population might prefer slightly higher resistance conditions to better exploit the substrate as a result of the competition with the electrogenic bacteria.

The maximum power density per projected anode surface area was 170 mW/m^2 for the MFC-C (Figure 3(b)) and 240 mW/m^2 for the MFC-U (Figure 3(c)) while the limiting current density recorded was 1304 mA/m^2 for the MFC-U and 992 mA/m^2 for the MFC-C. Overall, the electrochemical measurements showed comparable performances between the reactors demonstrating that electrogenic bacteria were present in the digestate and possibly selected by MFC conditions.

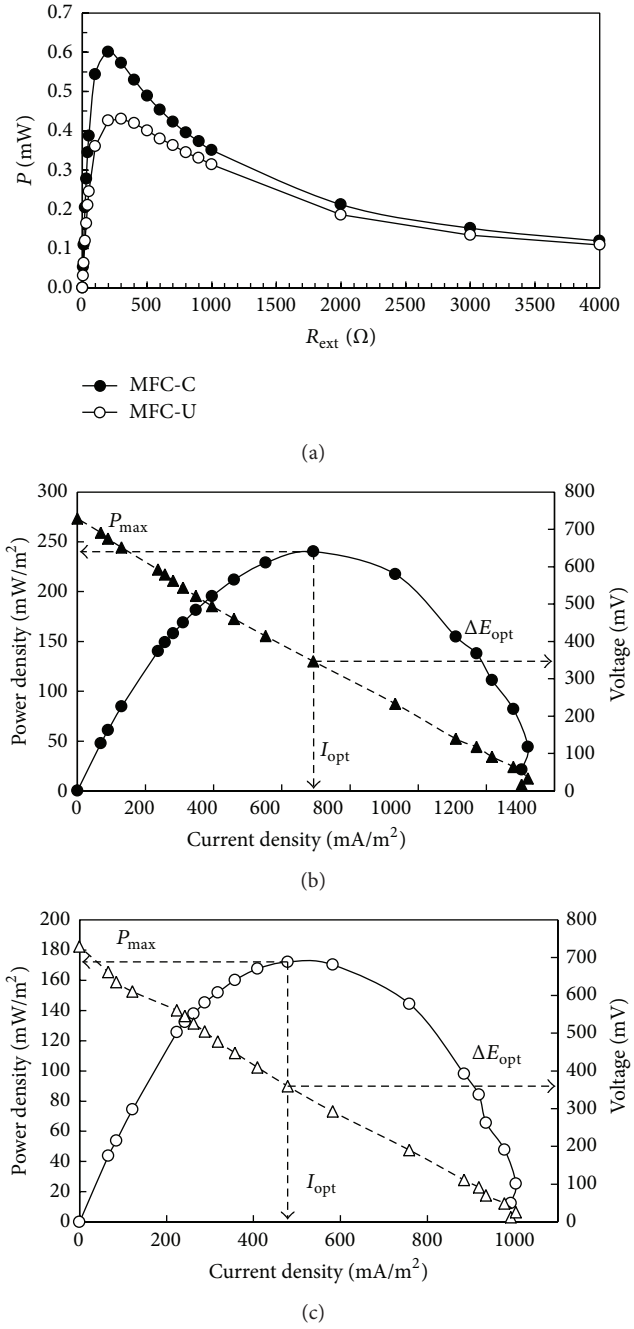

Figure 3: Maximum power transfer curves performed on MFC-C and MFC-U (a). Polarization curves with the maximum power density (P_{max}), the optimal voltage (ΔE_{opt}), and optimal current density (I_{opt}) performed on MFC-C (b) and MFC-U (c) at the end of the start-up procedure (day 28).

3.3. Coulombic Efficiency and Substrates Removal. MFC-U and MFC-C exhibited during days 35 and 42, a calculated CE

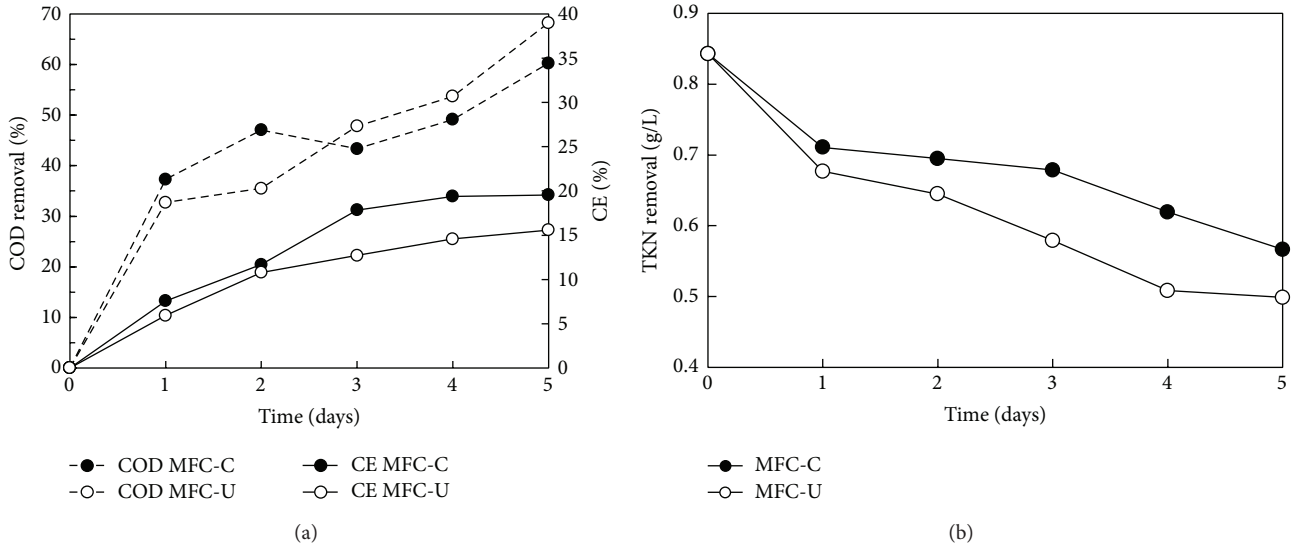

Figure 4: Total COD removal and Coulombic Efficiency (CE) in MFC-C and MFC-U (a); TKN removal as function of time (b) (days 36–41).

of 15.6 and 19.6%, respectively (Figure 4(a)), both of which were in the typical range observed for MFCs fed with waste or wastewater [19, 38] while CE, in MFC fed with acetate-based synthetic media, may rise up to 98% [13].

The absence of any gas development in both reactors allowed us to exclude methanogenic processes as the main cause of the resulting low Coulombic Efficiency. On the contrary, it could be attributed to the initial presence of nitrates, sulphates, and other terminal electron acceptors in the digestate.

The removal of the organic carbon by both reactors was quite efficient as demonstrated by the reduction of total COD up to 68 and 60% in the MFC-C and MFC-U, respectively, at the fifth day after feeding. Considering that the liquid digestate accounted for about 71% of the initial COD both reactors appeared to be very effective in the reduction of the organic content of the effluents from anaerobic digestion plants.

As regards to nitrogen TKN removals of about 40% and 32% in the MFC-C and MFC-U, respectively, were observed (Figure 4(b)). Ammonia in the cathodic chamber was always found at negligible level disfavouring the hypothesis of the ammonium ion transit to the cathodic chamber through the membrane [39]. Ammonia volatilization in the cathodic chamber can be also excluded since no oxygen was insufflated and the cathodic pH was neutral. Nitrogen sources in the MFCs were both the growth media (as ammonia) and the digestate (mainly as organic nitrogen and ammonia); the latter accounted for about 60% of nitrogen in each fed-batch cycle. Although, nitrogen consumption in the cells could be in part justified by the synthesis of new biomass in the anodic chamber, other mechanisms could be involved. According to the literature ammonia consumption in MFC can be also explained by several different specific pathways such as nitrification-denitrification, anammox, and nitrite reduction by lithotrophic ammonia oxidizers or by specific processes of ammonia oxidation coupled to electricity generation. Taking into consideration the lower Coulombic Efficiency and total COD consumption calculated for the unconditioned cell with respect to the conditioned one, electricity generation from direct ammonia oxidation appeared to be negligible. At the same time, since dissolved oxygen in the anodic chambers was always lower than 0.05 mg/L and that nitrates and nitrites at the end of each cycle were negligible in the anodic and cathodic chambers in both MFCs, it is reasonable to hypothesize that the main nitrogen removal mechanism was ammonia oxidation under anaerobic conditions.

Collectively our results suggest that H-type MFC reactors fed with digestate-based medium allowed the development of a microbial consortium able to oxidize ammonia anaerobically, as proposed in other studies [40]. However, further experiments are needed to better investigate the nitrogen removal mechanism and to evaluate the maximum nitrogen amount potentially degradable in such systems.

3.4. Biofilm Imaging. The morphology of the biofilm grown on the electrodes surface was analysed by scanning electron microscope (SEM) and fluorescence microscopy. Anode samples, about 1 cm^2 size, were taken from the reactors operating since two and three months; the sampling was done the day after feeding when the reactors reached the maximum power generation. SEM analysis showed that anodes from both reactors were covered by bacterial biofilm (Figures 5(a) and 5(d)). Measurements of biofilm thickness showed that the biofilm ranged from 141 ± 30 μm to 66 ± 1 μm without detectable differences between MFC-C and -U. Close-up images (Figures 5(b)–5(e)) revealed a different bacterial morphology with a predominance of bacilli, often tightly embedded into the biofilm matrix (Figure 5(e)). Comparative analysis of the biofilms from the MFC-C and MFC-U anodes showed a more uniform morphology in the former than in the latter. Accordingly, MFC-C images at higher magnification revealed the presence of a multilayered

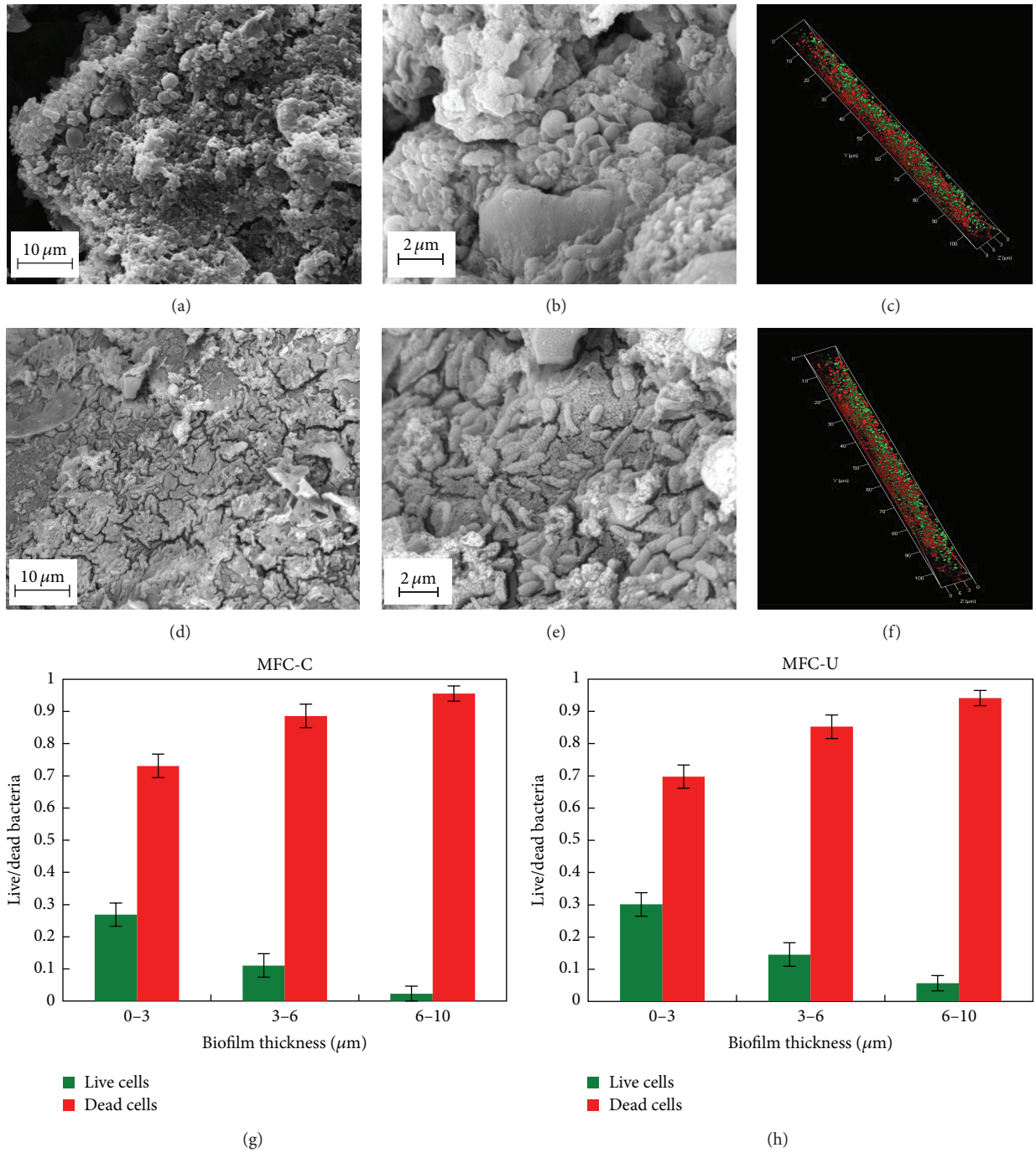

FIGURE 5: Biofilm imaging and cell viability. (a–f), SEM images of biofilms from MFC-C (a and b) and MFC-U (d and e). Live (green) and dead (red) bacteria within the biofilms from MFC-C (c) and MFC-U (f). (g and h) Fraction of live and dead bacteria in the anode biofilms from the indicated reactors. Cell viability was determined at the surface (0–3 μm), in the middle (3–6 μm), and at the base of the biofilms (6–10 μm).

biofilm in all the fields examined. On the contrary, MFC-U biofilm showed composite morphology with smooth and rough areas with bacteria mainly located on the surface of the matrix. Additionally, MFC-U biofilm showed the presence of complex aggregates, probably due to the entrapped digestate sediments. These different morphologies could be due to the fact that biofilm in MFC-C was previously colonized by *G. sulfurreducens* pure culture whereas MFC-U biofilm is developed on sterile anode by the unique contribution of the bacteria present in the digestate.

Next bacteria viability in biofilm samples was analysed using the LIVE/DEAD assay (Figures 5(c) and 5(f)). Fluorescence microscopy analysis did not reveal significant differences between MFC-C and MFC-U. 3D analysis showed

that live bacteria preferentially localized on the outer layer of the biofilm (Figures 5(c) and 5(f)), probably due to easier availability to substrate. Quantitative analysis of the green and red signals within the biofilms showed that most of the live bacteria stratified in the outer layer and account for about 30% of total (Figures 5(g) and 5(h)). The fraction of live bacteria was slightly higher in MFC-U than in MFC-C, probably due to the fact that the anodic biofilm in the latter was one month older than the former. Although the staining procedure cannot rigorously distinguish live and dead cells, since it is based on membrane permeability, the fraction of live bacteria in these reactors appeared much lower than previously described [13]. Some differences may account for this result such as anode materials (graphite versus carbon cloth) and the age of the biofilm. Nonetheless, current generation in the two reactors was similar to that reported by the aforementioned studies, suggesting that the anode biofilms developed from digestate are efficient in electricity production. Additionally, the presence of a subpopulation of dead cells in-between the metabolically active cells and the electrode surface did not appear to significantly dampen electron transfer possibly due to long-range electrons transfer via the conductive pili [12]. We cannot exclude that the layer of dead cells may overgrow with time, reducing the efficiency of electron transfer to the anode. Although, the cycling in current production observed during the operation period suggests that the subpopulations of live and dead cells found equilibrium compatible with sufficient electron transfer.

3.5. Molecular Analysis of Biofilms. MFC-C and MFC-U performed very similarly although small differences in CE, nitrogen removal and biofilm structure were recorded, suggesting similar microbial communities developed on both conditioned and unconditioned anodes. To address this hypothesis, at the end of the last feeding cycle, DNA samples from both reactors were analysed by using the 16S rRNA gene as a molecular marker and functional biomarkers such as genes involved in the nitrogen metabolism. Controls DNAs were extracted from the same digestate used to feed the reactors, from *G. sulfurreducens* and laboratory strains of *Escherichia coli*. First, the 16S rRNA genes were amplified with universal primers and then restricted with *Rsa*I and *Hinf* I to analyse genome similarities between the two reactors and control DNAs (see Supplementary Material available online at http://dx.doi.org/10.1155/2015/351014) (Supplementary Figure 1)). The resulting restriction profiles showed high similarities among digestate, MFC-C, and MFC-U samples and between the MFCs and *G. sulfurreducens*.

Next, 16S rRNA gene was also amplified by using specie-specific primers. *G. sulfurreducens* 16S rRNA gene was clearly detected in MFCs and digestate and the band intensity was higher in MFC-C than in MFC-U due to the *G. sulfurreducens* preconditioning (Figure 6(a)). Sequence analysis confirmed the presence of *G. sulfurreducens* in the digestate and in both reactors. No AmoA band targeting the ammonia oxidizing bacteria (AOB) [29] was observed in the reactors. This suggests that the anaerobic conditions of the anodic chamber, the accumulation of toxic compounds in the MFC, or the competition with better-adapted microorganisms negatively affected the growth of the AOB. On the contrary, by using primers targeting the 16S rRNA gene and the cd1 nitrite reductase (NIRS) of the anammox bacteria [41] (Figure 6(b)) we observed amplification products in both the reactors and the digestate. To quantify the abundance of anammox 16S rRNA in the bacterial populations of both reactors, we performed real-time PCR assays by using the relative quantification method and the digestate as calibrator (Figure 6(c)). The analysis showed an increase of the average abundance of the anammox specific 16S rRNA genes in the MFC-C (1.59 ± 0.28) and MFC-U (3.73 ± 1.01) compared with the digestate. This suggests a greater ability of anammox bacteria to colonize sterile MFCs than *G. sulfurreducens*-conditioned reactors.

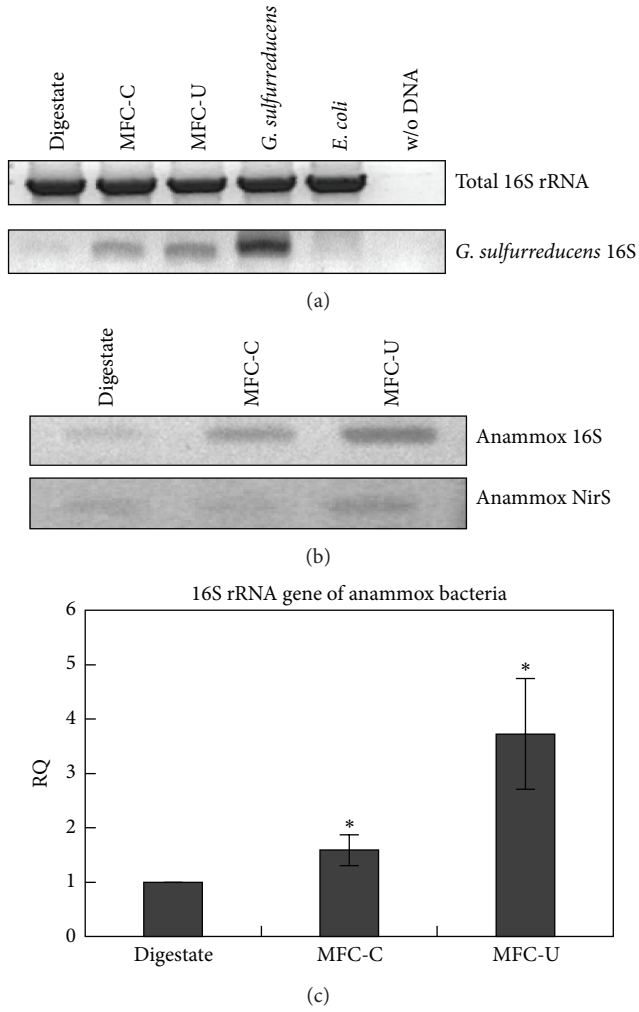

Figure 6: Molecular analysis of the biofilm. (a) PCR amplification of the indicated genes. 100 ng of DNA is used for each PCR reaction. (b) Upper panel, PCR amplification of the 16 rRNA gene, and the cd1 nitrite reductase (NirS) of the anammox bacteria. (c) Relative quantification (RQ) of the anammox 16S rRNA gene in the MFC-C and MFC-U biofilms with respect to digestate. Data are mean, standard deviation, $N = 3$; statistical analysis (t-test): MFC-C versus digestate $P = 0.018$; MFC-U versus digestate $P = 0.011$.

Finally, sequencing analysis of the anammox 16S rRNA gene confirmed presence of *Planctomycetes* closely related to *Candidatus brocadia anammoxidans* (sequence identity between 97-98%) in both reactors (Supplementary Figure 2).

Overall, the molecular analyses revealed that MFC bacterial communities were directly related to the microbial population found in the digestate; irrespective of *G. sulfurreducens* preconditioning, very similar microbial communities developed in the MFC-C and MFC-U reactors; MFC operating conditions selected electrogenic bacterial and provide favourable conditions for the cultivation of anammox bacteria.

4. Conclusions

Two-chamber MFC reactors fed with anaerobic digestate and operated in batch-mode were assembled to test for simultaneous nitrogen reductions and energy recovery. Appreciable removal of total COD (up to 60%) and TKN (up to 40%), together with good electricity generation, was achieved by the activity of bacterial consortia derived from digestate. Regardless of preacclimation of the anodic biofilm with *G. sulfurreducens* in one of the cells, the proposed MFCs allowed the development of biofilms containing anammox bacteria in the anaerobic compartment of the MFC, indicating the presence of favourable conditions (e.g., strict anaerobic conditions and high nitrogen content) for these bacteria. The comparable current production measured in both MFC-C and MFC-U suggests that electrogenic bacteria, such as *G. sulfurreducens,* were fostered in the electrode colonization.

However additional studies are needed to better understand how the MFC environment and the digestate influence bacteria proliferation and biofilm development electricity generation and ultimately nitrogen removal. Additionally, in scaling-up MFC or in the assembly of continuous flow systems, the treatment of undiluted digestate could represent a critical issue especially at an acceptable hydraulic retention time. Nevertheless, the proposed results represent a preliminary study to address the feasibility of MFC as bottoming bioremediation units in anaerobic digestor plants to generate electricity and simultaneously treat digestate for nitrogen removal in order to limit waters pollution caused by spreading of livestock effluents.

Conflict of Interests

The authors declare that there is no conflict of interests regarding the publication of this paper.

Acknowledgments

This research received the financial support from ENAMA under the "Biomass Project," sponsored and funded by the Italian Ministry of Agriculture, Food and Forestry. The partial support from Sapienza University (Grant nos. C26A11HBR2, C26A107ENC, C26A09ENBW, C26G105YMC, and C26F092PBW) is also acknowledged. The work of Enea Gino Di Domenico was supported by grants from Regione Lazio and by Istituto Pasteur-Fondazione Cenci Bolognetti, University of Rome "Sapienza".

References

[1] S. Philips, H. J. Laanbroek, and W. Verstraete, "Origin, causes and effects of increased nitrite concentrations in aquatic environments," *Reviews in Environmental Science and Biotechnology*, vol. 1, no. 2, pp. 115–141, 2002.

[2] H.-G. Zhang and S.-Q. Zhou, "Treating leachate mixture with anaerobic ammonium oxidation technology," *Journal of Central South University of Technology*, vol. 13, no. 6, pp. 663–667, 2006.

[3] M. S. Jetten, L. van Niftrik, M. Strous, B. Kartal, J. T. Keltjens, and H. J. Op den Camp, "Biochemistry and molecular biology of anammox bacteria," *Critical Reviews in Biochemistry and Molecular Biology*, vol. 44, no. 2-3, pp. 65–84, 2009.

[4] I. Tsushima, Y. Ogasawara, T. Kindaichi, H. Satoh, and S. Okabe, "Development of high-rate anaerobic ammonium-oxidizing (anammox) biofilm reactors," *Water Research*, vol. 41, no. 8, pp. 1623–1634, 2007.

[5] M. Strous, J. J. Heijnen, J. G. Kuenen, and M. S. M. Jetten, "The sequencing batch reactor as a powerful tool for the study of slowly growing anaerobic ammonium-oxidizing microorganisms," *Applied Microbiology and Biotechnology*, vol. 50, no. 5, pp. 589–596, 1998.

[6] K. Egli, U. Fanger, P. J. J. Alvarez, H. Siegrist, J. R. Van der Meer, and A. J. B. Zehnder, "Enrichment and characterization of an anammox bacterium from a rotating biological contactor treating ammonium-rich leachate," *Archives of Microbiology*, vol. 175, no. 3, pp. 198–207, 2001.

[7] W. R. L. van der Star, A. I. Miclea, U. G. J. M. van Dongen, G. Muyzer, C. Picioreanu, and M. C. M. van Loosdrecht, "The membrane bioreactor: a novel tool to grow anammox bacteria as free cells," *Biotechnology and Bioengineering*, vol. 101, no. 2, pp. 286–294, 2008.

[8] M. Oshiki, T. Awata, T. Kindaichi, H. Satoh, and S. Okabe, "Cultivation of planktonic anaerobic ammonium oxidation (anammox) bacteria using membrane bioreactor," *Microbes and Environments*, vol. 28, no. 4, pp. 436–443, 2013.

[9] S. M. Kotay, B. L. Mansell, M. Hogsett, H. Pei, and R. Goel, "Anaerobic ammonia oxidation (ANAMMOX) for side-stream treatment of anaerobic digester filtrate process performance and microbiology," *Biotechnology and Bioengineering*, vol. 110, no. 4, pp. 1180–1192, 2013.

[10] K. Rabaey and W. Verstraete, "Microbial fuel cells: Novel biotechnology for energy generation," *Trends in Biotechnology*, vol. 23, no. 6, pp. 291–298, 2005.

[11] A. Sydow, T. Krieg, F. Mayer, J. Schrader, and D. Holtmann, "Electroactive bacteria—molecular mechanisms and genetic tools," *Applied Microbiology and Biotechnology*, vol. 98, no. 20, pp. 8481–8495, 2014.

[12] D. R. Lovley, "Electromicrobiology," *Annual Review of Microbiology*, vol. 66, pp. 391–409, 2012.

[13] K. J. Chae, M. J. Choi, J. W. Lee, K. Y. Kim, and I. S. Kim, "Effect of different substrates on the performance, bacterial diversity, and bacterial viability in microbial fuel cells," *Bioresource Technology*, vol. 100, no. 14, pp. 3518–3525, 2009.

[14] P. T. Kelly and Z. He, "Nutrients removal and recovery in bioelectrochemical systems: a review," *Bioresource Technology*, vol. 153, pp. 351–360, 2014.

[15] H. I. Park, D. K. Kim, Y.-J. Choi, and D. Pak, "Nitrate reduction using an electrode as direct electron donor in a biofilm-electrode reactor," *Process Biochemistry*, vol. 40, no. 10, pp. 3383–3388, 2005.

[16] X. Xie, L. Hu, M. Pasta et al., "Three-dimensional carbon nanotube-textile anode for high-performance microbial fuel cells," *Nano Letters*, vol. 11, no. 1, pp. 291–296, 2011.

[17] B. Virdis, K. Rabaey, Z. Yuan, and J. Keller, "Microbial fuel cells for simultaneous carbon and nitrogen removal," *Water Research*, vol. 42, no. 12, pp. 3013–3024, 2008.

[18] B. Virdis, K. Rabaey, R. A. Rozendal, Z. Yuan, and J. Keller, "Simultaneous nitrification, denitrification and carbon removal in microbial fuel cells," *Water Research*, vol. 44, no. 9, pp. 2970–2980, 2010.

[19] B. Min, J. R. Kim, S. Oh, J. M. Regan, and B. E. Logan, "Electricity generation from swine wastewater using microbial fuel cells," *Water Research*, vol. 39, no. 20, pp. 4961–4968, 2005.

[20] R. K. Jung, Y. Zuo, J. M. Regan, and B. E. Logan, "Analysis of ammonia loss mechanisms in microbial fuel cells treating animal wastewater," *Biotechnology and Bioengineering*, vol. 99, no. 5, pp. 1120–1127, 2008.

[21] H. Yan, T. Saito, and J. M. Regan, "Nitrogen removal in a single-chamber microbial fuel cell with nitrifying biofilm enriched at the air cathode," *Water Research*, vol. 46, no. 7, pp. 2215–2224, 2012.

[22] H. Yan and J. M. Regan, "Enhanced nitrogen removal in single-chamber microbial fuel cells with increased gas diffusion areas," *Biotechnology and Bioengineering*, vol. 110, no. 3, pp. 785–791, 2013.

[23] D. R. Lovley, "Bug juice: harvesting electricity with microorganisms," *Nature Reviews Microbiology*, vol. 4, no. 7, pp. 497–508, 2006.

[24] F. Gioelli, E. Dinuccio, and P. Balsari, "Residual biogas potential from the storage tanks of non-separated digestate and digested liquid fraction," *Bioresource Technology*, vol. 102, no. 22, pp. 10248–10251, 2011.

[25] S. Ishii, T. Kosaka, K. Hori, Y. Hotta, and K. Watanabe, "Coaggregation facilitates interspecies hydrogen transfer between *Pelotomaculum thermopropionicum* and *Methanothermobacter thermautotrophicus*," *Applied and Environmental Microbiology*, vol. 71, no. 12, pp. 7838–7845, 2005.

[26] B. E. Logan, B. Hamelers, R. Rozendal et al., "Microbial fuel cells: methodology and technology," *Environmental Science and Technology*, vol. 40, no. 17, pp. 5181–5192, 2006.

[27] L. Pirone, A. Bragonzi, A. Farcomeni et al., "*Burkholderia cenocepacia* strains isolated from cystic fibrosis patients are apparently more invasive and more virulent than rhizosphere strains," *Environmental Microbiology*, vol. 10, no. 10, pp. 2773–2784, 2008.

[28] Z. Ren, L. M. Steinberg, and J. M. Regan, "Electricity production and microbial biofilm characterization in cellulose-fed microbial fuel cells," *Water Science and Technology*, vol. 58, no. 3, pp. 617–622, 2008.

[29] J.-H. Rotthauwe, K.-P. Witzel, and W. Liesack, "The ammonia monooxygenase structural gene amoa as a functional marker: molecular fine-scale analysis of natural ammonia-oxidizing populations," *Applied and Environmental Microbiology*, vol. 63, no. 12, pp. 4704–4712, 1997.

[30] C. R. Penton, A. H. Devol, and J. M. Tiedje, "Molecular evidence for the broad distribution of anaerobic ammonium-oxidizing bacteria in freshwater and marine sediments," *Applied and Environmental Microbiology*, vol. 72, no. 10, pp. 6829–6832, 2006.

[31] M. Li, T. Ford, X. Li, and J.-D. Gu, "Cytochrome *cd*1-containing nitrite reductase encoding gene *nirS* as a new functional biomarker for detection of anaerobic ammonium oxidizing (anammox) bacteria," *Environmental Science and Technology*, vol. 45, no. 8, pp. 3547–3553, 2011.

[32] I. Tsushima, T. Kindaichi, and S. Okabe, "Quantification of anaerobic ammonium-oxidizing bacteria in enrichment cultures by real-time PCR," *Water Research*, vol. 41, no. 4, pp. 785–794, 2007.

[33] R. J. Clifford, M. Milillo, J. Prestwood et al., "Detection of bacterial 16S rRNA and identification of four clinically important bacteria by real-time PCR.," *PloS one*, vol. 7, no. 11, Article ID e48558, 2012.

[34] M. Strous, J. A. Fuerst, E. H. M. Kramer et al., "Missing lithotroph identified as new planctomycete," *Nature*, vol. 400, no. 6743, pp. 446–449, 1999.

[35] B. Wett, "Development and implementation of a robust deammonification process," *Water Science and Technology*, vol. 56, no. 7, pp. 81–88, 2007.

[36] T. Lotti, W. R. L. van der Star, R. Kleerebezem, C. Lubello, and M. C. M. van Loosdrecht, "The effect of nitrite inhibition on the anammox process," *Water Research*, vol. 46, no. 8, pp. 2559–2569, 2012.

[37] K. P. Katuri, A.-M. Enright, V. O'Flaherty, and D. Leech, "Microbial analysis of anodic biofilm in a microbial fuel cell using slaughterhouse wastewater," *Bioelectrochemistry*, vol. 87, pp. 164–171, 2012.

[38] G. Zhang, Q. Zhao, Y. Jiao, K. Wang, D.-J. Lee, and N. Ren, "Efficient electricity generation from sewage sludge usingbiocathode microbial fuel cell," *Water Research*, vol. 46, no. 1, pp. 43–52, 2012.

[39] R. A. Rozendal, H. V. M. Hamelers, and C. J. N. Buisman, "Effects of membrane cation transport on pH and microbial fuel cell performance," *Environmental Science and Technology*, vol. 40, no. 17, pp. 5206–5211, 2006.

[40] Y. H. Ahn and B. E. Logan, "Effectiveness of domestic wastewater treatment using microbial fuel cells at ambient and mesophilic temperatures," *Bioresource Technology*, vol. 101, no. 2, pp. 469–475, 2010.

[41] M. Li and J.-D. Gu, "Advances in methods for detection of anaerobic ammonium oxidizing (anammox) bacteria," *Applied Microbiology and Biotechnology*, vol. 90, no. 4, pp. 1241–1252, 2011.

Hindawi Publishing Corporation
BioMed Research International
Volume 2015, Article ID 981829, 17 pages
http://dx.doi.org/10.1155/2015/981829

Research Article

Bacterial Diversity and Bioremediation Potential of the Highly Contaminated Marine Sediments at El-Max District (Egypt, Mediterranean Sea)

Ranya A. Amer,[1] Francesca Mapelli,[2] Hamada M. El Gendi,[3] Marta Barbato,[2] Doaa A. Goda,[3] Anna Corsini,[2] Lucia Cavalca,[2] Marco Fusi,[4] Sara Borin,[2] Daniele Daffonchio,[2,4] and Yasser R. Abdel-Fattah[5]

[1] *Environmental Biotechnology Department, Genetic Engineering and Biotechnology Research Institute, City of Scientific Research and Technology Applications, Alexandria, Egypt*
[2] *Department of Food, Environment and Nutritional Sciences (DeFENS), University of Milan, 20133 Milan, Italy*
[3] *Bioprocess Development Department, Genetic Engineering and Biotechnology Research Institute, City of Scientific Research and Technology Applications, Alexandria, Egypt*
[4] *Biological and Environmental Sciences and Engineering Division (BESE), King Abdullah University of Science and Technology (KAUST), Thuwal 23955, Saudi Arabia*
[5] *Genetic Engineering and Biotechnology Research Institute (GEBRI), City for Scientific Research and Technology Applications (SRTA City), New Burg El-Arab City, Universities and Research Institutes District, Alexandria 21934, Egypt*

Correspondence should be addressed to Yasser R. Abdel-Fattah; yasser1967@yahoo.com

Received 4 November 2014; Revised 1 February 2015; Accepted 1 February 2015

Academic Editor: Spyridon Ntougias

Coastal environments worldwide are threatened by the effects of pollution, a risk particularly high in semienclosed basins like the Mediterranean Sea that is poorly studied from bioremediation potential perspective especially in the Southern coast. Here, we investigated the physical, chemical, and microbiological features of hydrocarbon and heavy metals contaminated sediments collected at El-Max bay (Egypt). Molecular and statistical approaches assessing the structure of the sediment-dwelling bacterial communities showed correlations between the composition of bacterial assemblages and the associated environmental parameters. Fifty strains were isolated on mineral media supplemented by 1% crude oil and identified as a diverse range of hydrocarbon-degrading bacteria involved in different successional stages of biodegradation. We screened the collection for biotechnological potential studying biosurfactant production, biofilm formation, and the capability to utilize different hydrocarbons. Some strains were able to grow on multiple hydrocarbons as unique carbon source and presented biosurfactant-like activities and/or capacity to form biofilm and owned genes involved in different detoxification/degradation processes. El-Max sediments represent a promising reservoir of novel bacterial strains adapted to high hydrocarbon contamination loads. The potential of the strains for exploitation for *in situ* intervention to combat pollution in coastal areas is discussed.

1. Introduction

The Mediterranean Sea is exposed to a high risk of pollution by petroleum hydrocarbons (HC), due to the presence of tens of sites related to their extraction, refinery, and transport along its coastline [1]. This risk is exacerbated by several factors, including the semienclosed nature of this sea and the geographical location of most of the oil-producing and oil-consuming countries, placed, respectively, on the Southern and Northern sides of the basin, entailing the presence of pipeline terminal and oil tanker traffic. A recent analysis of the papers published in the last years about the microbiology of coastal and open-sea sites in the Mediterranean Sea clearly showed that the Southern side of the basin has been largely

neglected [2] although it hosts several polluted areas along its coasts, such as El-Max district area (Alexandria, Egypt). Due to the numerous industrial activities, the disposal of untreated waste effluents, and the shipping activities, El-Max bay is a coastal site chronically contaminated by crude oil and heavy metals [3] whose clean-up represents a challenge for the Egyptian country and for the entire research community. Crude oil is a mixture of organic compounds that may contain up to 20000 chemicals and it is hardly removable from polluted ecosystems by traditional methods [4]. Bioremediation is an alternative to physical and chemical methods and takes advantage of the natural ability of certain microbes to degrade HC, buffering the effect of oil pollution in natural ecosystems. Bioremediation can be achieved by adding nutrients to the autochthonous biodegrading microbes (biostimulation) or adding a microorganism's inoculum in the polluted environment (bioaugmentation). The successfulness of such approaches is still under debate [5–7]; however recent reports suggest the use of autochthonous bioaugmentation (ABA) as the best practice to restore polluted marine ecosystems [8]. The starting point for such approach is the detailed study of the diversity of microbial communities colonizing the polluted site of interest. Such survey should be accomplished through both molecular and cultivation dependent techniques that, respectively, allow (i) the correlation of the environmental parameters with the structure of the whole microbial communities and (ii) the enrichment, identification, and characterization of degrading microbes for traits of interest like the production of biosurfactant. Biosurfactants are molecules that have hydrophilic and hydrophobic moieties and, enhancing the bioavailability of oil hydrocarbons, are pivotal in microbial oil degradation network [8]. In this pipeline, the most promising microbes can be selected for subsequent laboratory scale experiments to test their degrading capability before *ex situ* and *in situ* field ABA trials.

This work represents the first holistic investigation of the bacterial communities inhabiting the marine sediments of different stations located in El-Max district bay. It aims to unravel the pattern of bacterial diversity, ecology, and degradation potential in polluted sediments and to obtain promising bacterial resources to be exploited for marine sites' clean-up. Chronically polluted El-Max district represents a very interesting site for this research topic since, due to the occurrence of strong selective pressure, most of the autochthonous bacteria should be able to cope with the environmental stressors induced by oil contamination.

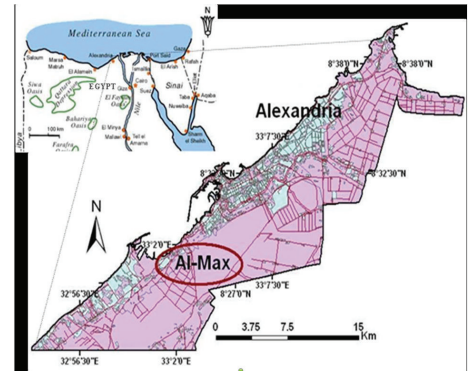

(a)

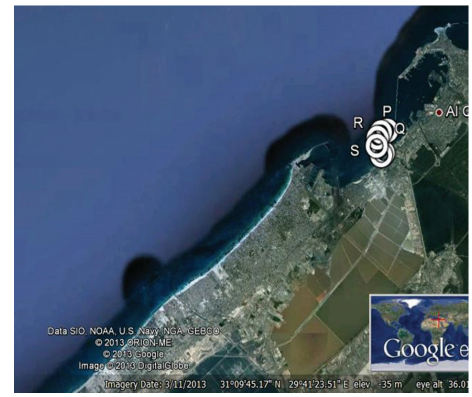

(b)

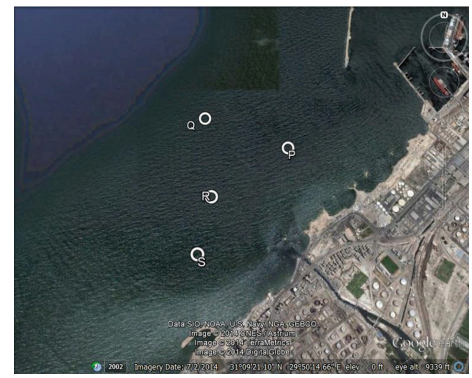

(c)

Figure 1: Location of the study area and sampling stations. (a) Overall area of El-Max district (Egypt) in the Mediterranean Sea and (b) satellite image of the sampling area, (c) showing the position of the four sampling sites.

2. Materials and Methods

2.1. Sites Description and Sampling. The sampling areas are located at El-Max bay, which lies in the western side of Alexandria at longitude 29°78 E and latitude 31°13 N (Figure 1(a)). The shoreline is mainly rocky with occurrences of narrow sandy beaches. There are pronounced differences in direction and intensity of marine currents in the bay near the outlets [9, 10]. Sediment samples were collected in triplicate at depth between 3 and 16 meters, using a grab sampler, from 4 stations (Figures 1(b) and 1(c)): P (31°9′31.20″N, 29°50′28.20″E), Q (31°9′28.40″N, 29°50′14.40″E), R (31°9′18.56″N, 29°50′5.89″E), and S (31°9′4.89″N, 29°50′2.49″E). Sediment samples were packed in aluminum foil for HC analysis and in plastic bags for the rest of the physicochemical parameters. The water content, particle size, and total organic carbon were determined immediately after sampling. Sediment samples were collected using sterile spoons and stored in sterile bags at 4°C for bacterial isolation and −20°C for molecular analyses.

2.2. Chemical Characterization of Sediment Samples. Phosphorus extraction was performed according to Aspila et al. [15]. Total phosphorus was extracted by ashing the sample at 550°C for 2.5 h and subsequent shaking with 1 N HCl for 16 hours while the inorganic phosphorus was extracted by shaking the oven-dried sediments (110°C) with 1 N HCl for 16 hours. Phosphorus determination in the two extracts was made according to the method of Murphy and Riley [16]. Organic phosphorus was calculated subtracting the value of the inorganic phosphorous from the total phosphorus.

Total nitrogen content in the sediment samples was determined by using Kjeldahl apparatus (Raypa, model: DNP–1500, R. Espinar S.L., Barcelona, Spanish) according to standard method [17].

The total organic content (TOC) was determined by the loss-on-combustion technique after removal of carbonate with dilute (IN) HCl; a portion of sediments was weighed into a porcelain crucible and ignited in a muffle furnace at 550°C for two hours. The crucible was cooled in a desiccator and reweighed and the total organic content (TOC) was calculated as the weight loss in percentage [18]. The analysis of total pesticides and polychlorinated biphenyls (PCBs) was performed as previously described [19–21].

The presence and abundance of different n-alkanes were estimated by chromatographic techniques. The n-alkane concentration was analyzed by Agilent 7890, USA. A HP-5 capillary chromatographic column (30 m × 0.32 mm I.D.) and a capillary column (30 m × 0.25 mm I.D.) were used for GC-FID and GC-MS analyses, respectively. Nitrogen was the carrier gas with 3 mL/min. Injector and detector temperature were maintained at 300°C and 320°C, respectively. The identification of n-paraffin peaks was established using a reference mixture of n-paraffin of known composition.

To determine the total content of heavy metals (copper (Cu), iron (Fe), zinc (Zn), chromium (Cr), nickel (Ni), cadmium (Cd), cobalt (Co), and lead (Pb)) and arsenic (As) in sediments, samples (0.1 g) were $HNO_3/HClO_4$ (4 : 1, v/v) digested in a microwave oven (CEM, MARS5). After digestion, the volume of each sample was adjusted to 20 mL using deionized water. Heavy metals and arsenic content was determined by inductively coupled plasma-mass spectrometry (ICP-MS, Agilent Technologies, Santa Clara, CA, USA). Standards of heavy metals and of arsenic for concentrations ranging from 0 to 1 mg/L were prepared from multielement calibration standard-2A solution (Agilent Technologies) and from sodium arsenite solution ($NaAsO_2$) (Sigma-Aldrich, St. Louis, MO, USA), respectively. For all the measures by ICP-MS an aliquot of a 2 mg/L of an internal standard solution (45Sc, 89Y, 159Tb, Agilent Technologies) was added both to samples and to a calibration curve to give a final concentration of 20 μg/L. The instrument was tuned daily with a multielement tuning solution for optimized signal-to-noise ratio.

2.3. Metagenome Extraction and 16S rRNA Amplification. Total DNA was extracted from 0.5 g of sediment using the "Power Soil" kit (MoBio Laboratories Inc., Carlsbad, CA, USA) following the manufacturer's instructions. DNA was quantified using a NanoDrop 1000 spectrophotometer (Thermo Scientific, Waltham, MA, USA). Bacterial 16S rRNA gene fragments (~550 bp) were amplified with polymerase chain reaction (PCR) using primers 907R (3′-CCGTCAATTCCTTTGAGTTT-5′) and GC-357F (3′-CCTACGGGAGGCAGCAG-5′ with a 5′-end GC-clamp) targeting a portion of the 16S rRNA gene that includes the hypervariable V3–V5 regions [22]. PCR reactions were performed as previously described [23]. Presence and length of PCR products were checked by electrophoresis in 1% w/v agarose gel prior to denaturing gradient gel electrophoresis (DGGE) analysis.

2.4. Denaturing Gradient Gel Electrophoresis. PCR products (~150 ng) were loaded in a 0.5 mm polyacrylamide gel (7% (w/v) acrylamide-bisacrylamide, 37.5 : 1) containing 43 to 56% urea-formamide denaturing gradient (100% corresponds to 7 M urea and 40% (v/v) formamide). The gels were run for 16 h at 60°C by applying a constant voltage of 90 V in 1X Tris-acetate-EDTA (TAE) buffer. After electrophoresis, the gels were stained for 30 min in 1X TAE buffer containing 1X SYBR Green (Molecular Probes, Leiden, Netherlands) according to manufacturer's instructions and rinsed twice for 10 min with distilled water. Gels images were captured using a Gel Doc 2000 apparatus (Bio-Rad, Milan, Italy). The band patterns of the DGGE gel were analysed using Image J software (available for free download at http://rsb.info.nih.gov/ij/). A Principal Coordinates Analysis (PCO) was performed using PRIMER v. 6.1 [24]. DGGE bands were excided from the gels with a sterile scalpel and eluted in 50 μL of sterile Milli-Q water at 37°C for 4 h. The eluted DNA was amplified by PCR using primers 357F and 907R and positive amplifications were sequenced by Macrogen Inc., Korea.

2.5. PCR Amplification of Functional Genes. The presence of *alkB* gene, encoding for alkane hydroxylase, in the metagenome extracted from the sediments was assessed using the primers D-alkF (5′-GCICAYGARYTIGGICAYAAR-3′) and D-alkR (5′-GCRTGRTGRTCISWRTG-3′) [25]. PCR amplification was performed in 50 μL reaction containing 1X buffer, 2 mM $MgCl_2$, 0.12 mM of dNTPs mixture, 1 μM of each primer, 5% DMSO, 1.5 U Taq polymerase, and 10 ng of template, applying the following thermic protocol: 94°C for 4′, followed by 30 cycles of 94°C for 45″, 55°C for 1′, and 72°C for 1′, and a final extension at 72°C for 10 min.

Primers nccA-F (5′-ACGCCGGACATCACGAACAAG-3′) and nccA-R (5′-CCAGCGCACCGAGACTCATCA-3′) were used as previously reported [12] to amplify the *nccA* gene that encode for nickel-cobalt-cadmium efflux pump. Primers dacr5F (5′-TGATCTGGGTCATGATCTTCCCVATGMTGVT-3′) and dacr4R (5′-CGGCCACGGCCAGYTCRAARAARTT-3′) were used for amplification of arsenite efflux pump (*ACR3(2)*) according to Achour et al. [13]. Primers Phn321F (5′-TTCTCGGTCGGG ACTTTCCAA-3′) and Phn671R (5′-GGCAACCAGATCTGTCATG-3′) were used for amplification of *phnA1* gene coding for 3,4-phenanthrene dioxygenase, according to Cavalca et al. [14].

PCR reactions were performed in a final volume of 25 μL containing 1X buffer, 1.75 mM $MgCl_2$, 0.2 mM of dNTPs mixture, 0.4 μM of each primer, 1.5 U Taq polymerase, and 10 ng of total DNA.

2.6. Bacteria Isolation and Identification. Bacteria were enriched and isolated using two different marine mineral media (artificial seawater (ASW) and ONR7a) [3, 26] supplemented with 1% crude oil (see [27] for composition details). Enrichment vials were incubated at 30°C under agitation until turbidity was observed before proceeding with isolation. Twenty-five bacterial isolates have been obtained in pure cultures from both media. DNA extraction was performed on each isolate by boiling lysis or using Thermo Scientific GeneJET Genomic DNA Purification Kit. The amplification of the bacterial 16S rRNA gene was performed using the universal primers 27F (3′-AGAGTTTGATCMTGGCTCAG-5′) and 1492R (3′-CTACGGCTACCTTGTTACGA-5′). The PCR amplification conditions and thermal protocol were set up as previously described [23] providing a PCR amplicon of approximately 1400 bp.

2.7. Nucleotide Sequence Analyses and Accession Numbers. Nucleotide sequences were edited in Chromas Lite 2.01 (http://www.technelysium.com.au) and subjected to BLAST search (http://blast.ncbi.nlm.nih.gov/Blast.cgi). The partial 16S rRNA gene sequences obtained from the bacterial isolates have been deposited in the GenBank and ENA (European Nucleotide Archive) databases and the related accession number is reported in Table 6. The sequences obtained from the excised DGGE bands are available at ENA under the accession numbers LN610485–LN610498.

2.8. Evaluation of Metabolic Traits, Biofilm, and Biosurfactant Production within the Bacteria Collection. The potential ability to produce biosurfactant has been assessed within the bacteria collection using different assays aimed at determining the surface tension reduction, hemolytic activity, and cell hydrophobicity as previously described [3].

Surface tension of cell-free ASW medium was measured after 7 days of enrichment by tensiometer (model TD 1 LAUD, Germany) using the ring method, at room temperature [28]. The results are reported in Table 7 as mean and standard deviation of three measurements. The reduction of surface tension was determined by comparing the surface tension of the noninoculated medium (65.66 ± 4 mN/m) with the cell-free medium obtained after the incubation of tested bacteria. Biofilm formation was evaluated by using 96-well microtiter plate according to published protocols [3, 29]. The inoculated plates were incubated for 48 h at 30°C. After incubation, quantitative analysis of biofilm production was performed by measuring the optical densities (OD) at 570 nm of stained adherent bacterial films using a microtiter-plate reader (Tecan Sunrise Remote, Austria). Each assay was performed in triplicate. The noninoculated medium was used as negative control to determine background OD. The average OD values were calculated for all tested strains and negative controls. All the OD measurements were normalized against the negative control for each microtiter plate separately. The isolates were considered biofilm producers if they showed an OD value of 0.12. If the OD exceeded 0.240, they were classified as strongly adherent. Strains displaying OD values greater than 0.12 but less than 0.240 were classified as weakly adherent [30, 31]. Cell hydrophobicity was determined for bacterial isolates according to previously established protocols [32, 33]. Bacterial cells were enriched in 20 mL ASW medium supplemented with crude oil (1% w/v) and incubated for 7 days in an orbital shaker at 30°C. Cells were harvested at the early log phase, washed with phosphate buffer, and resuspended to get an initial OD600 measure comprised between 0.4 and 0.6. Cell suspension (3 mL) and crude oil (150 μL) were mixed using a vortex for 120 seconds, the phases separated for 15 min, and the aqueous phase was carefully removed with a Pasteur pipette and transferred to a cuvette to measure the OD600. The decrease in the turbidity of the aqueous phase correlates with the hydrophobicity of the cells [34]. The percentage of cells bound to the hydrophobic phase (H) is calculated by the following formula $H = (1 - A/A_0) - 100\%$, where A_0 is the absorbance of the bacterial suspension without hydrophobic phase added and A is the absorbance after mixing with hydrophobic phase.

The capability of each of the bacteria to utilize different HC molecules (xylene, octane, pyrene, dibenzothiophene, phenanthrene, and naphthalene) as sole carbon source was tested in ASW agar medium with a final concentration of 25 mg/L of the different HC. Xylene, octane, and naphthalene were added in the inner side of the lids of Petri dishes and incubated upside down to allow the upwards diffusion of the HC through the medium, whereas the other HCs were spread on the medium surface. The plates were incubated at 30°C for two weeks: if colonies could be detected on the plates, the ability to grow in presence of a certain compound was considered positive [3].

2.9. Statistical Analyses. Significant differences in the bacterial community composition were analyzed by permutational analysis of variance (PERMANOVA, [35]) considering the sampling stations and the type of sediment as an orthogonal fixed factor. All the statistical tests were performed by PRIMER v. 6.1 [24], PERMANOVA+ for PRIMER routines [36]. To assess the significance correlation between environmental data with the bacterial community composition obtained by DGGE, a Mantel test was performed (R packageade4, mantel.rtest, 999 iterations [37]).

Furthermore, distance-based multivariate analysis for a linear model (DistLM [38]) was carried out to determine the significant environmental variables explaining the observed similarity among the samples. The Akaike information criterion (AIC) was used to select the significant predictor variables. The contribution of each environmental variable was assessed using a "sequential test" to evaluate the cumulative effect of the environmental variables explaining biotic similarity.

Table 1: Physical characteristics of El-Max district sediments samples.

Station	% sand	% silt	% clay	Mean size (phi)	Type of sediment	Water content %	Porosity %
P	95.18	4.82	0.00	0.11	Coarse sand	15.00	6.90
Q	85.82	8.7	5.49	0.49	Coarse sand	20.00	9.79
R	95.62	3.04	1.34	1.51	Medium sand	28.00	15.02
S	39.41	34.39	26.20	4.84	Coarse silt	35.00	20.22

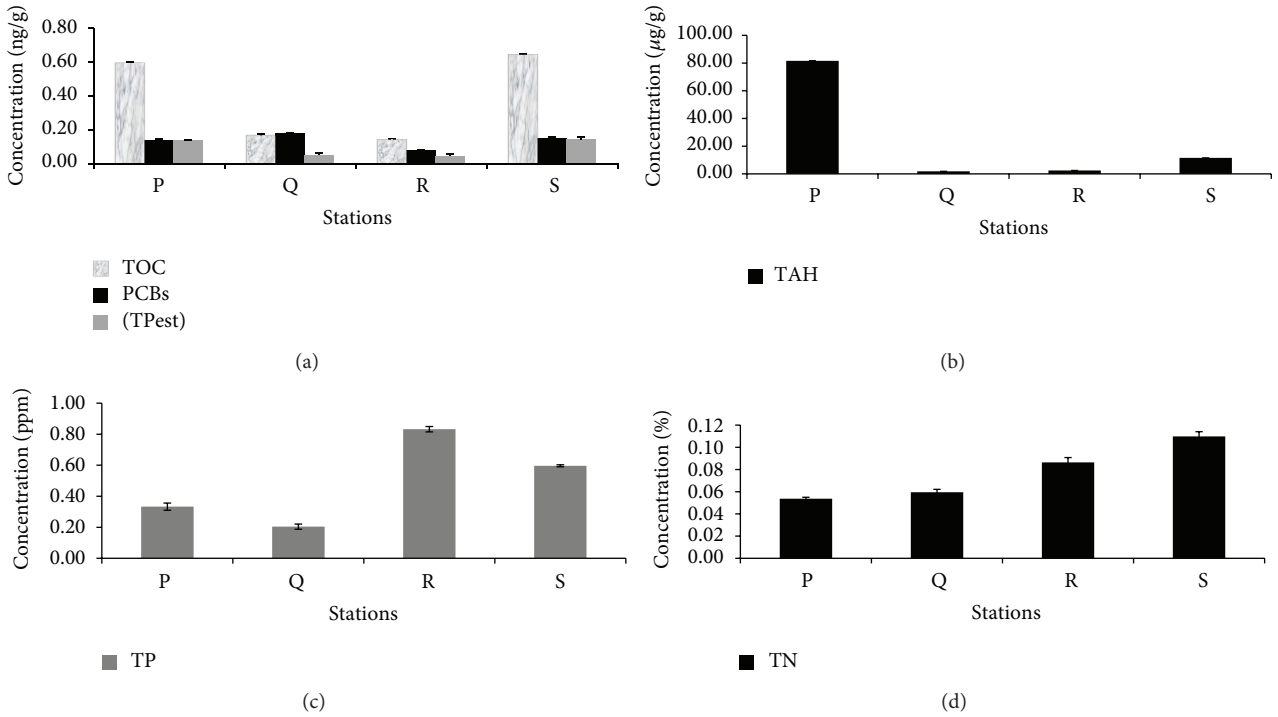

Figure 2: Chemical characterization of the sediments. Concentration in the sediment of (a) total nitrogen (TN); (b) total phosphorous (TP); (c) total organic carbon (TOC), total pesticides (TPest), and polychlorinated biphenyls (PCBs); (d) total aromatic hydrocarbons.

3. Results and Discussion

3.1. Physicochemical Analyses Indicate High Level of Pollution in El-Max District Sediments. Physical analyses showed that the sediments collected from the stations P, Q, and R are mainly composed of sand (85.82–95.62%) while the sediment of station S displayed a different composition, containing approximately the same percentage of sand (39.41%) and silt (34.39%) and a higher proportion of clay (26.20%) compared to the rest of the stations (0–5.49%) (Table 1). Grain size measurements of superficial sediment revealed that stations P and Q contained coarse sand whereas station R displayed medium size sand (Table 1). The highest water content percentage was detected in station S (35%) which contains a fine silty sediment type (Table 1). Such differences in the water content and grain size are known to influence the solubility of elements and nutrients in marine sediments, ultimately affecting the distribution of metals and other pollutants that preferentially bind to fine particles [39], determining as a consequence that the four stations analyzed constitute different environmental niches. All the stations showed total nitrogen content below 0.2% w/v (Figure 2(a)). Stations R and S showed a high content of total phosphorous with 0.83 and 0.59 ppm, respectively (Figure 2(b)). In the case of station R, which showed the highest concentration, this could be due to the close presence of the agricultural drain El-Umum. As shown in Figure 2(c), sediments of the stations P and S displayed the highest concentrations of total organic carbon (0.56 and 0.634 ng/g, resp.) and total pesticides (0.1362 and 0.1452 ng/g, resp.). Moreover, sediments P and S contained high concentrations of PCBs (Figure 2(c)), whose highest concentration was recorded in sediments of station Q (0.17 ng/g). The assessment of total polycyclic aromatic hydrocarbons (PAH) concentration in the sediment was performed by measuring the content of 16 different aromatic hydrocarbons and it indicated that station P has the highest PAH level (Figure 2(d)). Stations P and S, containing 81.6 and 11.6 μg/g of PAH, are active fishing area characterized by PAH concentration higher than the maximum indicated by the quality standards for marine water [40] and allowed by the EU (0.20 μgL^{-1}) and US (ΣPAH = 0.030 μgL^{-1}) Environmental Quality Criteria for

Table 2: Total heavy metal and arsenic content in El-Max district sediments.

	Cu (mg/kg)	Fe (g/kg)	Zn (mg/kg)	Cr (mg/kg)	Ni (mg/kg)	Cd (mg/kg)	Co (mg/kg)	Pb (mg/kg)	As (mg/kg)
P	22.63 ± 4.09	4.389 ± 0.21	45.77 ± 10.42	19.21 ± 1.27	7.83 ± 2.12	1.19 ± 1.93	1.58 ± 0.03	19.27 ± 4.87	3.31 ± 0.57
Q	65.98 ± 11.1	11.16 ± 1.69	142.97 ± 17.16	78.35 ± 10.19	15.93 ± 2.95	0.25 ± 0.14	3.71 ± 0.69	44.15 ± 0.44	4.90 ± 0.84
R	72.79 ± 1.66	11.23 ± 0.75	142.80 ± 11.16	86.6 ± .3.66	19.18 ± 0.74	0.28 ± 0.05	4.11 ± 0.31	45.57 ± 2.47	5.17 ± 0.93
S	118.15 ± 12.14	11.66 ± 0.93	247.71 ± 22.59	105.08 ± 7.69	26.37 ± 2.08	0.58 ± 0.11	4.45 ± 0.54	59.40 ± 5.01	7.06 ± 1.25

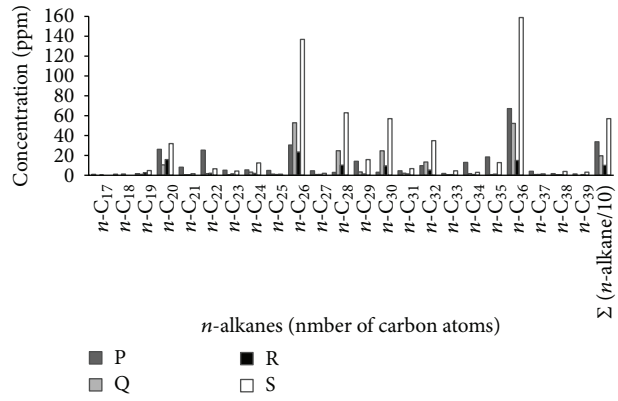

Figure 3: Concentration of n-alkanes in El-Max district sediments.

Table 3: PERMANOVA pairwise results. (a) Groups correspond to the different stations. (b) Groups correspond to the different type/granulometry of the sediment. *t*: *t* statistic; *P*: statistical significance. Significantly different groups are written in bold type.

(a)

Groups	*t*	*P*
P, Q	**2,1697**	**0,0385**
P, R	1,6055	0,1077
P, S	**3,7151**	**0,0044**
Q, R	**2,6056**	**0,0146**
Q, S	**5,9167**	**0,0009**
R, S	**5,1805**	**0,002**

(b)

Groups	*t*	*P*
Coarse sand, medium sand	1,2488	0,2166
Coarse sand, coarse silt	**4,3187**	**0,0006**
Medium sand, coarse silt	**5,1805**	**0,0021**

protection of human consumers of aquatic life [41]. GC analysis of HC compounds in the analyzed stations (Figure 3) revealed that the dominant n-alkanes were *n*-C_{20} (eicosane), *n*-C_{26} (hexacosane), *n*-C_{28} (octacosane), *n*-C_{30} (tricontane), and *n*-C_{36} (hexatriacontane). Sediment collected at station P contained the highest concentration of n-alkane of *n*-C_{22}, while the sediment of station S showed the highest concentrations of long chain n-alkanes of *n*-C_{26}, *n*-C_{28}, and *n*-C_{30}. Overall, the sediment collected at station S showed the highest total n-alkanes content (Figure 3).

Heavy metal and metalloids content in sediments was evaluated by measuring 8 different metals (Cu, Fe, Zn, Cr, Ni, Cd, Co, and Pb) and As. It is noted that station S has the highest metal and As content while station P showed the lowest content (Table 2). Unlike metal concentrations in surface water, where many countries adopted clear and unambiguous guidelines (i.e., [42, 43]), there are no accepted international or local standards of metal levels in marine sediments. Only few countries (i.e., Netherlands and Canada) have a long-standing legislative tradition developing criteria and regulations for sediment quality [44], while Egypt as the majority of the countries has not enforced any environmental protection laws or the existing legislation is not clear. Thus, the metals and arsenic levels assessed in this study were compared to the EU intervention limits imposed by the law for soil and subsoil of residential or industrial areas and to literature data. In all the sediments, metals content was below the threshold concentration of European Union Standard [45] and, in particular, Ni, Pb, and Cd were retrieved at a similar level present in rural soils of many countries [46]. In addition, arsenic content was present at a comparable level to the uncontaminated soils [47].

3.2. El-Max District Polluted Sediments Host Complex Bacterial Communities Whose Diversity Is Driven by Physicochemical Parameters. Denaturing Gradient Gel Electrophoresis (DGGE) was applied to the metagenome extracted from the sediments to provide a snapshot of the bacterial communities' structure. From each station, total sediment DNA was extracted and analyzed by DGGE. Fingerprinting performed in triplicate demonstrated the reliability of the obtained DGGE profiles (Figure 4(a)). DGGE patterns showed the occurrence of complex bacterial communities in all the analyzed sediments (Figure 4(a)) indicating that the pollution level did not affect the taxonomic diversity of bacterial communities. A positive correlation between the environmental data available for the analyzed sediments and the detected DGGE pattern was indicated by the Mantel test ($r = 0.597$; $P < 0.05$), revealing that the physical parameters, together with the measured nutrients and pollutants concentration, are the main drivers of the overall composition of the bacterial communities. The DGGE patterns of the sediments P, Q, and R appeared to be similar whereas differences could be observed with sediment S, concerning the presence of peculiar bands as well as differential abundance of some ubiquitous bands (Figure 4(a)). Principal Coordinates Analysis

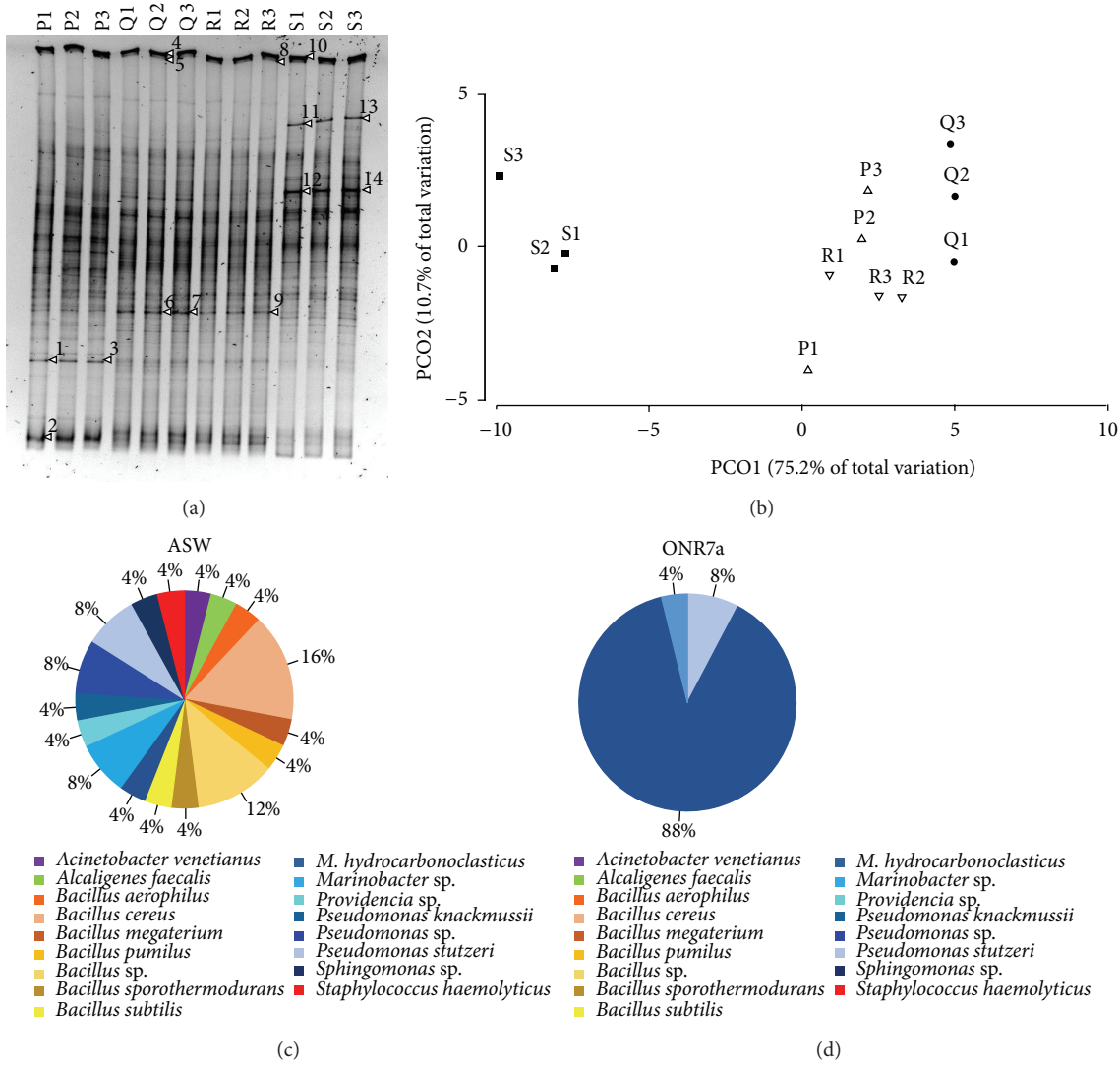

Figure 4: Cultivation dependent and independent analyses of the bacterial communities at El-Max district. (a) DGGE analysis performed of the 16S rRNA on the sediment metagenome. The numbers in the name of the samples represented the three analyzed replicates. Bands numbered have been excised from the gel and their DNA content has been sequenced (results are reported in Table 5). (b) Principal component analysis based on the DGGE profiles of the 16S rRNA gene in the sediments. (c) Identification and relative abundance of the bacteria isolated on ONR7a medium. (d) Identification and relative abundance of the bacteria isolated on ASW medium.

(PCO) of the DGGE fingerprints confirmed the observed differences showing a sharp clustering of sediments S1-2-3 separately from the other sediments (Figure 4(b)). Based on PCO1 (explaining 75.2% of the total variation) the bacterial community of the samples collected at station Q were also different from the sediments P and R (Figure 4(b)). Statistical analysis supported the PCO indications, confirming that both the bacterial community dwelling sediments S and Q were significantly different from those collected at stations P and R (see Table 3(a) for pairwise comparison). Moreover, PERMANOVA showed that the structure of sediments' bacterial community was influenced by the type of sediment (PERMANOVA, df = 2, $F = 12.7$, $P = 0.0001$), distinguishing sandy (P, Q, and R) and silty (S) sediments as statistically different (see Table 3(b) for pairwise comparison).

Physical and chemical parameters measured at the investigated stations were analyzed to assess their influence on the structure of the bacterial communities (Table 4). The sequential test showed that sand and clay percentage in the sediments are the statistically significant physical parameters involved in shaping the bacterial communities (Table 4(a)). Furthermore, DistLM analysis was performed on chemical data considering separately the metal concentration and the other available chemical parameters. The sequential tests showed that, among metals, Cu, Fe, and Zn concentration are the drivers of the bacterial community structure in the sediments (Table 4(b)) and that total organic carbon (TOC) and PCBs concentration were the other statistically significant parameters involved in the selection and assemblage of bacterial populations (Table 4(c)). Our data are in agreement

Table 4: (a) Sequential test (DistLM) explaining the total variation with the contribution of all the predictor variables accounted separately according to their division in (a) physical data, (b) metal/metalloid concentration, and (c) nutrients/pollutants concentration. F = statistic; P = probability; Prop. = proportion of total variation explained; Cumul. = cumulative explained by the listed variables; Res.df = residual degrees of freedom. Statistically significant variables are written in bold type.

(a)

	Sequential tests					
Variable	AIC	F	P	Prop.	Cumul.	Res.df
+% sand	**35,267**	**16,445**	**0,0036**	**0,62186**	**0,62186**	**10**
+% silt	**34,458**	**2,3747**	**0,0738**	**0,078943**	**0,70081**	**9**
+% clay	**28,526**	**7,493**	**0,0008**	**0,1447**	**0,84551**	**8**
Mean size	28,526	No test		−1,60E− 14	0,84551	8
Water content	28,526	No test		−1,59E− 16	0,84551	8
Porosity	28,526	No test		1,14E− 15	0,84551	8

(b)

	Sequential tests					
Variable	AIC	F	P	Prop.	Cumul.	Res.df
Cu	**40,706**	**6,8084**	**0,0092**	**0,40506**	**0,40506**	**10**
Fe	**30**	**16,947**	**0,0009**	**0,38858**	**0,79364**	**9**
Zn	**28,526**	**2,686**	**0,055**	**0,051871**	**0,84551**	**8**
Cr	28,526	No test		−4,67E− 16	0,84551	8
Ni	28,526	No test		−6,42E− 16	0,84551	8
Cd	28,526	No test		7,80E− 16	0,84551	8
Co	28,526	No test		−2,21E− 16	0,84551	8
Pb	28,526	No test		5,79E− 16	0,84551	8
As	28,526	No test		7,27E− 16	0,84551	8

(c)

	Sequential tests					
Variable	AIC	F	P	Prop.	Cumul.	Res.df
TAH	46,138	0,68916	0,506	6,45E − 02	6,45E− 02	10
TOC	**31,775**	**26,19**	**0,0006**	**0,69626**	**0,76073**	**9**
PCHs	**28,526**	**4,3898**	**0,0099**	**8,48E − 02**	**0,84551**	**8**
Tpest	28,526	No test		3,40E − 16	0,84551	8
TN	28,526	No test		−9,57E − 16	0,84551	8
TP	28,526	No test		8,47E − 16	0,84551	8

with a recent study, which indicated both sediment particle size and the concentration of metals, including Fe and Zn, as pivotal factors in shaping the sediment's bacterial community [48].

Aiming to identify the dominant taxa associated with the PCR-DGGE profiles several DGGE bands were excised from the gel. The successful sequencing of partial 16S rRNA could be obtained only for 14 bands (Figure 4(a)), pointing out the presence of bacteria typical of marine ecosystems and characterized by low identity percentage with any known sequence in the public databases (Table 5). According to DGGE band sequencing, the main phylum associated with El-Max district sediment was represented by Bacteroidetes, while Actinobacteria, Acidobacteria, and Spirochaetes were retrieved in lower abundance (Table 5). The phylum Bacteroidetes was previously indicated among the main actors involved in PAH degradation in river sediment based on DGGE analyses [49] and could possibly play a role in marine sediments. The phyla Actinobacteria, Acidobacteria, and Bacteroidetes were also detected by high-throughput sequencing in estuarine sediments [48] while Spirochaetes were identified within the metabolically active bacterial communities in microcosms established using chronically polluted estuarine sediments [50].

The presence of putative HC-oxidizers in El-Max district sediments was, moreover, demonstrated by the amplification of the *alkB* gene, codifying the alkane monooxygenase enzyme, from all the sediment metagenomes (data not shown).

3.3. Phylogenetically Different Hydrocarbonoclastic Bacterial Isolates Were Obtained Using Different Cultivation Media. Besides molecular analysis, a cultivation approach was applied to obtain and characterize bacterial isolates according to the biotechnological potential for bioremediation applications. Twenty-five bacteria were isolated from the four

Table 5: Phylogenetic identification of bacteria from sequenced DGGE bands (see Figure 4 for band correspondence). The column "Environment" reports the habitat in which the "Closest relative" sequence present in NCBI database was detected.

Band	Sample	Closest relative (Acc. No.)	Identity (%)	Phylum	Environment
1	P1	Unc. Bacterium (FR851749)	99	Actinobacteria	Coral reef sands
2	P1	Unc. Acidobacteria (JF344347)	97	Acidobacteria	Oil-polluted sediments
3	P3	Unc. Bacterium (FR851749)	99	Actinobacteria	Coral reef sands
4	Q2	Unc. Bacterium (JN453366)	95	Bacteroidetes	Hypersaline microbial mat
5	Q2	Unc. Bacterium (JN470103)	96	Bacteroidetes	Hypersaline microbial mat
6	Q2	Unc. Bacterium (JN530286)	98	Spirochaetes	Hypersaline microbial mat
7	Q3	Unc. Bacterium (JN530286)	97	Spirochaetes	Hypersaline microbial mat
8	R3	Unc. Bacterium (KC574864)	95	Bacteroidetes	—
9	R3	Unc. Bacterium (KC574864)	94	Bacteroidetes	Hypersaline microbial mat
10	S1	Unc. Bacterium (JN529047)	93	Bacteroidetes	Hypersaline microbial mat
11	S1	Unc. Bacteroidetes (AF507860)	97	Bacteroidetes	Meromictic soda lake
12	S1	Unc. Bacterium (KF268891)	99	Bacteroidetes	Marine sediment
13	S3	Unc. Bacteroidetes (AF507860)	97	Bacteroidetes	Meromictic soda lake
14	S3	Unc. Bacterium (KF268891)	99	Bacteroidetes	Marine sediment

stations on ASW medium supplemented with crude oil as the sole carbon source. This collection included Bacilli (13), Betaproteobacteria (1), and Gammaproteobacteria (11) divided into several families and genera (Table 6), with a high Shannon-Weaver index (2.69), calculated from the number of individuals per genus. The collection included bacterial genera widely studied for their ability to degrade oil hydrocarbons, such as *Acinetobacter venetianus* [51], *Pseudomonas stutzeri* [52], and *Marinobacter hydrocarbonoclasticus* [53] (Table 6, Figure 4(c)). Bacteria belonging to the genera *Acinetobacter, Pseudomonas,* and *Marinobacter* were isolated from a variety of oil contaminated sites around the world. Such environments included coastal oil-polluted site in Tunisia [54], intertidal sand affected by oil pollution after the Prestige spill [55], the Gulf of Mexico beach sand [56], and deep hypersaline anoxic basins [57]. Kostka and coauthors [56] recently proposed that Gram-positive bacteria like those of the genus *Bacillus*, representing the 48% of the bacteria we isolated on ASW medium, could be used as sentinel for the later stages of oil degradation, when PAH dominate the composition of the residual oil. Accordingly, other authors [58–60] previously reported the presence of hydrocarbon-degrading *Bacillus* strains from marine sediments and seawater. The fraction of El-Max sediment bacteria cultivable on ASW medium included representatives of the genera *Alcaligenes*, *Sphingomonas,* and *Providencia* (Table 6, Figure 4(d)), the latter showing high potential for the bioremediation of heavy metals [61, 62], which are abundantly present in the samples analyzed in this study. Marine bacteria able to resist high mercury concentrations and able to detoxify cadmium and lead were described also within the species *Bacillus pumilus* and *Alcaligenes faecalis* [63], present in our collection (Table 6). *A. faecalis* can perform phenanthrene degradation [64] and was also previously detected by DGGE analysis in weathered fuel enrichment established after the Prestige oil spill [65]. The ability of *Sphingomonas* spp. isolates to degrade a wide range of xenobiotics has been reported and their remediating capability has been assigned to a large plasmid harboring the genes codifying degrading enzymes [64].

Sediment from station S, which hosts a peculiar bacterial community according to the DGGE analysis, was used to perform second enrichment on ONR7a medium, adding crude oil as the sole carbon source. A second collection of twenty-five bacteria was obtained from the ONR7a enrichment, leading to the selection of three different species, thus showing a lower diversity compared to the ASW collection (Shannon-Weaver index: 0.44). All the bacteria isolated on ONR7a medium belonged to the known hydrocarbon-degrading species *Pseudomonas stutzeri* (2), *Marinobacter adhaerens* (1), and *Marinobacter hydrocarbonoclasticus* (22) (Table 6). It is worthy to note how much our perception of the cultivable fraction of oil-degrading bacteria in a certain environment can vary simply changing the medium applied for cultivation purposes. In fact, ONR7a medium exclusively selected Gammaproteobacteria from El-Max district polluted sediments, mainly represented by the well-known metabolic versatile *Marinobacter hydrocarbonoclasticus*. The cultivation approach based on the use of two different media provided a wider perspective on the cultivable fraction of the bacterial community present in the investigated sediments. Such strategy permitted identifying both (i) specialist and versatile bacterial species involved in the first stages of the degradation of aliphatic and aromatic hydrocarbons (i.e., Gammaproteobacteria) and (ii) bacterial species previously indicated as key players in the successional stages of the degradation process (i.e., *Bacillus*).

3.4. Hydrocarbonoclastic Bacteria of El-Max District Possessed Bioremediation Potential Traits. We screened the bacterial collection for the ability to grow on single hydrocarbon molecules as sole carbon source, showing that a variable percentage of the isolates were able to grow on the different tested HC (Table 7). A lower percentage of the strains were able to grow using pyrene (7%) and phenanthrene (8%) and

Table 6: List of the bacterial strains isolated from the polluted sediments of El-Max district (Egypt) and their phylogenetic affiliation. The codes of the strains isolated from station R are indicated in italics since their identification was previously reported by the same authors [11].

Strain code	Medium	Acc. No.	Class	Family	Closest described relative	Identity (%)
SCP2	ASW	KC573500	Bacilli	Bacillaceae	*Bacillus sporothermodurans*	96
SCuQ1	ASW	KC573503			*Bacillus megaterium*	99
SCR2[a]	ASW	KC573523			*Bacillus megaterium*	98
SCuR2[a]	ASW	KC573507			*Bacillus cereus*	98
SCR3[a]	ASW	KC573505			*Bacillus cereus*	99
SC∗R3[a]	ASW	KF217252			*Bacillus cereus*	99
SCuR5[a]	ASW	KF217249			*Bacillus* sp.	99
SC∗S1	ASW	KF217253			*Bacillus pumilus*	99
SCS2	ASW	KC573509			*Bacillus cereus*	99
SCS3	ASW	KC573510			*Bacillus subtilis*	99
SCS4	ASW	KF217259			*Bacillus* sp.	99
SC∗S6	ASW	KF217254			*Bacillus aerophilus*	99
SCP1	ASW	KC573499		Staphylococcaceae	*Staphylococcus haemolyticus*	99
SC∗CuP1	ASW	KC573501	Gammaproteobacteria	Pseudomonadaceae	*Pseudomonas xanthomarina*	98
SCuQ2	ASW	KC573504		Pseudomonadaceae	*Pseudomonas stutzeri*	99
SCuR3[a]	ASW	KC573508		Pseudomonadaceae	*Pseudomonas knackmussii*	98
SCuR4[a]	ASW	KC573524		Pseudomonadaceae	*Pseudomonas stutzeri*	99
SCS1	ASW	KC573525		Pseudomonadaceae	*Pseudomonas stutzeri*	100
SC∗Q2	ASW	KC573520		Moraxellaceae	*Acinetobacter venetianus*	99
SCR1[a]	ASW	KC573522		Alteromonadaceae	*Marinobacter hydrocarbonoclasticus*	99
SC∗Q3	ASW	KC573502			*Marinobacter hydrocarbonoclasticus*	98
SCS6	ASW	KC573526			*Marinobacter hydrocarbonoclasticus*	99
SC∗R2[a]	ASW	KF217251		Enterobacteriaceae	*Providencia vermicola*	99
SCuR1[a]	ASW	KC573506		Sphingomonadaceae	*Sphingomonas* sp.	95
SCP3	ASW	KF217258	Betaproteobacteria	Alcaligenaceae	*Alcaligenes faecalis*	99
S1_1	ONR7a	LN610460	Gammaproteobacteria	Pseudomonadaceae	*Pseudomonas stutzeri*	99
S1_24	ONR7a	LN610475			*Pseudomonas stutzeri*	99
S1_4	ONR7a	LN610461		Alteromonadaceae	*Marinobacter hydrocarbonoclasticus*	99
S1_5	ONR7a	LN610462			*Marinobacter hydrocarbonoclasticus*	100
S1_7	ONR7a	LN610463			*Marinobacter hydrocarbonoclasticus*	99
S1_9	ONR7a	LN610464			*Marinobacter hydrocarbonoclasticus*	99
S1_10	ONR7a	LN610465			*Marinobacter hydrocarbonoclasticus*	99
S1_11	ONR7a	LN610466			*Marinobacter hydrocarbonoclasticus*	99
S1_12	ONR7a	LN610467			*Marinobacter hydrocarbonoclasticus*	99
S1_13	ONR7a	LN610468			*Marinobacter hydrocarbonoclasticus*	100
S1_16	ONR7a	LN610469			*Marinobacter hydrocarbonoclasticus*	99
S1_17	ONR7a	LN610470			*Marinobacter hydrocarbonoclasticus*	100

Table 6: Continued.

Strain code	Medium	Acc. No.	Class	Family	Closest described relative	Identity (%)
S1_20	ONR7a	LN61047			*Marinobacter hydrocarbonoclasticus*	100
S1_21	ONR7a	LN610472			*Marinobacter hydrocarbonoclasticus*	100
S1_22	ONR7a	LN610473			*Marinobacter hydrocarbonoclasticus*	99
S1_23	ONR7a	LN610474			*Marinobacter hydrocarbonoclasticus*	99
S1_26	ONR7a	LN610476			*Marinobacter hydrocarbonoclasticus*	99
S1_28	ONR7a	LN610477			*Marinobacter hydrocarbonoclasticus*	99
S1_29	ONR7a	LN610478			*Marinobacter hydrocarbonoclasticus*	99
S1_30	ONR7a	LN610479			*Marinobacter hydrocarbonoclasticus*	99
S1_31	ONR7a	LN610480			*Marinobacter hydrocarbonoclasticus*	99
S1_32	ONR7a	LN610481			*Marinobacter adhaerens*	100
S1_33	ONR7a	LN610482			*Marinobacter hydrocarbonoclasticus*	99
S1_34	ONR7a	LN610483			*Marinobacter hydrocarbonoclasticus*	99
S1_36	ONR7a	LN610484			*Marinobacter hydrocarbonoclasticus*	99

Acc. No.: accession number of the 16S rRNA sequences amplified from the isolated strains and deposited in GenBank.

naphthalene (9.5%). A higher portion of the collection could grow using dibenzothiophene (DBT, 11%), octane (15.5%), and xylene (36%). Both the collections obtained on ASW and ONR7a media included similar amounts of strains able to use all the tested hydrocarbons, with the exception of DBT and octane degrading bacteria that were mainly isolated on ASW and ONR7a medium, respectively. The ability to grow using all the supplied HC molecules in minimal medium was recorded exclusively in few strains belonging to the species *Marinobacter hydrocarbonoclasticus* (Table 7), confirming the adaptable metabolisms of this species often isolated in marine contaminated environments. The low number of bacteria capable of utilizing all the tested substrates corroborates the reports of several studies that indicate the need of microbial consortia to degrade complex mixtures of hydrocarbons, such as crude oil, in soil [66], fresh water [67], and marine environments [4].

To widen the characterization of the HC-degrading bacteria isolated from El-Max district we performed PCR assays looking for functional genes codifying the 3,4-phenanthrene dioxygenase enzyme (*phnA*) and genes related to metal and metalloid detoxification systems, like the efflux pumps for arsenite (*ACR3(2)*) and for different heavy metals (*nccA*). Despite the fact that the sediments were not highly contaminated by metals and arsenic, isolates possessing arsenic and metals resistance genes were retrieved, confirming that bacteria capable of detoxification mechanism are widespread and their presence is not strictly related to metal and arsenic level [13, 68]. *ACR3(2)*, *nccA,* and *phnA* genes were successfully amplified in 14, 10, and 4 bacterial strains isolated on ONR7a medium, respectively. On the contrary, the amplification of these genes was unsuccessful for all the bacteria isolated on ASW medium, with the exception of the strain *Alcaligenes faecalis* SCP3, which resulted positive for *nccA* gene amplification and belongs to species previously described as Cd and Pb detoxifying [63]. Overall, apart from strain *A. faecalis* SCP3, all the bacteria positive for *ACR3(2)*, *nccA,* and *phnA* genes amplification belong to the species *M. hydrocarbonoclasticus*. Only one out of the 4 strains harboring the *phnA* gene was able to grow on phenanthrene as the sole carbon source in the tested conditions. On the other hand, those that could grow on this HC failed to give positive amplification, probably due to mismatches between the tested primers and gene sequence [69].

The biotechnological potential of the strains inhabiting oil-polluted ecosystems does not rely exclusively on their ability to degrade a certain HC mixture but it includes additional features. Different microorganisms were shown to possess multiple adaptations to facilitate oil degradation procedures, such as the synthesis of biosurfactants or emulsifiers and biofilm formation [70, 71], processes that enhance the bacterial adhesion to hydrocarbons, increasing their solubility and thus promoting their degradation [72, 73]. Biosurfactants, in particular, reduce the surface tension at the interface of immiscible fluids, increasing the surface area of insoluble compounds like oil and water, which leads

Table 7: Screening of the bioremediation potential in the bacteria collection established from the sediment of El-Max district.

Isolate	Biofilm	b.h.	ST ($mN\,m^{-1}$)	Hydro (%)	Growth on different hydrocarbons							PCR amplification of gene markers		
					Xyl	Oct	Pyr	DBT	Phe	Naph	Oil	*nccA*[(a)]	*ACR3(2)*[(b)]	*phnA*[(c)]
S1-1	0.023 ± 0.0071	−	39.33 ± 3.05	38 ± 2.466	+	+	+	−	+	+	+	−	+	−
S1-4	0.164 ± 0.0789	−	45.63 ± 0.55	n.d.	+	+	+	+	+	+	+	−	+	−
S1-5	0.024 ± 0.0081	−	10.42 ± 1.64	5.9 ± 1.322	−	+	−	−	−	−	+	−	−	+
S1-7	0.014 ± 0.0123	+	20.33 ± 1.52	5.1 ± 1.607	−	+	−	+	−	−	+	−	+	−
S1-9	0.0125 ± 0.0071	+	32.33 ± 1.52	20.3 ± 2.020	+	+	−	−	−	−	+	+	+	−
S1-10	0.0112 ± 0.0035	−	28.66 ± 1.52	46.2 ± 0.954	−	−	−	−	−	−	+	+	+	−
S1-11	0.041 ± 0.0111	+	18.66 ± 0.57	10.4 ± 1.527	−	+	−	−	−	−	+	+	+	−
S1-12	0.014 ± 0.0472	−	15.83 ± 0.76	40.8 ± 0.831	−	+	−	+	−	−	+	−	+	+
S1-13	0.024 ± 0.0081	+	12.96 ± 0.55	n.d.	−	+	−	−	−	+	+	−	+	−
S1-16	0.035 ± 0.0135	−	28.66 ± 0.57	21.98 ± 1.527	−	+	−	−	−	−	+	+/−	−	+
S1-17	0.013 ± 0.0086	+	29.3 ± 1.57	9.3 ± 0.5	−	+	−	+	−	−	+	+/−	+	−
S1-20	0.0145 ± 0.0092	−	25.23 ± 1.05	n.d.	+	+	+	+	+	+	+	−	−	−
S1-21	0.418 ± 0.0920	−	28.36 ± 1.28	10.4 ± 1.261	+	+	+	+	+	+	+	−	−	−
S1-22	0.0297 ± 0.0113	−	20.33 ± 0.57	n.d.	+	+	−	−	−	−	+	−	−	−
S1-23	0.009 ± 0.0054	+	27.23 ± 0.68	7.5 ± 0.550	+	+	−	−	−	−	+	−	−	−
S1-24	0.0126 ± 0.0034	−	23.66 ± 1.52	n.d.	+	+	+	+	+	+	+	+/−	−	−
S1-26	0.0525 ± 0.0147	+	29.1 ± 0.85	13.3 ± 0.941	+	+	+	−	−	+	+	−	+	−
S1-28	0.013 ± 0.0081	−	40.5 ± 1.32	16.3 ± 0.774	−	+	−	−	−	−	+	−	+	−
S1-29	0.004 ± 0.0021	+	20.63 ± 3.05	14.2 ± 1.286	−	+	−	−	+	+	+	−	−	+
S1-30	0.012 ± 0.0046	+	47.26 ± 0.57	21.3 ± 1.382	+	+	−	−	−	−	+	−	+	−
S1-31	0.012 ± 0.0058	−	20.36 ± 1.15	13.8 ± 0.694	−	+	−	−	−	−	+	−	−	−
S1-32	0.0183 ± 0.0078	−	40.26 ± 1.44	15.8 ± 0.390	+	+	−	−	−	−	+	+	−	−
S1-33	0.004 ± 0.0015	−	40.83 ± 0.76	34.7 ± 0.375	−	−	−	−	−	−	+	+/−	+	−
S1-34	0.0134 ± 0.007	−	15.16 ± 1.75	22.2 ± 2.450	−	+	−	−	−	−	+	−	+	−
S1-36	0.024 ± 0.0081	+	20.63 ± 3.05	n.d.	+	+	−	−	−	−	+	+	−	−
SCP1	0.011 ± 0.0075	−	47.16 ± 1.52	n.d.	−	−	−	−	−	−	−	−	−	−
SCP2	0.028 ± 0.0053	+	51.25 ± 0.77	11.3 ± 1.734	−	−	+	+	+	+	+	−	−	−
SCP3	0.417 ± 0.0156	−	48.30 ± 1.34	31.6 ± 1.443	+	+	−	+	+	+	−	+	−	−
SCR1[a]	0.046 ± 0.0122	+	53.50 ± 1.25	77.3 ± 2.508	n.d.	−	−	−	−	−	+	−	−	−
SCR2[a]	0.040 ± 0.0083	+	46.67 ± 0.84	26.8 ± 1.527	−	−	−	−	+	−	−	−	−	−
SCR3[a]	0.030 ± 0.0083	−	57.64 ± 0.50	23.5 ± 1.702	−	−	+	−	+	+	−	−	−	−
SCS1	0.037 ± 0.0132	−	52.52 ± 0.77	10.2 ± 1.297	−	−	−	−	−	+	−	−	−	−
SCS2	0.037 ± 0.0132	−	22.90 ± 1.48	23.6 ± 1.950	+	−	+	+	+	+	−	−	−	−
SCS3	0.065 ± 0.0140	+	41.56 ± 1.05	n.d.	+	+	−	+	−	−	++	−	−	−
SCS4	0.075 ± 0.0018	+	46.20 ± 1.00	2.7 ± 1.322	−	−	+	+	−	−	−	−	−	−
SCS6	0.032 ± 0.0016	−	44.35 ± 0.70	n.d.	−	+	+	+	n.d.	n.d.	+	−	−	−
SCuP1	0.022 ± 0.0106	+	50.95 ± 1.52	46.4 ± 2.466	−	−	−	+	+	+	+	−	−	−
SCuQ1	0.081 ± 0.0240	−	52.30 ± 1.07	0.96 ± 0.076	−	−	−		+	−	+	−	−	−
SCuQ2	0.007 ± 0.0097	−	59.82 ± 0.53	28.8 ± 1.258	−	−	−	−	−	−	−	−	−	−
SCuR1[a]	0.049 ± 0.0131	−	59.70 ± 1.36	7.1 ± 1.294	+	+	−	+	+	+	−	−	−	−
SCuR2[a]	0.003 ± 0.0081	−	50.09 ± 1.51	6.7 ± 0.475	−	−	−	−	−	−	−	−	−	−

Table 7: Continued.

Isolate	Biofilm	b.h.	ST (mN m^{-1})	Hydro (%)	Growth on different hydrocarbons							PCR amplification of gene markers		
					Xyl	Oct	Pyr	DBT	Phe	Naph	Oil	*nccA*[(a)]	*ACR3(2)*[(b)]	*phnA*[(c)]
SCuR3[a]	0.086 ± 0.0116	+	59.40 ± 0.72	8.7 ± 1.189	−	+	+	+	+	+	−	−	−	−
SCuR4[a]	0.051 ± 0.0116	+	35.87 ± 0.93	29.1 ± 1.322	+	+	+	+	−	−	+	−	−	−
SCuR5[a]	0.022 ± 0.0097	+	38.30 ± 1.07	22.7 ± 1.875	−	+	+	+	−	+	++	−	−	−
SC∗Q2	0.032 ± 0.0142	+	47.84 ± 1.11	9 ± 0.304	−	−	−	+	−	+	−	−	−	−
SC∗Q3	0.026 ± 0.005	−	48.71 ± 2.23	3 ± 0.132	n.d.	−	−	+	−	−	−	−	−	−
SC∗R2[a]	0.177 ± 0.0512	−	55.60 ± 1.92	6.6 ± 0.25	+	+	−	+	+	+	−	−	−	−
SC∗R3[a]	0.366 ± 0.0361	+	42.6 ± 0.808	n.d.	n.d.	n.d.	−	+	−	−	n.d.	−	−	−
SC∗S1	0.067 ± 0.0272	−	16.88 ± 0.76	36.6 ± 2.432	−	−	−	−	+	+	++	−	−	−
SC∗S6	0.012 ± 0.0083	−	51.25 ± 1.86	18.3 ± 0.125	−	−	−	−	−	−	−	−	−	−

+: growth; −: no growth; n.d.: not detected.

Xyl: xylene; Oct: octane; Pyr: pyrene; DBT: dibenzothiophene; Phe: phenanthrene; Naph: naphthalene; oil: crude oil.

ST: surface tension; Hydro: hydrophobicity ratio (%); b.h.: blood haemolysis; biofilm: biofilm formation.

[(a)]Ni, Co, and Cd efflux pump, amplified with primer nccA [12]; [(b)]arsenite efflux pump [13]; [(c)]3,4-phenanthrene dioxygenase large subunit amplified with primer Phn321F/P671R [14].

to increased bioavailability and subsequent biodegradation of the hydrocarbons [4, 74, 75]. In this study, we applied several methods to assess the ability of the isolated bacteria to produce biosurfactant molecules. One of the simplest methods used for screening the production of some types of biosurfactants is the blood haemolysis method [11]. In our study, 20 isolates (40% of the collection) showed haemolytic activity on blood agar media (Table 7). They belong to the *Marinobacter* (11), *Bacillus* (5), *Pseudomonas* (3), and *Acinetobacter* (1) genera. The reduction of the surface tension (ST) of the medium, resulting from the emulsification of crude oil by the surfactants produced by microorganism, represents an alternative method for testing the biosurfactant production [76]. All the isolates in our collections were able to reduce surface tension when compared to the noninoculated medium surface tension (65.66 ± 4 mN/m) (Table 7); in particular those isolated on the ONR7a medium (average value within the collection: 27.4 ± 10.2), namely, *M. hydrocarbonoclasticus*, demonstrated higher ST reduction compared to those belonging to the ASW collection (average value within the collection: 47.25 ± 10.36). Furthermore, bacterial adhesion to hydrocarbons (BATH) test was applied to measure the cell surface hydrophobicity, a property related to the structure and composition of cell surface [77]. The uptake mechanism of hydrophobic substrate occurs by the direct contact between the hydrocarbon and cell surface and can be thus dependent on its hydrophobicity [28, 77, 78]. The highest hydrophobicity (77.3%) was recorded for the strain *M. hydrocarbonoclasticus* SCS6 (Table 7).

Hydrocarbonoclastic bacteria have been detected in both monospecies and multispecies biofilms developing on hydrocarbons [79]. Hence, the ability to produce biofilm was also investigated (Table 7) allowing the identification of 5 strains, representing 10% of the collection, as biofilm producers. Such strains belong to the *M. hydrocarbonoclasticus, A. faecalis, B. cereus,* and *P. vermicola* species. According to the literature [30, 31] two strains were classified as weakly adherent, while two resulted in being strongly adherent (Table 7), the latter including the *M. hydrocarbonoclasticus* strain S1-21. A proteomic study realized on *M. hydrocarbonoclasticus* previously showed a differential protein expression for biofilm attached and detached cells, displaying the ability of recently detached cells to reinitiate the formation of a new biofilm at the hexadecane-water interface [79], a trait that might confer competitive advantage for hydrocarbon uptakes in the environment. The two *M. hydrocarbonoclasticus* isolates (S1-4 and S1-21) positive for biofilm formation were also able to grow using the entire set of hydrocarbons tested in this study, further demonstrating the high potential of this species for marine oil remediation.

4. Conclusions

Thisstudy represents the first holistic microbiological investigation of biodiversity occurring at El-Max district sediments taking advantage of both molecular and cultivation techniques. The adopted molecular approach, coupled with statistical analyses, clarified that a significant correlation exists between biotic and abiotic data in the polluted ecosystems, allowing identifying (i) sand and clay composition, (ii) TOC and PCBs, and (iii) the concentration of different heavy metals (Cu, Fe, and Zn) as the driving forces shaping the structure of the bacterial microbiome. The establishment of a bacterial collection exploiting different growth media permitted isolating species described for their pivotal role in the different successional stages of oil hydrocarbons' biodegradation, such as the highly abundant classes Gammaproteobacteria and Bacilli. Most of the isolates, belonging to different genera, showed one or more metabolic traits of interest for bioremediation purposes (e.g., the capability to grow on single hydrocarbon molecules, presence of genes involved in detoxification systems, and traits related to the production of biosurfactants). Our investigation contributed to filling the gap of knowledge on the microbial diversity of Southern Mediterranean Sea sites, shedding light on the potential of the contaminated sediments of El-Max district as a reservoir of microbial resources selected (and adapted) by the peculiar environmental conditions of the site and possibly exploitable for future *in situ* intervention to combat pollution.

Disclosure

Professor Yasser R. Abdel-Fattah is the Secretary of Supreme Council for Research Centers and Institutes, Ministry of Scientific Research, Cairo, Egypt.

Conflict of Interests

The authors declare that there is no conflict of interests regarding the publication of this paper.

Authors' Contribution

Ranya A. Amer and Francesca Mapelli contributed equally to this work.

Acknowledgments

This work was funded by FP-7 projects ULIXES (no. 266473, "Unravelling and Exploiting Mediterranean Sea Microbial Diversity and Ecology for Xenobiotics' and Pollutants' Clean Up") and KILLSPILL (no. 312139, "Integrated Biotechnological Solutions for Combating Marine Oil Spills") and the support of King Abdullah University of Science and Technology (baseline research funds to Daniele Daffonchio). Francesca Mapelli was supported by Università degli Studi di Milano, DeFENS, European Social Fund (FSE), and Regione Lombardia (contract "Dote Ricerca"). Anna Corsini was supported by MIUR-PRIN2010 Project 2010JBNLJ7.

References

[1] D. Daffonchio, F. Mapelli, A. Cherif et al., "ULIXES, unravelling and exploiting Mediterranean Sea microbial diversity and ecology for xenobiotics' and pollutants' clean up," *Reviews in Environmental Science and Biotechnology*, vol. 11, no. 3, pp. 207–211, 2012.

[2] D. Daffonchio, M. Ferrer, F. Mapelli et al., "Bioremediation of Southern Mediterranean oil polluted sites comes of age," *New Biotechnology*, vol. 30, no. 6, pp. 743–748, 2013.

[3] R. A. Amer and Y. R. Abdel Fattah, "Hydrocarbonoclastic marine bacteria in Mediterranean Sea, El-Max, Egypt: isolation, identification and site characterization," *Jökull Journal*, vol. 64, no. 4, pp. 223–243, 2014.

[4] I. M. Head, D. M. Jones, and W. F. M. Röling, "Marine microorganisms make a meal of oil," *Nature Reviews. Microbiology*, vol. 4, no. 3, pp. 173–182, 2006.

[5] R. M. M. Abed, J. Al-Sabahi, F. Al-Maqrashi, A. Al-Habsi, and M. Al-Hinai, "Characterization of hydrocarbon-degrading bacteria isolated from oil-contaminated sediments in the Sultanate of Oman and evaluation of bioaugmentation and biostimulation approaches in microcosm experiments," *International Biodeterioration and Biodegradation*, vol. 89, pp. 58–66, 2014.

[6] M.-E. Guazzaroni, F.-A. Herbst, I. Lores et al., "Metaproteogenomic insights beyond bacterial response to naphthalene exposure and bio-stimulation," *The ISME Journal*, vol. 7, no. 1, pp. 122–136, 2013.

[7] B. A. McKew, F. Coulon, M. M. Yakimov et al., "Efficacy of intervention strategies for bioremediation of crude oil in marine systems and effects on indigenous hydrocarbonoclastic bacteria," *Environmental Microbiology*, vol. 9, no. 6, pp. 1562–1571, 2007.

[8] M. Nikolopoulou, N. Pasadakis, and N. Kalogerakis, "Evaluation of autochthonous bioaugmentation and biostimulation during microcosm-simulated oil spills," *Marine Pollution Bulletin*, vol. 72, no. 1, pp. 165–173, 2013.

[9] A. M. Samir and A. B. El-Din, "Benthic foraminiferal assemblages and morphological abnormalities as pollution proxies in two Egyptian bays," *Marine Micropaleontology*, vol. 41, no. 3-4, pp. 193–227, 2001.

[10] M. A. Okbah, A. M. A. Ibrahim, and M. N. M. Gamal, "Environmental monitoring of linear alkylbenzene sulfonates and physicochemical characteristics of seawater in El-Mex Bay (Alexandria, Egypt)," *Environmental Monitoring and Assessment*, vol. 185, no. 4, pp. 3103–3115, 2013.

[11] I. M. Banat, "The isolation of a thermophilic biosurfactant producing *Bacillus SP*," *Biotechnology Letters*, vol. 15, no. 6, pp. 591–594, 1993.

[12] I. Kamika and M. N. B. Momba, "Assessing the resistance and bioremediation ability of selected bacterial and protozoan species to heavy metals in metal-rich industrial wastewater," *BMC Microbiology*, vol. 13, no. 1, article 28, 2013.

[13] A. R. Achour, P. Bauda, and P. Billard, "Diversity of arsenite transporter genes from arsenic-resistant soil bacteria," *Research in Microbiology*, vol. 158, no. 2, pp. 128–137, 2007.

[14] L. Cavalca, N. Guerrieri, M. Colombo, S. Pagani, and V. Andreoni, "Enzymatic and genetic profiles in environmental strains grown on polycyclic aromatic hydrocarbons," *Antonie van Leeuwenhoek, International Journal of General and Molecular Microbiology*, vol. 91, no. 4, pp. 315–325, 2007.

[15] K. I. Aspila, H. Agemian, and A. S. Y. Chau, "A semi-automated method for the determination of inorganic, organic and total phosphate in sediments," *The Analyst*, vol. 101, no. 1200, pp. 187–197, 1976.

[16] J. Murphy and J. P. Riley, "A modified single solution method for the determination of phosphate in natural waters," *Analytica Chimica Acta*, vol. 27, no. C, pp. 31–36, 1962.

[17] AOAC, *Official Methods of Analysis*, Association of Official Analytical Chemists, Arlington, Va, USA, 2000.

[18] E. Gaudette, R. Flight, L. Toner, and W. Folger, "An inexpensive titration method for the determination of organic carbon in recent sediments," *Sedimentary Petrology*, vol. 4, pp. 249–253, 1974.

[19] R.-A. Doong, Y.-C. Sun, P.-L. Liao, C.-K. Peng, and S.-C. Wu, "Distribution and fate of organochlorine pesticide residues in sediments from the selected rivers in Taiwan," *Chemosphere*, vol. 48, no. 2, pp. 237–246, 2002.

[20] B. Era-Miller and R. Coots, *Potholes Reservoir: Screening Survey for Dieldrin, Other Chlorinated Pesticides, and PCBs in Fish, Water, and Sediments*, Toxic Studies Unit Environmental Assessment Program Washington State Department of Ecology, Olympia Wash, USA, 2010.

[21] J. P. Giesy, D. J. Jude, D. E. Tillitt et al., "Polychlorinated dibenzo-*p*-dioxins, dibenzofurans, biphenyls and 2,3,7,8-tetrachlorodibenzo-*p*-dioxin equivalents in fishes from Saginaw Bay, Michigan," *Environmental Toxicology and Chemistry*, vol. 16, no. 4, pp. 713–724, 1997.

[22] G. Muyzer, E. C. de Waal, and A. G. Uitterlinden, "Profiling of complex microbial populations by denaturing gradient gel electrophoresis analysis of polymerase chain reaction-amplified genes coding for 16S rRNA," *Applied and Environmental Microbiology*, vol. 59, no. 3, pp. 695–700, 1993.

[23] F. Mapelli, R. Marasco, E. Rolli et al., "Potential for plant growth promotion of rhizobacteria associated with *Salicornia* growing in Tunisian hypersaline soils," *BioMed Research International*, vol. 2013, Article ID 248078, 13 pages, 2013.

[24] K. Clarke and R. Gorley, "PRIMER v6. User manual/tutorial," Plymouth routine in multivariate ecological research, Plymouth Marine Laboratory, 2006.

[25] H. Li, X.-L. Wang, B.-Z. Mu et al., "Molecular detection, quantification and distribution of alkane-degrading bacteria in production water from low temperature oilfields," *International Biodeterioration and Biodegradation*, vol. 76, pp. 49–57, 2013.

[26] S. E. Dyksterhouse, J. P. Gray, R. P. Herwig, J. C. Lara, and J. T. Staley, "*Cycloclasticus pugetii* gen. nov., sp. nov., an aromatic hydrocarbon—degrading bacterium from marine sediments," *International Journal of Systematic Bacteriology*, vol. 45, no. 1, pp. 116–123, 1995.

[27] R. A. Amer, N. Sh. El-Gendy, T. Taha, S. Farag, and Y. R. Abdel Fattah, "Biodegradation of crude oil and its kinetics using indigenous bacterial consortium isolated from contaminated area in Egyptian Mediterranean ecosystem," *Jökull Journal*, vol. 64, no. 4, pp. 42–58, 2014.

[28] B. Kumari, S. N. Singh, and D. P. Singh, "Characterization of two biosurfactant producing strains in crude oil degradation," *Process Biochemistry*, vol. 47, no. 12, pp. 2463–2471, 2012.

[29] S. Stepanović, D. Vuković, V. Hola et al., "Quantification of biofilm in microtiter plates: overview of testing conditions and practical recommendations for assessment of biofilm production by staphylococci," *APMIS*, vol. 115, no. 8, pp. 891–899, 2007.

[30] G. D. Christensen, W. A. Simpson, J. J. Younger et al., "Adherence of coagulase-negative staphylococci to plastic tissue culture plates: a quantitative model for the adherence of staphylococci to medical devices," *Journal of Clinical Microbiology*, vol. 22, no. 6, pp. 996–1006, 1985.

[31] E. G. A. Fredheim, C. Klingenberg, H. Rohde et al., "Biofilm formation by *Staphylococcus haemolyticus*," *Journal of Clinical Microbiology*, vol. 47, no. 4, pp. 1172–1180, 2009.

[32] M. Rosenberg, D. Gutnick, and E. Rosenberg, "Adherence of bacteria to hydrocarbons: a simple method for measuring cell-surface hydrophobicity," *FEMS Microbiology Letters*, vol. 9, no. 1, pp. 29–33, 1980.

[33] M. Rosenberg, M. Barki, R. Bar-Ness, S. Goldberg, and R. J. Doyle, "Microbial adhesion to hydrocarbons (math)," *Biofouling*, vol. 4, no. 1–3, pp. 121–128, 1991.

[34] W. van der Vegt, H. C. van der Mei, J. Noordmans, and H. J. Busscher, "Assessment of bacterial biosurfactant production through axisymmetric drop shape analysis by profile," *Applied Microbiology and Biotechnology*, vol. 35, no. 6, pp. 766–770, 1991.

[35] M. J. Anderson, "A new method for non-parametric multivariate analysis of variance," *Austral Ecology*, vol. 26, no. 1, pp. 32–46, 2001.

[36] M. J. Anderson, R. N. Gorley, and K. R. Clarke, *PERMANOVA+for PRIMER: Guide to Software and Statistical Methods*, PRIMER-E, Plymouth, UK, 2008.

[37] S. Dray and A.-B. Dufour, "The ade4 package: implementing the duality diagram for ecologists," *Journal of Statistical Software*, vol. 22, no. 4, pp. 1–20, 2007.

[38] M. J. Anderson, *DISTLM v.2: A FORTRAN Computer Program to Calculate a Distance-Based Multivariate Analysis for a Linear Model*, Department of Statistics, University of Auckland, Auckland, New Zealand, 2002.

[39] W. R. Oschwald, "Sediment-water interactions," *Journal of Environment Quality*, vol. 1, no. 4, pp. 360–366, 1972.

[40] F. Murkowski and E. Ballard, *Water Quality Standards*, Alaska Department of Environmental Conservation, 2003.

[41] EPA, *National Recommended Water Quality Criteria*, US Environmental Protection Agency, 2009.

[42] European Union, "EU Water Framework Directive—Directive 2000/60/EC of the European Parliament and of the Council establishing a framework for the community action in the field of water policy," http://eur-lex.europa.eu/legal-content/EN/TXT/?uri=CELEX:32000L0060.

[43] US EPA, "Supplemental guidance for developing soil screening levels for superfund sites," Office of Solid Waste and Emergency Response, Washington, DC, USA, 2002, http://www.epa.gov/superfund/health/conmedia/soil/index.htm.

[44] N. Milenkovic, M. Damjanovic, and M. Ristic, "Study of heavy metal pollution in sediments from the Iron Gate (Danube River), Serbia and Montenegro," *Polish Journal of Environmental Studies*, vol. 14, no. 6, pp. 781–787, 2005.

[45] European Union, *Heavy Metals in Wastes*, European Commission on Environment, 2002, http://ec.europa.eu/environment/waste/studies/pdf/heavy_metalsreport.pdf.

[46] Z. S. Chen, D. Y. Lee, C. F. Lin, S. L. Lo, and Y. P. Wang, "Contamination of rural and urban soils in Taiwan," in *Contaminants and the Soil Environment in the Australasia-Pacific Region*, R. Naidu, R. S. Kookuna, D. P. Oliver, S. Rogers, and M. J. McLaughlin, Eds., pp. 691–709, Kluwer Academic Publishers, London, UK, 1999.

[47] R. Mukhopadhyay, B. P. Rosen, L. T. Phung, and S. Silver, "Microbial arsenic: from geocycles to genes and enzymes," *FEMS Microbiology Reviews*, vol. 26, no. 3, pp. 311–325, 2002.

[48] M. Y. Sun, K. A. Dafforn, E. L. Johnston, and M. V. Brown, "Core sediment bacteria drive community response to anthropogenic contamination over multiple environmental gradients," *Environmental Microbiology*, vol. 15, no. 9, pp. 2517–2531, 2013.

[49] E. J. Hilyard, J. M. Jones-Meehan, B. J. Spargo, and R. T. Hill, "Enrichment, isolation, and phylogenetic identification of polycyclic aromatic hydrocarbon-degrading bacteria from Elizabeth River sediments," *Applied and Environmental Microbiology*, vol. 74, no. 4, pp. 1176–1182, 2008.

[50] S. Païssé, M. Goñi-Urriza, F. Coulon, and R. Duran, "How a bacterial community originating from a contaminated coastal sediment responds to an oil input," *Microbial Ecology*, vol. 60, no. 2, pp. 394–405, 2010.

[51] M. Fondi, E. Rizzi, G. Emiliani et al., "The genome sequence of the hydrocarbon-degrading *Acinetobacter venetianus* VE-C3," *Research in Microbiology*, vol. 164, no. 5, pp. 439–449, 2013.

[52] E. Kaczorek, T. Jesionowski, A. Giec, and A. Olszanowski, "Cell surface properties of *Pseudomonas stutzeri* in the process of diesel oil biodegradation," *Biotechnology Letters*, vol. 34, no. 5, pp. 857–862, 2012.

[53] M. J. Gauthier, B. Lafay, R. Christen et al., "*Marinobacter hydrocarbonoclasticus* gen. nov., sp. nov., a new, extremely halotolerant, hydrocarbon-degrading marine bacterium," *International Journal of Systematic Bacteriology*, vol. 42, no. 4, pp. 568–576, 1992.

[54] M. Mahjoubi, A. Jaouani, A. Guesmi et al., "Hydrocarbonoclastic bacteria isolated from petroleum contaminated sites in Tunisia: isolation, identification and characterization of the biotechnological potential," *New Biotechnology*, vol. 30, no. 6, pp. 723–733, 2013.

[55] M. Mulet, Z. David, B. Nogales, R. Bosch, J. Lalucat, and E. García-Valdés, "*Pseudomonas* diversity in crude-oil-contaminated intertidal sand samples obtained after the prestige oil spill," *Applied and Environmental Microbiology*, vol. 77, no. 3, pp. 1076–1085, 2011.

[56] J. E. Kostka, O. Prakash, W. A. Overholt et al., "Hydrocarbon-degrading bacteria and the bacterial community response in Gulf of Mexico beach sands impacted by the deepwater horizon oil spill," *Applied and Environmental Microbiology*, vol. 77, no. 22, pp. 7962–7974, 2011.

[57] T. Brusa, S. Borin, F. Ferrari, C. Sorlini, C. Corselli, and D. Daffonchio, "Aromatic hydrocarbon degradation patterns and catechol 2,3-dioxygenase genes in microbial cultures from deep anoxic hypersaline lakes in the eastern Mediterranean sea," *Microbiological Research*, vol. 156, no. 1, pp. 49–58, 2001.

[58] E. AL-Saleh, H. Drobiova, and C. Obuekwe, "Predominant culturable crude oil-degrading bacteria in the coast of Kuwait," *International Biodeterioration & Biodegradation*, vol. 63, no. 4, pp. 400–406, 2009.

[59] V. Patel, J. Patel, and D. Madamwar, "Biodegradation of phenanthrene in bioaugmented microcosm by consortium ASP developed from coastal sediment of Alang-Sosiya ship breaking yard," *Marine Pollution Bulletin*, vol. 74, no. 1, pp. 199–207, 2013.

[60] L. Wang, N. Qiao, F. Sun, and Z. Shao, "Isolation, gene detection and solvent tolerance of benzene, toluene and xylene degrading bacteria from nearshore surface water and Pacific Ocean sediment," *Extremophiles*, vol. 12, no. 3, pp. 335–342, 2008.

[61] M. M. Naik, D. Khanolkar, and S. K. Dubey, "Lead-resistant *Providencia alcalifaciens* strain 2EA bioprecipitates Pb^{+2} as lead phosphate," *Letters in Applied Microbiology*, vol. 56, no. 2, pp. 99–104, 2013.

[62] U. Thacker, R. Parikh, Y. Shouche, and D. Madamwar, "Hexavalent chromium reduction by *Providencia* sp," *Process Biochemistry*, vol. 41, no. 6, pp. 1332–1337, 2006.

[63] J. De, N. Ramaiah, and L. Vardanyan, "Detoxification of toxic heavy metals by marine bacteria highly resistant to mercury," *Marine Biotechnology*, vol. 10, no. 4, pp. 471–477, 2008.

[64] R.-H. Peng, A.-S. Xiong, Y. Xue et al., "Microbial biodegradation of polyaromatic hydrocarbons," *FEMS Microbiology Reviews*, vol. 32, no. 6, pp. 927–955, 2008.

[65] N. Jiménez, M. Viñas, C. Guiu-Aragonés, J. M. Bayona, J. Albaigés, and A. M. Solanas, "Polyphasic approach for assessing changes in an autochthonous marine bacterial community in the presence of *Prestige* fuel oil and its biodegradation potential," *Applied Microbiology and Biotechnology*, vol. 91, no. 3, pp. 823–834, 2011.

[66] R. Bartha and I. Bossert, "The treatment and disposal of petroleum wastes," in *Petroleum Microbiology*, R. M. Atlas, Ed., pp. 553–578, Macmillan, New York, NY, USA, 1984.

[67] J. J. Cooney, "The fate of petroleum pollutants in fresh water ecosystems," in *Petroleum Microbiology*, R. M. Atlas, Ed., pp. 399–434, Macmillan, New York, NY, USA, 1984.

[68] L. Cavalca, A. Corsini, P. Zaccheo, V. Andreoni, and G. Muyzer, "Microbial transformations of arsenic: perspectives for biological removal of arsenic from water," *Future Microbiology*, vol. 8, no. 6, pp. 753–768, 2013.

[69] G.-C. Ding, H. Heuer, S. Zühlke et al., "Soil type-dependent responses to phenanthrene as revealed by determining the diversity and abundance of polycyclic aromatic hydrocarbon ring-hydroxylating dioxygenase genes by using a novel PCR detection system," *Applied and Environmental Microbiology*, vol. 76, no. 14, pp. 4765–4771, 2010.

[70] T. J. McGenity, B. D. Folwell, B. A. McKew, and G. O. Sanni, "Marine crude-oil biodegradation: a central role for interspecies interactions," *Aquatic Biosystems*, vol. 8, no. 1, article 10, 2012.

[71] S. Schneiker, V. A. P. M. dos Santos, D. Bartels et al., "Genome sequence of the ubiquitous hydrocarbon-degrading marine bacterium *Alcanivorax borkumensis*," *Nature Biotechnology*, vol. 24, no. 8, pp. 997–1004, 2006.

[72] L. Yuste, M. E. Corbella, M. J. Turiégano, U. Karlson, A. Puyet, and F. Rojo, "Characterization of bacterial strains able to grow on high molecular mass residues from crude oil processing," *FEMS Microbiology Ecology*, vol. 32, no. 1, pp. 69–75, 2000.

[73] G.-L. Zhang, Y.-T. Wu, X.-P. Qian, and Q. Meng, "Biodegradation of crude oil by *Pseudomonas aeruginosa* in the presence of rhamnolipids," *Journal of Zhejiang University Science B*, vol. 6, no. 8, pp. 725–730, 2005.

[74] M. Hassanshahian, G. Emtiazi, and S. Cappello, "Isolation and characterization of crude-oil-degrading bacteria from the Persian Gulf and the Caspian Sea," *Marine Pollution Bulletin*, vol. 64, no. 1, pp. 7–12, 2012.

[75] S. B. Batista, A. H. Mounteer, F. R. Amorim, and M. R. Tótola, "Isolation and characterization of biosurfactant/bioemulsifier-producing bacteria from petroleum contaminated sites," *Bioresource Technology*, vol. 97, no. 6, pp. 868–875, 2006.

[76] S. K. Satpute, A. G. Banpurkar, P. K. Dhakephalkar, I. M. Banat, and B. A. Chopade, "Methods for investigating biosurfactants and bioemulsifiers: a review," *Critical Reviews in Biotechnology*, vol. 30, no. 2, pp. 127–144, 2010.

[77] M. Bouchez-Naïtali, H. Rakatozafy, R. Marchal, J.-Y. Leveau, and J.-P. Vandecasteele, "Diversity of bacterial strains degrading hexadecane in relation to the mode of substrate uptake," *Journal of Applied Microbiology*, vol. 86, no. 3, pp. 421–428, 1999.

[78] C.-W. Liu and H.-S. Liu, "*Rhodococcus erythropolis* strain NTU-1 efficiently degrades and traps diesel and crude oil in batch and fed-batch bioreactors," *Process Biochemistry*, vol. 46, no. 1, pp. 202–209, 2011.

[79] P.-J. Vaysse, P. Sivadon, P. Goulas, and R. Grimaud, "Cells dispersed from *Marinobacter hydrocarbonoclasticus* SP17 biofilm exhibit a specific protein profile associated with a higher ability to reinitiate biofilm development at the hexadecane-water interface," *Environmental Microbiology*, vol. 13, no. 3, pp. 737–746, 2011.

Hindawi Publishing Corporation
BioMed Research International
Volume 2015, Article ID 857639, 8 pages
http://dx.doi.org/10.1155/2015/857639

Research Article

A High Diversity in Chitinolytic and Chitosanolytic Species and Enzymes and Their Oligomeric Products Exist in Soil with a History of Chitin and Chitosan Exposure

Malathi Nampally,[1,2] M. B. Govinda Rajulu,[1,3] Dominique Gillet,[4] T. S. Suryanarayanan,[3] and Bruno B. Moerschbacher[1]

[1] *Institute for Biology and Biotechnology of Plants, WWU Münster, Schlossplatz 8, 48143 Münster, Germany*
[2] *Research and Development Laboratory, Sri Biotech Laboratories India Ltd., Hyderabad 500 034, India*
[3] *Vivekananda Institute of Tropical Mycology (VINSTROM), Ramakrishna Mission Vidyapith, Chennai 600 004, India*
[4] *Gillet Chitosan EURL, Laurent Bonnevay 17, 54100 Nancy, France*

Correspondence should be addressed to Bruno B. Moerschbacher; moersch@uni-muenster.de

Received 11 December 2014; Revised 31 March 2015; Accepted 15 April 2015

Academic Editor: Spyridon Ntougias

Chitin is one of the most abundant biomolecules on earth, and its partially de-N-acetylated counterpart, chitosan, is one of the most promising biotechnological resources due to its diversity in structure and function. Recently, chitin and chitosan modifying enzymes (CCMEs) have gained increasing interest as tools to engineer chitosans with specific functions and reliable performance in biotechnological and biomedical applications. In a search for novel CCME, we isolated chitinolytic and chitosanolytic microorganisms from soils with more than ten-years history of chitin and chitosan exposure and screened them for chitinase and chitosanase isoenzymes as well as for their patterns of oligomeric products by incubating their secretomes with chitosan polymers. Of the 60 bacterial strains isolated, only eight were chitinolytic and/or chitosanolytic, while 20 out of 25 fungal isolates were chitinolytic and/or chitosanolytic. The bacterial isolates produced rather similar patterns of chitinolytic and chitosanolytic enzymes, while the fungal isolates produced a much broader range of different isoenzymes. Furthermore, diverse mixtures of oligosaccharides were formed when chitosan polymers were incubated with the secretomes of select fungal species. Our study indicates that soils with a history of chitin and chitosan exposure are a good source of novel CCME for chitosan bioengineering.

1. Introduction

Shrimp and crab shell wastes are used commercially for the extraction of chitin which can then be converted into its partially de-N-acetylated forms, chitosans. Chitosans are a family of molecules differing with respect to their degree of polymerisation (DP), degree of acetylation (DA), and pattern of acetylation (PA). Such variations influence the physicochemical solution properties as well as the biological functionalities of chitosans [1–5] which find use in agricultural, food, and pharmaceutical industries [6]. Therefore, well characterized chitosans with broad ranges of specific DPs, DAs, and PAs are crucial for detailed structure-function analyses. To this end, chitin and chitosan modifying enzymes (CCMEs) such as chitinase, chitin deacetylase, and chitosanase could be used to complement the chemical methods currently used for this purpose [7–9]. Furthermore, chitosans could be broken down to soluble derivatives called chitooligosaccharides (CHOS) which are vested with desirable technological properties [10]. Since enzymatic conversion of chitin to chitosan and CHOS is ecofriendly, more specific and a cheaper option compared to the chemical methods [11] and could potentially augment the existing chemical methods [12, 13] for characterization of chitosans, search for novel CCME is a worthwhile exercise. With the expectation that soils with a long history of exposure to chitin and chitosan would select organisms elaborating diverse chitinolytic and chitosanolytic enzymes, we proceeded with the current work.

Although fungi are reported to contribute more than bacteria to environmental degradation of chitin [14], much less is known about the fungi involved compared to chitinolytic bacteria; bacterial CCMEs have been studied in much more detail than fungal enzymes. In terrestrial soils, the most prevalent chitin degrading bacteria are species of *Bacillus, Stenotrophomonas,* Gammaproteobacteria, and *Arthrobacter* [15, 16] while those in marine sludges are species of *Actinobacterium, Pantoea,* and *Pseudomonas* [17, 18]. Fungi such as *Trichoderma viride* [15] and species of *Mortierella* and *Fusarium* isolated from soil exhibit appreciable chitinolytic activity in the presence of chitin in the culture medium [19]. Here, we looked at the diversity of chitinolytic and chitosanolytic fungi and bacteria in soils of a chitin and chitosan producing company in Gujarat, India. These soils had been exposed to dry or fresh shrimp shells or to chitin or different types of chitosan for more than ten years. In addition to species diversity, we also analysed the diversity of CCME present in these organisms, as well as the diversity of products produced by these CCMEs.

2. Materials and Methods

2.1. Soil Samples. Seven soil samples were collected from different sites of Mahtani Chitosan Pvt. Ltd., Veraval (Gujarat, India), a chitin/chitosan producing company from a depth of 5 to 10 cm, and stored at 4°C for a maximum of two months before further processing.

2.2. Preparation of Colloidal Chitin and Chitosans. Colloidal chitin was prepared according to the method of Berger and Reynolds [20]. To 10 g of β-chitin, 500 mL of conc. HCl was added, stirred to get a homogeneous mixture, and incubated at 4°C overnight. Two litres of double-distilled water was then added, stirred for 48 hours at 4°C, and then washed with double-distilled water until the pH was neutral.

Chitosan (average DA 3%, average DPn ca. 2,000) was dissolved in an aqueous acetic acid (0.1 M) solution and purified by successive filtration and extensive washing by repeated precipitation and centrifugation; following this, chitosans with DA 35%, DP 900, and DA 50%, DP 820 were prepared by partial re-N-acetylation using acetic anhydride in 1,2-propanediol [21]. The DA of the resulting chitosans was determined using ^{1}H NMR spectroscopy [22], and the DP using HP-SEC coupled to RI and MALLS detectors [3].

2.3. Preparation of Chitin and Chitosan Agar Plates. For visualizing chitinolytic activity, Petri dishes with M9 minimal medium amended with 0.5% of colloidal chitin as sole carbon source were used. Petri dishes with Luria-Bertani (LB) agar medium with 0.9% chitosan (DA 3%) as the sole carbon source were used to identify chitosanolytic activity. The appearance of a clear zone around the colony of a bacterium or fungus growing on M9 and LB medium indicated chitinolytic and chitosanolytic activity, respectively.

2.4. Isolation of Chitinolytic and Chitosanolytic Fungi and Bacteria from Soil Samples. Fungi were isolated from the soil samples by dilution plating and Warcup soil-plate methods [23]. For dilution plate, 2 g of soil was suspended in 1 mL of sterile distilled water, and tenfold dilutions of this were spread on PDA (Difco Potato Dextrose Agar medium, Becton and Dickinson, Sparks, USA) plates containing chloramphenicol (150 mg/L) to obtain individual fungal colonies. For soil plates, 2 g of soil was placed in a sterile Petri dish, cooled PDA medium (15 mL) was added, and soil particles were spread in the medium. All plates had replicates and were incubated at 28°C for 20 days to obtain fungal colonies. The fungi were isolated and subcultured in PDA slants. Slide cultures of these isolated fungi were then prepared, stained, and observed under microscope to identify them based on standard keys [24].

Bacteria were isolated using a modified serial dilution method of Maltseva and Oriel [25]. Initially, 10 g of soil was inoculated in M9 minimal medium amended with colloidal chitin (0.5%) to enrich chitinolytic bacteria; a few mL of the enriched cultures was spread on LB agar plates and incubated at 37°C for isolating bacteria. Pure cultures were obtained by restreaking the colonies several times until single colonies were obtained.

2.5. Preparation of Samples for Zymography and Thin Layer Chromatography. Each fungal isolate was grown in potato dextrose broth for 5 days as static culture at 28°C and 100 mL of this culture filtrate (secretome) was dialyzed (MWCO 1,000 kDa) for 24 h against distilled water at 4°C; 10 mg of the lyophilized secretome was mixed in 1 mL of 50 mM sodium acetate buffer (pH 5.2) and centrifuged at 16,000 g for 5 min (20°C). An aliquot (5–10 μL) of sample was used for dot activity assay or zymography. Bacterial isolates were grown in 10 mL of LB medium for 48 h at 37°C, centrifuged, and the secretomes were lyophilised. Lyophilised samples were dissolved in 1 mL of 5 mM sodium acetate buffer (pH 5.0) and used for assessing enzyme activities.

2.6. Detection of Chitinase and Chitosanase Activity by Dot Assay and Zymography. Chitinolytic and chitosanolytic enzyme activities were detected using a dot activity assay as described previously [26]. Briefly, 5 μL from a fungal secretome preparation was applied on the gels prepared with glycol-chitin (0.3 mg/mL) or chitosan DA 35% (0.1 mg/mL). Gels were incubated at 37°C overnight and then stained l with Calcofluor White. A dark spot under UV transillumination on the gel indicated enzyme activity.

For detecting isoenzymes, seminative SDS-PAGE (12%) was run in gels containing 0.3 mg/mL of glycol-chitin for chitinase or 0.1 mg/mL of either of two chitosans (DA 50% or DA 35%) [27]. After electrophoresis (50 mA for 4 h), the gel was washed twice for 20 min each in 50 mM sodium acetate buffer (pH 5.2, with 1% Triton X-100), followed by two washes in buffer without Triton X-100. The gel was incubated at 37°C for 12 h under shaking in 50 mM sodium acetate buffer (pH 5.2) and stained with 0.01% Calcofluor White (Sigma, Steinheim, Germany) in 0.5 M Tris/HCl-buffer (pH 8.9) for 5 min and finally washed in deionized water for 1 h. The isozymes were visualized on a UV transilluminator. A crude extract of a known chitinolytic strain of *Bacillus licheniformis* [28] was run as a positive control.

Alternatively, zymography was done using isoelectric focusing (IEF) over the pH range 3–10 in a polyacrylamide gel containing Ampholine (Amersham Bioscience, Uppsala, Sweden) followed by activity staining using overlay gels containing 0.1 mg/mL of either of the chitosans mentioned above. After incubation in 50 mM ammonium acetate buffer (pH 5.2) overnight at 37°C, overlay gels were stained with Calcofluor White as described above.

2.7. Detection of Chitosan Oligomers by Thin Layer Chromatography. A sample (20 μL) of secretome of selected fungal isolates was mixed with 20 μL of chitosan DA 35% solution (1 mg/mL) and incubated overnight at 37°C in 50 mM sodium acetate buffer (pH 5.5). Samples were concentrated under reduced pressure to scale down the volume, and aliquots of 10 μL were applied on TLC plates (Merck, Berlin, Germany), run in butanol : methanol : ammonia : water (5 : 4 : 2 : 1, v/v/v/v) and stained using aniline-diphenylamine reagent (4 mL of aniline, 4 g of diphenylamine, 200 mL of acetone, and 30 mL of 85% phosphoric acid). Oligomers were visualised by heating the plate at 180°C for 3–5 min. Oligomers were compared with authentic N-acetyl-D-glucosamine (DP 1, 2, 3, 5, 6) and D-glucosamine (DP 1, 3, 4) standards (Seikagaku, Tokyo, Japan).

2.8. 16S-rDNA Analysis of Bacterial Isolates. PCR was performed on the bacterial soil isolates using bacterial universal primers: forward primer (5′AGAGTTTGATC(AC)TGGCTCAG3′), reverse primer (5′AAGGAGGTGATCCA(AGCT)CC(AG)CA3′) [29]. Amplicons were cloned into PCRII-TOPO vector and sequenced at MWG, Ebersberg, Germany. Blast analyses were performed with the sequences in the NCBI database. Sequences obtained were deposited in NCBI under Gene Bank with sequence id's JN593073–JN593080.

Table 1: Chitinase and chitosanase activity of the fungal isolates screened from soil samples.

Isolate number	Name of the fungus	Activity in dot assays	
		Chitinase*	Chitosanase*
1	*Fusarium* sp.	+	−
2	Unidentified	−	+
3	*Penicillium* sp.	+	+
4	*Aspergillus* sp.	+	−
5	*Acremonium* sp.	−	−
6	*Cladosporium* sp.	+	+
7	*Cladosporium* sp.	−	+
8	*Aureobasidium pullulans*	+	−
9	*Aureobasidium pullulans*	+	−
10	Unidentified	+	+
11	Unidentified	−	+
12	Unidentified	−	+
13	Unidentified	+	−
14	*Aspergillus* sp.	−	−
15	*Curvularia* sp.	−	−
16	Unidentified	−	−
17	*Aspergillus* sp.	+	+
18	*Aspergillus niger*	+	+
19	*Sporormiella intermedia*	−	−
20	*Cladosporium cladosporioides*	−	+
21	*Drechslera* sp.	+	+
22	*Drechslera* sp.	+	−
23	*Aspergillus* sp.	−	+
24	*Acremonium* sp.	+	+
25	Unidentified	−	+

*Glycol-chitin and chitosan DA 36% were used as substrates to detect chitinase and chitosanase activity, respectively; + = positive; − = negative.

3. Results

3.1. Isolation and Screening for Chitinolytic or Chitosanolytic Bacteria and Fungi. A total of sixty bacterial strains were isolated from seven soil samples collected from different sites of the chitin/chitosan producing company. On a minimal medium with 0.5% colloidal chitin as the sole carbon source, eight strains consistently produced clear zones around their colonies indicating a chitinolytic activity (Figure 1(a)). Microscopic observations indicated that all of them were *Bacillus* species differing in their motility, sporulation, and arrangement of spores. The overall 16S-rDNA sequence identity between these *Bacillus* strains ranged from 99.5 to 100%. 16S-rDNA sequence identities of 99 and 99.7% corroborated this to the *cereus/anthracis/thuringiensis* group of *Bacillus*.

A total of 25 fungal strains were isolated from two different soil samples. Many of them were *Aspergillus* species; other genera included *Acremonium*, *Aureobasidium*, *Cladosporium*, *Curvularia*, *Drechslera*, *Fusarium*, *Penicillium*, and *Sporormiella* (Table 1). Of the seven randomly chosen isolates from these, two produced clearing zones on chitin medium (Figure 1(b)), and two others on chitosan medium (Figure 1(c)). Of the 25 isolates, 13 were positive for chitinase, 14 were positive for chitosanase, and 7 produced both the enzymes as visualized by dot assay (Table 1). Among the 20 fungal isolates which were chitinolytic and/or chitosanolytic, 14 identified fungi belong to seven different genera, namely, *Acremonium, Aspergillus*, *Aureobasidium*, *Cladosporium*, *Drechslera, Fusarium*, and *Penicillium* which are common saprotrophs found in soils [30].

3.2. Chitinolytic and Chitosanolytic Enzymes of Bacterial and Fungal Isolates. The crude extract of *B. licheniformis* (control) showed activity on all three substrates whereas the secretomes from the different soil bacterial strains showed differences in their activities. Isolates 2, 3, 5, and 7 showed the same two high-molecular weight chitinases as *B. licheniformis,* while the extracts from isolates 1, 4, 6, and 8 were not active on glycol-chitin (Figure 2(a)). All isolates including *B. licheniformis* produced one high MW isoenzyme degrading chitosan (DA 56%) and isolates 2, 4, and possibly 7 possessed an additional isoenzyme with a MW between 50 and 75 kDa

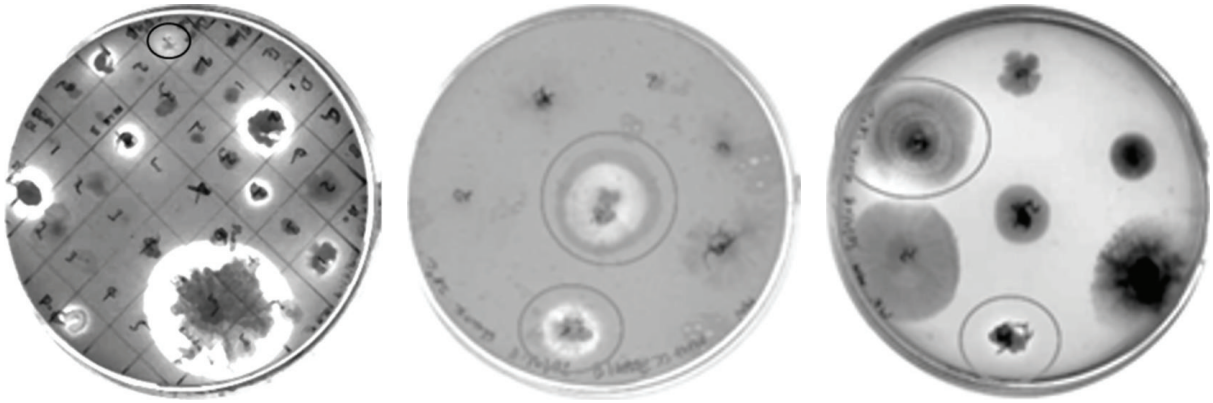

(a) (b) (c)

Figure 1: Chitinolytic and chitosanolytic activities in bacterial and fungal isolates from soil samples. (a) Bacterial strains showing clearing zones on minimal medium agar plates containing colloidal chitin; one strain showing weak chitinolytic activity (top, marked with circle) was excluded from further studies as it did not show the activity consistently; (b) and (c) examples of fungal strains showing clearing zones on agar plates containing colloidal chitin in minimal medium (b) or chitosan DA 3% in LB medium (c).

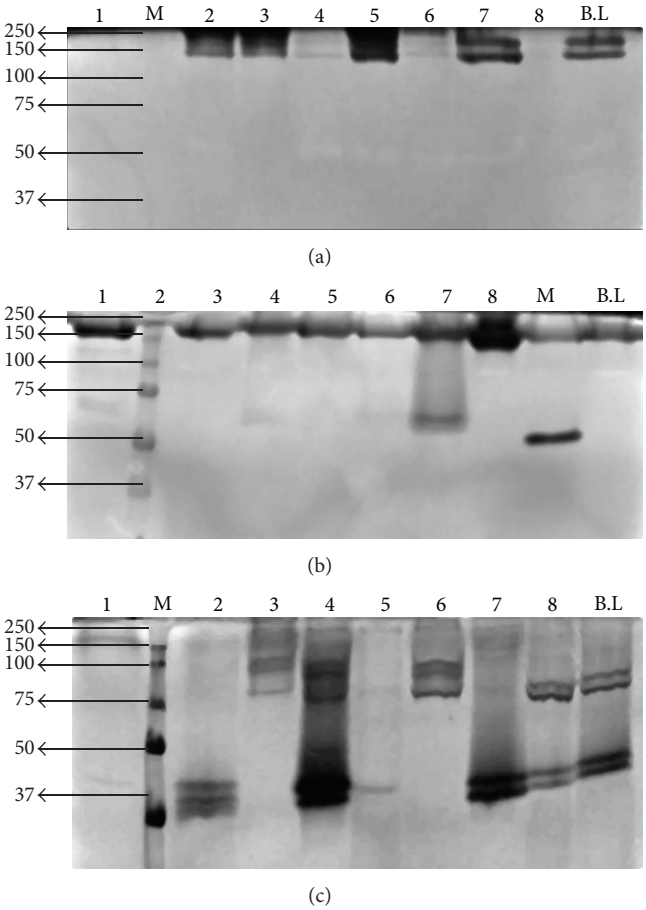

Figure 2: Seminative SDS-PAGE of crude extracts of the bacterial soil isolates (1–8), followed by zymography using glycol-chitin (a), chitosan DA 56% (b), or chitosan DA35% (c) as a substrate. A known chitinolytic strain of *Bacillus licheniformis* (B.L) was used as a positive control. The positions of marker proteins (M) are given on the sides of the gels.

capable of degrading this chitosan (Figure 2(b)). All of the strains including *B. licheniformis* had isoenzymes degrading chitosan DA 35% (Figure 2(c)). Isolates 1 and 5 produced fewer and weakly active chitosanase isoforms and isolates 4 and 7 produced chitosanase of highest MW. Considering the activities on all three substrates, it was clear that all eight isolates differ from each other and from *B. licheniformis* in their chitinolytic and chitosanolytic isoenzymes, but their diversity was limited.

PCR was performed on genomic DNA of the eight bacterial soil isolates using primers designed from conserved regions of known *Bacillus* chitosanases. Amplicons were observed at 1.3 Kb only in strains 1, 3, 6, and 7 (data not shown); the other strains did not show any amplification. Blast results showed that the sequences were identical to the known chitosanase sequence of *Bacillus* sp. strain KCTC 0377BP [31].

To analyse the chitosanolytic isoenzymes of fungi, crude extracts of fungal isolates which were positive in the dot assay with chitosan DA 35% as a substrate were subjected to seminative SDS-PAGE in a gel containing chitosan DA 35% (Figure 3). Isoenzyme activity was observed in all isolates; the isolates differed in the number of isoforms and in their overall activity. The number of isoenzymes ranged from one to three and their MW ranged from very low to very high. Isolates 3, 10, 17, 18, and 23 (*Penicillium* and all three chitosanolytic *Aspergillus* isolates) had a strong activity at MW of ca. 250 kDa; two of the three *Cladosporium* isolates (7 and 20) showed one sharp band around 50 kDa; isolates 11, 12, and 18 had one or two low MW isoforms between 10 and 20 kDa.

Samples which differed clearly in their isoenzyme spectrum were selected, and their proteins were separated by isoelectric focusing (IEF). For zymography, polyacrylamide gels containing different chitosans with DA 35% and DA 56% were overlaid on the IEF gel after the run (Figure 4). Gels

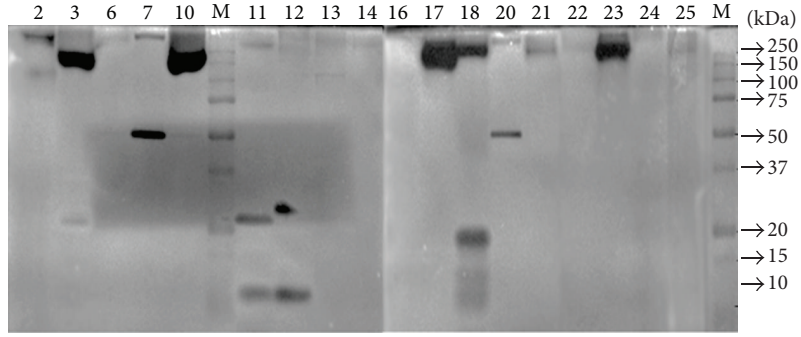

Figure 3: Seminative SDS-PAGE of crude extracts of selected fungal soil isolates (numbers correspond to Table 1), followed by zymography using chitosan DA 35% as a substrate. The positions of marker proteins (M) are given on the right side.

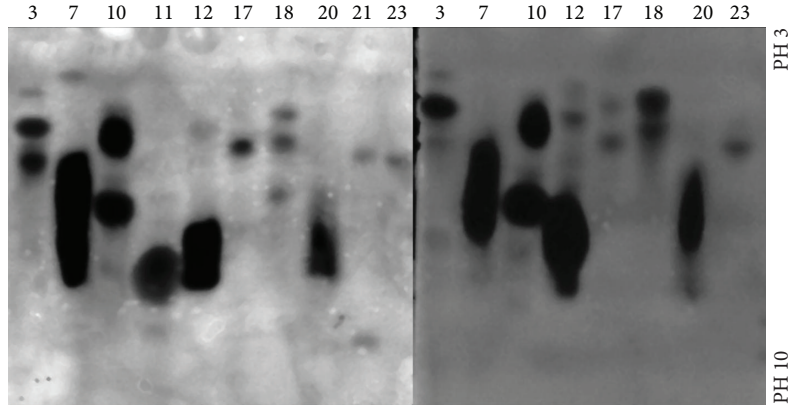

Figure 4: Isoelectric focusing of crude extracts of selected fungal soil isolates (numbers correspond to Table 1), followed by zymography using overlay gels containing chitosan DA 35% (a) or chitosan DA 56% (b) as a substrate. The pH range of the gels is indicated at the right side.

were incubated at 37°C overnight and stained with Calcofluor White to detect chitosanolytic activity. All fungal isolates had one to four chitosanolytic isoenzymes with isoelectric points ranging from pH 4 to pH 8. While few differences were seen between the two substrates tried, clear differences were obvious between the different isolates.

3.3. Chitosan Oligomers Produced by Chitosanolytic Enzymes of Select Fungal Isolates. Secretomes from fungal isolates which showed a single dominant isoenzyme in zymography (isolates 3, 7, 10, 12, 17, 20, and 23) were incubated with chitosan DA 35% overnight at 37°C, and the chitosan oligomers produced were analysed using TLC (Figures 5(a) and 5(b)). This preliminary analysis showed that different oligomer mixtures were produced by each fungal isolate, ranging from the monomers GlcN and GlcNAc (isolates 3, 23) to a mixture of small oligomers ranging in degree of polymerization from 2 to 6 (isolates 7, 10, 12, and 20). Isolate 17 produced only larger oligomers.

4. Discussion

We argued that soils with a long history of exposure to chitin and chitosan would select microbes with an ability to degrade chitin and/or chitosan. Hence, we studied the soils of a chitin and chitosan producing company which has been processing ca. 5,000 tons of fresh and dried shrimp annually since the year 1995. Earlier, our collaborators from India reported that Gammaproteobacteria were dominant in these soils [16]. We found eight different *Bacillus* species belonging to the *cereus/anthracis/thuringiensis* group which is well known for their potential to degrade chitin and chitosan [32–35]. With regard to the CCME, chitosanases were more diverse than chitinases in these species. Using degenerate primers of known *Bacillus* chitosanases [36], we could amplify a chitosanase gene from four of the eight strains which was identical to a chitosanase gene from *Bacillus* sp. strain KCTC 0377BP [31]. We have now set up a pooled genomic DNA library of these strains and are screening it for chitinase and chitosanase genes.

Although fungi with CCME activities have been reported from soils [37–39], to our knowledge, this is the first report on fungal diversity in soils with a history of chitin/chitosan exposure. We identified the fungi based on spore morphology, but a molecular approach will be essential to authenticate their identity at the species level. Though fungi produce chitinolytic enzymes *per se* for cell wall remodelling during their developmental processes [40], the diversity of these

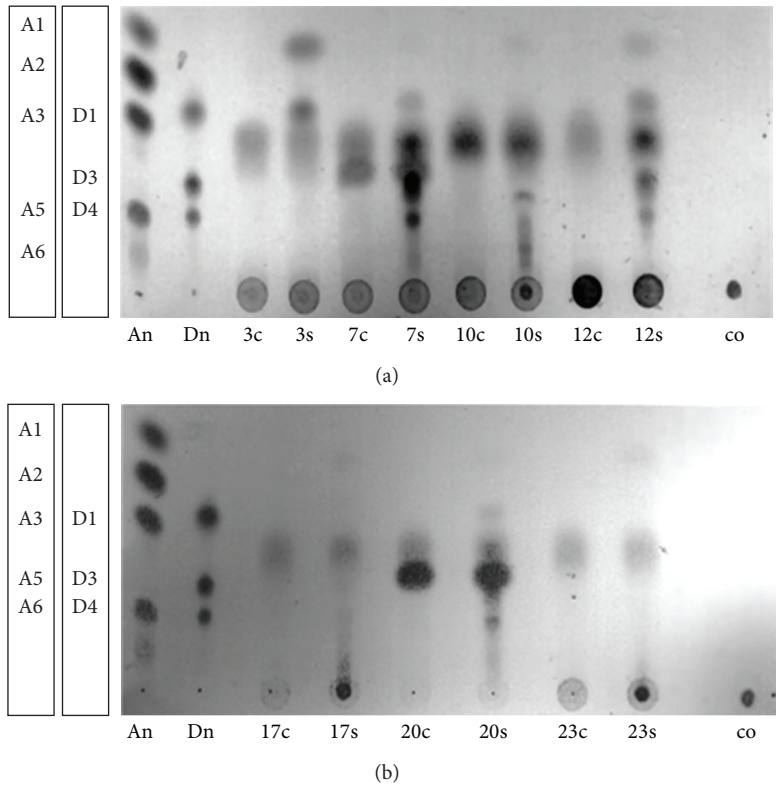

Figure 5: (a) and (b). TLC analysis of the products of chitosan (DA 35%) incubation with crude extracts of selected fungal soil isolates (numbers correspond to Table 1). Crude extracts were incubated with (samples labeled 3s, 7s, 10s, 12s, 17s, 20s, and 23s) or without chitosan (samples labeled 3c, 7c, 10c, 12c, 17c, 20c, and 23c) as a substrate. Chitosan incubated without any crude extract (co) was used as a control, and oligomers of GlcNAc (An) and GlcN (Dn) were used as standards. The DP of the standards is given on the left sides of the plates.

enzymes could be higher in fungi present in soils with spent chitin material since the fungi here could possibly be utilizing chitin and chitosan polysaccharides as carbon and nitrogen source [41]. This could be the reason why almost all of the fungi screened here were positive for chitin and/or chitosan degrading enzymes: 13 were chitinolytic, 14 were chitosanolytic, and 7 isolates were both chitinolytic and chitosanolytic. Furthermore, isolates belonging to the same genus differed significantly in their chitinolytic and chitosanolytic potential. A typical case is the genus *Aspergillus* which dominated the fungal isolates. Of the five *Aspergillus* isolates, one was chitinolytic but not chitosanolytic, one was chitosanolytic but not chitinolytic, two were both chitinolytic and chitosanolytic, and one was neither chitinolytic nor chitosanolytic. Similarly, of the two *Acremonium* isolates, one was negative for both activities and one was positive for both activities; all three *Cladosporium* isolates were chitosanolytic but only one was also chitinolytic; both the *Drechslera* isolates were chitinolytic and one was also chitosanolytic. Thus, soils with a history of chitin and chitin exposure appear to be a promising source of fungi with high CCME diversity useful for technological exploitation. This assumption was further substantiated by the isoenzyme patterns of chitosanases discerned based on size and isoelectric point. Most fungal isolates produced more than one chitosanolytic isoenzyme. IEF was superior to native PAGE for visualizing isozymes as more isoforms were visible for isolates 3, 10, 12, 17, and 20 in the latter method of detection. A few fungal isolates which tested positive for chitosanase in the dot activity assay (with chitosan DA 35% as substrate) showed weak activities in the zymograms with this substrate possibly owing to improper renaturation of the enzymes when the SDS was washed out. In spite of the multiplicity of enzymes, chitosan DA 35% was not fully degraded to monomers or very small oligomers by any of the crude enzyme preparations; pentamers and larger oligomers were produced by isolates 7, 10, 12, 17, and 20.

5. Conclusions

In conclusion, we observed strong and diverse chitinolytic and chitosanolytic activities among the microorganisms present in soil samples with a history of chitin/chitosan exposure, and the diversity in fungal species and their CCME here was higher than the bacterial diversity. Analysing the biodiversity of microorganisms in an environmental sample by screening for the diversity of isoenzymes and for the oligomers produced by these enzymes is a novel but promising approach. The high diversity found is of biotechnological relevance as isolated bacterial and fungal chitinases and chitosanases [42, 43] as well as the oligomers produced by purified or crude chitinolytic and chitosanolytic enzymes

[31, 44, 45] have interesting and diverse biological activities and may, thus, be useful in a wide range of applications.

Conflict of Interests

The authors declare that there is no conflict of interests regarding the publication of this paper.

Acknowledgments

The research leading to these results has received funding from the European Union Sixth Framework Programme ([FP6/2002–2006]) in the framework of the PolyModE project under Grant Agreement KBBE-2007-3-3-07, coordinated by BMM. Further financial support came from travel grants to M. B. Govinda Rajulu and T. S. Suryanarayanan in the framework of a joint project of the German Federal Ministry of Education and Research BMBF and the Department of Biotechnology, Govt. of India (BT/IN/FRG/09/TSS/2007), and a PhD fellowship to Malathi Nampally by the German Academic Exchange Service DAAD. The authors thank Mr. Kamlesh Fofandi, Mahtani Chitosan Pvt. Ltd., Veraval 362266, India, for support, Dr. Nour Eddine El Gueddari for help with the generation and characterisation of chitosans, Dr. Ratna Singh for help with 16S-rDNA phylogenetic trees, and Ursula Fassin for technical assistance.

References

[1] N. E. El Gueddari, U. Rauchhaus, B. M. Moerschbacher, and H. B. Deising, "Developmentally regulated conversion of surface-exposed chitin to chitosan in cell walls of plant pathogenic fungi," *New Phytologist*, vol. 156, no. 1, pp. 103–112, 2002.

[2] N. E. El Gueddari and B. M. Moerschbacher, "A bioactivity matrix for chitosans as elicitors of disease resistance reactions in wheat," *Advances in Chitin Science*, vol. 7, pp. 56–59, 2004.

[3] G. Lamarque, J. M. Lucas, C. Viton, and A. Domard, "Physicochemical behavior of homogeneous series of acetylated chitosans in aqueous solution: role of various structural parameters," *Biomacromolecules*, vol. 6, no. 1, pp. 131–142, 2005.

[4] B. M. Moerschbacher, "Bio-activity matrices of chitosans in plant protection," in *Emerging Trends in Plant-Microbe Interactions*, S. S. Gnanamanickam, R. Balasubramanian, and N. Anand, Eds., pp. 186–190, University of Madras, Chennai, India, 2005.

[5] A. Domard, "A perspective on 30 years research on chitin and chitosan," *Carbohydrate Polymers*, vol. 84, no. 2, pp. 696–703, 2011.

[6] W. Arbia, L. Arbia, L. Adour, and A. Amrane, "Chitin extraction from crustacean shells using biological methods—a review," *Food Technology and Biotechnology*, vol. 51, no. 1, pp. 12–25, 2013.

[7] S.-K. Kim and N. Rajapakse, "Enzymatic production and biological activities of chitosan oligosaccharides (COS): a review," *Carbohydrate Polymers*, vol. 62, no. 4, pp. 357–368, 2005.

[8] N. E. El Gueddari, A. Schaaf, M. Kohlhoff, C. Gorzelanny, and B. M. Moerschbacher, "Substrates and products of chitin and chitosan modifying enzymes," *Advances in Chitin Science*, vol. 10, pp. 119–126, 2007.

[9] M. Kohlhoff, N. E. El Gueddari, C. Gorzelanny et al., "Bio-engineering of chitosans with non-random patterns of acetylation—a novel sequence-specific chitosan hydrolase generating oligomers with block-PA," *Advances in Chitin Science*, vol. 11, pp. 463–468, 2009.

[10] W. Xia, P. Liu, J. Zhang, and J. Chen, "Biological activities of chitosan and chitooligosaccharides," *Food Hydrocolloids*, vol. 25, no. 2, pp. 170–179, 2011.

[11] I. Tsigos, A. Martinou, D. Kafetzopoulos, and V. Bouriotis, "Chitin deacetylases: new, versatile tools in biotechnology," *Trends in Biotechnology*, vol. 18, no. 7, pp. 305–312, 2000.

[12] M. Chen, X. Zhu, Z. Li, X. Guo, and P. Ling, "Application of matrix-assisted laser desorption/ionization time-of-flight mass spectrometry (MALDI-TOF-MS) in preparation of chitosan oligosaccharides (COS) with degree of polymerization (DP) 5-12 containing well-distributed acetyl groups," *International Journal of Mass Spectrometry*, vol. 290, no. 2-3, pp. 94–99, 2010.

[13] B. M. Moerschbacher, F. Bernard, and N. E. El Gueddari, "Enzymatic/mass spectrometric fingerprinting of partially acetylated chitosans," *Advances in Chitin Science*, vol. 11, pp. 185–191, 2011.

[14] M. Swiontek-Brzezinska, E. Lalke-Porczyk, and W. Donderski, "Chitinolytic activity of bacteria and fungi isolated from shrimp exoskeletons," *Oceanological and Hydrobiological Studies*, vol. 36, no. 3, pp. 101–111, 2007.

[15] N. A. Manucharova, A. N. Vlasenko, G. M. Zenova, T. G. Dobrovol'skaya, and A. L. Stepanov, "Methodological aspects of assessing chitin utilization by soil microorganisms," *Biology Bulletin*, vol. 35, no. 5, pp. 549–553, 2008.

[16] S. N. Das, P. V. S. R. N. Sarma, C. Neeraja, N. Malati, and A. R. Podile, "Members of Gammaproteobacteria and Bacilli represent the culturable diversity of chitinolytic bacteria in chitin-enriched soils," *World Journal of Microbiology and Biotechnology*, vol. 26, no. 10, pp. 1875–1881, 2010.

[17] A. C. Metcalfe, M. Krsek, G. W. Gooday, J. I. Prosser, and E. M. H. Wellington, "Molecular analysis of a bacterial chitinolytic community in an upland pasture?" *Applied and Environmental Microbiology*, vol. 68, no. 10, pp. 5042–5050, 2002.

[18] V. Gohel, T. Chaudhary, P. Vyas, and H. S. Chhatpar, "Isolation and identification of marine chitinolytic bacteria and their potential in antifungal biocontrol," *Indian Journal of Experimental Biology*, vol. 42, no. 7, pp. 715–720, 2004.

[19] W. de Boer, S. Gerards, P. J. A. Klein Gunnewiek, and R. Modderman, "Response of the chitinolytic microbial community to chitin amendments of dune soils," *Biology and Fertility of Soils*, vol. 29, no. 2, pp. 170–177, 1999.

[20] L. R. Berger and D. M. Reynolds, "Colloidal chitin preparation," *Methods in Enzymology*, vol. 161, pp. 140–142, 1988.

[21] L. Vachoud, N. Zydowicz, and A. Domard, "Formation and characterisation of a physical chitin gel," *Carbohydrate Research*, vol. 302, no. 3-4, pp. 169–177, 1997.

[22] A. Hirai, H. Odani, and A. Nakajima, "Determination of degree of deacetylation of chitosan by 1H NMR spectroscopy," *Polymer Bulletin*, vol. 26, no. 1, pp. 87–94, 1991.

[23] J. H. Warcup, "The soil-plate method for isolation of fungi from soil," *Nature*, vol. 166, no. 4211, pp. 117–118, 1950.

[24] R. W. Riddell, "Permanent stained mycological preparations obtained by slide culture," *Mycologia*, vol. 42, no. 2, pp. 265–270, 1950.

[25] O. Maltseva and P. Oriel, "Monitoring of an alkaline 2,4,6-trichlorophenol-degrading enrichment culture by DNA fingerprinting methods and isolation of the responsible organism, haloalkaliphilic *Nocardioides* sp. Strain M6," *Applied and Environmental Microbiology*, vol. 63, no. 11, pp. 4145–4149, 1997.

[26] M. B. G. Rajulu, N. Thirunavukkarasu, T. S. Suryanarayanan, J. P. Ravishankar, N. E. El Gueddari, and B. M. Moerschbacher, "Chitinolytic enzymes from endophytic fungi," *Fungal Diversity*, vol. 47, no. 1, pp. 43–53, 2011.

[27] J. Trudel and A. Asselin, "Detection of chitinase activity after polyacrylamide gel electrophoresis," *Analytical Biochemistry*, vol. 178, no. 2, pp. 362–366, 1989.

[28] C. Songsiriritthigul, S. Lapboonrueng, P. Pechsrichuang, P. Pesatcha, and M. Yamabhai, "Expression and characterization of *Bacillus licheniformis* chitinase (ChiA), suitable for bioconversion of chitin waste," *Bioresource Technology*, vol. 101, no. 11, pp. 4096–4103, 2010.

[29] J. C. Hogg and M. J. Lehane, "Identification of bacterial species associated with the sheep scab mite (*Psoroptes ovis*) by using amplified genes coding for 16S rRNA," *Applied and Environmental Microbiology*, vol. 65, no. 9, pp. 4227–4229, 1999.

[30] N. Satish, S. Sultana, and V. Nanjundiah, "Diversity of soil fungi in a tropical deciduous forest in Mudumalai, southern India," *Current Science*, vol. 93, no. 5, pp. 669–677, 2007.

[31] Y. J. Choi, E. J. Kim, Z. Piao, Y. C. Yun, and Y. C. Shin, "Purification and characterization of chitosanase from *Bacillus* sp. strain KCTC 0377BP and its application for the production of chitosan oligosaccharides," *Applied and Environmental Microbiology*, vol. 70, no. 8, pp. 4522–4531, 2004.

[32] R. M. Cody, "Distribution of chitinase and chitobiase in *Bacillus*," *Current Microbiology*, vol. 19, no. 4, pp. 201–205, 1989.

[33] T. Nishijima, K. Toyota, and M. Mochizuki, "Predominant culturable *Bacillus* species in Japanese arable soils and their potential as biocontrol agents," *Microbes and Environments*, vol. 20, no. 1, pp. 61–68, 2005.

[34] L. D. Alcaraz, G. Moreno-Hagelsieb, L. E. Eguiarte, V. Souza, L. Herrera-Estrella, and G. Olmedo, "Understanding the evolutionary relationships and major traits of *Bacillus* through comparative genomics," *BMC Genomics*, vol. 11, no. 1, article 332, 2010.

[35] N. Ivanova, A. Sorokin, I. Anderson et al., "Genome sequence of *Bacillus cereus* and comparative analysis with *Bacillus anthracis*," *Nature*, vol. 423, no. 6935, pp. 87–91, 2003.

[36] C. X. Su, D. M. Wang, L. M. Yao, and Z. L. Yu, "Purification, characterization, and gene cloning of a chitosanase from *Bacillus* species strain S65," *Journal of Agricultural and Food Chemistry*, vol. 54, no. 12, pp. 4208–4214, 2006.

[37] A. A. Sherief, M. M. A. Elsawah, and M. A. A. Elnaby, "Some properties of chitinase produced a potent *Aspergillus carneus* strain," *Applied Microbiology and Biotechnology*, vol. 35, no. 2, pp. 228–230, 1991.

[38] E. F. Sharaf, "A potent chitinolytic activity of *Alternaria alternata* isolated from Egyptian black sand," *Polish Journal of Microbiology*, vol. 54, no. 2, pp. 145–151, 2005.

[39] A. A. Shindia and K. A. El-Sherbiny, "Chitosanase production using some fungi optimization of fermentation conditions of chitosanase produced by *Aspergillus ornatus*," in *Proceeding of the 2nd Scientific Environmental Conference*, pp. 97–113, Zagazig University, 2007.

[40] D. J. Adams, "Fungal cell wall chitinases and glucanases," *Microbiology*, vol. 150, no. 7, pp. 2029–2035, 2004.

[41] E. Battaglia, I. Benoit, J. van den Brink et al., "Carbohydrate-active enzymes from the zygomycete fungus *Rhizopus oryzae*: a highly specialized approach to carbohydrate degradation depicted at genome level," *BMC Genomics*, vol. 12, article 38, 2011.

[42] N. Dahiya, R. Tewari, and G. S. Hoondal, "Biotechnological aspects of chitinolytic enzymes: a review," *Applied Microbiology and Biotechnology*, vol. 71, no. 6, pp. 773–782, 2006.

[43] C. Neeraja, K. Anil, P. Purushotham et al., "Biotechnological approaches to develop bacterial chitinases as a bioshield against fungal diseases of plants," *Critical Reviews in Biotechnology*, vol. 30, no. 3, pp. 231–241, 2010.

[44] C. Y. Cheng and Y.-K. Li, "An *Aspergillus* chitosanase with potential for large-scale preparation of chitosan oligosaccharides," *Biotechnology and Applied Biochemistry*, vol. 32, no. 3, pp. 197–203, 2000.

[45] T.-W. Liang, Y.-J. Chen, Y.-H. Yen, and S.-L. Wang, "The antitumor activity of the hydrolysates of chitinous materials hydrolyzed by crude enzyme from *Bacillus amyloliquefaciens* V656," *Process Biochemistry*, vol. 42, no. 4, pp. 527–534, 2007.

Hindawi Publishing Corporation
BioMed Research International
Volume 2015, Article ID 194540, 15 pages
http://dx.doi.org/10.1155/2015/194540

Research Article

Bacterial Diversity Associated with the Coccolithophorid Algae *Emiliania huxleyi* and *Coccolithus pelagicus* f. *braarudii*

David H. Green,[1] Virginia Echavarri-Bravo,[1,2] Debra Brennan,[1] and Mark C. Hart[1]

[1] *Microbial & Molecular Biology, Scottish Association for Marine Science, Oban, Argyll PA37 1QA, UK*
[2] *School of Life Science, Heriot-Watt University, Edinburgh EH14 4AS, UK*

Correspondence should be addressed to David H. Green; david.green@sams.ac.uk

Received 28 August 2014; Accepted 30 January 2015

Academic Editor: Ameur Cherif

Coccolithophores are unicellular calcifying marine phytoplankton that can form large and conspicuous blooms in the oceans and make significant contributions to oceanic carbon cycling and atmospheric CO_2 regulation. Despite their importance, the bacterial diversity associated with these algae has not been explored for ecological or biotechnological reasons. Bacterial membership of *Emiliania huxleyi* and *Coccolithus pelagicus* f. *braarudii* cultures was assessed using cultivation and cultivation-independent methods. The communities were species rich compared to other phytoplankton cultures. Community analysis identified specific taxa which cooccur in all cultures (*Marinobacter* and *Marivita*). Hydrocarbon-degrading bacteria were found in all cultures. The presence of Acidobacteria, Acidimicrobidae, *Schlegelella*, and *Thermomonas* was unprecedented but were potentially explained by calcification associated with coccolith production. One strain of Acidobacteria was cultivated and is closely related to a marine Acidobacteria isolated from a sponge. From this assessment of the bacterial diversity of coccolithophores, a number of biotechnological opportunities are evident, from bioprospecting for novel taxa such as Acidobacteria to helping understand the relationship between obligate hydrocarbonoclastic bacteria occurrence with phytoplankton and to revealing bacterial taxa that have a specific association with algae and may be suitable candidates as a means to improve the efficiency of mass algal cultivation.

1. Introduction

Marine phytoplankton are responsible for primary production in the oceans, using sunlight and inorganic nutrients to fix carbon dioxide that becomes the organic matter that supports the biological productivity of our oceans. Crucially, the availability of inorganic nutrients, such as N, P, and Si, necessary for phytoplankton growth, is indirectly controlled by a vast array of heterotrophic bacteria and Archaea that are responsible for remineralizing the organic matter produced by the phytoplankton. In this way, the fates of both phytoplankton and bacteria in the oceans are indirectly tied to one another. Additionally, some bacteria interact directly with phytoplankton cells in ways that can be beneficial or antagonistic. Overall, this makes the diversity of bacteria associated with phytoplankton of significant biotechnological interest for the discovery of novel and exploitable biodiversity and functions, such as tropodithietic acids produced by members of the *Roseobacter* clade [1], and, more recently, as a source of beneficial bacteria to promote and sustain mass algal culture systems [2, 3] that could be used to enhance the production of products such as pigments, lipids, and polysaccharides.

Remarkably, the bacterial diversity associated with one of the most important groups of marine phytoplankton, the coccolithophores, has not previously been investigated. This is surprising given the ecological importance of coccolithophorid algae, which by forming calcified scales (coccoliths) contribute significantly to the production of pelagic carbonate, as well as making a significant contribution to oceanic carbon cycling and regulation of atmospheric CO_2 levels [4]. From a biotechnological perspective, these calcareous structures serve as solid surfaces on which bacterial colonisation can occur, which are very different mineralogically and biochemically from the organic or siliceous matrices of other phytoplankton such as dinoflagellates (e.g., cellulose armour)

and diatoms (ridged silica structures). Together, these properties suggest that there may be associated bacterial taxa that are specific to coccolithophores, as the surface of coccoliths may facilitate the formation of complex bacterial communities containing unique biodiversity as well as a complex chemical signalling and secondary metabolite production [5].

Considerable effort is now being focused on the efficient cultivation of range of algae in closed growth systems, such as photobioreactors [6]. While mass culture of coccolithophorid algae is presently of modest biotechnological interest as a means of CO_2 sequestration and lipid production [7], there is some indirect evidence that bacteria could be important to this process if it is to be developed because at least one species of coccolithophore, *Emiliania huxleyi*, has been shown to have an intimate reliance on bacterial presence [8]. Such observations are increasingly leading researchers to the suggestion that algal-associated bacteria should be considered for use in mass algal cultures systems [9, 10] and the broader realisation that there is a need to understand more about the ecological role of algal-associated bacteria, such as which taxa may be symbionts [2, 11] and the mechanisms by which they benefit their host [12, 13] and, ultimately, how to exploit this knowledge to improve the efficiency of mass algal culture systems.

The present study catalogued the cultivable and total bacterial diversity associated with laboratory cultures of *E. huxleyi* and *Coccolithus pelagicus* f. *braarudii* with the aim of uncovering associations and potential interactions between bacterial taxa and coccolithophores and generating a library of taxonomically defined cultivable bacteria for biotechnological exploitation. The study describes the total bacterial diversity of four coccolithophore cultures identified using a combination of 16S rRNA gene clone libraries and bacterial cultivation and fluorescence *in situ* hybridisation. The data revealed the presence of complex and taxonomically rich communities with a number of taxa that were unique to coccolithophores. The biotechnological potential of this diversity is discussed.

2. Materials and Methods

2.1. Algal Culture. Growth of all coccolithophore cultures (Table 1) was at 15°C in K medium diluted to (1/5)th full strength (K/5) [21] in 25 cm^2 vented tissue culture flasks (Nunc) under cool-white fluorescent light of ca. 75 μmol photons m^2 s^1 with a 12 : 12 light : dark (L : D) photoperiod. All cultures were actively calcifying. Cultures were handled aseptically to prevent bacterial contamination and cross-contamination between cultures.

The coccolithophore cultures used in this study (Table 1) were isolated using two different techniques. CCAP 920/8 was isolated by directly recovering a single calcifying cell from a water sample collected from a mesocosm experiment, using a glass capillary micropipette and growing them in an appropriate medium (J. Green pers. comm.). This mesocosm experiment (Bergen, Norway) used natural fjordic water collected and supplemented with nutrients [22, 23]. The RCC cultures were derived using a two-stage process initiated by addition of a small volume of water sample to culture media (e.g., K/5) to stimulate coccolithophore growth and, subsequently, isolate single calcifying cells by micropipette from patches of actively calcifying cells on the bottom of the growth vessel (RCC1200, RCC1203, RCC1214, and RCC1216; I. Probert pers. comm.) These cultures were derived from water samples collected as part of research cruises in oceanic and coastal regions of the Northern and Southern hemispheres. Further details can be obtained from the Roscoff Culture Collection (http://roscoff-culture-collection.org).

2.2. Bacterial Cultivation. Samples for molecular analysis were harvested by pipette from late *log* phase cultures that had been gently agitated to evenly suspend the nonmotile calcifying coccolithophores. A volume of the harvested cell suspension was serially diluted 10-fold and cell dilutions were plated onto ZM/10 agar (pH 7.8), a low organic concentration agar medium [24], and ONR7a [25] amended with trace metals and vitamins as used in ZM/10. ONR7a plates were amended with *n*-hexadecane soaked sterile filter paper. All plates were incubated in the dark at ca. 20°C for up to 8 weeks. Thereafter, unique colony morphologies were selected with the aid of a binocular microscope and were serially passaged on ZM/10 or ONR7a agar until a single colony morphotype was achieved. Several colonies of each morphology were then inoculated into 3 mL ZM/10 and ZM/1 [24] or for fastidious oil degraders and ZM/1 amended with 0.1% sodium pyruvate and grown with gentle shaking (ca. 20°C) until turbidity was visible. From each broth culture 1-2 mL was harvested for DNA extraction, and 1 mL was amended with sterile glycerol (20% v/v) and frozen at −80°C.

2.3. 16S rRNA Gene Analysis. 16S rRNA gene clone libraries were constructed from 1 mL of the suspended late *log* phase culture (as above). Bacterial and algal cells were harvested by centrifugation (13,000 ×g for 10 min), the spent medium discarded and the cell pellets stored frozen at −80°C until DNA was extracted. DNA extraction used a cetyltrimethylammonium bromide purification method [26] amended to suspend the cell pellet in 100 mM Tris-HCl (pH 8.0), 150 mM NaCl, and 10 mM EDTA, to which lysozyme (5 mg mL^{-1} final concentration) was then added and incubated at 37°C for 30 min. Bacterial 16S rRNA gene sequences were amplified by the PCR from extracted DNA based on the universal bacterial primers 27f and 1492r [27], except that 27f primer was modified to include the underlined 5′ adapter sequence (27f adapter; CTAATACGACTCAGCTATGCACTA G R-GTTTGATCMTGGCTCAG). The PCR reaction contained a final concentration of 1.8 mM Mg^{2+}, 0.5 μM of each primer, 1 U Taq polymerase and 1x PCR buffer (New England Biolabs). The amplification protocol was 94°C for 5 min, followed by 20 cycles of 55°C for 30 s, 72°C for 3 min, and 94°C for 10 s, followed by 72°C for 10 min. For each coccolithophore culture, the amplicons from three independent 50 μL PCR reactions were pooled and purified with Montage PCR filters (Millipore) and then cloned using the pGEM-T Easy vector kit (Promega). 16S clones from

Table 1: Coccolithophorid cultures examined in this study.

Coccolithophore[1]	Origin	Location	Isolation date	Culture collection
E. huxleyi				
CCAP 920/8	Bergen mesocosm, Norway	Coastal	1992	CCAP
RCC 1214	Bay of Napoli, Italy	Coastal	2000	Roscoff
RCC 1216	Tasman Sea, New Zealand	Oceanic	1998	Roscoff
C. pelagicus f. *braarudii*				
RCC 1200	South Atlantic, Namibia	Oceanic	2000	Roscoff
RCC 1203	Bay of Biscay, North Atlantic	Coastal	1999	Roscoff

[1]Cultures are also known as CCAP 920/8 = PLY B92/11; RCC 1214 = AC475; RCC 1216 = AC472; RCC 1200 = AC400; RCC 1203 = AC392.

each library were picked by sterile toothpick and reamplified using the forward adapter primer sequence (27fSeqAdapter; CTAATACGACTCAGCTATGCACT) and 1492r. This primer combination prevents amplification of the *Escherichia coli* DH5α host 16S rRNA gene. Amplicon products were cleaned using shrimp alkaline phosphatase (Promega) and exonuclease I (New England Biolabs) and then sequenced using BigDye version 3.1 terminator chemistry (Applied Biosystems) primed using the 27fSeqAdapter oligonucleotide. DNA sequence products were called on an ABI3730 instrument (Applied Biosystems). The method of DNA extraction, the primer combination of 27f and 1492r, and DNA sequencing were used for cultivable bacterial strains (cloning was omitted and the products of a single PCR amplification were submitted for DNA sequencing as above).

2.4. Phylogenetic Analysis. Bacterial 16S rRNA gene sequences were classified using the RDP II Classifier [15]. Where clone library operational taxonomic units (OTUs) corresponded to cultivable strains (>99% identity) from the same coccolithophore culture, the cultivable strain number was used to denote the OTU. All 16S sequences were screened for chimeric sequences using Bellerophon [28]. Phylogenetic inference was performed using the ARB software suite [29]. Alignments were built using NAST aligner [30] and imported into ARB and corrected as necessary. Tree constructions used a masked alignment (lanePH) and the maximum likelihood model as implemented in PhyML [31]. UniFrac analysis [32] was used to generate various statistics and principal coordinate analysis (PCoA) based on the inferred ARB PhyML tree and an unweighted dataset (i.e., not weighted for species abundance). Analysis of the clone libraries at varying levels of OTU clustering, rarefaction, and reclassification of OTU identities were performed using MOTHUR [14]. 16S rRNA gene sequences are available with the following accession numbers: EF140750-EF140751, EF140753-EF140754, EU052756, EU052761-EU052762, EU052764-EU052765, EU732746, KC295293-KC295413, and KM279011-KM279029. All cultivable strain and clone 16S sequence data were generated and sequenced in 2008, but 16S data were submitted at later dates in relationship to specific manuscript submissions.

2.5. Fluorescence In Situ Hybridisation (FISH). Cy3 labelled Acidobacteria group specific probe SS_HOL1400 [33] and EUB338 [34] were used in this study. The SS_HOL1400 probe was confirmed by pairwise alignment to have a 100% match to the two Acidobacteria identified in this study (DG1540 and OTU AC472_G8). Briefly, coccolithophore cultures were gently suspended prior to removing ca. 1 mL that was then fixed with formaldehyde (3% final concentration) for 1 hr in the dark at room temperature. Volumes of 10 to 100 μL of fixed cells were then filtered onto 25 mm 0.2 μm track-etched white polycarbonate filters and washed with 10 mL of 0.2 μm filtered deionised water. Filters were air dried, dehydrated in ethanol (50, 80, 100%), and air dried and stored at −20°C. Hybridisation and washing proceeded as described [33, 35]. Hybridised filters were mounted with Vectashield which contains the DNA stain DAPI and antifade agent and viewed by epifluorescence microscopy in the normal way using Axioskop 2plus and images captured using AxioCam HRc and processed using AxioVision (Zeiss) and Cy3 and DAPI composite epifluorescent images compiled and montaged using Adobe Photoshop CS4.

3. Results and Discussion

3.1. Community Analysis. Five cultures were sampled for cultivable bacteria and cell pellets frozen at −80°C prior to 16S rRNA gene clone library construction and analysis. Clone libraries were constructed from 16S amplicons produced from a total of 20 thermal cycles to reduce the potential for PCR artefacts and heteroduplexes [36]. A total of 316 clones from four of the five libraries were sequenced leading to the identification of 85 bacterial operational taxonomic units (OTUs) representing five bacterial phyla (Table 2). The Chao-1 estimator of species richness indicated two of the libraries to have ca. 100 phylotypes. Bacterial cultivation using a low organic strength marine agar and extended incubation periods of up to eight weeks were used and increased the overall assessment of total species richness by ca. 33% compared to clone library data alone. Cultivation identified a total of 105 unique isolates (Table 3), and, in comparison to clone library data, cultivation success varied across the different phyla, with ca. 77% of Alphaproteobacteria, 62% of Gammaproteobacteria, and 55% of Bacteroidetes being cultivable. Overall, based on the cultures with clone and cultivation data, a total of 127 phylotypes were identified which results in an average species richness of 32 phylotypes per culture (Table 2).

Table 2: Bacterial species richness deduced from cultivation and clone library studies.

Coccolithophore	OTUs[1]				Cultivable	Total
	No.	Chao-1	Shannon	Evenness		
E. huxleyi						
CCAP 920/8	17	18	2.61	0.9212	17	27
RCC 1214	25	103	2.84	0.8823	25	35
RCC 1216	15	18	2.28	0.8419	19	26
C. pelagicus f. *braarudii*						
RCC 1200	28	96	2.76	0.8282	23	39
RCC 1203	ND	ND	ND	ND	21	—

[1]Number of OTUs, Chao-1, and Shannon index calculated at 0.01 distance as calculated in MOTHUR [14]. Evenness was calculated as $(J') = H'/\ln(S)$, where H' is Shannon diversity index; S is species richness. ND: not determined.

The bacterial species richness of the coccolithophore cultures was higher than the average range of 17–19 phylotypes per dinoflagellate culture [37, 38] where the same methods were used, and higher than the 9–14 phylotypes that were identified in diatom cultures [39–41], although diatom analyses used denaturing gradient gel electrophoresis which may underestimate species richness compared to clone libraries. Nevertheless, in comparison to dinoflagellates, coccolithophores appear to maintain a more species rich bacterial community. This increased richness could have originated from the presence of higher levels of bacteria attached to coccolithophorid cells when they were isolated from field material. This may be an intrinsic property of the cell surface (e.g., coccolith production) or it could be linked to the method of culture isolation from the field (see materials and methods). Alternatively, it may be because actively growing and calcifying coccolithophores create a more complex biochemical and biophysical environment than do dinoflagellates (e.g., algal exudates, acidic polysaccharides, calcite, and increased surface area), which supports the greater diversity of bacteria observed. Illustrating the role calcified cell plates can have as an attachment point is a report describing the attachment of a nitrogen-fixing cyanobacterial symbiont to its calcifying picoeukaryote host [42].

UniFrac analysis did not detect any significant differences in pairwise comparisons between the total unweighted diversity of the four communities (OTU and cultivable; $P = 1.0$), although each community was clearly separated by UniFrac PCoA (Figure 1(b)). Rarefaction analysis of the shared diversity showed that, at the 0.01 OTU identity level, the rate of new diversity discovered was still increasing (Figure 1(a)), but that at the level of ca. family and below (≤0.10) the amount of shared diversity was nearing an asymptote (Figure 1(a)). This indicates that the communities contained a high proportion of unique species-level microdiversity [36], while the community taxonomic composition at and below the family level is conserved across the cultures. The broad diversity observed may be a product of taxonomically similar groups of bacteria being adapted to or are selected by the coccolithophores. Whereas the fine scale microdiversity seen in the 16S rRNA sequences could possibly be due to the different geographic origins of the cultures (Table 1) or selection of different ecotypes based on adaption to the coccolithophore strains or neutral sequence variation. The origin of this 16S rRNA variation is unknown but could be revealed by more in-depth analyses of a greater number and range of coccolithophore species as well as analysis of genomic variation in some of the diverse clusters [36].

The bacterial diversity of coccolithophore cultures was spread across five phyla (Figure 2). Species richness was dominated by Alphaproteobacteria (average 53%), of which just under half (43%) belonged to the *Roseobacter* clade. Gammaproteobacteria (21% on average) and Bacteroidetes (17% on average) comprised the next most prominent taxonomic groups present in all the cultures. Within the Bacteroidetes, Sphingobacteria were present in all cultures, but Flavobacteria were present in only three cultures and were relatively species poor. Betaproteobacteria and Planctomycetes were each identified in three of four cultures. Actinobacteria and Acidobacteria were each present in two cultures. The broad taxonomic composition was similar to that of dinoflagellates [37, 43–45] and diatoms [40, 41, 46] where Alphaproteobacteria dominate, with varying numbers of Bacteroidetes and Gammaproteobacteria. Qualitatively, the gammaproteobacterial composition in the coccolithophore cultures bore a greater similarity to that observed with dinoflagellates than that from diatoms. For example, *Marinobacter*, *Alcanivorax,* and oligotrophic marine Gammaproteobacteria- (OMG-) like bacteria were more common in coccolithophore as well as dinoflagellate cultures [12, 37], whereas diatom gammaproteobacterial diversity is more typically dominated by *Pseudoalteromonas* and *Alteromonas* [39, 40]. A notable difference of the coccolithophore cultures to that of dinoflagellates and diatoms was that Bacteroidetes diversity of the coccolithophores was dominated by Sphingobacteria (Figure 2) and not Flavobacteria, the latter being typically more prevalent with dinoflagellates and diatoms [47]. This shift in laboratory culture diversity may be a reflection of natural coccolithophore blooms, as the most abundant bacterial taxa (~19%) in the coccolithophore-attached fraction recovered from the Bay of Biscay were Sphingobacteria [48].

3.2. Cooccurring Bacterial Taxa: Marivita and Marinobacter. Phylotypes belonging to two phylogenetic clusters were observed in all five cultures. Strains in the first cluster

Table 3: Bacterial isolates cultivated from *E. huxleyi* and *C. pelagicus* f. *braarudii*.

Strain number	Host	Accession	Taxonomy[1]			
			Phylum/class	Family	Genus	Conf.
	E. huxleyi					
DG1395	CCAP 920/8	KC295338	Alphaproteobacteria	Sphingomonadaceae	*Sphingorhabdus*	99
DG1397	CCAP 920/8	KC295339	Alphaproteobacteria	Rhodobacteraceae	*Marivita*	100
DG1398	CCAP 920/8	KC295340	Alphaproteobacteria	Rhodobacteraceae	*Loktanella*	52
DG1399	CCAP 920/8	KC295341	Flavobacteria	Flavobacteriaceae	*Aureitalea*	60
DG1400	CCAP 920/8	KC295342	Flavobacteria	Flavobacteriaceae	*Maribacter*	100
DG1402	CCAP 920/8	EF140754	Gammaproteobacteria	Alteromonadaceae	*Marinobacter*	100
DG1403	CCAP 920/8	KC295343	Gammaproteobacteria	Piscirickettsiaceae	*Methylophaga*	100
DG1404	CCAP 920/8	KC295344	Gammaproteobacteria	Alcanivoracaceae	*Alcanivorax*	100
DG1405	CCAP 920/8	KC295345	Alphaproteobacteria	Rhodobacteraceae	*Roseovarius*	100
DG1406	CCAP 920/8	KC295346	Alphaproteobacteria	Rhodobacteraceae	*Sulfitobacter*	98
DG1407	CCAP 920/8	KC295347	Alphaproteobacteria	Rhodobacteraceae	*Sulfitobacter*	32
DG1408	CCAP 920/8	KC295348	Alphaproteobacteria	Phyllobacteriaceae	*Hoeflea*	100
DG1410	CCAP 920/8	KC295349	Sphingobacteria	Chitinophagaceae	*Balneola*	100
DG1412	CCAP 920/8	KC295350	Flavobacteria	Flavobacteriaceae	*Arenibacter*	100
DG1413	CCAP 920/8	KC295351	Sphingobacteria	Flammeovirgaceae	*Marinoscillum*	100
DG1414	CCAP 920/8	KC295352	Alphaproteobacteria	Rhodobacteraceae	*Ahrensia*	35
DG1417	CCAP 920/8	EU052756	Alphaproteobacteria	Rhodospirillaceae	*Thalassospira*	100
DG1442	RCC 1216	KC295353	Alphaproteobacteria	Phyllobacteriaceae	*Ahrensia*	29
DG1443	RCC 1216	KC295354	Alphaproteobacteria	Rhodobacteraceae	*Roseovarius*	47
DG1444	RCC 1216	KC295355	Alphaproteobacteria	Rhodobacteraceae	*Ahrensia*	42
DG1445	RCC 1216	KC295356	Sphingobacteria	Flammeovirgaceae	*Fabibacter*	82
DG1447	RCC 1216	KC295357	Alphaproteobacteria	Rhodospirillaceae	*Nisaea*	100
DG1448	RCC 1216	KC295358	Alphaproteobacteria	Hyphomonadaceae	*Hyphomonas*	73
DG1449	RCC 1216	KC295359	Alphaproteobacteria	Rhodobacteraceae	*Marivita*	100
DG1452	RCC 1216	KC295360	Alphaproteobacteria	Phyllobacteriaceae	*Hoeflea*	100
DG1453	RCC 1216	KC295361	Alphaproteobacteria	Rhodobiaceae	*Roseospirillum*	37
DG1457	RCC 1216	KC295362	Gammaproteobacteria	Oceanospirillaceae	*Oceaniserpentilla*	20
DG1459	RCC 1216	KC295363	Gammaproteobacteria	Gammaproteobacteria	Unclassified	—
DG1462	RCC 1216	KC295364	Alphaproteobacteria	Rhodobacteraceae	*Roseovarius*	52
DG1468	RCC 1216	KC295365	Alphaproteobacteria	Phyllobacteriaceae	*Hoeflea*	100
DG1471	RCC 1216	KC295366	Gammaproteobacteria	Alteromonadaceae	*Marinobacter*	100
DG1473	RCC 1216	KC295367	Alphaproteobacteria	Kordiimonadaceae	*Kordiimonas*	100
DG1475	RCC 1216	KC295368	Alphaproteobacteria	Rhodobacteraceae	*Roseovarius*	91
DG1476	RCC 1216	KC295369	Alphaproteobacteria	Rhodobacteraceae	*Phaeobacter*	100
DG1477	RCC 1216	KC295370	Gammaproteobacteria	Gammaproteobacteria	*Congregibacter*	100
DG1592	RCC 1216	EU052761	Gammaproteobacteria	Alcanivoracaceae	*Alcanivorax*	100
DG1516	RCC 1214	KC295392	Alphaproteobacteria	Rhodospirillaceae	*Nisaea*	100
DG1517	RCC 1214	KC295393	Alphaproteobacteria	Rhodobacteraceae	*Marivita*	100
DG1519	RCC 1214	KC295394	Alphaproteobacteria	Rhodobacteraceae	*Oceanicola*	65
DG1520	RCC 1214	KC295395	Alphaproteobacteria	Rhodobacteraceae	*Roseovarius*	47
DG1521	RCC 1214	KC295396	Alphaproteobacteria	Rhodobacteraceae	*Roseovarius*	100
DG1523	RCC 1214	KC295397	Alphaproteobacteria	Hyphomonadaceae	*Hyphomonas*	100
DG1524	RCC 1214	KC295398	Sphingobacteria	Chitinophagaceae	*Balneola*	83
DG1525	RCC 1214	KC295399	Alphaproteobacteria	Kordiimonadaceae	*Kordiimonas*	100
DG1526	RCC 1214	KC295400	Alphaproteobacteria	Sneathiellaceae	*Oceanibacterium*	44
DG1530	RCC 1214	KC295401	Alphaproteobacteria	Rhodobacteraceae	*Oceanicola*	14

Table 3: Continued.

Strain number	Host	Accession	Taxonomy[1]			
			Phylum/class	Family	Genus	Conf.
DG1531	RCC 1214	KC295402	Alphaproteobacteria	Erythrobacteraceae	*Altererythrobacter*	96
DG1532	RCC 1214	KC295403	Alphaproteobacteria	Rhodobacteraceae	*Ahrensia*	35
DG1533	RCC 1214	KC295404	Alphaproteobacteria	Rhodobacteraceae	*Loktanella*	67
DG1534	RCC 1214	KC295405	Gammaproteobacteria	Gammaproteobacteria	*Congregibacter*	100
DG1536	RCC 1214	KC295406	Gammaproteobacteria	Alteromonadaceae	*Marinobacter*	100
DG1538	RCC 1214	KC295407	Actinobacteria	Acidimicrobiaceae	*Ilumatobacter*	100
DG1540	RCC 1214	KC295408	Acidobacteria	Acanthopleuribacteraceae	*Acanthopleuribacter*	100
DG1544	RCC 1214	KC295409	Sphingobacteria	Flammeovirgaceae	*Echidna*	100
DG1545	RCC 1214	KC295410	Sphingobacteria	Cytophagaceae	*Leadbetterella*	82
DG1546	RCC 1214	KC295411	Alphaproteobacteria	Rhodobacteraceae	*Roseovarius*	82
DG1548	RCC 1214	KC295412	Alphaproteobacteria	Rhodospirillaceae	*Tistlia*	31
DG1588	RCC 1214	KC295413	Alphaproteobacteria	Hyphomonadaceae	*Hyphomonas*	93
DG1593	RCC 1214	EU052762	Gammaproteobacteria	Alcanivoracaceae	*Alcanivorax*	100
DG1594	RCC 1214	EF140750	Gammaproteobacteria	Alteromonadaceae	*Marinobacter*	100
DG1595	RCC 1214	EF140751	Gammaproteobacteria	Alteromonadaceae	*Marinobacter*	100
	C. pelagicus f. *braarudii*					
DG1479	RCC 1200	KC295371	Alphaproteobacteria	Rhodobacteraceae	*Oceanicola*	70
DG1481	RCC 1200	KC295372	Flavobacteria	Flavobacteriaceae	*Tenacibaculum*	81
DG1483	RCC 1200	KC295373	Alphaproteobacteria	Sneathiellaceae	*Oceanibacterium*	51
DG1484	RCC 1200	KC295374	Alphaproteobacteria	Rhodobacteraceae	*Marivita*	100
DG1486	RCC 1200	KC295375	Alphaproteobacteria	Phyllobacteriaceae	*Hoeflea*	100
DG1487	RCC 1200	KC295376	Alphaproteobacteria	Rhodobacteraceae	*Marivita*	100
DG1489	RCC 1200	KC295377	Alphaproteobacteria	Rhodobacteraceae	*Ahrensia*	46
DG1492	RCC 1200	KC295378	Alphaproteobacteria	Rhodobacteraceae	*Sulfitobacter*	64
DG1494	RCC 1200	KC295379	Alphaproteobacteria	Rhodospirillaceae	*Magnetospira*	73
DG1498	RCC 1200	KC295380	Alphaproteobacteria	Rhodobacteraceae	*Roseovarius*	100
DG1500	RCC 1200	KC295381	Alphaproteobacteria	Hyphomonadaceae	*Hyphomonas*	100
DG1501	RCC 1200	KC295382	Actinobacteria	Acidimicrobidae	*Ilumatobacter*	100
DG1502	RCC 1200	KC295383	Sphingobacteria	Chitinophagaceae	*Balneola*	100
DG1503	RCC 1200	KC295384	Alphaproteobacteria	Rhodobacteraceae	*Jannaschia*	40
DG1504	RCC 1200	KC295385	Alphaproteobacteria	Rhodobacteraceae	*Roseovarius*	80
DG1506	RCC 1200	KC295386	Alphaproteobacteria	Sphingomonadaceae	*Sphingopyxis*	55
DG1507	RCC 1200	KC295387	Gammaproteobacteria	Piscirickettsiaceae	*Methylophaga*	100
DG1510	RCC 1200	KC295388	Flavobacteria	Cryomorphaceae	*Wandonia*	62
DG1511	RCC 1200	KC295389	Alphaproteobacteria	Rhodobacteraceae	*Loktanella*	68
DG1512	RCC 1200	KC295390	Gammaproteobacteria	Oleiphilaceae	*Oleiphilus*	61
DG1513	RCC 1200	KC295391	Alphaproteobacteria	Hyphomonadaceae	*Hyphomonas*	65
DG1597	RCC 1200	EF140753	Gammaproteobacteria	Alteromonadaceae	*Marinobacter*	100
DG1599	RCC 1200	EU052764	Alphaproteobacteria	Rhodobacteraceae	*Maritimibacter*	59
DG1554	RCC 1203	KM279011	Alphaproteobacteria	Rhodobacteraceae	*Marivita*	100
DG1555	RCC 1203	KM279012	Alphaproteobacteria	Phyllobacteriaceae	*Hoeflea*	100
DG1556	RCC 1203	EU732746	Gammaproteobacteria	Alteromonadaceae	*Marinobacter*	100
DG1557	RCC 1203	KM279013	Alphaproteobacteria	Rhodobacteraceae	*Loktanella*	74
DG1558	RCC 1203	KM279014	Alphaproteobacteria	Rhodobacteraceae	*Roseovarius*	55
DG1561	RCC 1203	KM279015	Gammaproteobacteria	Alteromonadaceae	*Aestuariibacter*	71
DG1562	RCC 1203	KM279016	Alphaproteobacteria	Rhodobacteraceae	*Roseovarius*	62
DG1563	RCC 1203	KM279017	Alphaproteobacteria	Rhodospirillaceae	*Magnetospira*	64

Table 3: Continued.

Strain number	Host	Accession	Taxonomy[1]			
			Phylum/class	Family	Genus	Conf.
DG1564	RCC 1203	KM279018	Alphaproteobacteria	Hyphomonadaceae	*Hyphomonas*	100
DG1565	RCC 1203	KM279019	Gammaproteobacteria	Oceanospirillaceae	*Oceaniserpentilla*	16
DG1566	RCC 1203	KM279020	Alphaproteobacteria	Rhodobacteraceae	*Roseovarius*	46
DG1567	RCC 1203	KM279021	Alphaproteobacteria	Rhodobacteraceae	*Roseovarius*	100
DG1568	RCC 1203	KM279022	Cytophagia	Flammeovirgaceae	*Marinoscillum*	100
DG1569	RCC 1203	KM279023	Alphaproteobacteria	Rhodobacteraceae	*Loktanella*	64
DG1570	RCC 1203	KM279024	Alphaproteobacteria	Rhodobacteraceae	*Roseovarius*	100
DG1572	RCC 1203	KM279025	Alphaproteobacteria	Rhodobacteraceae	*Sulfitobacter*	57
DG1575	RCC 1203	KM279026	Gammaproteobacteria	Gammaproteobacteria	*Porticoccus*	98
DG1576	RCC 1203	KM279027	Cytophagia	Flammeovirgaceae	*Marinoscillum*	100
DG1579	RCC 1203	KM279028	Flavobacteriia	Cryomorphaceae	*Brumimicrobium*	54
DG1582	RCC 1203	KM279029	Betaproteobacteria	Burkholderiaceae	*Limnobacter*	100

[1]Taxonomic assignment was determined using the RDP II naive Bayesian classifier [15]; Conf.: Bayesian confidence for the rank of genera only is shown.

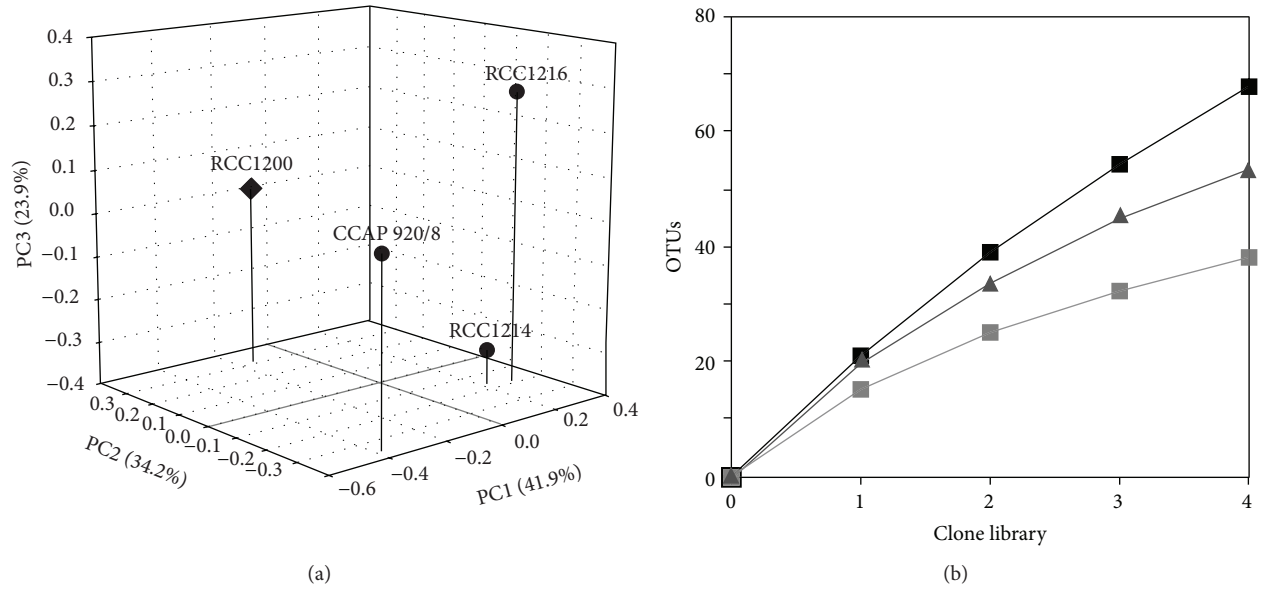

Figure 1: Total bacterial community analysis. (a) Unweighted UniFrac principal coordinate analysis of the total bacterial diversity of *E. huxleyi* (●) and *C. pelagicus* f. *braarudii* (◆) cultures. (b) Rarefaction analysis of shared 16S clone library diversity at OTU clustering levels of 0.01 (black ■), 0.05 (grey ▲), and 0.1 (grey ■) was based on an average of 79 sequenced clones per library.

(DG1397, 1449, 1484, 1487, 1517, and 1554) were closely related (≥98.2% identity) to the type strains of the genus *Marivita* (Figure 3(a)). To date, there is relatively little known about the genus Marivita, but related phylotypes have been identified with a range of algal cultures [24, 38, 49, 50], as well as representing ca. 4–6% of the phylotype abundance in summer and autumn clone libraries from productive surface waters off the north west of Spain [51]. In other work, we have observed that strains of *Marivita* (as well as other taxa) act as dinoflagellate symbionts promoting dinoflagellate growth (D. Green and C. J. S. Bolch, publication in prep.). Collectively, this suggests that *Marivita* may have a specific adaptation to associating with phytoplankton, including coccolithophores, and could be analogous to the other Roseobacters that are regarded as algal symbionts, such as *Dinoroseobacter shibae* [52].

The second phylogenetic cluster was cultivable isolates belonging to the gammaproteobacterial genus *Marinobacter* (Figure 3(b)). *Marinobacter* have been found with a range of algae, principally dinoflagellates [37, 38, 43, 45, 53] and some diatoms [12]. Despite an apparent algal culture association, their abundance in the marine environment is typically low; for example, the multiyear average in the Western English Channel was ca. 0.18% (min. 0.00% and max. 4.5%) of total pyrosequencing reads [19]. One explanation for this disparity could be that the frequent association with laboratory cultures represents a laboratory-induced artefact caused by algal cultivation that is selecting for *Marinobacter*, possibly

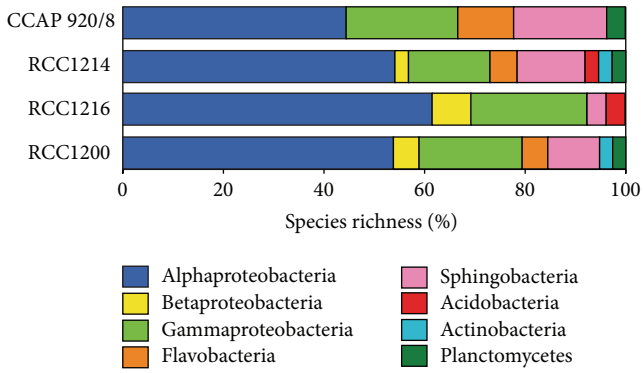

Figure 2: Taxonomic composition of the total bacterial community. Percentage species richness was based on the number of unique clone library and cultivable phylotypes identified in each culture.

based on their utilisation of algal aliphatics. However, their markedly lower frequency in diatom cultures (~22%, as compared to ≥83% in coccolithophore and dinoflagellate cultures; [12]) argues against their presence being a simple laboratory artefact because algal culture media and methodology are similar for all three algal lineages and this should not cause such a bias. We speculate that *Marinobacter* have a specific adaptation to coccolithophores and dinoflagellates. As *Marinobacter* have been recognised in the context of algal-bacterial interactions, such as increasing iron bioavailability to dinoflagellates [12], promoting growth of the dinoflagellate *G. catenatum* [54] and the cyanobacterium *Prochlorococcus* [55], this provides some support to the hypothesis that this association represents a specific adaptation to life with these algae.

In the context of applying bacteria to improve the mass cultivation of algae, the evidence from this study and others point toward *Marivita* and *Marinobacter* as two candidate bacterial groups that have some potential because of their common cooccurrence with algal cultures, as well as evidence that strains of both genera can have beneficial effects such as growth promotion. Furthermore, neither genus has been linked to antagonistic interactions with algae that we are aware of.

3.3. Hydrocarbon-Degrading Bacteria. In the present study, we sought to identify whether there were hydrocarbon-degrading bacteria present in these cultures, as we have previously observed an association with algae [24]. We identified and confirmed that all the *Alcanivorax* and *Marinobacter* strains that were isolated could utilise *n*-hexadecane as the sole carbon and energy source (Figure 3). This is consistent with a number of reports showing that both genera are important and are often highly abundant in the marine environment during oil spill events (e.g. [56]). Four strains that did not belong to these two genera were also shown to use *n*-hexadecane: one was a member of the Alteromonadaceae (DG1561), three were members of Alphaproteobacteria belonging to *Maritimibacter* of the *Roseobacter* clade (DG1599), and *Thalassospira* (DG1417) and *Nisaea* (DG1516) both belonged to the Rhodospirillaceae. This study and others reporting the coassociation of oil-degrading bacteria and algae [24, 57–59] suggest that there may be a specific association between the two. The simplest explanation for this may reflect the fact that many microalgae are lipid-rich [60] and that, in the natural environment, algal cells provide an abundant source of energy-rich aliphatic compounds available to hydrocarbonoclastic bacteria.

The presence of hydrocarbon-degrading bacteria living with algae presents a number of biotechnological opportunities. First, we believe that it is important to understand their ecological relationship to algae in the marine environment and then to use this knowledge to try improving natural oil spill bioremediation: for example, will there be better natural bioremediation of oil spills in regions that are dominated by primary production? Or is the use of iron fertilization during oil spill events beneficial in stimulating both primary production and the associated bacterial community that clearly comprises many key hydrocarbonoclastic bacteria such as *Alcanivorax*, as well as ensuring a sufficient supply of iron for the iron-requiring alkane hydroxylases of all oil-degrading bacteria [61]? Second, specific genes and activities of oil-degraders can potentially be exploited for biosurfactant, bioemulsifier [62, 63], or polyhydroxyalkanoate production [64], or the potential development of alkane hydroxylases to catalyze difficult-to-synthesize molecules [65]. While hydrocarbon-degrading strains from coccolithophores have not been explored for polycyclic aromatic hydrocarbon (PAH) degradation, related research with other algae shows that they do harbor highly fastidious PAH degrading bacteria [58, 59]. Overall, coccolithophore and other phytoplankton cultures are a useful starting point for bioprospecting for specialist hydrocarbon-degrading microorganisms. They may also be used as model systems to study the ecological underpinnings of this interrelationship, with the aim to use this knowledge to help enhance oil bioremediation.

3.4. Atypical Bacterial Taxa. A number of the phylotypes identified were not typical of bacterial taxa found previously with algal cultures. First was the identification of two phylotypes belonging to the phylum Acidobacteria (Figure 3(b)), which have not previously been identified in any algal culture. OTU AC472G8 was affiliated to Group IV Acidobacteria, which appear to be rare in the marine environment (e.g., the closest marine phylotypes is DQ071127; 95.6% id). The other Acidobacteria, DG1540 (KC295408), was affiliated to the Holophagales (group VIII). This isolate was cultivated on the low organic strength marine agar ZM/10 at ca. pH 7.8. Subsequent cultivation experiments with this strain demonstrated that it did not grow at pH values below pH 7.0 but grew abundantly up to pH 9.5, the highest pH tested (data not shown). This indicates that while it is related to the phylum Acidobacteria, it is not acidophilic as is characteristic of this phylum. The closest 16S rRNA gene sequences to DG1540 were all marine and belonged to coral-associated bacterial clones (FJ202764.1, FJ203188.1; 89.3 and 88.4% id resp.), a sponge-associated bacterial isolate (EF629834; 95.6% id), and *Acanthopleuribacter pedis* (AB303221; 88.6% id) isolated from a marine chiton [66]. The second atypical taxon was

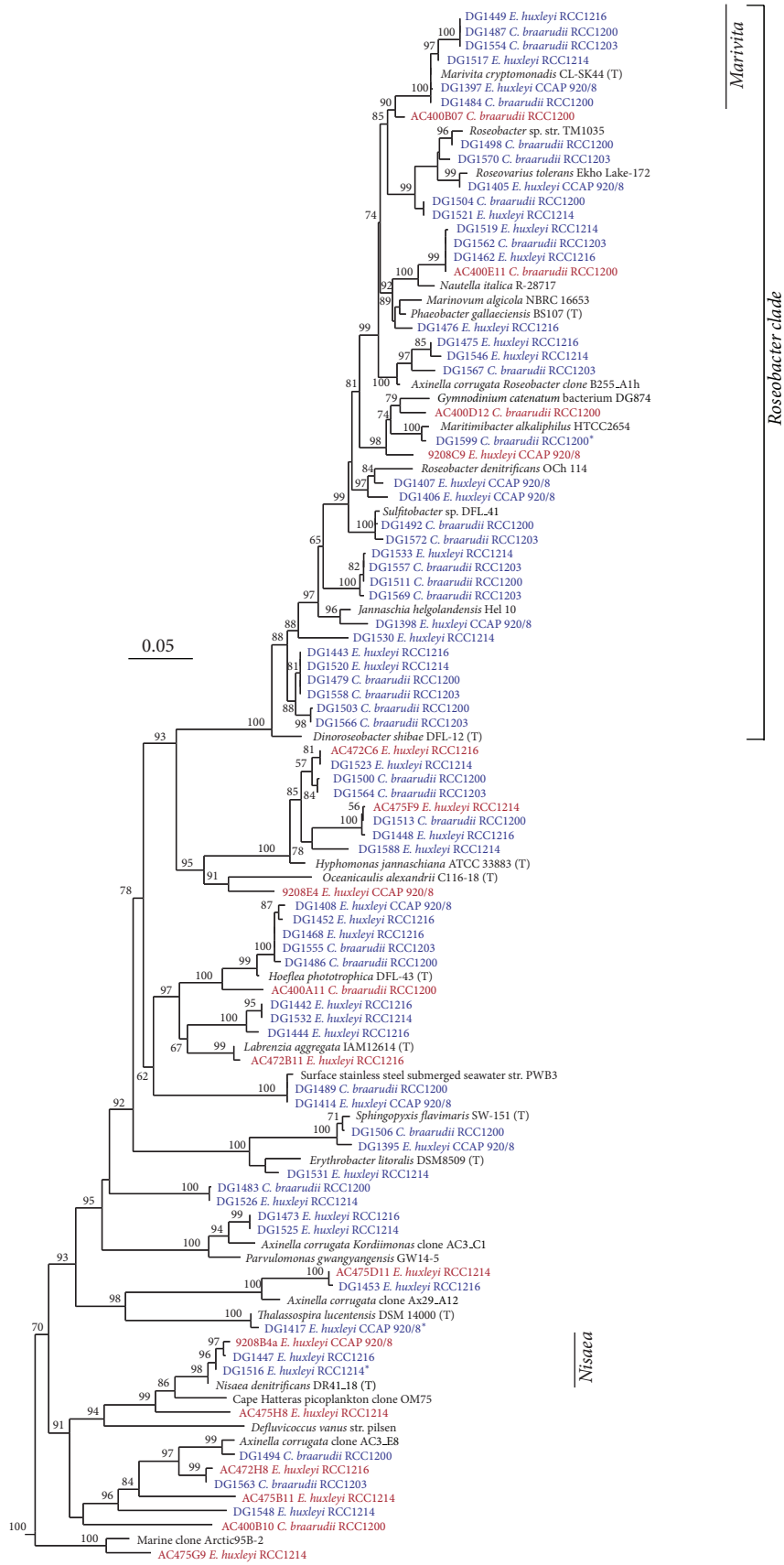

(a)

Figure 3: Continued.

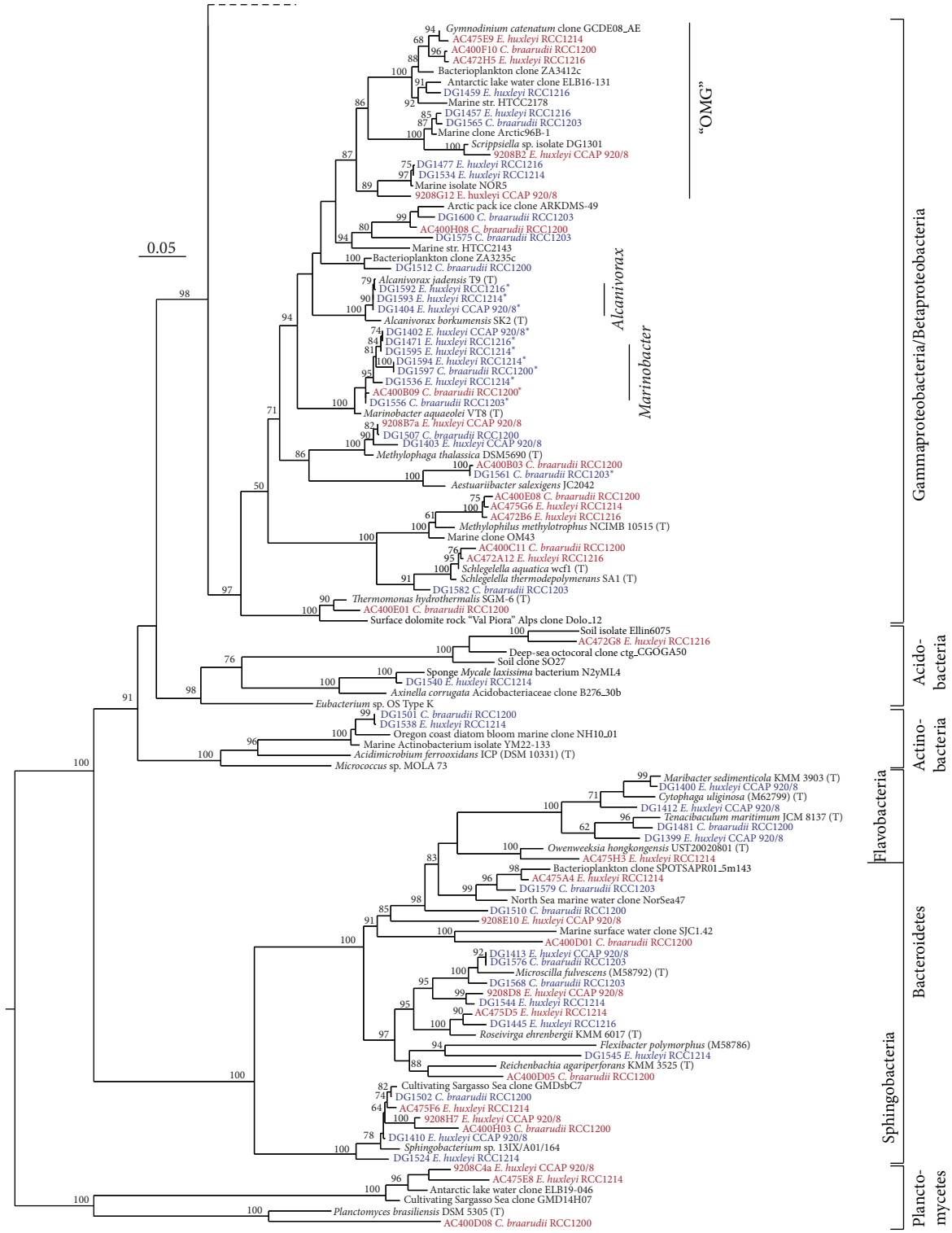

(b)

Figure 3: Phylogenetic affiliation (16S rRNA gene) of coccolithophore-associated bacteria, depicting (a) Alphaproteobacteria and (b) Gammaproteobacteria, Betaproteobacteria, Acidobacteria, Actinobacteria, Bacteroidetes, and Planctomycetes. Dendrograms were constructed using a lanePH filtered alignment using maximum likelihood and the HKY model of nucleotide substitution (PhyML). Bootstrap support ≥50% support for the branching is shown. ∗ denotes strains shown to use *n*-hexadecane as a sole carbon source. Clones (red font) and strains (blue font) identified in this study and representative clones or strains from public databases (black font). Scale bar: 0.05 nucleotide substitutions per base.

Table 4: Biogeography of rare bacterial taxa in the marine environment.

Project[1]	Acidobacteria	Acidimicrobiales	*Schlegelella*	*Thermomonas*
ICoMM surface seawater (≤50 m)				
CAM	0.006	0.215	0	0.009
AWP	0.010	0.327	0	0
AOT	0.005	3.248	0	<0.001
ABR	0.001	1.435	0	0
LCR	0.038	2.696	0.004	0.008
PML	0.054	0.726	0.001	<0.001
ICoMM coral, sponge, and microbial mats				
CCB	1.368	1.065	0	0
CMM	0.955	6.806	0.001	0.002
SPO	7.718	5.318	0	0

[1] Average percentage abundance identified from each ICoMM project, normalised for sequencing effort. Data was compiled from publically accessible data at ICoMM Marine Microbes Database (http://vamps.mbl.edu/). CAM: census of Antarctic marine life [16]; AWP: Azores water profile; AOT: Atlantic Ocean transect; ABR: active but rare (Nth and Sth Pacific) [17]; LCR: latitudinal gradient from South Atlantic to the Caribbean [18]; PML, English Channel L4, UK [19]; CCB: microbial diversity in Caribbean coral species; CMM: coastal microbial mats; SPO: marine sponge-associated bacteria [20].

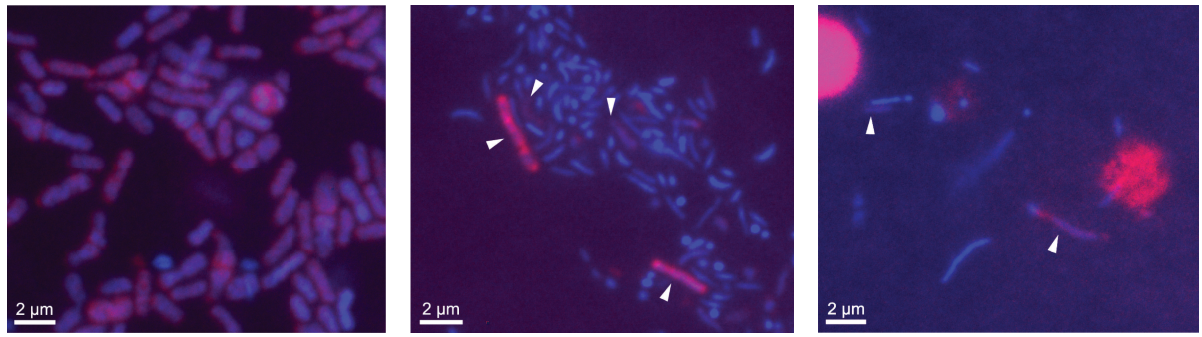

(a) (b) (c)

Figure 4: Composite DAPI-Cy3 FISH detection of Acidobacteria in coccolithophore cultures. (a) Positive control DG1540 (isolated from *E. huxleyi* RCC1214). (b) *E. huxleyi* RCC1214 culture and (c) *E. huxleyi* Bergen_05_08 (Bergen mesocosm, 2008). Arrowheads indicate Acidobacteria cells present on the DAPI-Cy3 composite images. Scale bar: 2 μm.

two cultivable Actinobacteria strains (DG1501 and DG1538) affiliated to the family Acidimicrobidae. A single Acidimicrobidae OTU (DQ376149; 97.0% id) has previously been identified in a diatom culture. Related Acidimicrobidae OTUs and isolates have been found in a range of marine samples (Table 4), including corals (GU118194; ca. 92.9% id), sponges (EU236418; ca. 94.8% id), marine sediment (AB286031; ca. 96.8% id), and surface waters (GQ850547 and DQ372838; ca. 98.1 and 94.5% id resp.). Third, a gammaproteobacterial OTU affiliated to *Thermomonas* was identified in one culture only. This genus has been identified in thermal springs [67] and at several oceanic stations and in microbial mat communities (Table 4). Fourth, two OTUs belonging to the genus *Schlegelella* (Betaproteobacteria) were identified in two separate cultures. Like *Thermomonas*, this genus has been observed in mineral springs [67, 68] and has been recorded in the marine environment from the same sites as *Thermomonas* (Table 4). Finally, three very closely related OTUs (≥97.5% ID) affiliated to the Methylophilaceae (Betaproteobacteria) were identified but not cultured. These OTUs are distantly related to the well-described OM43 clade (≥87.9% ID) of obligate methylotrophic bacteria linked with phytoplankton blooms [69], and, to our knowledge, only a single related OTU has previously been identified in an algal culture (KEppi37, AF188168; [43]).

As the observation of Acidobacteria in algal cultures was apparently unusual, an additional three *E. huxleyi* cultures were screened using a phylum-level Acidobacteria FISH probe, these were LY1_05 (LY1 2005, Oban, Scotland), Bergen_05_08 (Bergen Mesocosm, 2008, Norway), and CS_08 (Celtic Sea 2008, UK). The positive control, DG1540 (Figure 4(a)), was identified in RCC1214 from where it had originally been isolated (Figure 4(b)). However, Acidobacteria were not detected in RCC1216 from which the group IV acidobacterial OTU AC472G8 had been identified. Acidobacteria were detected in the Bergen mesocosm culture isolated in 2008 (Bergen _05_08) (Figure 4(c)).

The presence of Acidobacteria (DG1540 and AC472G8, as well as FISH detection in one other *E. huxleyi* culture; Figure 4) and the Acidimicrobidae (Actinobacteria) led us to consider why putatively acidophilic bacteria were associated with *E. huxleyi*. We speculate that this may reflect a pattern

of finding marine Acidobacteria associated with calcareous organisms or structures such as the chiton [66], corals [70], and stromatolites [71]. The reasons for their association with carbonate structures are unclear, but these organisms may be involved in catabolizing the organic matrix associated with the coccoliths and potentially driving calcite dissolution through acid production [72]. The observation of *Schlegelella* and *Thermomonas* in the cultures may also be attributable to calcification in the cultures because both *Schlegelella* and *Thermomonas* OTUs have been isolated from thermal spring waters containing a high mineral and carbonate loading [67, 68]. As both genera have been identified by pyrosequencing from marine environmental samples (Table 4), this suggests that their presence could be related to the high mineral content of calcifying coccolithophores and not the product of external contamination of the cultures.

The lack of phylogenetic coherence amongst the atypical taxa detected does not appear to be an ecological pattern, but we suggest that, from the biochemical associations of related taxa to those detected in this study (Figure 3(b)), this points at carbonate chemistry as the most likely reason explaining their presence. This may also explain why these taxa have not previously been identified with diatoms and dinoflagellates, because the latter are not calcifying organisms. Thus, we speculate that the atypical taxa such as Acidobacteria, *Schlegelella,* and *Thermomonas* are evidence that actively calcifying coccolithophores chemically and physically structure the bacterial community to include organisms adapted to calcareous material. This is analogous to the way in which diatom exudates structure the bacterial associates in culture [40] and of estuarine sediments [73].

Cultivation of DG1540 and related Acidobacteria (N2yML4; EF629834) from sponge aquaculture [74] represent a potentially valuable biotechnological and ecological resource because of their taxonomic relationship to prevalent groups of bacteria in sponge and coral microbial communities [20, 75]. Whether or not these Acidobacteria produce secondary metabolites is of clear interest given the importance of the marine sponge microbiome for production of a wide range of novel chemical entities [76]. However, cultivation of these and other marine Acidobacteria has clearly been sporadic (totalling three: this study, Mohamed et al. 2008 [74], and Fukunaga et al. 2008 [66]) despite the many efforts to cultivate sponge and coral bacteria. This indicates a need to develop different primary isolation media and strategies to improve discovery of these and related Acidobacteria, as well as the other atypical taxa identified in this study. The inclusion of solid carbonate (or siliceous) material in agar or in liquid enrichment media may be one starting point; and addition of 5% CO_2 (v/v) has been successfully used to improve isolation of soil Acidobacteria [77]. The question of whether all or any marine Acidobacteria are acidophilic is unclear given that ambient seawater pH is typically nearer to pH 8 and the evidence that DG1540 would not grow below pH 7. Genomic analysis of DG1540 is now underway, and this data will be mined to address questions of their ecological, metabolic and biotechnological potential, as well as contribute to cultivation efforts of related marine Acidobacteria found with corals and sponges.

4. Conclusions

The present study is the first to catalogue the bacterial diversity associated with two important species of coccolithophorid phytoplankton. It revealed that both *E. huxleyi* and *C. pelagicus* f. *braarudii* cultures had relatively species rich bacterial communities compared to dinoflagellates. It identified a number of bacterial taxa not previously detected in other phytoplankton cultures and included the unexpected finding of a number of putatively acidophilic bacteria. Overall, this is suggested to signify that coccolithophores possess a greater range of available niches, as well as novel niches, compared to other kinds of phytoplankton such as dinoflagellates and diatoms. It is proposed that the presence of some of the atypical taxa may represent selection of specific bacterial taxa adapted to the active calcification occurring in these coccolithophore cultures. The cultures were observed to share bacterial diversity with other algal cultures, most notably, dinoflagellates. Two genera, *Marinobacter* and *Marivita*, were observed to occur in all of the coccolithophore cultures, and whilst these genera may be a product of laboratory culture induced artefacts, closely related bacteria have been shown to benefit dinoflagellate and *Prochlorococcus* growth, suggesting that the common occurrence of these bacteria may represent a specific interdependence between the bacteria and algae. Hydrocarbon-degrading bacteria were found in all cultures, and, most notably, each *E. huxleyi* culture had a closely related strain of *Alcanivorax*, a well-known and highly fastidious oil-degrading bacterium.

Knowledge of the biodiversity contained within these coccolithophore cultures has a number of potential uses, that include the types of bacteria that could be employed to improve the efficiency of mass cultivation of marine algae, and, as a model system to help uncover the ecological relationship of why oil-degrading bacteria cooccur with phytoplankton, and how this knowledge may be used to improve oil-spill bioremediation. Furthermore, the cultivation of a marine bacterium related to Acidobacteria found with marine sponges represents a rare opportunity to understand more about the ecology of these bacteria and to explore the biotechnological potential this may entail.

Conflict of Interests

The authors declare that there is no conflict of interests regarding the publication of this paper.

Acknowledgments

The authors are grateful to I. Probert (AlgoBank) and C. Campbell (CCAP) for algal strain provision. Virginia Echavarri-Bravo was very kindly supported by a SAMS Research Bursary. DNA sequencing was supported by a UK Natural Environment Research Council (NERC) NBAF facilities access Grant no. 5172 and NERC Oceans 2025 funding.

References

[1] T. Brinkhoff, G. Bach, T. Heidorn, L. Liang, A. Schlingloff, and M. Simon, "Antibiotic production by a *Roseobacter* clade-affiliated species from the German Wadden Sea and its antagonistic effects on indigenous isolates," *Applied and Environmental Microbiology*, vol. 70, no. 4, pp. 2560–2565, 2004.

[2] M. Le Chevanton, M. Garnier, G. Bougaran et al., "Screening and selection of growth-promoting bacteria for *Dunaliella* cultures," *Algal Research*, vol. 2, no. 3, pp. 212–222, 2013.

[3] Suminto and K. Hirayama, "Application of a growth-promoting bacteria for stable mass culture of three marine microalgae," *Hydrobiologia*, vol. 358, pp. 223–230, 1997.

[4] A. Ridgwell, D. N. Schmidt, C. Turley et al., "From laboratory manipulations to Earth system models: scaling calcification impacts of ocean acidification," *Biogeosciences*, vol. 6, no. 11, pp. 2611–2623, 2009.

[5] C. Holmström and S. Kjelleberg, "Marine *Pseudoalteromonas* species are associated with higher organisms and produce biologically active extracellular agents," *FEMS Microbiology Ecology*, vol. 30, no. 4, pp. 285–293, 1999.

[6] E. Molina Grima, F. G. A. Fernández, F. García Camacho, and Y. Chisti, "Photobioreactors: light regime, mass transfer, and scaleup," *Journal of Biotechnology*, vol. 70, no. 1–3, pp. 231–247, 1999.

[7] N. R. Moheimani, J. P. Webb, and M. A. Borowitzka, "Bioremediation and other potential applications of coccolithophorid algae: a review," *Algal Research*, vol. 1, no. 2, pp. 120–133, 2012.

[8] K. E. Helliwell, G. L. Wheeler, K. C. Leptos, R. E. Goldstein, and A. G. Smith, "Insights into the evolution of vitamin B12 auxotrophy from sequenced algal genomes," *Molecular Biology and Evolution*, vol. 28, no. 10, pp. 2921–2933, 2011.

[9] E. Kazamia, D. C. Aldridge, and A. G. Smith, "Synthetic ecology—a way forward for sustainable algal biofuel production?" *Journal of Biotechnology*, vol. 162, no. 1, pp. 163–169, 2012.

[10] V. H. Smith and T. Crews, "Applying ecological principles of crop cultivation in large-scale algal biomass production," *Algal Research*, vol. 4, no. 1, pp. 23–34, 2014.

[11] H. Geng and R. Belas, "Molecular mechanisms underlying roseobacter-phytoplankton symbioses," *Current Opinion in Biotechnology*, vol. 21, no. 3, pp. 332–338, 2010.

[12] S. A. Amin, D. H. Green, M. C. Hart, F. C. Küpper, W. G. Sunda, and C. J. Carrano, "Photolysis of iron-siderophore chelates promotes bacterial-algal mutualism," *Proceedings of the National Academy of Sciences of the United States of America*, vol. 106, no. 40, pp. 17071–17076, 2009.

[13] M. T. Croft, A. D. Lawrence, E. Raux-Deery, M. J. Warren, and A. G. Smith, "Algae acquire vitamin B12 through a symbiotic relationship with bacteria," *Nature*, vol. 438, no. 7064, pp. 90–93, 2005.

[14] P. D. Schloss, S. L. Westcott, T. Ryabin et al., "Introducing mothur: open-source, platform-independent, community-supported software for describing and comparing microbial communities," *Applied and Environmental Microbiology*, vol. 75, no. 23, pp. 7537–7541, 2009.

[15] Q. Wang, G. M. Garrity, J. M. Tiedje, and J. R. Cole, "Naïve Bayesian classifier for rapid assignment of rRNA sequences into the new bacterial taxonomy," *Applied and Environmental Microbiology*, vol. 73, no. 16, pp. 5261–5267, 2007.

[16] J. F. Ghiglione, P. E. Galand, T. Pommier et al., "Pole-to-pole biogeography of surface and deep marine bacterial communities," *Proceedings of the National Academy of Sciences of the United States of America*, vol. 109, no. 43, pp. 17633–17638, 2012.

[17] Y. Tada, A. Taniguchi, I. Nagao et al., "Differing growth responses of major phylogenetic groups of marine bacteria to natural phytoplankton blooms in the Western North Pacific Ocean," *Applied and Environmental Microbiology*, vol. 77, no. 12, pp. 4055–4065, 2011.

[18] F. L. Thompson, T. Bruce, A. Gonzalez et al., "Coastal bacterioplankton community diversity along a latitudinal gradient in Latin America by means of V6 tag pyrosequencing," *Archives of Microbiology*, vol. 193, no. 2, pp. 105–114, 2011.

[19] J. A. Gilbert, J. A. Steele, J. G. Caporaso et al., "Defining seasonal marine microbial community dynamics," *The ISME Journal*, vol. 6, no. 2, pp. 298–308, 2012.

[20] N. S. Webster, M. W. Taylor, F. Behnam et al., "Deep sequencing reveals exceptional diversity and modes of transmission for bacterial sponge symbionts," *Environmental Microbiology*, vol. 12, no. 8, pp. 2070–2082, 2010.

[21] M. D. Keller, R. C. Selvin, W. Claus et al., "Media for the culture of oceanic ultraphytoplankton," *Journal of Phycology*, vol. 23, pp. 633–638, 1987.

[22] G. L. A. Barker, J. C. Green, P. K. Hayes et al., "Preliminary results using the RAPD analysis to screen bloom populations of *Emiliania huxleyi* (Haptophyta)," *Sarsia*, vol. 79, pp. 301–306, 1994.

[23] J. K. Egge and B. R. Heimdal, "Blooms of phytoplankton including *Emiliania huxleyi* (Haptophyta). Effects of nutrient supply in different N:P ratios," *Sarsia*, vol. 79, pp. 333–348, 1994.

[24] D. H. Green, L. E. Llewellyn, A. P. Negri, S. I. Blackburn, and C. J. S. Bolch, "Phylogenetic and functional diversity of the cultivable bacterial community associated with the paralytic shellfish poisoning dinoflagellate *Gymnodinium catenatum*," *FEMS Microbiology Ecology*, vol. 47, no. 3, pp. 345–357, 2004.

[25] S. E. Dyksterhouse, J. P. Gray, R. P. Herwig, J. C. Lara, and J. T. Staley, "*Cycloclasticus pugetii* gen. nov., sp. nov., an aromatic hydrocarbon- degrading bacterium from marine sediments," *International Journal of Systematic Bacteriology*, vol. 45, no. 1, pp. 116–123, 1995.

[26] F. M. Ausubel, R. Brent, R. E. Kingston et al., *Short Protocols in Molecular Biology*, John Wiley & Sons, 1999.

[27] W. G. Weisburg, S. M. Barns, D. A. Pelletier, and D. J. Lane, "16S ribosomal DNA amplification for phylogenetic study," *Journal of Bacteriology*, vol. 173, no. 2, pp. 697–703, 1991.

[28] T. Huber, G. Faulkner, and P. Hugenholtz, "Bellerophon: a program to detect chimeric sequences in multiple sequence alignments," *Bioinformatics*, vol. 20, no. 14, pp. 2317–2319, 2004.

[29] W. Ludwig, O. Strunk, R. Westram et al., "ARB: a software environment for sequence data," *Nucleic Acids Research*, vol. 32, no. 4, pp. 1363–1371, 2004.

[30] T. Z. DeSantis, P. Hugenholtz, N. Larsen et al., "Greengenes, a chimera-checked 16S rRNA gene database and workbench compatible with ARB," *Applied and Environmental Microbiology*, vol. 72, no. 7, pp. 5069–5072, 2006.

[31] S. Guindon and O. Gascuel, "A simple, fast, and accurate algorithm to estimate large phylogenies by maximum likelihood," *Systematic Biology*, vol. 52, no. 5, pp. 696–704, 2003.

[32] C. Lozupone, M. E. Lladser, D. Knights, J. Stombaugh, and R. Knight, "UniFrac: an effective distance metric for microbial community comparison," *ISME Journal*, vol. 5, no. 2, pp. 169–172, 2011.

[33] D. B. Meisinger, J. Zimmermann, W. Ludwig et al., "*In situ* detection of novel *Acidobacteria* in microbial mats from a chemolithoautotrophically based cave ecosystem (Lower Kane Cave, WY, USA)," *Environmental Microbiology*, vol. 9, no. 6, pp. 1523–1534, 2007.

[34] H. Daims, A. Brühl, R. Amann, K.-H. Schleifer, and M. Wagner, "The domain-specific probe EUB338 is insufficient for the detection of all *Bacteria*: development and evaluation of a more comprehensive probe set," *Systematic and Applied Microbiology*, vol. 22, no. 3, pp. 434–444, 1999.

[35] R. I. Amann, L. Krumholz, and D. A. Stahl, "Fluorescent-oligonucleotide probing of whole cells for determinative, phylogenetic, and environmental studies in microbiology," *Journal of Bacteriology*, vol. 172, no. 2, pp. 762–770, 1990.

[36] S. G. Acinas, V. Klepac-Ceraj, D. E. Hunt et al., "Fine-scale phylogenetic architecture of a complex bacterial community," *Nature*, vol. 430, no. 6999, pp. 551–554, 2004.

[37] D. H. Green, M. C. Hart, S. I. Blackburn, and C. J. S. Bolch, "Bacterial diversity of *Gymnodinium catenatum* and its relationship to dinoflagellate toxicity," *Aquatic Microbial Ecology*, vol. 61, no. 1, pp. 73–87, 2010.

[38] A. D. Hatton, D. M. Shenoy, M. C. Hart, A. Mogg, and D. H. Green, "Metabolism of DMSP, DMS and DMSO by the cultivable bacterial community associated with the DMSP-producing dinoflagellate *Scrippsiella trochoidea*," *Biogeochemistry*, vol. 110, no. 1–3, pp. 131–146, 2012.

[39] M. L. Guannel, M. C. Horner-Devine, and G. Rocap, "Bacterial community composition differs with species and toxigenicity of the diatom *Pseudo-nitzschia*," *Aquatic Microbial Ecology*, vol. 64, no. 2, pp. 117–133, 2011.

[40] M. Sapp, A. S. Schwaderer, K. H. Wiltshire, H.-G. Hoppe, G. Gerdts, and A. Wichels, "Species-specific bacterial communities in the phycosphere of microalgae?" *Microbial Ecology*, vol. 53, no. 4, pp. 683–699, 2007.

[41] H. Schäfer, B. Abbas, H. Witte, and G. Muyzer, "Genetic diversity of 'satellite' bacteria present in cultures of marine diatoms," *FEMS Microbiology Ecology*, vol. 42, no. 1, pp. 25–35, 2002.

[42] A. W. Thompson, R. A. Foster, A. Krupke et al., "Unicellular cyanobacterium symbiotic with a single-celled eukaryotic alga," *Science*, vol. 337, no. 6101, pp. 1546–1550, 2012.

[43] M. Alavi, T. Miller, K. Erlandson, R. Schneider, and R. Belas, "Bacterial community associated with *Pfiesteria*-like dinoflagellate cultures," *Environmental Microbiology*, vol. 3, no. 6, pp. 380–396, 2001.

[44] G. L. Hold, E. A. Smith, M. S. Rappé et al., "Characterisation of bacterial communities associated with toxic and non-toxic dinoflagellates: *Alexandrium* spp. and *Scrippsiella trochoidea*," *FEMS Microbiology Ecology*, vol. 37, no. 2, pp. 161–173, 2001.

[45] S. Jasti, M. E. Sieracki, N. J. Poulton, M. W. Giewat, and J. N. Rooney-Varga, "Phylogenetic diversity and specificity of bacteria closely associated with *Alexandrium* spp. and other phytoplankton," *Applied and Environmental Microbiology*, vol. 71, no. 7, pp. 3483–3494, 2005.

[46] H.-P. Grossart, F. Levold, M. Allgaier, M. Simon, and T. Brinkhoff, "Marine diatom species harbour distinct bacterial communities," *Environmental Microbiology*, vol. 7, no. 6, pp. 860–873, 2005.

[47] A. Barberán and E. O. Casamayor, "Global phylogenetic community structure and β-diversity patterns in surface bacterioplankton metacommunities," *Aquatic Microbial Ecology*, vol. 59, no. 1, pp. 1–10, 2010.

[48] N. Van Oostende, W. Vyverman, J. Harlay et al., "Coccolithophore bloom dynamics shape bacterioplankton communities in the northern Bay of Biscay," in *Proceedings of the 12th International Symposium on Microbial Ecology (ISME '08)*, 2008.

[49] C. Y. Hwang, G. D. Bae, W. Yih, and B. C. Cho, "*Marivita cryptomonadis* gen. nov., sp. nov. and *Marivita litorea* sp. nov., of the family *Rhodobacteraceae*, isolated from marine habitats," *International Journal of Systematic and Evolutionary Microbiology*, vol. 59, no. 7, pp. 1568–1575, 2009.

[50] T. Yoshikawa, K. Iwamoto, and T. Sakata, "Pigment compositions and phylogenetic positions of filamentous bacteria coexisting in marine microalgal cultures," *Microbes and Environments*, vol. 16, no. 1, pp. 59–62, 2001.

[51] J. Alonso-Gutiérrez, I. Lekunberri, E. Teira, J. M. Gasol, A. Figueras, and B. Novoa, "Bacterioplankton composition of the coastal upwelling system of 'Ría de Vigo', NW Spain," *FEMS Microbiology Ecology*, vol. 70, no. 3, pp. 161–173, 2009.

[52] I. Wagner-Döbler, B. Ballhausen, M. Berger et al., "The complete genome sequence of the algal symbiont *Dinoroseobacter shibae*: a hitchhiker's guide to life in the sea," *ISME Journal*, vol. 4, no. 1, pp. 61–77, 2010.

[53] A. Seibold, A. Wichels, and C. Schütt, "Diversity of endocytic bacteria in the dinoflagellate *Noctiluca scintillans*," *Aquatic Microbial Ecology*, vol. 25, no. 3, pp. 229–235, 2001.

[54] C. J. S. Bolch, T. A. Subramanian, and D. H. Green, "The toxic dinoflagellate *Gymnodinium catenatum* (Dinophyceae) Requires marine bacteria for growth," *Journal of Phycology*, vol. 47, no. 5, pp. 1009–1022, 2011.

[55] D. Sher, J. W. Thompson, N. Kashtan, L. Croal, and S. W. Chisholm, "Response of *Prochlorococcus* ecotypes to co-culture with diverse marine bacteria," *ISME Journal*, vol. 5, no. 7, pp. 1125–1132, 2011.

[56] J. E. Kostka, O. Prakash, W. A. Overholt et al., "Hydrocarbon-degrading bacteria and the bacterial community response in Gulf of Mexico beach sands impacted by the deepwater horizon oil spill," *Applied and Environmental Microbiology*, vol. 77, no. 22, pp. 7962–7974, 2011.

[57] F. Coulon, P.-M. Chronopoulou, A. Fahy et al., "Central role of dynamic tidal biofilms dominated by aerobic hydrocarbonoclastic bacteria and diatoms in the biodegradation of hydrocarbons in coastal mudflats," *Applied and Environmental Microbiology*, vol. 78, no. 10, pp. 3638–3648, 2012.

[58] T. Gutierrez, D. H. Green, P. D. Nichols, W. B. Whitman, K. T. Semple, and M. D. Aitken, "*Polycyclovorans algicola* gen. nov., sp. nov., an aromatic-hydrocarbon-degrading marine bacterium found associated with laboratory cultures of marine phytoplankton," *Applied and Environmental Microbiology*, vol. 79, no. 1, pp. 205–214, 2013.

[59] T. Gutierrez, D. H. Green, W. B. Whitman, P. D. Nichols, K. T. Semple, and M. D. Aitken, "*Algiphilus aromaticivorans* gen. nov., sp. nov., an aromatic hydrocarbon-degrading bacterium isolated from a culture of the marine dinoflagellate *Lingulodinium polyedrum*, and proposal of *Algiphilaceae* fam. nov.," *International Journal of Systematic and Evolutionary Microbiology*, vol. 62, no. 11, pp. 2743–2749, 2012.

[60] J. K. Volkman, S. M. Barrett, S. I. Blackburn, M. P. Mansour, E. L. Sikes, and F. Gelin, "Microalgal biomarkers: a review of recent research developments," *Organic Geochemistry*, vol. 29, no. 5–7, pp. 1163–1179, 1998.

[61] R. N. Austin, G. E. Kenney, and A. C. Rosenzweig, "Perspective: what is known, and not known, about the connections between alkane oxidation and metal uptake in alkanotrophs in the

marine environment," *Metallomics*, vol. 6, no. 6, pp. 1121–1125, 2014.

[62] W.-R. Abraham, H. Meyer, and M. Yakimov, "Novel glycine containing glucolipids from the alkane using bacterium *Alcanivorax borkumensis*," *Biochimica et Biophysica Acta*, vol. 1393, no. 1, pp. 57–62, 1998.

[63] T. Gutiérrez, B. Mulloy, K. Black, and D. H. Green, "Glycoprotein emulsifiers from two marine *Halomonas* species: chemical and physical characterization," *Journal of Applied Microbiology*, vol. 103, no. 5, pp. 1716–1727, 2007.

[64] J. S. Sabirova, M. Ferrer, H. Lünsdorf et al., "Mutation in a '*tesB*-like' hydroxyacyl-coenzyme A-specific thioesterase gene causes hyperproduction of extracellular polyhydroxyalkanoates by *Alcanivorax borkumensis* SK2," *Journal of Bacteriology*, vol. 188, no. 24, pp. 8452–8459, 2006.

[65] J. B. van Beilen and E. G. Funhoff, "Expanding the alkane oxygenase toolbox: new enzymes and applications," *Current Opinion in Biotechnology*, vol. 16, no. 3, pp. 308–314, 2005.

[66] Y. Fukunaga, M. Kurahashi, K. Yanagi, A. Yokota, and S. Harayama, "*Acanthopleuribacter pedis* gen. nov., sp. nov., a marine bacterium isolated from a chiton, and description of *Acanthopleuribacteraceae* fam. nov., *Acanthopleuribacterales* ord. nov., *Holophagaceae* fam. nov., *Holophagales* ord. nov. and *Holophagae classis* nov. in the phylum 'Acidobacteria'," *International Journal of Systematic and Evolutionary Microbiology*, vol. 58, no. 11, pp. 2597–2601, 2008.

[67] M. P. Alves, F. A. Rainey, M. Fernanda Nobre, and M. S. da Costa, "*Thermomonas hydrothermalis* sp. nov., a new slightly thermophilic γ-proteobacterium isolated from a hot spring in central Portugal," *Systematic and Applied Microbiology*, vol. 26, no. 1, pp. 70–75, 2003.

[68] Y.-J. Chou, S.-Y. Sheu, D.-S. Sheu, J.-T. Wang, and W.-M. Chen, "*Schlegelella aquatica* sp. nov., a novel thermophilic bacterium isolated from a hot spring," *International Journal of Systematic and Evolutionary Microbiology*, vol. 56, part 12, pp. 2793–2797, 2006.

[69] R. M. Morris, K. Longnecker, and S. J. Giovannoni, "Pirellula and OM43 are among the dominant lineages identified in an Oregon coast diatom bloom," *Environmental Microbiology*, vol. 8, no. 8, pp. 1361–1370, 2006.

[70] R. A. Littman, B. L. Willis, and D. G. Bourne, "Bacterial communities of juvenile corals infected with different Symbiodinium (dinoflagellate) clades," *Marine Ecology Progress Series*, vol. 389, pp. 45–59, 2009.

[71] F. Goh, M. A. Allen, S. Leuko et al., "Determining the specific microbial populations and their spatial distribution within the stromatolite ecosystem of Shark Bay," *ISME Journal*, vol. 3, no. 4, pp. 383–396, 2009.

[72] R. H. M. Godoi, K. Aerts, J. Harlay et al., "Organic surface coating on coccolithophores—*Emiliania huxleyi*: its determination and implication in the marine carbon cycle," *Microchemical Journal*, vol. 91, no. 2, pp. 266–271, 2009.

[73] K. Haynes, T. A. Hofmann, C. J. Smith, A. S. Ball, G. J. C. Underwood, and A. M. Osborn, "Diatom-derived carbohydrates as factors affecting bacterial community composition in estuarine sediments," *Applied and Environmental Microbiology*, vol. 73, no. 19, pp. 6112–6124, 2007.

[74] N. M. Mohamed, J. J. Enticknap, J. E. Lohr, S. M. McIntosh, and R. T. Hill, "Changes in bacterial communities of the marine sponge *Mycale laxissima* on transfer into aquaculture," *Applied and Environmental Microbiology*, vol. 74, no. 4, pp. 1209–1222, 2008.

[75] M. E. Mouchka, I. Hewson, and C. D. Harvell, "Coral-associated bacterial assemblages: current knowledge and the potential for climate-driven impacts," *Integrative and Comparative Biology*, vol. 50, no. 4, pp. 662–674, 2010.

[76] U. R. Abdelmohsen, K. Bayer, and U. Hentschel, "Diversity, abundance and natural products of marine sponge-associated actinomycetes," *Natural Product Reports*, vol. 31, no. 3, pp. 381–399, 2014.

[77] B. S. Stevenson, S. A. Eichorst, J. T. Wertz, T. M. Schmidt, and J. A. Breznak, "New strategies for cultivation and detection of previously uncultured microbes," *Applied and Environmental Microbiology*, vol. 70, no. 8, pp. 4748–4755, 2004.

Hindawi Publishing Corporation
BioMed Research International
Volume 2015, Article ID 179597, 10 pages
http://dx.doi.org/10.1155/2015/179597

Research Article

Isolation and Characterization of Phages Infecting *Bacillus subtilis*

Anna Krasowska,[1] Anna Biegalska,[1] Daria Augustyniak,[2] Marcin Łoś,[3,4,5] Malwina Richert,[6] and Marcin Łukaszewicz[1]

[1]*Department of Biotransformation, Faculty of Biotechnology, University of Wroclaw, Fryderyka Joliot-Curie 14a, 50-383 Wroclaw, Poland*
[2]*Department of Pathogen Biology and Immunology, Institute of Genetics and Microbiology, University of Wroclaw, Przybyszewskiego 63-77, 51-148 Wroclaw, Poland*
[3]*Department of Molecular Biology, University of Gdańsk, Kładki 24, 80-822 Gdańsk, Poland*
[4]*Institute of Physical Chemistry, Polish Academy of Sciences, Kasprzaka 44/52, 01-224 Warsaw, Poland*
[5]*Phage Consultants, Tenisowa 10/5, 80-180 Gdańsk, Poland*
[6]*Laboratory of Electron Microscopy, Faculty of Biology, University of Gdańsk, Kładki 24, 80-822 Gdańsk, Poland*

Correspondence should be addressed to Marcin Łukaszewicz; marcin.lukaszewicz@uni.wroc.pl

Received 6 July 2014; Revised 15 September 2014; Accepted 25 September 2014

Academic Editor: Dimitrios Karpouzas

Bacteriophages have been suggested as an alternative approach to reduce the amount of pathogens in various applications. Bacteriophages of various specificity and virulence were isolated as a means of controlling food-borne pathogens. We studied the interaction of bacteriophages with *Bacillus* species, which are very often persistent in industrial applications such as food production due to their antibiotic resistance and spore formation. A comparative study using electron microscopy, PFGE, and SDS-PAGE as well as determination of host range, pH and temperature resistance, adsorption rate, latent time, and phage burst size was performed on three phages of the *Myoviridae* family and one phage of the *Siphoviridae* family which infected *Bacillus subtilis* strains. The phages are morphologically different and characterized by icosahedral heads and contractile (SIOΦ, SUBω, and SPOσ phages) or noncontractile (ARπ phage) tails. The genomes of SIOΦ and SUBω are composed of 154 kb. The capsid of SIOΦ is composed of four proteins. Bacteriophages SPOσ and ARπ have genome sizes of 25 kbp and 40 kbp, respectively. Both phages as well as SUBω phage have 14 proteins in their capsids. Phages SIOΦ and SPOσ are resistant to high temperatures and to the acid (4.0) and alkaline (9.0 and 10.0) pH.

1. Introduction

Recent investigations show that bacteriophages could be used as a means of controlling food-borne pathogens [1–3]. New phages are therefore being isolated and characterized [4, 5]. One of the bacterial genera with the highest prevalence in food industry, which could potentially be controlled by bacteriophages, is *Bacillus*, which belong to the heterogeneous group of Gram-positive, endospore-forming, facultative anaerobic bacteria [6, 7]. Despite the numerous advantages of *Bacillus* species in industry applications, they may also cause damage. The pathogenicity of *Bacillus anthracis* for mammals is well known, and other *Bacillus* species infections have been documented since the beginning of the last century [8, 9]. *Bacillus cereus* is considered a pathogenic species causing local infections, bacteremia, septicemia endocarditis and pericarditis, and infection of the central nervous system and respiratory tract [10–15]. *Bacillus cereus* is the main factor in food poisoning resulting from toxin production [16]. Beside the well-known pathogenic *Bacillus* species, recent studies have detected the production of enterotoxins and emetic toxin by *B. subtilis, B. pumilus*, and *B. licheniformis*, resulting in food-borne illnesses [17–19]. *Bacillus subtilis* contaminated 25% of samples of food products in The Netherlands (milk, yeast, flour, pasta products, cocoa, chocolate, bakery products, meat products, herbs, and spices) [20] and 12% of raw

Table 1: *Bacillus subtilis* strains and bacteriophages.

Number	Strain	Origin	Bacteriophage typing			
			SUBω	SPOσ	SIOΦ	ARπ
1	*B. subtilis* ATCC 6633	Polish Academy of Sciences, Wroclaw	+	+	−	−
2	*B. subtilis* 168	Institute, Rijksuniversiteit Groningen, Holland	0	+	0	0
3	*B. subtilis* SWV215		+	+	−	−
4	*B. subtilis* 10	University of Wroclaw, Faculty of Biotechnology	−	−	+	−
5	*B. subtilis* B3	Wroclaw University of Environmental and Life Sciences, Faculty of Food Science	+	+	−	+
6	*B. subtilis* Ż7-mutant B3		+	+	−	+
7	*B. subtilis* Ż17-mutant B3		+	+	−	+
8	*B. subtilis* Ż25-mutant B3		+	+	−	+
9	*B. subtilis* Hb36-mutant B3		+	+	−	+
10	*B. subtilis* B20		0	+	−	0
11	*B. subtilis* P22		+	+	−	+
12	*B. subtilis* KT20		0	−	0	0
13	*B. subtilis* 172		+	+	−	+
14	*B. subtilis* B24		0	+	−	0
15	*B. subtilis* PCM1938	Polish Academy of Sciences, Wroclaw	+	+	−	−
16	*B. subtilis* PCM 2226		+	+	+	−
17	*B. subtilis* PCM 486		0	+	−	0
18	*B. subtilis* PCM 2189		+	+	−	−
19	*B. subtilis* PCM 2005		+	+	−	0
20	*B. subtilis* PCM 2224		+	+	−	−

(−) Plaques not formed, (+) distinct clear plaques, and (0) hazy plaques.

materials, dough and bread samples in South Africa [21]. Moreover, *B. subtilis* spore contamination has been found in wheat flour, ropy bread [22], and gelatin [23].

The removal of *Bacillus* contamination is limited due to its resistance to physicochemical decontaminations methods. Usually the food industry uses physical methods of sterilization or disinfection such as *uv*, gamma radiation, or high temperature, but, unfortunately, they are often not effective against the highly resistant *Bacillus* spores [24, 25]. One option for *Bacillus* contamination treatment could be phagotherapy [26].

Bacteriophages are the largest group of viruses [27, 28]. They are very useful for people in phage therapy [29]. On the other hand, preventive phage therapy may eliminate pathogenic bacteria from food products. Phages are host-specific and infect only specific species or strains [1] with a few exceptions [30]. Although investigations have shown that bacteriophages can aid in successful eradications of food-borne pathogens such as *Listeria monocytogenes, Escherichia coli, Salmonella typhimurium*, or *Campylobacter* [1, 31], there are few commercial products, such as LISTEX P100, which have received the GRAS status [32]. Thus, it is necessary to determine the criteria for the application of phages in the control of bacteria in food and therefore all newly isolated phages with the potential application in antibacterial therapy should be characterized in detail. Beside using isolated phages as decontamination agents, they could be used in bacterial detection and serotyping or strain improvement recently described by Petty et al. [33]. However, the commercial application of bacteriophages requires the optimization of culture conditions and detailed determination of the physical and chemical factors influencing phage viability [34, 35]. The first attempts to control *Bacillus subtilis* infections by phages were carried out by Ackermann et al. [36]. The results showed an extreme heterogeneity of *B. subtilis* strains. Ackermann's phagotype system was used by Inatsu et al. [37] for the differentiation of *B. subtilis* (natto) and other *B. subtilis* strains isolated from fermented soybean foods [38].

The aim of this work was to isolate and characterize *Bacillus* bacteriophages in view of their potential application in phagotyping, strain improvement, and eradication of unwanted *Bacillus* strains in food industries. We have isolated four bacteriophages with different specificity to 20 *B. subtilis* strains. Detailed data on their morphology, thermal and pH stability, genome size, and capsid protein mass are described for bacteriophages specified for four representative *B. subtilis* strains.

2. Materials and Methods

2.1. Bacillus Strains and Bacteriophages. The origins of bacteriophages used in this study as well as their host strains are shown in Table 1. *Bacillus* strains 10 (isolated from soil), SWV215 [39], B3 [40], and ATTC6633 [41] were used for detailed investigation (Table 1). *Bacillus* strains were maintained as frozen stocks at −80°C in 1.5%, nutrient broth (Biocorp, Poland) with 2% agar-agar (BioShop, Canada Inc) supplemented with 15% (v/v) of glycerol. For experiments,

the strains were cultured on the nutrient agar and then cultured overnight in a liquid nutrient broth. The *Bacillus subtilis*-specific bacteriophages SUBω, SPOσ, SIOΦ (Acc. number KC699836), and ARπ were isolated from soil supplemented with a liter of *Bacillus subtilis* cultures. After a week, soil samples (1 g) were suspended in water, shaken (200 rpm/30 min), and centrifuged (4500 rpm/10 min), and the supernatant was filtered through a polyethersulfone (PES) 0.22 μm Millipore filter. Phage propagation was performed as follows: 45 mL of filtered soil samples and 5 mL culture of *Bacillus* strain grown overnight in nutrient broth were added to 20 mL of fresh nutrient broth and incubated for 24 h at 37°C. The suspension was centrifuged (4500 rpm/10 min) and the supernatant was filtered through a PES 0.22 μm Millipore filter. The bacteriophage titer in the filtrate was assessed using the double-agar layer technique of Adams [42].

Phage stocks were prepared in nutrient broth and then stored at 4°C.

2.2. Electron Microscopy. A high-titer phage lysate filtered through a PES 0.22 μm Millipore filter was centrifuged at 25,000 ×g for 60 min, and the pellet was washed twice in ammonium acetate (0.1 M, pH 7.0). A portion of the resuspended sediment was deposited on carbon-coated Formvar films, stained with 1% uranyl acetate for 30 s, and examined in a Philips CM 100 (Philips CM 100, Japan) transmission electron microscope at 80 kV with 39,000x magnification. The phage size was determined from the average of five to seven independent measurements using T4 phage tail (114 nm) as the magnification control.

2.3. Thermal Treatment. The thermal resistance of all bacteriophages was determined at 23, 50, 60, 70, 80, 90, and 100°C in a temperature-controlled thermo-block (Labnet International. Inc.), at 121°C in an autoclave, at 4°C and −20°C in a standard refrigerator, and at −80°C in a low temperature freezer (REVCO Sanyo, Japan). Equal volumes of phage (10^7 pfu/mL in sterile water) were incubated for 1, 2, 5, 10, 15, 30, 60, and 180 min at 4°C and then placed in an ice bath or thawed. Samples were assayed to determine surviving pfu using the double-agar layer technique [42].

2.4. pH Treatment. The influence of pH on the bacteriophages was assayed in CP (citrate-phosphate) buffer (0.2 M Na_2HPO_4/0.1 M citrate) within the pH range of 2.0 to 8.0 and in carbonate buffer (0.2 M H_2CO_3/0.2 M $NaHCO_3$) within the pH range of 9.0 to 11.0. Experiments were carried out at room temperature (25°C) for 1 and 6 h. Samples were assayed to determine pfu using the double-agar layer technique [42].

2.5. Host Range Determination. The host range of bacteriophages was assayed according to Yang et al. [43] as follows: 10^8 bacterial cells were mixed with molten 0.6% agar and the mixture was poured on 2% solid agar to make double layer agar plates. After solidification, 10 μL of bacteriophage (>10^6 pfu/mL) was spotted on each plate with each of the different *Bacillus* strains, incubated, and the presence of lysed plates was examined to determine host range.

2.6. Adsorption Rate, Latent Time, and Phage Burst Size. Experiments were performed as described previously [42, 44, 45] with slight modifications. Equal volume of phages (10^6–10^7 pfu/mL) was added to 0.9 mL of overnight cultures of host bacterial species and incubated at 37°C for 5 min. After incubation, the mixture was diluted to 10^{-5} and filtered through a PES 0.22 μm Millipore filter. The number of free phages in the filtrate was determined in duplicate, using the double-agar layer method.

To determine the phage latent time and burst size a one-step experiment was carried out according to the previous descriptions [46] with modifications. To 0.9 mL of overnight cultures of host bacteria was added 0.1 mL of the bacteriophage suspension. The bacteria were allowed to adsorb the bacteriophages for 5 min at 37°C; the mixture was diluted to 10^{-5} or 10^{-4} and further incubated for 135 min at 37°C. Samples were taken at 10 min intervals and phage titer was determined by the double layer-agar plate method. Burst size was calculated as the ratio of the final amount of liberated phage particles to the initial number of infected bacterial cells during the latent period [42].

2.7. Phage DNA Extraction. Phage particles were partially purified by PEG precipitation [47]. High titer suspensions (10^{10} pfu/mL) of filtered phage lysate were mixed with NaCl (1 M final conc.) and incubated on ice for 1.5 h. Then PEG 8000 was added to a final concentration of 10% and the mixture was incubated on ice for 2.5 h. This was followed by the centrifugation of precipitated phages (10 000 g, 4°C, 20 min). Pellets were suspended in 10 mM TE buffer (pH 8.0) or TM buffer (10 mM Tris-HCl, 100 mM NaCl, 10 mM $MgCl_2$; pH 7.4). The residual PEG and bacterial debris were next removed by gentle extraction for 30 s with an equal volume of chloroform, followed by centrifugation at 3000 ×g, 4°C for 15 min.

2.8. Pulsed-Field Gel Electrophoresis PFGE. Determination of bacteriophage genome size by PFGE was performed according to Lingohr et al. [48]. Purified phage particles in 10 mM TE buffer (pH 8.0) were incorporated in 1 : 1 proportion into 2% low-melting agarose in 10 mM TE. The solid gel plugs were incubated for 2.5 h at 54°C in 1 mL of phage lysis buffer containing 50 mM pH 8.0 Tris-HCl, 50 mM EDTA, 1% (w/v) SDS, and 100 μg/mL (final conc.) of proteinase K (phages SUBω, SPOσ, SIOΦ) or 1 mg/mL of proteinase K (phage ARπ). The plugs were washed at least 4 times in 10 mM Tris/EDTA buffer (TE, pH 8.0) and pulsed-field gel electrophoresis (PFGE) was performed (Bio-Rad, UK) in 1% agarose in 0.5X TBE buffer (pH 8.3). The PFGE parameters were as follows: 0.5X TBE buffer; 6 V/cm, initial switch time 1 s; final switch time 15 s; run time 16 h; temperature 12°C. Gels were stained with ethidium bromide followed by destaining in miliQ water. The genome size was determined with BioRad Quantity One software, using the Low Range PFG marker (New England BioLabs, UK) as a standard.

2.9. Preparation of Phage Structural Proteins and SDS-PAGE. Concentrated phage particles in TM buffer were extracted with chloroform (1 : 1 v/v) and, after gentle mixing, were

Table 2: Phage titers (pfu/mL) for *B. subtilis* strains.

Phage	SIOΦ	SUBω	SPOσ	ARπ
Bacillus strain	*B. subtilis* 10	*B. subtilis* ATCC 6633	*B. subtilis* SWV215	*B. subtilis* B3
Phage titer (pfu/mL)	10^{13}	10^{10}	10^{10}	10^{12}

centrifuged at 3000 ×g, 4°C for 15 min. Partly purified phage particles in the aqueous phase were pelleted by ultracentrifugation (Beckman Coulter) at 50 000 rpm at 4°C for 60 min. The pellets were resuspended in 1X Laemmli loading buffer (62.5 mM Tris-HCl, 2% SDS (w/v), 5% β-mercaptoethanol (v/v), 10% glycerol (v/v), 0.04% (w/v) bromophenol blue; pH 6.8), boiled for 5 min, and separated on the SDS-PAGE 12% gel. All gels were run at 40 mA using a mini Protean apparatus (BioRad) and Laemmli buffer. Gels were stained with Gel Code Blue stain reagent (Thermo Scientific). Biorad Quantity One software was used for the molecular analysis of the phage structural proteins based upon a PageRuler prestained protein ladder plus (Fermentas).

2.10. Statistical Analysis. All experiments were performed at least in triplicate. For the statistical analysis of data obtained, Microsoft Excel 2007 (SD and t-test) and R (ANOVA) programs were applied. Standard deviation was included in figures. Statistical significance was determined using Student's t-test. The significance level was set at $P < 0.05$.

3. Results

3.1. Phage Isolation. *Bacillus subtilis*-specific bacteriophages were isolated from soil inoculated with four distinct (isolated from different locations) *B. subtilis* strains: 10, B3, ATTC 6633, and SWV215. All isolated phages formed clear plaques with the strains used for isolation. Phage titers ranged from 10^{10} for SUBω and SPOσ to 10^{13} for SIOΦ (Table 2).

3.2. Phage Typing. Twenty *Bacillus subtilis* strains were used to determine the specificity of the four isolated bacteriophages: SUBω, SPOσ, SIOΦ, and ARπ (Table 1). Phage SUBω infected all *Bacillus* strains tested with the exception of *B. subtilis* 10. For *B. subtilis* 168, B20, KT20, B24, and PCM 486 the resulting plaques were hazy. Phage SPOσ did not form plaques with *B. subtilis* 10 and KT20 strains, but formed distinct clear plaques with all other strains. Phage SIOΦ formed plaques with *B. subtilis* strains 168, 10, KT20, and PCM 2226 but clear plaques were observed only with *Bacillus* strains 10 and PCM 2226. Phage ARπ did not form plaques with strains ATCC 6633, SWV215, 10, PCM1938, PCM 2226, PCM 2189, and PCM 2224. Clear plaques were observed for P22 and 172 strains and for B3 and its mutants (Table 1).

3.3. Phage Morphology. The phages belonged to two morphotypes. Three phages (SIOΦ, SUBω, and SPOσ) were classified to *Myoviridae* because of the appearance of icosahedral heads and contractile tails with necks, collars, and base plates (Figures 1(a), 1(b), and 1(c)). Phage head and tail length also indicated relationship to the *Myoviridae* (Table 3).

Table 3: Particle sizes of SIOΦ, SUBω, SPOσ, and ARπ phages.

Host	Phage	Head diameter [nm × nm]	Tail length [nm]
B. subtilis 10	SIOΦ	100 × 90	208
B. subtilis ATCC 6633	SUBω	67 × 67	223
B. subtilis SWV215	SPOσ	91 × 87	70
B. subtilis B3	ARπ	41 × 47	342

Bacteriophage ARπ had icosahedral heads and noncontractile, long tails (Figure 1(d), Table 3) and is thus morphologically similar to phages belonging to *Siphoviridae* family.

3.4. Thermal and pH Stability Test. The thermal stability test was carried out to determine the heat resistance of tested phages at pH 7.0. All phages were stable after 180 min at −80°C, −20°C, 4°C, 23°C, 30°C, 37°C, and 50°C, and all phages retained 100% infection activity after a 1 min incubation at 90°C, 100°C, and 121°C (data not shown). An ANOVA test was done and the interaction between the types of phage tested parameters was found statistically important. Thus, it can be said that the inactivation rate of the phages varies for different types of phages.

Phage SIOΦ lost total activity after 2 min at 80°C, 30 min at 70°C, and at 60°C only 1% of original activity was observed after a 3 h incubation period. Phage SUBω lost its infective ability after 1 min at 80°C, 5 min at 70°C, and 180 min at 60°C. Phage SPOσ was inactive after 2 min at 80°C, 15 min at 70°C, and 60 min at 60°C, respectively. Phage ARπ lost its activity after 2 min at 80°C, 10 min at 70°C, and 3 hours at 60°C (Figures 2(a), 2(b), 2(c), and 2(d)).

Optimal pH was determined by testing the stability of phages at different pH after 60 min (data not shown) and 6 h of incubation at room temperature (25°C). After 1-hour incubation at pH 2.0 all tested phages lost infective ability. Statistically significant differences between tested phages were found. Phage SPOσ seems to be extremely stable in the pH range 6.0–8.0; after a 6 h incubation the SPOσ activity was reduced from 10^7 to 10^4 pfu/mL at pH 3.0 and pH 4.0 (Figure 3(c)). At alkaline pH of 10.0 and pH 11.0 the activity was reduced by one order of magnitude (Figure 3(c)).

Bacteriophage ARπ was the most sensitive to acid and alkaline conditions and only showed 100% activity at pH 7.0 and pH 8.0 (Figure 3(d)). Similar results were observed after only 1 hour incubation (data not shown).

Phages SIOΦ and SUBω had 100% activity in the pH range of 6.0–8.0 and SIOΦ had reduced activity at pH 4.0, 5.0, and 9.0 from 10^7 to 10^2, 10^3, and 10^3, respectively (Figures 3(a) and 3(b)).

Phage SIOΦ was the most active in the adsorption (50%) to the *B. subtilis* 10 strain. The one-step growth curve of SIOΦ indicated that the latent period was 55–65 min and the estimated burst size was ~74 phage particles per infected

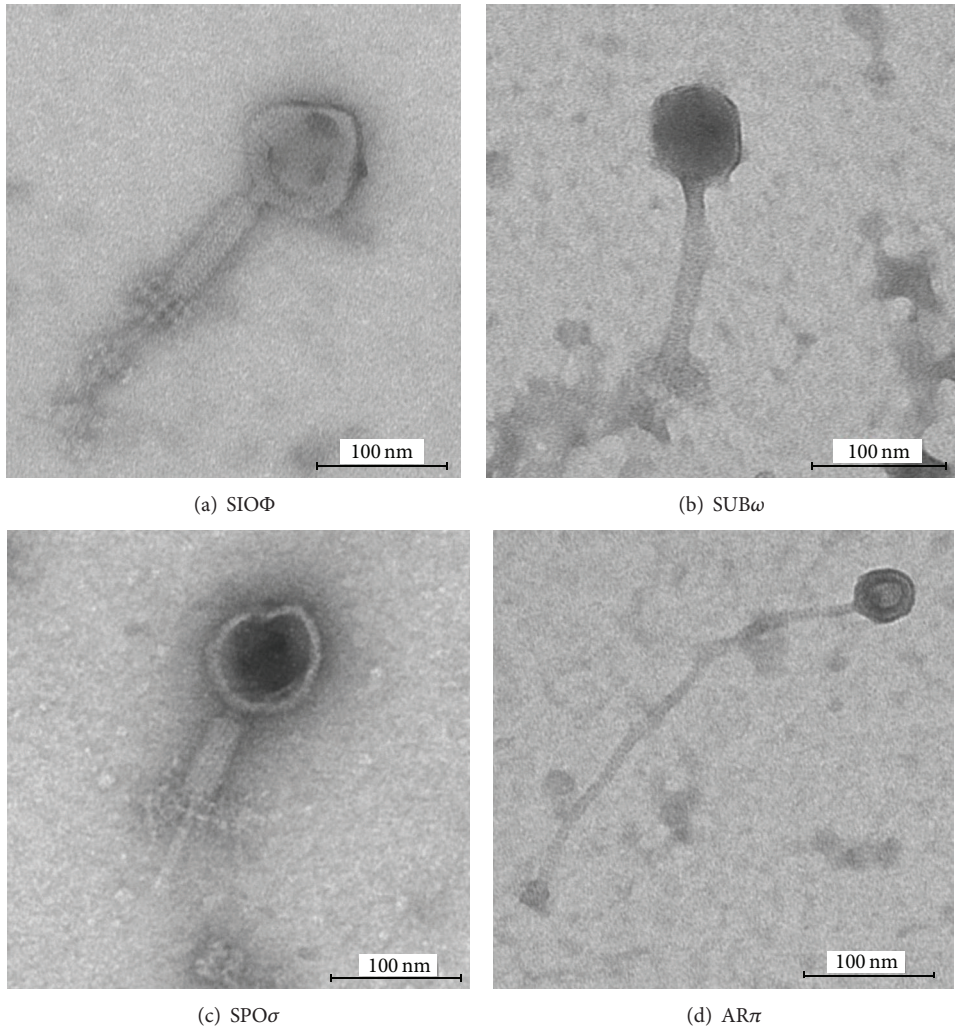

(a) SIOΦ (b) SUBω

(c) SPOσ (d) ARπ

Figure 1: Transmission electron microscopic images of (a) *B. subtilis* 10 phage SIOΦ, (b) *B. subtilis* ATCC 6633 phage SUBω, (c) *B. subtilis* SWV215 phage SPOσ, and *B. subtilis* B3 phage ARπ.

Table 4: Biological characteristics of SIOΦ, SUBω, SPOσ, and ARπ phages.

Phage	Adsorption [%]	Burst size [pfu/mL]	Latent period [min]	Growth time [min]
SIOΦ	50	~74	55–65	40
SUBω	12	~8	55–65	30
SPOσ	7.5	~23	75–85	40
ARπ	12	~37	55–65	30

bacterial cell (Table 4). Phage SPOσ was less active. It was adsorbed by only 7.5% of the *B. subtilis* SWV215 strain. The latent period of SPOσ was 75–85 min and the estimated burst size was ~23 phage particles per infected bacterial cell (Table 4). The latent periods of phages SUBω and ARπ were the same as that of phage SIOΦ, but the adsorption was lower (12%) and growth times were shorter (30 min). A difference between phages SUBω and ARπ was observed in their burst size: for SUBω it was only ~8 phage particles per infected bacterial cell while for ARπ it was ~37 phage particles (Table 4).

3.5. Phage Genome Size Estimated by PFGE. The size of the intact genomic DNA of the four phages in this study was estimated by pulse-field electrophoresis (PFGE). For phages SIOΦ, SUBω, and SPOσ belonging to *Myoviridae* family the size of their genomes was, respectively, 154, 154, and 25 kbp (Figure 4). The genome size of Arπ, the only phage from *Siphoviridae* family, was 40 kbp (Figure 4). The determined genome size values are comparable with values estimated by ICTV for the indicated phage families.

3.6. Protein Composition. SDS-PAGE was used to determine the content of structural proteins of phage particles. Virions of phages SIOΦ, SUBω, and SPOσ contained structural proteins with predominant protein bands corresponding, respectively, to ~52 kDa (SIOΦ), ~45, 31 kDa (SUBω), and 45 kDa (SPOσ) (Figure 5). Phage ARπ contained at least 14 structural proteins and was found to produce three major

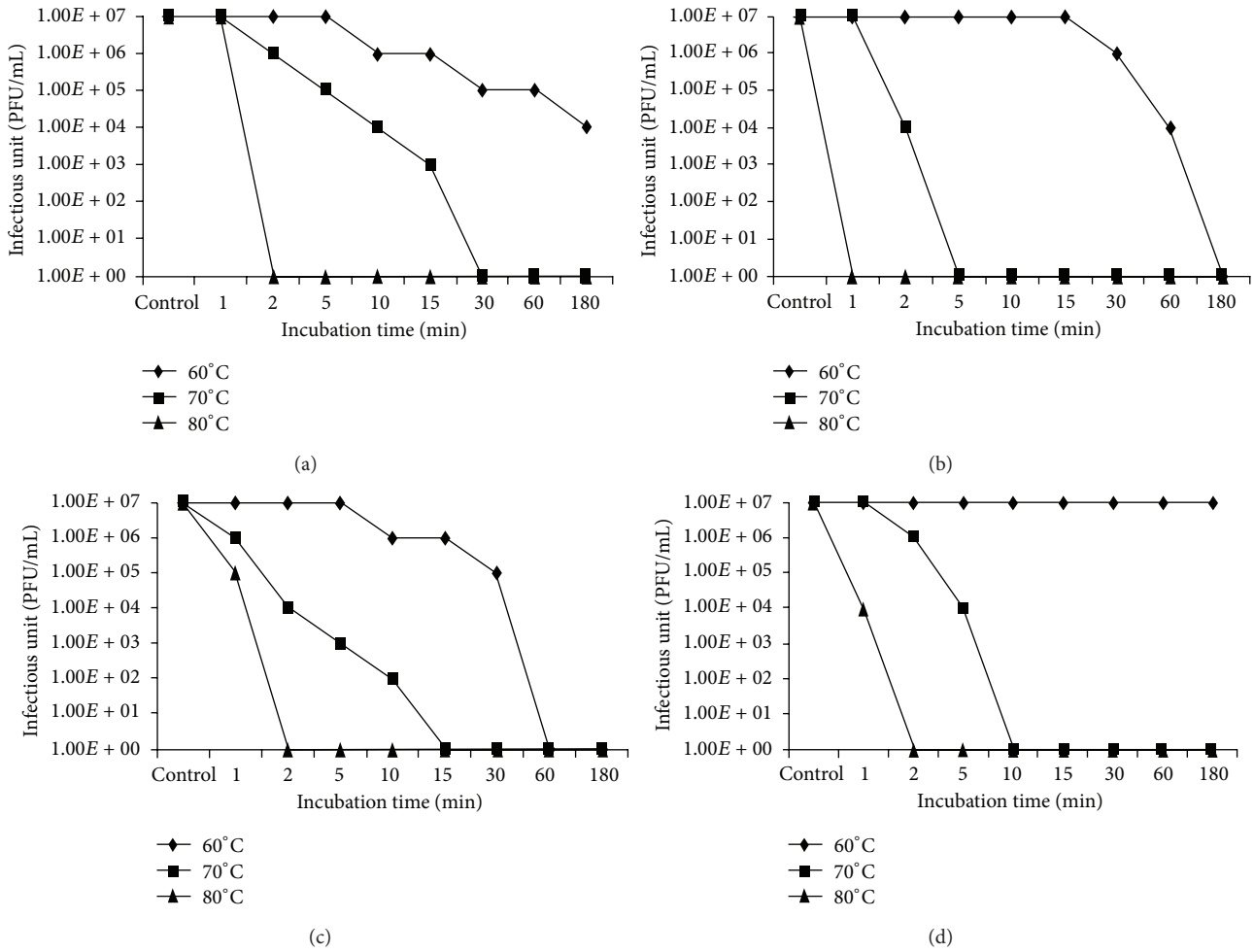

Figure 2: Thermal stability test of phages: (a) SIOΦ, (b) SUBω, (c) SPOσ, and (d) ARπ.

protein bands at molecular masses of approximately 42, 37, and 31 kDa (Figure 5).

4. Discussion

Bacillus has a high prevalence in nature and ability to form heat-resistant endospores; hence it is difficult to eradicate it from, for example, fermented food, and the constant presence of beneficial microorganisms is critical to maintaining the expected food quality. Bacteriophages are host-specific natural enemies of bacteria and the efficient eradication of bacterial pathogens with the use of phages is an effective way to control harmful bacteria [2, 49].

Bacteriophages may have distinct applications, such as biocontrol (eradication) of unwanted species (strains), improvement (selection) of strains used for production, and strain typing. All these applications depend on phage specificity [50]. Both a wide and a narrow host range may be useful. While a rather narrow host range will enable distinction of closely related strains in strain typing, a rather wide host range will be beneficial for biocontrol. In comparison to biocontrol, application of bacteriophages for improvement and selection of industrial strains has been poorly described. In fact, it is well known that in a large-scale production phage infection may lead to the collapse of the production, as it was in the case of acetone-butanol fermentation [51]. Thus, in industrial practice either various strains are used every month or a cocktail of strains is used for inoculum. Rotation of strains with various resistance decreases the risk of accumulation of bacteriophages infecting producer strain in industrial environment [52].

We found four bacteriophages with different specificity toward twenty *Bacillus subtilis* strains (Table 1). The classification of bacteriophages is in most cases based on morphological criteria and rarely on molecular data, for example, nucleotide sequence homology [53]. Considering the morphology, 96% of all bacteriophages belong to the order *Caudovirales* and this order is subdivided into three families: the *Myoviridae* (25%), characterized by a contractile tail; the *Siphoviridae* (61%) with a noncontractile tail; and the *Podoviridae* (14%) with a short, noncontractile tail [54, 55]. In 2009 the International Committee on the Taxonomy of Viruses (ICTV) proposed the creation the *Myoviridae* subfamily *Spounavirinae* with genera of SPO1-like viruses and Twort-like viruses and eight phage species [56]. Recently, Klumpp et al. [57] proposed a revision of current taxonomic

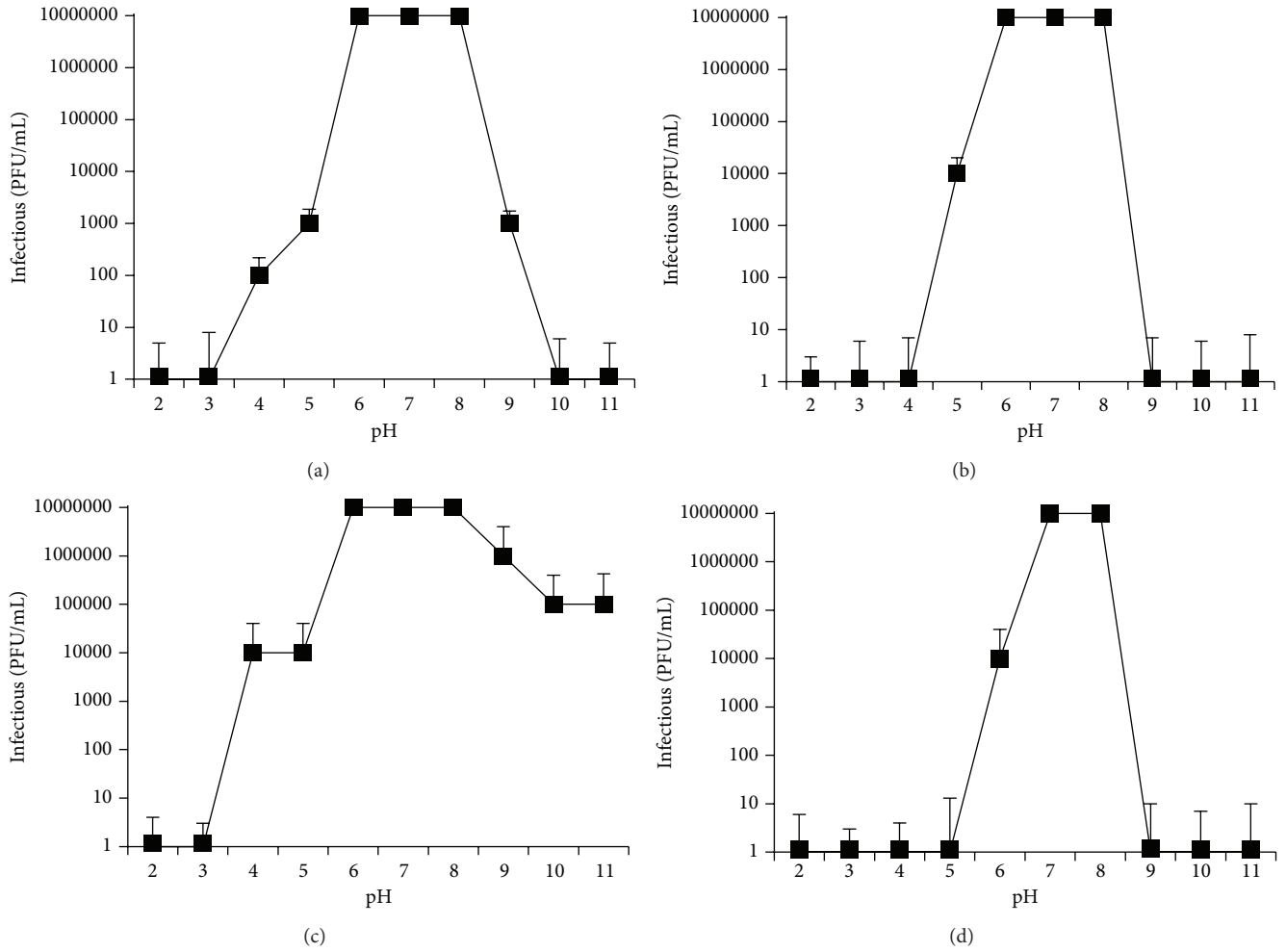

Figure 3: pH stability test of phages: (a) SIOΦ, (b) SUBω, (c) SPOσ, and (d) ARπ. Data are the means from three independent experiments +SD.

organization of the family *Myoviridae* and evaluated new members of this group. In this work we isolated three phages, SIOΦ, SUBω, and SPOσ, which morphologically belong to the *Myoviridae* family and phage ARπ which is classified in the *Siphoviridae* family (Figure 1). The genomes of SIOΦ and SUBω are 154 kbp each and are similar to the other phages of *Bacillus subtilis* such as SPO1 (145.7 kbp), SP8, SP82G, H1, 2C, Φe, or Φ25 (~150) [57]. SIOΦ has only four capsid proteins like the ΦH-like viruses; however, viruses of the ΦH type have a mere 59 kbp genome [58]. Bacteriophage SPOσ has a genome size of 25 kbp and ~14 capsid proteins and these features allow it to fall into the group of P2-like or Mu-like viruses but, unfortunately, viruses in this class have Gram-negative bacteria as hosts [58]. ARπ phage genome is sized 40 kbp and it has ~14 capsid proteins. On the basis of these characteristics it can be classified as N_{15}-like virus but the very long tail (342 nm) excludes it from the known classification [58]. The bacteriophages with the longest tails in *Siphoviridae* family belong to ΦM_1-like viruses (210 nm) and their tail is terminated with a knob as in ARπ phage.

The use of bacteriophages in biotechnological processes requires the knowledge of their characteristics such as the host range, latent period, growth time, or the resistance to stress conditions, for example, different temperatures or pH. Temperature plays a crucial role in bacteriophage survival, capacity for attachment, and the length of the latent period [59]. SIOΦ, SUBω, SPOσ, and ARπ bacteriophages retain a stable activity following 3 hours at temperatures ranging from −80°C to 50°C (Figure 2). Phages SIOΦ, SPOσ, and ARπ proved to be resistant to high temperatures and all of them survive after 2 min at 80°C, 5 min or longer at 70°C, and 180 min (except for 60 min for SPOσ) at 60°C (Figure 2). In general, members of *Myoviridae* and *Siphoviridae* families are considered to be resistant to large temperature fluctuations [35].

Acidity and alkalinity of the environment are other important factors influencing phage stability. SIOΦ and SPOσ phages are the most resistant to acid (4.0) and alkaline (9.0 and 10.0) pH; ARπ phage is the least resistant to pH fluctuations. The optimum pH values for all investigated phages were 7.0 and 8.0 (Figure 3). Lasobras et al. [60] have suggested that members of *Siphoviridae* family are the most resistant to adverse conditions. However, phage Arπ, which we morphologically classified as a member of *Siphoviridae*, is only active in a narrow pH range (6.0–8.0).

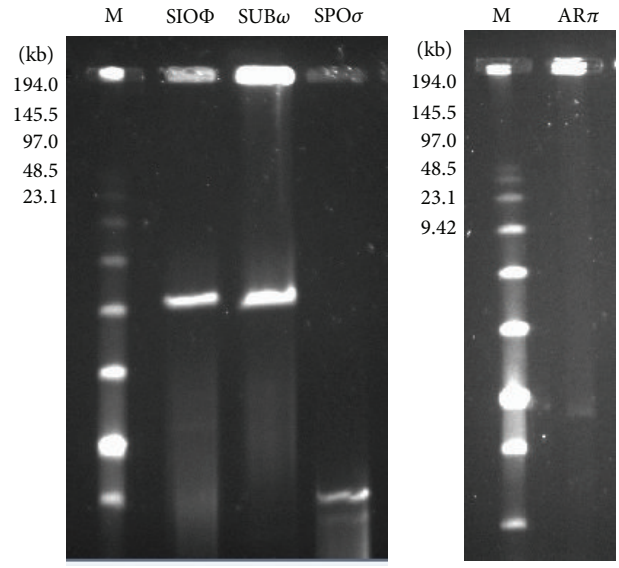

Figure 4: Pulsed-field gel electrophoresis of undigested phage DNAs. Genome sizes were estimated by using Low Range PFG marker (M).

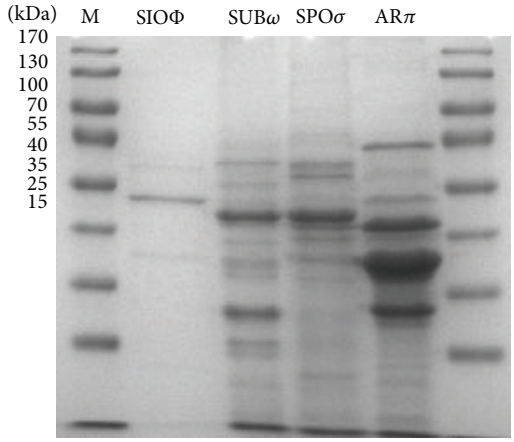

Figure 5: SDS-polyacrylamide gel electrophoretic analysis of indicated virion proteins estimated by using PageRuler prestained protein ladder plus (M).

Bacteriophage SIOΦ had the highest percent adsorption to the *Bacillus* host (50%) and released the largest number of particles (~74) from host cells (Table 4) and its phage titer was the highest (10^{13}) (Table 2). Due to high activity at low and high temperature and pH, SIOΦ seems to be the best candidate for use in industry.

The literature contains many descriptions of experiments conducted under different conditions and hence with varying results. Some *Bacillus subtilis* phages such as SP02c1 or SP82 have a higher percent of adsorption than our phages [61] while, on the other hand, phage SPO1 has the same burst size as SIOΦ [62].

At least one of the characterized isolated bacteriophages was lytic for each tested strain of *Bacillus subtilis*. Thus, they could be suitable for the phagotyping of this bacterial species.

Conflict of Interests

The authors declare that there is no conflict of interests regarding the publication of this paper.

Acknowledgments

This work was supported by grants from the Polish National Centre for Research and Development KB/48/13639/IT1-B/U/08, Grant EU POIG.01.01.02-00-016/2008, grant of the Ministry of Science and Higher Education (Poland) and the European Union within European Regional Development Fund, through Innovative Economy Grant (POIG.01.01.02-00-008/08), and by Wroclaw Centre of Biotechnology, programme The Leading National Research Centre (KNOW) for years 2014–2018.

References

[1] S. Hagens and M. J. Loessner, "Application of bacteriophages for detection and control of foodborne pathogens," *Applied Microbiology and Biotechnology*, vol. 76, no. 3, pp. 513–519, 2007.

[2] S. Guenther, D. Huwyler, S. Richard, and M. J. Loessner, "Virulent bacteriophage for efficient biocontrol of listeria monocytogenes in ready-to-eat foods," *Applied and Environmental Microbiology*, vol. 75, no. 1, pp. 93–100, 2009.

[3] L. Y. Brovko, H. Anany, and M. W. Griffiths, "Bacteriophages for detection and control of bacterial pathogens in food and food-processing environment," in *Advances in Food and Nutrition Research*, H. Jeyakumar, Ed., chapter 6, pp. 241–288, Academic Press, New York, NY, USA, 2012.

[4] J.-H. Lee, H. Shin, B. Son, S. Heu, and S. Ryu, "Characterization and complete genome sequence of a virulent bacteriophage B4 infecting food-borne pathogenic *Bacillus cereus*," *Archives of Virology*, vol. 158, no. 10, pp. 2101–2108, 2013.

[5] N. Bandara, J. Jo, S. Ryu, and K.-P. Kim, "Bacteriophages BCP1-1 and BCP8-2 require divalent cations for efficient control of *Bacillus cereus* in fermented foods," *Food Microbiology*, vol. 31, no. 1, pp. 9–16, 2012.

[6] H. Shin, N. Bandara, E. Shin, S. Ryu, and K.-P. Kim, "Prevalence of Bacillus cereus bacteriophages in fermented foods and characterization of phage JBP901," *Research in Microbiology*, vol. 162, no. 8, pp. 791–797, 2011.

[7] T. Nagai and F. Yamasaki, "*Bacillus subtilis* (*natto*) bacteriophages isolated in Japan," *Food Science and Technology Research*, vol. 15, no. 3, pp. 293–298, 2009.

[8] W. E. Farrar Jr., "Serious infections due to "non-pathogenic" organisms of the genus bacillus. Review of their status as pathogens," *The American Journal of Medicine*, vol. 34, no. 1, pp. 134–141, 1963.

[9] J. McFarland, "*Bacillus anthracis* similis," *Zentralbl Bakteriol Parasitenkd Abt I*, vol. 24, pp. 556–557, 1898.

[10] A. Akesson, S. A. Hedstrom, and T. Ripa, "Bacillus cereus: a significant pathogen in postoperative and post-traumatic wounds on orthopaedic wards," *Scandinavian Journal of Infectious Diseases*, vol. 23, no. 1, pp. 71–77, 1991.

[11] D. Barrie, J. A. Wilson, P. N. Hoffman, and J. M. Kramer, "Bacillus cereus meningitis in two neurosurgical patients: an investigation into the source of the organism," *Journal of Infection*, vol. 25, no. 3, pp. 291–297, 1992.

[12] D. J. Cotton, V. J. Gill, D. J. Marshall, J. Gress, M. Thaler, and P. A. Pizzo, "Clinical features and therapeutic interventions in 17 cases of Bacillus bacteremia in an immunosuppressed patient population," *Journal of Clinical Microbiology*, vol. 25, no. 4, pp. 672–674, 1987.

[13] C. S. Block, M. L. Levy, and V. U. Fritz, "Bacillus cereus endocarditis—a case report," *South African Medical Journal*, vol. 53, no. 4, pp. 556–557, 1978.

[14] J. E. Carbone and J. L. Stauffer, "Bacillus cereus pleuropulmonary infection in a normal host," *The Western Journal of Medicine*, vol. 143, no. 5, pp. 676–677, 1985.

[15] C. P. Craig, W.-S. Lee, and M. Ho, "Bacillus cereus endocarditis in an addict," *Annals of Internal Medicine*, vol. 80, no. 3, pp. 418–419, 1974.

[16] F. A. Drobniewski, "Bacillus cereus and related species," *Clinical Microbiology Reviews*, vol. 6, no. 4, pp. 324–338, 1993.

[17] C. From, R. Pukall, P. Schumann, V. Hormazábal, and P. E. Granum, "Toxin-producing ability among Bacillus spp. outside the Bacillus cereus group," *Applied and Environmental Microbiology*, vol. 71, no. 3, pp. 1178–1183, 2005.

[18] P. B. Pedersen, M. E. Bjørnvad, M. D. Rasmussen, and J. N. Petersen, "Cytotoxic potential of industrial strains of *Bacillus* sp," *Regulatory Toxicology and Pharmacology*, vol. 36, no. 2, pp. 155–161, 2002.

[19] M. S. Salkinoja-Salonen, R. Vuorio, M. A. Andersson et al., "Toxigenic strains of Bacillus licheniformis related to food poisoning," *Applied and Environmental Microbiology*, vol. 65, no. 10, pp. 4637–4645, 1999.

[20] M. C. Te Giffel, R. R. Beumer, S. Leijendekkers, and F. M. Rombouts, "Incidence of *Bacillus cereus* and *Bacillus subtilis* in foods in the Netherlands," *Food Microbiology*, vol. 13, no. 1, pp. 53–58, 1996.

[21] C. P. Bailey and A. von Holy, "Bacillus spore contamination associated with commercial bread manufacture," *Food Microbiology*, vol. 10, no. 4, pp. 287–294, 1993.

[22] I. B. Sorokulova, O. N. Reva, V. V. Smirnov, I. V. Pinchuk, S. V. Lapa, and M. C. Urdaci, "Genetic diversity and involvement in bread spoilage of Bacillus strains isolated from flour and ropy bread," *Letters in Applied Microbiology*, vol. 37, no. 2, pp. 169–173, 2003.

[23] E. de Clerck, T. Vanhoutte, T. Hebb, J. Geerinck, J. Devos, and P. de Vos, "Isolation, characterization, and identification of bacterial contaminants in semifinal gelatin extracts," *Applied and Environmental Microbiology*, vol. 70, no. 6, pp. 3664–3672, 2004.

[24] R. Moeller, G. Horneck, R. Facius, and E. Stackebrandt, "Role of pigmentation in protecting *Bacillus* sp. endospores against environmental UV radiation," *FEMS Microbiology Ecology*, vol. 51, no. 2, pp. 231–236, 2005.

[25] C. Faille, F. Fontaine, and T. Bénézech, "Potential occurrence of adhering living Bacillus spores in milk product processing lines," *Journal of Applied Microbiology*, vol. 90, no. 6, pp. 892–900, 2001.

[26] E. J. Vandamme, "Phage therapy and phage control: to be revisited urgently!!," *Journal of Chemical Technology and Biotechnology*, vol. 89, no. 3, pp. 329–333, 2014.

[27] R. W. Hendrix, "Bacteriophages: evolution of the majority," *Theoretical Population Biology*, vol. 61, no. 4, pp. 471–480, 2002.

[28] G. W. Hanlon, "Bacteriophages: an appraisal of their role in the treatment of bacterial infections," *International Journal of Antimicrobial Agents*, vol. 30, no. 2, pp. 118–128, 2007.

[29] A. Sulakvelidze, Z. Alavidze, and J. G. Morris Jr., "Bacteriophage therapy," *Antimicrobial Agents and Chemotherapy*, vol. 45, no. 3, pp. 649–659, 2001.

[30] R. Zink and M. J. Loessner, "Classification of virulent and temperate bacteriophages of Listeria spp. on the basis of morphology and protein analysis," *Applied and Environmental Microbiology*, vol. 58, no. 1, pp. 296–302, 1992.

[31] C. E. D. Rees, C. E. R. Dodd, S. S. Allen, and I. Laskin, "Phage for rapid detection and control of bacterial pathogens in food," in *Advances in Applied Microbiology*, pp. 159–186, Academic Press, New York, NY, USA, 2006.

[32] M. Skurnik, M. Pajunen, and S. Kiljunen, "Biotechnological challenges of phage therapy," *Biotechnology Letters*, vol. 29, no. 7, pp. 995–1003, 2007.

[33] N. K. Petty, T. J. Evans, P. C. Fineran, and G. P. C. Salmond, "Biotechnological exploitation of bacteriophage research," *Trends in Biotechnology*, vol. 25, no. 1, pp. 7–15, 2007.

[34] H. W. Ackermann, D. Tremblay, and S. Moineau, "Long-term bacteriophage preservation," *WFCC Newsletter*, vol. 38, pp. 35–40, 2004.

[35] E. Jończyk, M. Kłak, R. Miedzybrodzki, and A. Górski, "The influence of external factors on bacteriophages—review," *Folia Microbiologica*, vol. 56, no. 3, pp. 191–200, 2011.

[36] H.-W. Ackermann, R. R. Azizbekyan, R. L. Bernier et al., "Phage typing of *Bacillus subtilis* and *B. thuringiensis*," *Research in Microbiology*, vol. 146, no. 8, pp. 643–657, 1995.

[37] Y. Inatsu, K. Kimura, and Y. Itoh, "Characterization of Bacillus subtilis strains isolated from fermented soybean foods in Southeast Asia: comparison with B. subtilis (natto) starter strains," *Japan Agricultural Research Quarterly*, vol. 36, no. 3, pp. 169–175, 2002.

[38] K. Kimura and Y. Itoh, "Characterization of poly-γ-glutamate hydrolase encoded by a bacteriophage genome: possible role in phage infection of bacillus subtilis encapsulated with poly-γ-glutamate," *Applied and Environmental Microbiology*, vol. 69, no. 5, pp. 2491–2497, 2003.

[39] K. Xu and M. A. Strauch, "Identification, sequence, and expression of the gene encoding γ-glutamyltranspeptidase in Bacillus subtilis," *Journal of Bacteriology*, vol. 178, no. 14, pp. 4319–4322, 1996.

[40] S. Yao, X. Gao, N. Fuchsbauer, W. Hillen, J. Vater, and J. Wang, "Cloning, sequencing, and characterization of the genetic region relevant to biosynthesis of the lipopeptides iturin A and surfactin in Bacillus subtilis," *Current Microbiology*, vol. 47, no. 4, pp. 0272–0277, 2003.

[41] L. K. Nakamura, "Taxonomic relationship of black-pigmented Bacillus subtilis strains and a proposal for Bacillus atrophaeus sp. nov," *International Journal of Systematic Bacteriology*, vol. 39, no. 3, pp. 295–300, 1989.

[42] M. Adams, *Bacteriophages*, Interscience, New York, NY, USA, 1959.

[43] H. Yang, L. Liang, S. Lin, and S. Jia, "Isolation and characterization of a virulent bacteriophage AB1 of Acinetobacter baumannii," *BMC Microbiology*, vol. 10, no. 1, p. 131, 2010.

[44] R. Gallet, Y. Shao, and I.-N. Wang, "High adsorption rate is detrimental to bacteriophage fitness in a biofilm-like environment," *BMC Evolutionary Biology*, vol. 9, no. 1, article 241, 2009.

[45] C. Roncero, A. Darzins, and M. J. Casadaban, "Pseudomonas aeruginosa transposable bacteriophages D3112 and B3 require pili and surface growth for adsorption," *Journal of Bacteriology*, vol. 172, no. 4, pp. 1899–1904, 1990.

[46] M. Pajunen, S. Kiljunen, and M. Skurnik, "Bacteriophage φYeO3-12, specific for Yersinia enterocolitica serotype O:3, is related to coliphages T3 and T7," *Journal of Bacteriology*, vol. 182, no. 18, pp. 5114–5120, 2000.

[47] J. Sambrook and D. W. Russell, *Molecular Cloning*, Cold Spring Harbor Laboratory, New York, NY, USA, 2001.

[48] E. Lingohr, S. Frost, and R. P. Johnson, "Determination of bacteriophage genome size by pulsed-field gel electrophoresis," *Methods in Molecular Biology*, vol. 502, pp. 19–25, 2009.

[49] P. García, B. Martínez, J. M. Obeso, and A. Rodríguez, "Bacteriophages and their application in food safety," *Letters in Applied Microbiology*, vol. 47, no. 6, pp. 479–485, 2008.

[50] S. Hagens and M. J. Loessner, "Bacteriophage for biocontrol of foodborne pathogens: calculations and considerations," *Current Pharmaceutical Biotechnology*, vol. 11, no. 1, pp. 58–68, 2010.

[51] W. Kuit, N. P. Minton, A. M. López-Contreras, and G. Eggink, "Disruption of the acetate kinase (ack) gene of Clostridium acetobutylicum results in delayed acetate production," *Applied Microbiology and Biotechnology*, vol. 94, no. 3, pp. 729–741, 2012.

[52] A. Gálvez, H. Abriouel, R. L. López, and N. B. Omar, "Bacteriocin-based strategies for food biopreservation," *International Journal of Food Microbiology*, vol. 120, no. 1-2, pp. 51–70, 2007.

[53] H.-W. Ackermann, "Phage classification and characterization," *Methods in Molecular Biology*, vol. 501, pp. 127–140, 2009.

[54] H. W. Ackermann, "Bacteriophage observations and evolution," *Research in Microbiology*, vol. 154, no. 4, pp. 245–251, 2003.

[55] H.-W. Ackermann, "5500 Phages examined in the electron microscope," *Archives of Virology*, vol. 152, no. 2, pp. 227–243, 2007.

[56] R. Lavigne, P. Darius, E. J. Summer et al., "Classification of myoviridae bacteriophages using protein sequence similarity," *BMC Microbiology*, vol. 9, article 224, 2009.

[57] J. Klumpp, R. Lavigne, M. J. Loessner, and H.-W. Ackermann, "The SPO1-related bacteriophages," *Archives of Virology*, vol. 155, no. 10, pp. 1547–1561, 2010.

[58] C. M. Fauquet, M. A. Mayo, J. Maniloff, U. Desselberger, and A. Ball, *VIII Report of the International Committe on the Taxonomy of Viruses—Virus Taxonomy Classification and Nomenclature*, Elsevier/Academic Press, London, UK, 2005.

[59] M. R. Olson, R. P. Axler, and R. E. Hicks, "Effects of freezing and storage temperature on MS2 viability," *Journal of Virological Methods*, vol. 122, no. 2, pp. 147–152, 2004.

[60] J. Lasobras, M. Muniesa, J. Frías, F. Lucena, and J. Jofre, "Relationship between the morphology of bacteriophages and their persistence in the environment," *Water Science and Technology*, vol. 35, no. 11-12, pp. 129–132, 1997.

[61] S. Palefski, H. E. Hemphill, P. E. Kolenbrander, and H. R. Whiteley, "Dominance relationships in mixedly infected *Bacillus subtilis*," *Journal of Virology*, vol. 9, no. 4, pp. 594–601, 1972.

[62] A. Sampath and C. R. Stewart, "Roles of genes 44, 50, and 51 in regulating gene expression and host takeover during infection of *Bacillus subtilis* by bacteriophage SPO1," *Journal of Bacteriology*, vol. 186, no. 6, pp. 1785–1792, 2004.

Hindawi Publishing Corporation
BioMed Research International
Volume 2015, Article ID 816102, 12 pages
http://dx.doi.org/10.1155/2015/816102

Research Article

Bioprecipitation of Calcium Carbonate Crystals by Bacteria Isolated from Saline Environments Grown in Culture Media Amended with Seawater and Real Brine

G. A. Silva-Castro,[1] I. Uad,[1] A. Gonzalez-Martinez,[2] A. Rivadeneyra,[3] J. Gonzalez-Lopez,[1] and M. A. Rivadeneyra[1]

[1]*Department of Microbiology, Faculty of Farmacy, University of Granada, University Campus of Cartuja, 18071 Granada, Spain*
[2]*Department Civil Engineering, School of Civil Engineering, University of Granada, Campus of Fuentenueva, 18071 Granada, Spain*
[3]*Department of Electronic and Computer Technology, School of Computer Sciences and Telecomunications, University of Granada, University Campus of Almanjayar, 18071 Granada, Spain*

Correspondence should be addressed to A. Gonzalez-Martinez; agon@ugr.es

Received 12 September 2014; Revised 8 January 2015; Accepted 9 March 2015

Academic Editor: Ameur Cherif

The precipitation of calcium carbonate and calcium sulphate by isolated bacteria from seawater and real brine obtained in a desalination plant growth in culture media containing seawater and brine as mineral sources has been studied. However, only bioprecipitation was detected when the bacteria were grown in media with added organic matter. Biomineralization process started rapidly, crystal formation taking place in the beginning a few days after inoculation of media; roughly 90% of total cultivated bacteria showed. Six major colonies with carbonate precipitation capacity dominated bacterial community structure cultivated in heterotrophic platable bacteria medium. Taxonomic identification of these six strains through partial 16S rRNA gene sequences showed their affiliation with Gram-positive *Bacillus* and *Virgibacillus* genera. These strains were able to form calcium carbonate minerals, which precipitated as calcite and aragonite crystals and showed bacterial fingerprints or bacteria calcification. Also, carbonic anhydrase activity was observed in three of these isolated bacteria. The results of this research suggest that microbiota isolated from sea water and brine is capable of precipitation of carbonate biominerals, which can occur *in situ* with mediation of organic matter concentrations. Moreover, calcium carbonate precipitation ability of this microbiota could be of importance in bioremediation of CO_2 and calcium in certain environments.

1. Introduction

Carbon dioxide (CO_2) can be released to the environment from fixed sources (such as power generation facilities of industries) and from mobile sources (such as cars and trucks). The Intergovernmental Panel on Climate Change Special Report on Emission Scenarios [1] estimates CO_2 emissions to be as high as 29–44 Gt per year in 2020 and 23–84 Gt per year by 2050. It is estimated that 60% of fixed emissions occur at specific locations and in a large-scale scenario. Most can be remediated by CO_2 sequestration and storage, which also incurs in economic cost [2].

Different technologies can be applied for CO_2 capture and store [3]. In this context, one form for CO_2 capture is the geological carbon sequestration (GCS), which stores CO_2 for indefinite periods of time at geological sites such as deep saline aquifers or depleted oil or gas wells. This is particularly attractive due to the possibility of usage of fossil fuels and, at the same time, consideration is paid to global warming phenomenon. However, there may be some doubts about the application of GCS. One of the most important concerns is the CO_2 leakage through wells, faults, or fractures in the low-permeability cap rock [4]. Risk of leakage is a more pressing concern given that $scCO_2$ is less dense and less viscous than natural pore fluid, which offers the possibility of CO_2 upwards migration through sequestrating geological formation [5]. However, biological approaches such as the use of engineered

biofilms or biomineralisation processes have been proposed to mitigate leakage and enhance CO_2 storage [6].

It has been also proposed that the bioprecipitation of minerals such as calcium carbonates could be considered a new strategy to remove carbon dioxide or to prevent its emission [7]. In this context, several possible mechanisms of microorganisms-mediated mineral precipitation in natural and engineered environments have been proposed [8–10]. In spite of this, the role that microorganisms have in the biological process and their influence over the crystal characteristics of precipitates is still not understood [11]. Thus, certain microbial species have been found to be associated with biomineral precipitation in many different environments such as saline habitats (seawater, brine), biofilms, and soils [12, 13]. Relationships between microorganisms species and biomineral characteristics have been suggested [11], although the biological precipitation mechanisms as well as the impact of this process in the microbial ecology of precipitating organisms are still unknown.

Several studies have reported the bacterial precipitation of carbonates [9, 10, 14] and have suggested different mechanisms for the microorganism-mediated precipitation of carbonate biominerals [15, 16]. The formation of calcium and magnesium carbonates has been explained by the production of NH_4^+ and CO_2 in presence of calcium and magnesium ionic species. Other authors have proposed that adsorption of calcium, magnesium, and metallic cations to cell surface could trigger bacterial-mediated biomineralization, with bacterial cell serving as nucleus for precipitation; in this sense, characteristics of extracellular polymeric substances impact biomineral precipitation [15, 16]. However, the influence of abiogenic features over bioprecipitation process is still unresolved, and thus optimal microbially mediated precipitation conditions are still not known. Among these abiogenic factors, the ionic composition of the medium and its salt concentrations are thought to be the most important factors in carbonate minerals bioprecipitation, along with fluid chemistry and fluid flow or viscosity [17].

Halophilic bacteria or microorganisms that have adapted to high-range salinity-changing environments can be used for the determination of the effect of the ionic characterization of the medium over the bacterial carbonate mineralization and therefore over CO_2 sequestration [10]. Furthermore, previous studies have reported mineralogical differences of biominerals formed by precipitation mediated by halophilic bacteria [10, 18] as well as the different roles that these bacteria play in carbonate mineralization at both natural environments and laboratory culture media.

As reported above, and considering the amounts of CO_2 in the atmosphere, one alternative is to create new equilibrium conditions in calcium and carbon cycles by storing and sequestering CO_2 in the stable form of calcium carbonate [7]. As a result, research is now being carried out regarding the use of microorganisms to produce calcium carbonate precipitations that are extremely stable in certain environments. In this context, carbonic anhydrase (CA) enzyme catalyses the reversible hydration of CO_2 in many organisms. Even though the enzyme has been found in many environments, its precise functions and mechanisms of action are not well known [19]. CA has an important role in carbonate precipitation in different marine organisms [20] and algae [21] and in the formation of calcified structures of corals and diatoms [22]. The presence of CA in metabolically diverse species within both *Bacteria* and *Archaea* domains is indicative of the significant role of this enzyme in prokaryotic microorganisms [23], even though little is known about its function. Sánchez-Moral et al. (2003) [24] suggest that CA could also be responsible for the capture of an important fraction of carbon dioxide by heterotrophic bacteria in underground environments.

In this paper, we studied biomineral precipitation by different bacteria isolated from saline environments and its capability for biomineral formation including calcium carbonate in both liquid media and solid media. The morphology, mineralogy, and texture of the precipitates in laboratory cultures, amended or not with brine obtained from a desalination plant as the only calcium source, were also studied. Finally, the role of the carbonic anhydrase (CA) in carbonate precipitation and capture of CO_2 was determined and discussed.

2. Materials and Methods

2.1. Bacterial Strains. The experiments were performed with bacterial strains isolated from natural brine produced in a desalination plant located in Ibiza Island (Spain) and from seawater samples obtained from the Mediterranean Sea in the area close to the desalination plant. The isolation, selection, and study of capacity of these bacterial strains for biomineral precipitation were carried out in a specific medium for bacterial carbonate precipitation. The medium M1 composition (wt/vol) was the following: 1% yeast extract, 0.5% protease peptone, 0.1% glucose 0.4% calcium acetate, and 20 g/L Bacto-Agar and a mixture of sea salts to achieve a 3% final concentration (wt/vol). 1 M KOH was used to set the pH to 7.2.

0.1 mL brine or seawater dilutions in sterile saline solution were used for the inoculation of M1 medium plates (5 plates per dilution). Inoculated plates were incubated under aerobic conditions at 25°C temperature. Total heterotrophic aerobic bacteria were counted. Also, all plates were examined through optical microscopy periodically to check the presence of crystals, and the crystal-forming and non-crystal-forming colonies were counted. Isolated representatives of the dominant colony morphologies (3 major colony types from brine samples and 3 major colony types from seawater samples) were selected and purified, by restreaking them.

2.2. Identification of Selected Strains. All of the selected strains (with carbonate precipitation capacity) were taxonomically classified by analysing the partial sequence of the gene encoding 16S rRNA. DNA extraction procedures, PCR amplification process, purification techniques, and sequencing methods were done following Rivadeneyra Torres et al. (2013) [13]. Phylogenetic affiliation of isolated strains was done using the hypervariable V1–V3 (650 bp) regions of the sequenced 16S rRNA gene. Bioinformatic processing

Table 1: Chemical composition of the soil media used in the study.

Medium	Yeast extract (g/L)	Protease-peptone (g/L)	Glucose (g/L)
SM1	10	5	1
SM2	7.5	3.75	0.75
SM3	7.5	—	2
SM4	7.5	—	3
SM5	—	5	2
SM6	—	5	3

All of the culture media were prepared with real brine as mineral source.

of isolated strains partial 16S rRNA gene corresponding to sequence similarity searching, phylogenetic analysis, and phylogenetic tree conformation was done in accordance with Rivadeneyra Torres et al. (2013) [13].

2.3. Study of Carbonates Formation. In order to study whether brine may be a suitable source of cations for the carbonate, bioprecipitation experiments with the selected bacterial strains were performed in solid and liquid media. In this context, the chemical composition (data reported by Aqualia, Ibiza, Spain) of the brine used in our study was as follows (mg/L): Ca^{+2} 770; Mg^{+2} 2340; Na^{+} 11800; K^{+} 450; Cl^{-} 21100; SO_4^{-2} 3166; HCO_3^{-2} 238; pH 6.97.

2.3.1. Carbonate Crystal Formation in Solid Medium. Solid media used for carbonate precipitation were composed of real brine amended with different amounts and sources of organic matter, as indicated in Table 1. The main purpose of the selection of these different culture media for the study of the carbonate precipitation was to evaluate the effects that different concentrations and types of carbon sources have on the crystal formation. For the purpose of solid media conformation, 18 g/L of Bacto-Agar was added, while pH was set to 7.2 by 0.1 M KOH addition. The media was then autoclaved during 20 minutes at 112°C temperature.

The strains were inoculated onto different solid media and incubated under aerobic conditions at 25°C temperature. Optical microcopy was used for periodical examination of crystal presence in the media up to the 30 days after media inoculation. pH-indicator paper was used for the measurement of pH at the end of both growth and mineral formation experiments. After 30 days of incubation, precipitates produced by all strains were collected from solid culture media and studied by X-ray diffraction (XRD). The experiments were carried out in triplicate and were repeated three times. Control experiments consisting of media inoculated with autoclaved cells and of noninoculated media were also conducted.

2.3.2. Liquid Media. Two selected strains (S3 and M3) were inoculated into two Erlenmeyer flasks of 1 L containing 200 mL of SM2 medium (Table 1). SM2 medium was selected for this study because an optimal condition for the formation of carbonate crystals was detected. Culture media were incubated at 25°C under aerobic conditions during 30 days. The dynamics of the following parameters was monitored: pH, Ca, and Mg ions concentrations; total organic carbon (TOC); and inorganic carbon (IC). The pH was measured with a pH Meter Basic 20 (Crison); Ca_2^{+} and Mg_2^{+} were measured with a Perkin-Elmer 5100ZL atomic absorption spectrophotometer with flame photometry, graphite camera, and automatic sample analyzer equipment; TOC and IC were measured with a Rosemount Analytical TOC Analyzer. Precipitates after 30 d were collected following the methods described in Rivadeneyra et al. (2004) [18]. Control experiments were conducted using autoclaved cells as inoculum and using noninoculated culture medium.

2.4. Mineralogical Study. X-ray diffraction examination of obtained minerals from both solid and liquid culture media was done following Rivadeneyra Torres et al. (2013) [13] using the XPowder software [25, 26].

2.5. Morphological Studies. Observations and morphologic studies of the bacterial precipitates obtained were also carried out by scanning electron microscopy (SEM), using an LEO 1430VP and an LEO 1430VP equipped with an EDX system INCA350, or a Zeiss DMS scanning electron microscope. In order to provide better resolution images, the samples were golden and covered with carbon to carry out EDX microanalysis. In order to obtain high resolution images, we used a scanning electron microscope (FESEM) 2-3 kV LEO 1525 and samples covered with carbon.

2.6. Carbonic Anhydrase Assay. A carbonic anhydrase (CA) assay was performed, following Ramanan et al. (2009) [27]. The reaction is based on hydration, in the presence of the CA enzyme, of p-nitrophenyl-acetate (p-NPA) to p-nitrophenol and acetate, which produces a yellow coloration. Bacterial strains were inoculated onto TSA agar and incubated at 28°C for 24 hours over a period of five days. The plates were subsequently sprayed with a solution of 10 mM of p-NPA (p-nitrophenyl acetate), and the positive colonies showed yellow colour zones.

2.7. Geochemical Study. PHREEQC software version 2.17.01 [28] was used to determine the activity of the dissolved species and saturation degree in the initial solutions assayed. Total phosphorous was measured using the colorimetric analysis in the nitrogen digests. The total carbon and nitrogen in culture media were measured by Elemental Analysis with an organic elemental analyser that had a thermal conductivity detection system (Thermo Scientific Flash 2000). In solid media, values of C, P, and NH_4^{+} were calculated on the assumption that all of the organic substrates added had been metabolised. The C, P, and N data in the culture solutions correspond to the values of the metabolised organic matter in the cultures of the bacterial strains. All of the calculations were performed with the values presented in Table 2.

Table 2: Ionic composition (mg/L) of different solid and liquid media used in this study. The liquid medium used in the experiment was SM2 medium which was inoculated with strain M3 (*Bacillus marisflavi*) or strain S3 (*Virgibacillus pantothenticus*).

Compounds	Solid medium							Liquid medium	
	M1	SM1	SM2	SM3	SM4	SM5	SM6	M3	S3
Ca^{+2}	1040	770	770	770	770	770	770	556	535
Mg^{+2}	890	2340	2340	2340	2340	2340	2340	213	103
Na^{+}	756	11800	11800	11800	11800	11800	11800	11800	11800
K^{+}	260	450	450	450	450	450	450	450	450
SO_4^{-2}	1910	3166	3166	3166	3166	3166	3166	3166	3166
Cl^{-}	1504	21100	21100	21100	21100	21100	21100	21100	21100
TC	6484	6484	4863	2386	2003	2920	3333	1828	1678
NH_4^{+}	1728	1728	1296	651	434	642	642	487	447
P	150	150	112	90	60	0	0	42	39
pH	8.4	8.2	8.1	8.0	8.2	8.1	8.0	7.9	7.8

TC: total carbon.

Table 3: Taxonomic identification of selected strains through partial 16S rRNA gene sequence.

Strain		Accession number	Gene sequence of 16s rRNA	% identity	Sequence length (bp)
Brine	S1	KP721634	NR_025240 *Bacillus marisflavi*	91	593
	S2	KP721635	NR_118437 *Bacillus marisflavi*	95	1466
	S3	KP721636	NR_114091 *Virgibacillus pantothenticus*	89	1382
Seawater	M1	KP721631	NR_074977.1 *Bacillus pumilus*	99	1505
	M2	KP721632	NR_074977.1 *Bacillus pumilus*	99	1501
	M3	KP721633	NR_118437.1 *Bacillus marisflavi*	97	1396

3. Results and Discussion

The number of heterotrophic bacteria (CFU) per mL brine and seawater samples was in the range of 5.5×10^5 and 2.8×10^6, respectively. The carbonate-forming bacteria percentage in M1 soil medium was 85% in brine samples and 94% in seawater samples. The role of microorganisms in biomineral precipitation has been reported for different mineral formation processes. In this sense, several researches have highlighted the role of microorganisms in mineral precipitation in natural ecosystems [29, 30]. In general, biomineralization does not have to be related to any specific microbial group, even though when these bioprocesses have been reported in numerous ecosystems. In this context, our results showed that both seawater and brine samples presented higher bacterial populations with the ability to precipitate carbonate crystals in culture media containing real brine as a source of calcium and magnesium.

Six major colonies with the greatest production capacity of crystal formation (three from brine samples and three from seawater samples) were selected for taxonomic identification and the study of crystal formation using brine as a calcium source. The taxonomic identification of selected strains is shown in Table 3. Isolated bacterial populations were closely related to Firmicutes phylum, according to the phylogenetic tree (Figure 1). Specifically, all isolates with the ability to precipitate minerals were classified into two closely related genera *Bacillus* (5 strains) and *Virgibacillus* (1 strain). BLAST search of selected strains sequence showed that strain M1 was related to *Bacillus pumilus* (99% identity), strain M2 to *Bacillus pumilus* (99% similarity), strain M3 to *Bacillus marisflavi* (97% identity), strain S1 to *Bacillus marisflavi* (91% similarity), strain S2 to *Bacillus marisflavi* (95% identity), and strain S3 to *Virgibacillus pantothenticus* (89% similarity). It has been found that microorganisms belonging to the Firmicutes phylum are the dominant phylotypes involved in carbonate precipitation in extreme environments [31], while Bacillales-related bacteria have been reported for their role in organic matter hydrolysis and biodegradation.

The capability of the selected strains to bioprecipitate carbonate in solid media with added brine and its carbonic anhydrase activity is shown in Table 4. The incubation time required for the formation of crystal carbonates by the bacterial strains was affected by the particular strain and culture medium used. Thus, crystal formation by M3 and S3 strain growth in SM1 and SM2 medium took place rapidly, beginning at 2 days after inoculation, while M3 and S3 strain growth in SM5 and SM6 medium formed carbonate crystals after 14 days of inoculation. Obviously, after this period of time, all of the strains formed larger amounts of crystals both in quantity and in size.

Regarding the carbonic anhydrase activity (Table 4), it was observed that three strains (M1, M2, and M3) isolated from seawater samples showed an intense yellow colour when its colonies were sprayed with a solution of 10 mM p-NPA, indicating a positive reaction to the presence of the enzyme. However, the strains isolated from brine samples (S1, S2, and S3) did not reveal any carbonic anhydrase activity.

All of the strains selected from seawater samples showed CA activity while the strains selected from real brine had

Table 4: Carbonate mineral precipitation in solid media and carbonic anhydrase activity.

Strain	Number of days strains take to precipitate Culture media tested						Carbonic anhydrase
	SM1	SM2	SM3	SM4	SM5	SM6	
Bacillus marisflavi S1	4	6	NF	8	14	14	NR
Bacillus marisflavi S2	4	6	NF	10	NF	NF	NR
Virgibacillus pantothenticus S3	2	2	8	8	14	14	NR
Bacillus pumilus M1	6	8	NF	8	NF	NF	PR
Bacillus pumilus M2	6	10	8	10	16	14	PR
Bacillus marisflavi M3	2	2	8	8	14	14	PR

PR: positive reaction; NR: negative reaction (no yellow colouration). NF: non-crystal-formation.

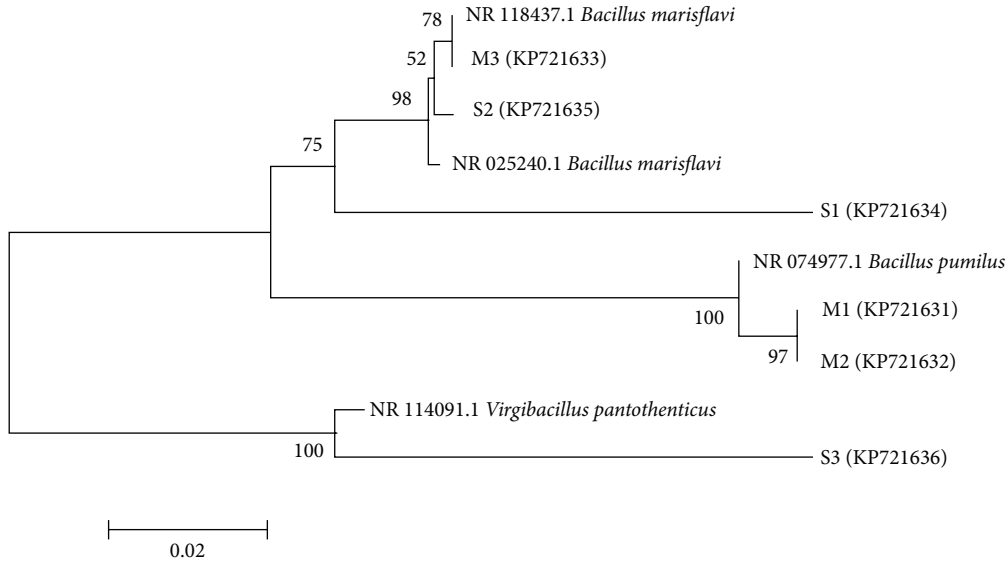

Figure 1: Phylogenetic tree of the six bacterial isolates based on 16S rRNA gene partial sequences.

negative enzymatic activity (Table 4). Liu et al. (2005) [20] reported that CA catalyses the reversible hydration balance from carbon dioxide to bicarbonate in many organisms, which decisively influences biological carbonate precipitation in different types of organisms, both prokaryotic and eukaryotic. In the same sense, Sánchez-Moral et al. (2003) [24] concluded that CA could also be responsible for the sequestration of CO_2 by heterotrophic bacteria. In addition, scientists have now begun to study the potential use of CA for the storage and capture of CO_2 through its precipitation in the form of insoluble carbonates [7, 27]. In our study, CA activity was detected in three of the six strains, with the capacity to precipitate calcium carbonate; consequently, it might be suggested that this enzyme could not affect carbonate precipitation. However, more experimental data is needed in order to confirm this preliminary hypothesis, since other factors can probably affect this biomineralisation process. Nevertheless, the efficient ecological or industrial application of carbonate precipitation by bacteria or carbonic anhydrase activity requires greater knowledge of these processes and the action of the enzyme that characterises them. In this context, more experiments are in progress.

Figure 2 shows the values of pH (a), total organic carbon and inorganic carbon (b), calcium concentration (c), and magnesium concentration (d) during the growth of S3 and M3 strains in SM2 liquid medium. *Virgibacillus pantothenticus* S3 and *Bacillus marisflavi* M3 initially decreased the pH of the culture medium at values of 5.0 and 5.8, respectively. However, after 4 days of incubation, the pH values in the liquid media were slowly increased until values became close to 8.0 at the end of the experiments. *Virgibacillus pantothenticus* S3 decreased calcium, magnesium, and organic matter concentrations at values of 69.5%, 4.4%, and 34.5%, respectively, while *Bacillus marisflavi* M3 reduced concentrations of calcium, magnesium, and organic matter 72.3%, 9.1%, and 37.6%, respectively. Obviously, changes in pH, TOC consumption, calcium, and magnesium were not detected in the control experiments.

The metabolic activity of bacteria has an important role in the mineralisation process. The pH of the liquid cultures (Figure 2) as well as solid media increased significantly from a pH value of 7 to a value of 8. The reduction of organic carbon in the cultures of the selected bacteria strains was approximately 40% (*Bacillus* and *Virgibacillus*). In this sense,

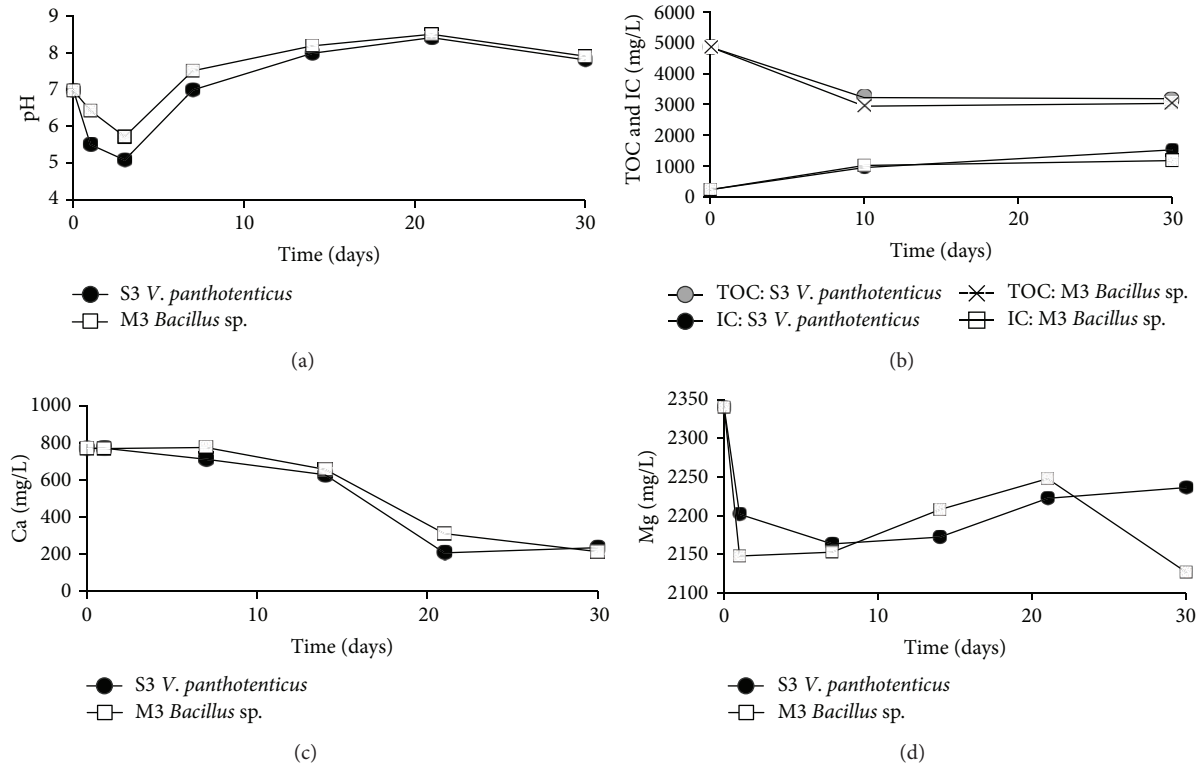

Figure 2: pH (a), total organic carbon and inorganic carbon (b), calcium concentration (c), and magnesium concentration (d) in SM2 liquid medium inoculated with *Virgibacillus pantothenticus* S3 and *Bacillus marisflavi* M3.

according to previous research [8], the release of CO_3^{2-} and NH_4^+ ions (with an increasing pH), in the presence of Ca^{2+} or Ca^{2+} and Mg^{2+} ions, produces carbonate precipitation. In our culture media, which contained high concentrations of Ca^{+2} and Mg^{+2} ions and high concentrations of organic matter (in the forms of glucose, peptone, and yeast extract), a similar mechanism could have occurred. Organic matter consumption produces CO_2 and NH_4^+, which is totally or partially utilized for the bioformation of carbonates. Since no precipitation was observed in the control experiments of noninoculated media, the importance of microbial activity in bioprecipitation processes was demonstrated. Accordingly, this data suggests that nutrient composition or nutrient concentration in brine used was not enough for biominerals precipitation. Nevertheless, crystal formation was successful in the organic matter-amended brine. Finally, when the carbon source was peptone, no carbonate precipitation was observed.

Castanier et al. (1999) [32], as well as McConnaughey and Whelan (1997) [33], proposed that ion transport (especially Ca^{2+}) across cellular membrane is linked to bacteria-mediated crystal precipitation. In *Bacillus* and *Virgibacillus*, the calcium concentration progressively decreased over time, reaching percentages of 25% after 20 days of culture. However, the percentages of magnesium reduction were always lower than the calcium percentages with values ranging to 80% after 20 days of culture. Greater power for ionic selectivity produces more adsorption of Ca^{2+} than of Mg^{2+} in the bacteria cellular envelope [34, 35]. As pointed out by Rosen (1987) [36], the bacterial Ca^{2+} pump is displaced close to the outside of the cell, whereas the Mg^{2+} pump is located towards the inside. It has been defended that extracellular Ca^{2+} concentrations are around 103-fold higher than intracellular Ca^{2+} concentrations [37, 38]. These findings explain the greater tendency of these bacterial strains to precipitate calcium carbonate or calcium sulphate and calcium carbonate instead of magnesium minerals, even when the concentration of magnesium ions in the brine was much higher than the concentration of calcium ions.

Table 5: Semiquantitative analysis (%) of precipitates produced in solid media cultures containing brine as calcium source by the six selected strains.

Medium	Aragonite	Bassanite	Calcite	Dolomite	Gypsum
SM1	02.8	74.3	01.4	08.5	13.2
SM2	02.3	84.5	00.0	06.3	06.8
SM3	02.8	80.2	00.0	07.7	09.3
SM4	04.1	48.8	01.5	19.3	26.2
SM5	00.5	79.4	00.0	00.0	20.1
SM5	00.0	70.4	00.0	00.0	30.6

Figure 3 (X-ray map of the precipitate formed) and Table 5 (semiquantitative analysis of precipitates) show the results of crystal formation of the six selected strains grown in M1, SM1, SM2, SM3, SM4, SM5, and SM6 solid media. In

Table 6: Saturation index values (SI) for mineral formation in culture solid medium (M1, SM1, SM2, SM3, SM4, SM%, and SM6) and liquid medium SM2 inoculated with strains S3 and M3. All of the culture media contained added artificial brine.

Mineral	Solid medium							Liquid medium	
	M1	SM1	SM2	SM3	SM4	SM5	SM6	S3	M3
Anhydrite	−0.70	−0.72	−0.69	−0.65	−0.64	−0.65	−0.65	−0.63	−0.63
Aragonite	2.43	2.25	2.15	1.87	1.80	1.95	2.01	1.63	1.68
Calcite	2.57	2.40	2.29	2.01	1.94	2.10	2.15	1.78	1.83
Dolomite	5.47	5.69	5.47	4.91	4.77	5.08	5.19	3.23	3.63
Dolomite (d)	4.92	5.14	4.92	4.36	4.22	4.53	4.64	2.68	3.08
Gypsum	−0.49	−0.52	−0.49	−0.45	−0.44	−0.45	−0.45	−0.43	−0.43
Huntite	6.92	7.92	7.49	6.36	6.08	6.72	6.93	1.79	2.88
Hydroxyapatite	13.41	12.18	11.85	11.65	11.14	—	—	11.4	11.41
Magnesite	2.32	2.71	2.60	2.32	2.25	2.41	2.46	0.87	1.22
Monohydrocalcite	−1.83	−2.00	−2.11	−2.39	−2.46	−2.3	−2.25	−2.62	−2.57
Nesquehonite	−0.12	0.26	0.16	−0.12	−0.19	−0.03	0.02	−1.57	−1.22
Struvite	2.39	2.64	2.38	1.99	1.63	—	—	0.62	0.95
Vaterite	18.7	18.53	18.42	18.14	18.07	18.22	18.28	17.91	17.95

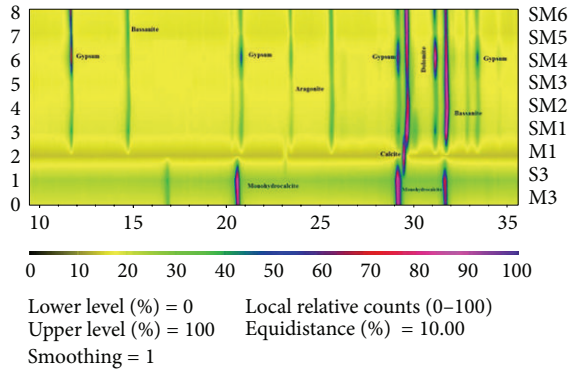

Figure 3: X-ray map of the precipitate formed in the solid medium (SM1, SM2, SM3, SM4, SM5, SM6, and M1) and SM2 liquid medium inoculated with the strain S3 and strain M3. Calcite $CaCO_3$; dolomite Ca Mg $(CO_3)_2$; aragonite $CaCO_3$; gypsum $CaSO_4 \cdot H_2O$; bassanite $2CaSO_4 \cdot H_2O$; and monohydrocalcite $CaCO_3 \cdot H_2O$.

this context, X-ray diagrams showed that precipitated crystals were 100% calcite in M1 medium and calcium sulphate (gypsum and bassanite) and calcium carbonate (aragonite, dolomite, and calcite) in the rest of the culture media. In this sense, when yeast extract was added to the culture media, carbonate crystals were formed. Finally, in culture media containing protease peptone and glucose, most of the crystalline precipitates were composed of gypsum and bassanite. However, carbonate crystals such as monohydroxycalcite ($CaCO_3 \cdot H_2O$) were formed by *Virgibacillus pantothenticus* S3 and Bacillus marisflavi M3 in liquid medium after 30 d of growth.

Several researches have demonstrated that bacteria can become the nucleus of mineral precipitation due to cellular surface membrane, cell wall, or EPS layers cation adsorption [16, 39–41]. Hammes and Verstraete (2002) [42] observed that thin, watery layers around bacterial cells create microenvironments subjected to different pH and dissolved organic carbon concentrations, in which calcium cations can prevail. Our results suggested that precipitation of different minerals is induced by the different cellular envelopes of the different bacteria found in this study. These results are similar to those of Rivadeneyra et al. (2004) [18], who showed that different bacterial strains can create microenvironments with different concentrations of calcium and magnesium cations and therefore result in different characteristics of precipitated minerals. They also agreed with Schultze-Lam et al. (1996) [43], who also claimed that the electronegative nature of the cell membrane can set up a unique precipitation environment on a microscale.

The PHREEQC results (Table 6) are presented in terms of the saturation index (SI) for each mineral. SI is defined by SI = log (IAP/Ksp), where IAP is the ion activity product of the dissolved constituents and Ksp is the solubility product for the mineral. Thus, SI < 0 indicates undersaturation with respect to the mineral, while SI > 0 indicates supersaturation. The geochemical study indicated that the ionic conditions of the media were suitable for the generation of vaterite, hydroxyapatite, aragonite, calcite, dolomite, huntite, magnesite, and struvite. When the selected strains were grown in M1, only calcite was precipitated. However, in SM1, SM2, SM3, and SM4 solid media, carbonates such as dolomite, aragonite, and calcite and calcium sulphates such as bassanite and gypsum were formed. In addition, in SM5 and SM6 solid media, only bassanite and gypsum were precipitated. Also, in SM2 liquid medium inoculated with strains M3 and S3, monohydrocalcite was the only mineral precipitated. Finally, vaterite, hydroxyapatite, huntite, and struvite were never detected in our experiments, despite being, from a geochemical viewpoint, the most often formed minerals.

In the results of the geochemical analysis software PHREEQC, vaterite, hydroxyapatite, aragonite, calcite, dolomite, huntite, magnesite, and struvite could possibly be inorganically precipitated in the solutions since their SI was greater than 0 (Table 6). However, when the selected strains were cultivated in culture media containing real brine

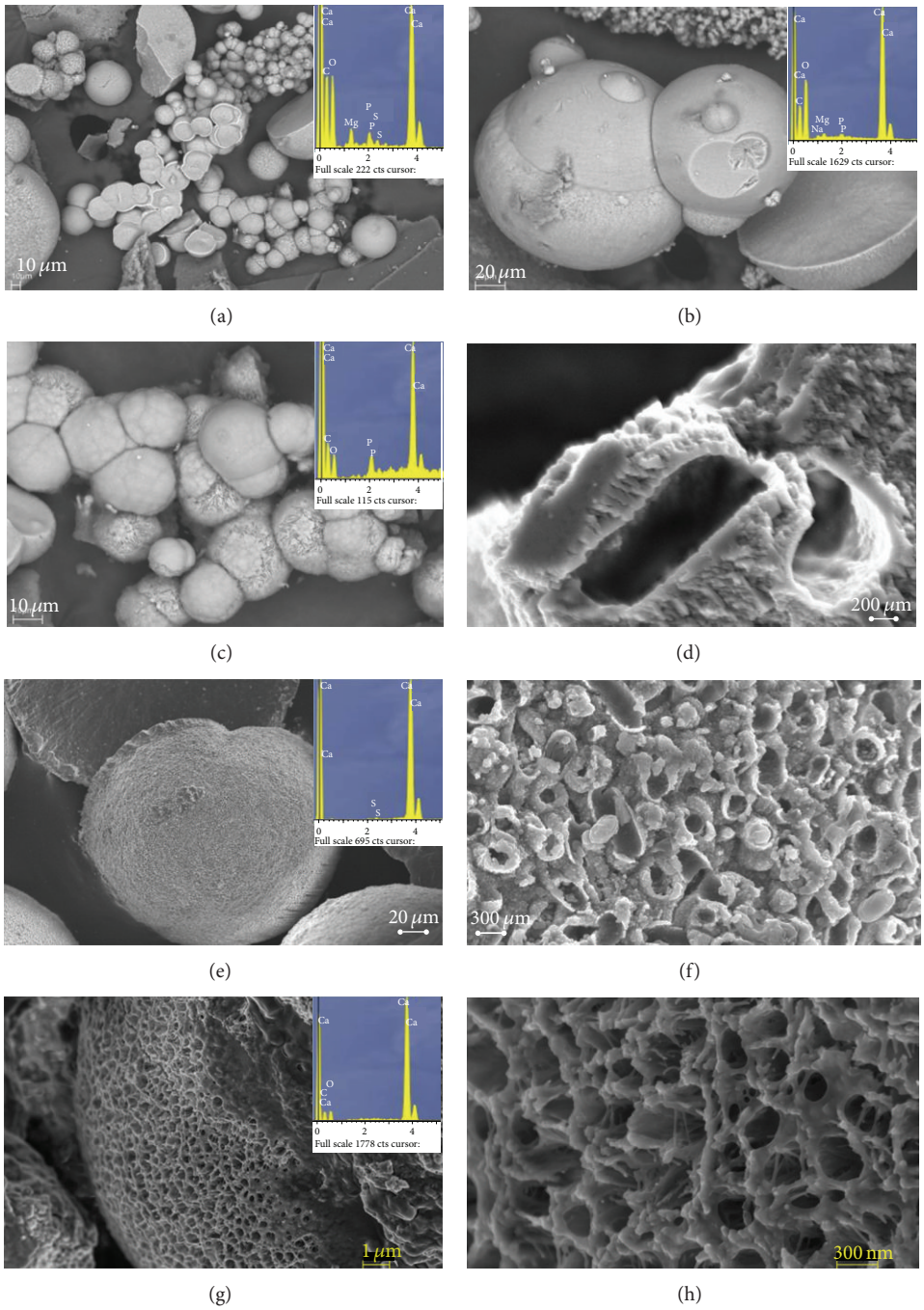

Figure 4: Scanning electron micrographs (SEM and FESEM) of calcium carbonate crystals precipitated. (a), (b), (c), and (e) show bioliths produced in solid media in different stages of formation with morphologies of spheres and hemispheres and EDX spectrum; some bioliths show bacteria fingerprints on the surface. (d) and (g) are detail of the surface of some bioliths. (d) shows the surface of one calcified cell. (f) shows detail of (e), where the abundance of calcite nanoparticles delimiting the bacterial cell contours is evident. (g) and (h) show bioliths of monohydrocalcite precipitates in liquid medium and EDX spectrum. (h) shows detail of the biolith surface.

from a desalination plant, lower amounts of carbonates such as dolomite, aragonite, and calcite were produced compared to the amounts of sulphates such as bassanite and gypsum formed. These results show that, in media containing real brine with a high concentration of sulphates (Table 2), the bacteria promote the biomineralisation of sulphates compared to carbonates. Probably, this fact is a consequence of the complex ion composition of the brine and also of the different ion interactions produced in this habitat. Moreover, our data suggest that high concentrations of sulphate may compete with the carbonate for the calcium ions present in the brine. This fact can be observed in

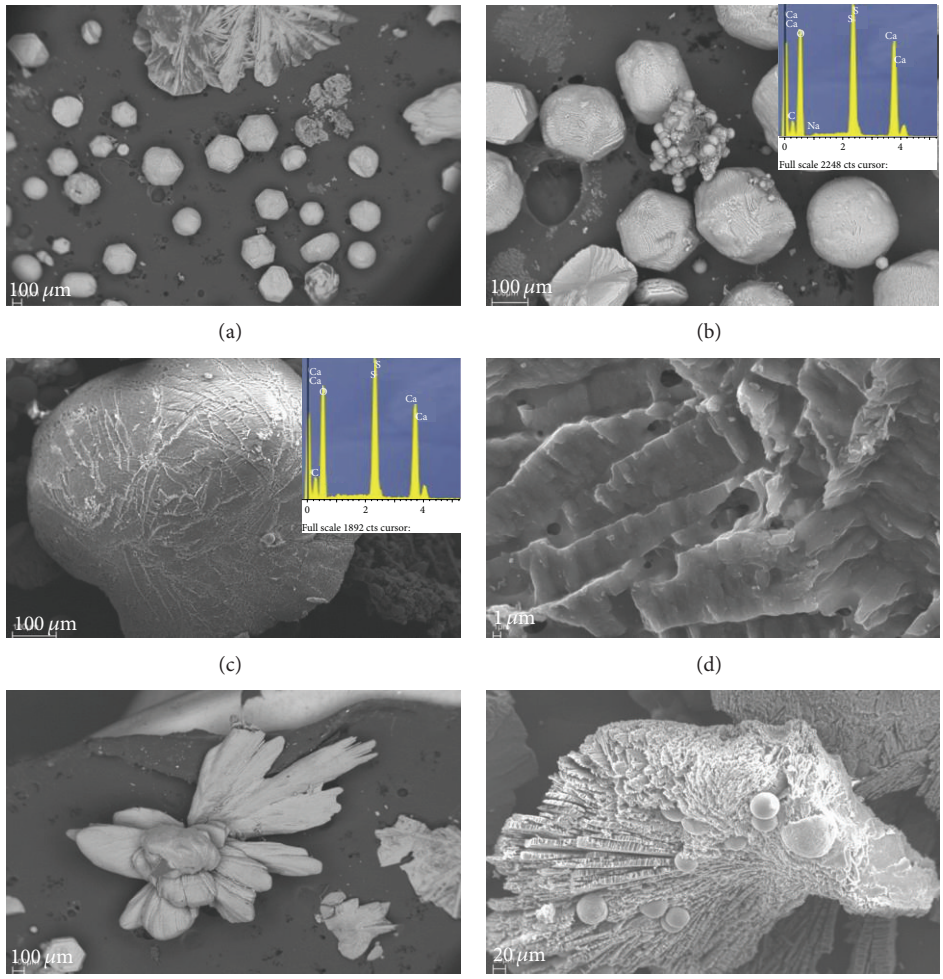

Figure 5: Scanning electron micrographs (SEM and FESEM) of calcium sulphate crystals precipitated in solid media. (a), (b), and (c) show polyhedral and pseudospheres shapes and EDX spectrum. (a) and (b) also show some spherulites of carbonate. (d) is detail of (c), where the surface of a biolith of sulphate mineral without mineralised cells can be observed. (e) and (f) show different morphologies of sulphate bioliths. (e) shows small spheres of calcium carbonate.

Table 5, where the importance of concentration and type of organic matter on the precipitation of carbonate and sulphates minerals is evident. Also, water solubility of CO_2 depends on temperature, pressure, pH, and brine salinity [2]. These environmental parameters need to be understood given that they determine bioprecipitation process and CO_2 sequestration in brines. Consequently, modification of these environmental parameters could affect the precipitation of biominerals.

The XRD analysis confirmed the bioprecipitation in all of the culture media, irrespective of the strain tested. A variety of shapes was observed in both types of mineral study. Particularly in the case of carbonate minerals, the most important morphologies were spheres and hemispheres forms, which appeared either in isolation or in groups. Most of the carbonate crystals formed in all culture media had surfaces with small holes, and high porosity (Figure 4). Shape and size of many holes resembled those of bacteria, and mineralised cells were frequently evident. However, calcium sulphate crystals had pseudospheres, polyhedral shapes, and crystal twinning (Figure 5). Finally, mineralised cells were never detected on the surfaces of the minerals.

The SEM of the carbonate crystals shows bioliths with spheroidal morphologies in the cultures (Figure 4). In many cases, mineralised bacteria are evident on spherulite surfaces, and bacterial mould entirely covers the surfaces of certain bioliths (Figures 4(a), 4(d), 4(f) and 4(h)). This confirms that the crystals were formed by an accumulation of calcified organisms. More detailed images of the spherulite surfaces (Figure 4(d)) showed that carbonate precipitates were nucleated on bacterial nanoglobules. These nanoglobules occurred in the external bacterial envelope. Carbonate nanoglobule formation is thought to be the first stage of microbially-mediated precipitation processes [44]. The observation of nanoglobules and calcified cells are clear evidence that the bacteria accumulate and precipitate carbonates on the cell surface during bacterial growth.

It has been shown that carbonate precipitation mediated by moderately halophilic bacteria *Chromohalobacter marismortui* started with the early appearance of amorphous

calcium phosphate, nanoparticles formed by the union of Ca^{2+} ions, and the phosphate groups of the outer membrane and cytoplasmic membrane components [16]. The transformation of phosphates into amorphous calcium carbonate during maturation of spherulites led to formation of aragonite and increase in crystallinity. In this sense, EDX analysis performed on different bioliths suggests this formation mechanism; the presence or absence of phosphate during the formation and maturation process of bioliths is evident (Figure 5).

The bioliths, formed by the union of calcified cells, increase in size as new calcified cells are progressively added. In the same way, our study suggested that mineralisation of the external envelopes of the bacteria (Figure 5) produces cell death since it inhibits an exchange of substances with the environment and causes the cells to break down; the release of the intracytoplasmatic contents may provide nutrients for other cells in the population and also contribute to recrystallisation processes in bioliths. Moreover, according to the hypothesis of programmed cell death, a percentage of the population will be genetically programmed to commit suicide. It has thus been observed that, in certain situations of extreme stress, a significant part of the population may commit mass suicide. This is for the greater good, since the death of these individuals guarantees the survival of other members, who will thus be able to resist until conditions improve [45]. In this context, in environments with a high calcium concentration (especially of Ca^{2+}), such as brines, carbonate precipitation may very well be a survival mechanism, which allows certain individuals of the population to survive, thanks to the sacrifice of the other members, as previously reported by Silva-Castro et al. (2013) [46]. If this hypothesis is confirmed, it would add an interesting dimension to the study of bacterially mediated carbonate precipitation and concomitantly to CO_2 capture. This would mean that, in addition to its ecological importance in carbon and calcium cycles, it would also be a key element that enables the survival of bacteria populations.

The most important finding of this research study is probably the fact that the heterotrophic bacterial community from saline environments (seawater and real brine) showed the potential ability to precipitate biominerals such as aragonite, calcite, dolomite, gypsum, and bassanite in culture media amended with a high concentration of real brine from desalination plants. However, precipitation only occurred when the microbiota were grown in environments with concentrations of organic matter and never when the microbiota were grown in environments derived from real brines without the addition of organic matter. This result suggests that, in the brines used in our experiments, the precipitation of biominerals, such as calcium carbonate, through autochthonous microbiota action cannot take place *in situ*, as a consequence of the low organic matter concentration present in this waste. However, if the brines are added with a sufficient concentration of organic matter, then biomineralisation could be produced. Consequently, if this circumstance is produced, the biosequestration of CO_2 can take place. The search for alternative sources of organic matter that can be used in these processes is a challenge for future research.

Conflict of Interests

The authors declare that they have no conflict of interests in this paper.

Acknowledgment

This investigation was funded by the EC FP7 CO2SolStock research consortium.

References

[1] B. Mertz, O. Davidson, H. de Coninck, M. Loos, and L. Meyers, *Carbon Dioxide Capture and Storage*, Intergovernmental Panel on Climate Change, New York, NY, USA, 2005.

[2] M. L. Druckenmiller and M. M. Maroto-Valer, "Carbon sequestration using brine of adjusted pH to form mineral carbonates," *Fuel Processing Technology*, vol. 86, no. 14-15, pp. 1599–1614, 2005.

[3] A. C. Mitchell, A. J. Phillips, L. Schultz et al., "Microbial $CaCO_3$ mineral formation and stability in an experimentally simulated high pressure saline aquifer with supercritical CO_2," *International Journal of Greenhouse Gas Control*, vol. 15, pp. 86–96, 2013.

[4] I. Pan, C. M. Oldenburg, Y.-S. Wu, and K. Pruess, "Wellbore flow model for carbon dioxide and brine," *Energy Procedia*, vol. 1, pp. 71–78, 2009.

[5] J. P. Nicot, C. M. Oldenburg, S. L. Bryant, and S. D. Hovorka, "Pressure perturbations from geologic carbon sequestration: area-of-review boundaries and borehole leakage driving forces," *Energy Procedia*, vol. 1, pp. 47–54, 2009.

[6] A. C. Mitchell, A. J. Phillips, R. Hiebert, R. Gerlach, L. H. Spangler, and A. B. Cunningham, "Biofilm enhanced geologic sequestration of supercritical CO_2," *International Journal of Greenhouse Gas Control*, vol. 3, no. 1, pp. 90–99, 2009.

[7] A. Sharma, A. Bhattacharya, R. Pujari, and A. Shrivastava, "Characterization of carbonic anhydrase from diversified genus for biomimetic carbon-dioxide sequestration," *Indian Journal of Microbiology*, vol. 48, no. 3, pp. 365–371, 2008.

[8] L. Ehrlich and D. K. Newman, *Geomicrobiology*, CRC Press, Taylor & Francis Group, New York, NY, USA, 5th edition, 2009.

[9] M. A. Rivadeneyra, A. Martín-Algarra, A. Sánchez-Navas, and D. Martín-Ramos, "Carbonate and phosphate precipitation by *Chromohalobacter marismortui*," *Geomicrobiology Journal*, vol. 23, no. 1, pp. 1–13, 2006.

[10] M. A. Rivadeneyra, R. Delgado, J. Párraga, A. Ramos-Cormenzana, and G. Delgado, "Precipitation of minerals by 22 species of moderately halophilic bacteria in artificial marine salts media: influence of salt concentration," *Folia Microbiologica*, vol. 51, no. 5, pp. 445–453, 2006.

[11] T. Bosak, V. Souza-Egipsy, and K. Newman, "A laboratory model of abiotic peloid formation," *Geobiology*, vol. 2, no. 3, pp. 189–198, 2004.

[12] F. Hammes, N. Boon, G. Clement, J. de Villiers, S. D. Siciliano, and W. Verstraete, "Molecular, biochemical and ecological characterisation of a bio-catalytic calcification reactor," *Applied Microbiology and Biotechnology*, vol. 62, no. 2-3, pp. 191–201, 2003.

[13] A. Rivadeneyra Torres, M. V. Martinez-Toledo, A. Gonzalez-Martinez, J. Gonzalez-Lopez, D. Martín-Ramos, and M. A. Rivadeneyra, "Precipitation of carbonates by bacteria isolated from wastewater samples collected in a conventional wastewater treatment plant," *International Journal of Environmental Science and Technology*, vol. 10, no. 1, pp. 141–150, 2013.

[14] M. Sanchez-Roman, M. A. Rivadedeneyra, C. Vascancelos, and J. A. McKenzie, "Biomineralisation of carbonate and phosphate by halophilic bacteria: influence of Ca^{2+} and Mg^{2+} ions," *FEMS Microbiology Ecology*, vol. 61, pp. 273–281, 2007.

[15] Y. van Lith, R. Warthmann, C. Vasconcelos, and J. A. McKenzie, "Microbial fossilization in carbonate sediments: a result of the bacterial surface involvement in dolomite precipitation," *Sedimentology*, vol. 50, no. 2, pp. 237–245, 2003.

[16] M. A. Rivadeneyra, A. Martín-Algarra, M. Sánchez-Román, A. Sánchez-Navas, and J. D. Martín-Ramos, "Amorphous Ca-phosphate precursors for Ca-carbonate biominerals mediated by *Chromohalobacter marismortui*," *The ISME Journal*, vol. 4, no. 7, pp. 922–932, 2010.

[17] C. Buczynski and H. S. Chafetz, "Habit of bacterially induced precipitates of calcium carbonate and the influence of medium viscosity on mineralogy," *Journal of Sedimentary Petrology*, vol. 61, no. 2, pp. 226–233, 1991.

[18] M. A. Rivadeneyra, J. Párraga, R. Delgado, A. Ramos-Cormenzana, and G. Delgado, "Biomineralization of carbonates by *Halobacillus trueperi* in solid and liquid media with different salinities," *FEMS Microbiology Ecology*, vol. 48, no. 1, pp. 39–46, 2004.

[19] B. E. Alber and J. G. Ferry, "A carbonic anhydrase from the archaeon *Methanosarcina thermophila*," *Proceedings of the National Academy of Sciences of the United States of America*, vol. 91, no. 15, pp. 6909–6913, 1994.

[20] N. Liu, G. M. Bond, A. Abel, B. J. McPherson, and J. Stringer, "Biomimetic sequestration of CO_2 in carbonate form: role of produced waters and other brines," *Fuel Processing Technology*, vol. 86, no. 14-15, pp. 1615–1625, 2005.

[21] O. Quiroga and E. L. Gonzalez, "Carbonic anhydrase in the chloroplast of a Coccolithophorid (Prymnesiophyceae)," *Journal of Phycology*, vol. 29, no. 3, pp. 321–324, 1993.

[22] B. M. Hopkinson, C. L. Dupont, A. E. Allen, and F. M. M. Morela, "Efficiency of the CO_2-concentrating mechanism of diatoms," *Proceedings of the National Academy of Sciences of the United States of America*, vol. 108, no. 10, pp. 3830–3837, 2011.

[23] K. S. Smith and J. G. Ferry, "Prokaryotic carbonic anhydrases," *FEMS Microbiology Reviews*, vol. 24, no. 4, pp. 335–366, 2000.

[24] L. Sánchez-Moral, J. C. Cañavas, L. Laiz, V. Jurado, B. Hermosin, and C. Saiz-Jimenez, "Bioinduced precipitation of calcium carbonate metastable phases in hypogean environments: a short review," *Geomicrobiology Journal*, vol. 20, pp. 491–500, 2003.

[25] J. D. Martín, *Using XPowder—A Software Package for Powder X-ray Diffraction Analysis*, D.L. GR-1001/04, XPowder, Madrid, Spain, 2004, http://www.xpowder.com/.

[26] J. D. Martín-Ramos, J. L. Díaz-Hernández, A. Cambeses, J. H. Scarrow, and A. López-Galindo, "Pathways for quantitative analysis by X-ray diffraction," in *An Introduction to the Study of Mineralogy*, InTech, Rijeka, Croatia, 2012.

[27] R. Ramanan, K. Kannan, S. Devi Sivanesan et al., "Bio-sequestration of carbon dioxide using carbonic anhydrase enzyme purified from *Citrobacter freundii*," *World Journal of Microbiology and Biotechnology*, vol. 25, no. 6, pp. 981–987, 2009.

[28] D. L. Parkhust and C. A. J. Appelo, "User's guide to PHREEQC (version 2). A computer program for speciation, batch-reaction, one-dimensional transport and inverse geochemical calculations," Water Resources Investigations Report 99-4259, U.S. Geological Survey, Denver, Colo, USA, 1999.

[29] J. Párraga, M. A. Rivadeneyra, J. M. Martín-García, R. Delgado, and G. Delgado, "Precipitation of carbonates by bacteria from a saline soil, in natural and artificial soil extracts," *Geomicrobiology Journal*, vol. 21, no. 1, pp. 55–66, 2004.

[30] G. Delgado, R. Delgado, J. Párraga, M. A. Rivadeneyra, and V. Aranda, "Precipitation of carbonates and phosphates by bacteria in extract solutions from a semi-arid saline soil. Influence of Ca^{2+} and Mg^{2+} concentrations and Mg^{2+}/Ca^{2+} molar ratio in biomineralisation," *Geomicrobiology Journal*, vol. 25, no. 1, pp. 1–13, 2008.

[31] K. Calderón, B. Rodelas, N. Cabirol, J. González-López, and A. Noyola, "Analysis of microbial communities developed on the fouling layers of a membrane-coupled anaerobic bioreactor applied to wastewater treatment," *Bioresource Technology*, vol. 102, no. 7, pp. 4618–4627, 2011.

[32] S. Castanier, G. Le Métayer-Levrel, and J.-P. Perthuisot, "Ca-carbonates precipitation and limestone genesis—the microbiogeologist point of view," *Sedimentary Geology*, vol. 126, no. 1–4, pp. 9–23, 1999.

[33] T. A. McConnaughey and J. F. Whelan, "Calcification generates protons for nutrient and bicarbonate uptake," *Earth-Science Reviews*, vol. 42, no. 1-2, pp. 95–117, 1997.

[34] J. D. Wolt, *Soil Solution Chemistry: Applications to Environmental Science and Agriculture*, John Wiley & Sons, New York, NY, USA, 1994.

[35] R. M. Maier, I. L. Pepper, and C. P. Gerba, *Environmental Microbiology*, Academic Press, San Diego, Calif, USA, 2000.

[36] B. P. Rosen, "Bacterial calcium transport," *Biochimica et Biophysica Acta—Reviews on Biomembranes*, vol. 906, no. 1, pp. 101–110, 1987.

[37] M. G. Desrosiers, L. J. Gately, A. M. Gambel, and D. R. Menick, "Purification and characterization of the Ca^{2+}-ATPase of *Flavobacterium odoratum*," *The Journal of Biological Chemistry*, vol. 271, no. 7, pp. 3945–3951, 1996.

[38] V. Norris, S. Grant, P. Freestone et al., "Calcium signalling in bacteria," *Journal of Bacteriology*, vol. 178, no. 13, pp. 3677–3682, 1996.

[39] M. A. Rivadeneyra, A. Ramos-Cormenzana, G. Delgado, and R. Delgado, "Process of carbonate precipitation by *Deleya halophila*," *Current Microbiology*, vol. 32, no. 6, pp. 308–313, 1996.

[40] O. Braissant, G. Cailleau, C. Dupraz, and E. P. Verrecchia, "Bacterially induced mineralization of calcium carbonate in terrestrial environments: the role of exopolysaccharides and amino acids," *Journal of Sedimentary Research*, vol. 73, no. 3, pp. 485–490, 2003.

[41] C. Dupraz, P. T. Visscher, L. K. Baumgartner, and R. P. Reid, "Microbe-mineral interactions: early carbonate precipitation in a hypersaline lake (Eleuthera Island, Bahamas)," *Sedimentology*, vol. 51, no. 4, pp. 745–765, 2004.

[42] F. Hammes and W. Verstraete, "Key roles of pH and calcium metabolism in microbial carbonate precipitation," *Reviews in Environmental Science and Biotechnology*, vol. 1, no. 1, pp. 3–7, 2002.

[43] S. Schultze-Lam, D. Fortin, B. S. Davis, and T. J. Beveridge, "Mineralization of bacterial surfaces," *Chemical Geology*, vol. 132, no. 1–4, pp. 171–181, 1996.

[44] G. Aloisi, A. Gloter, M. Krüger, K. Wallman, F. Guyot, and P. Zuddas, "Nucleation of calcium carbonate on bacterial nanoglobules," *Geology*, vol. 34, no. 12, pp. 1017–1020, 2006.

[45] E. Aizenman, H. Engelberg-Kulka, and G. Glaser, "An *Escherichia coli* chromosomal 'addiction module' regulated by 3′,5′-bispyrophosphate: a model for programmed bacterial cell death," *Proceedings of the National Academy of Sciences of the United States of America*, vol. 93, no. 12, pp. 6059–6063, 1996.

[46] G. A. Silva-Castro, I. Uad, A. Rivadeneyra et al., "Carbonate precipitation of bacterial strains isolated from sediments and seawater: formation mechanisms," *Geomicrobiology Journal*, vol. 30, no. 9, pp. 840–850, 2013.

Hindawi Publishing Corporation
BioMed Research International
Volume 2015, Article ID 401672, 8 pages
http://dx.doi.org/10.1155/2015/401672

Research Article

Characterization, Microbial Community Structure, and Pathogen Occurrence in Urban Faucet Biofilms in South China

Huirong Lin, Shuting Zhang, Song Gong, Shenghua Zhang, and Xin Yu

Institute of Urban Environment, Chinese Academy of Science, Xiamen 361021, China

Correspondence should be addressed to Xin Yu; xyu@iue.ac.cn

Received 1 July 2014; Revised 16 December 2014; Accepted 27 January 2015

Academic Editor: George Tsiamis

The composition and microbial community structure of the drinking water system biofilms were investigated using microstructure analysis and 454 pyrosequencing technique in Xiamen city, southeast of China. SEM (scanning electron microscope) results showed different features of biofilm morphology in different fields of PVC pipe. Extracellular matrix material and sparse populations of bacteria (mainly rod-shaped and coccoid) were observed. CLSM (confocal laser scanning microscope) revealed different distributions of attached cells, extracellular proteins, α-polysaccharides, and β-polysaccharides. The biofilms had complex bacterial compositions. Differences in bacteria diversity and composition from different tap materials and ages were observed. Proteobacteria was the common and predominant group in all biofilms samples. Some potential pathogens (Legionellales, Enterobacteriales, Chromatiales, and Pseudomonadales) and corrosive microorganisms were also found in the biofilms. This study provides the information of characterization and visualization of the drinking water biofilms matrix, as well as the microbial community structure and opportunistic pathogens occurrence.

1. Introduction

During the past decades, scientists have paid great attention to the biofilms formation in drinking water distribution systems (DWDSs) since biofilms formation and its resistance to disinfection were considered to be potential risk in DWDSs [1–3]. Bacteria can grow in bulk water and become attached to pipe walls as biofilms. Biofilms formation in DWDSs can lead to public health issues, such as protecting pathogenic bacterial regrowth, and depletion of disinfectant [4–6]. The microbial quality of tap water is closely related to consumers' health. Thus, knowledge of biofilms behavior in DWDSs and faucet can contribute to the design of effective control strategies.

DWDSs are engineered environments that are subject to frequent, variable disturbances caused by many factors including long residence times, each associated with loss of disinfectant residual and generating higher levels of biofilms growth. These changes are reflected in the new phenotypic characteristics developed by biofilm bacteria and occurred in response to a variety of environmental signals. Phylogenetically diverse bacterial groups can inhabit the biofilms attached to the pipes and the bulk water. The study of bacterial ecology can improve the understanding of the persistence of biofilms and pathogens.

Studies to date suggest that the planktonic-biofilm transition is a complex and highly regulated process. Several methods including culture-based and independent analyses showed that members of the class Proteobacteria, including the Alpha-, Beta-, and Gammaproteobacteria were considered to be the most predominant bacterial groups in water distribution systems [7]. Recent genetic and molecular approaches used to study bacterial and fungal biofilms have identified genes and regulatory circuits important for initial cell-surface interactions, biofilm maturation, and the return of biofilm microorganisms to a planktonic mode of growth [1, 3, 7]. However, the characterization of microbial communities of biofilms in DWDSs is far from being fully understood. To give insight into the characterization and bacterial diversity of biofilms in drinking water distribution systems, microstructure analysis (SEM, CLSM and XRF) was used for the characterization of biofilms on faucet. The bacterial community compositions of real biofilms from

Table 1: The biofilms samples used in this study and water quality parameters at each sampling location.

Samples	A1	A2	A3	A4	A5	A6	A7	A8	A9	A10	A11	A12
Tap material	Stainless steel	PVC	Stainless steel	Cast iron	Cast iron	Stainless steel	Stainless steel	Cast iron	Cast iron	Stainless steel	PVC	PVC
Age (year)	2	1	4	9	8	3	5	12	15	6	1	0.5
pH	7.08	6.8	7.01	6.62	7.11	7.03	6.94	7.35	7.26	6.83	6.98	6.7
TSS	40	49	99	75	81	69	39	80	69	73	52	47
Turbidity	0.6	0.3	0.3	0.2	0.4	0.2	0.1	0.3	0.2	0.1	0.4	0.3
Residual chlorine (mg/L Cl_2)	0.55	0.54	0.62	0.46	0.49	0.63	0.65	0.57	0.61	0.62	0.3	0.4
Sulfate (mg/L)	10.4	12.9	31.8	24.2	30.6	13.8	24.2	22	27.8	19.8	17.8	16.5

12 urban household taps (Xiamen, southeast of China) were detected using 454 pyrosequencing technique. Potential pathogens and corrosive microorganisms occurrence was also discussed.

2. Methods

2.1. Characterization and Visualization of the Biofilms Matrix in DWDSs. In order to observe the biofilms formed on drinking water pipe surface, five 5 × 5 mm removable PVC sheets were inserted in real PVC DWDSs pipe for biofilm attachment. They were sterilized by immersion in 70% ethanol for 2 min individually and air dried. The PVC tap in our lab was twisted off and the sheets were transferred with sterile forceps to the tap; then, the tap was screwed on. After three months, PVC sheets were took out for scanning electron microscopy (SEM) and staining. One PVC sheet was fixed, dried, and viewed with a scanning electron microscope (Hitachi S-4800, Japan). The other four were stained with DAPI (4,6-diamidino-2-phenylindole) for attach cells, FITC (fluorescein isothiocyanate) for extracellular protein, Con-A (concanavalin A) for α-polysaccharide, and CW (calcofluor white) for β-polysaccharide, respectively. Each kind of stain was added on each sheet in the dark. After 15 min the sheets were analyzed using CLSM. CLSM 3D-image was used to visualize the staining biofilms. The CLSM scanned different layers of the staining biofilms. The thickness of the biofilms was got from signals of different layers using the software ZEN 2008 Light Edition.

2.2. Biofilms Sampling for 454 Pyrosequencing. It is difficult to get the information on the microbial diversity of biofilms within DWDSs due to limited access and the high cost involved in sampling. In this study, biofilms in taps were collected from a drinking water distribution system of Xiamen, Fujian Province in southeast of China. Different taps with different materials and different ages were studied (Table 1). The taps were removed and ethanol-sterilized cotton swabs were then used to collect biofilms on the taps. Then, the collected biofilms were moved to 2 mL sterilized EP tubes and put into an ice box during transportation. For each sampling point, the physicochemical water quality parameters were measured and listed in Table 1.

2.3. X-Ray Fluorescence (XRF) Analysis of Biofilms A3 on Corroded Tap. Among the biofilms samples, A3 was red, indicating that the pipe was corroded. In order to analyze the element contents in the biofilms, XRF analysis of the biofilms A3 was performed at the XRF microprobe station (beam line 4W1B) of Beijing Synchrotron Radiation Facility (BSRF), Institute of High Energy Physics of China. The electron energy in the storage ring was 2.2 GeV, with a current range from 78 to 120 mA. The size of the exciting X-ray beam was 10 μm × 20 μm. XRF spectra were collected by a PGY Si (Li) solid detector, positioned at 90° to the beam line. The scanning point of the sample was selected and observed by a microscope.

2.4. DNA Extraction, 16S rRNA Genes Amplification, and Pyrosequencing. Total DNA of the biofilms samples was extracted and purified using a bead beating method (FastDNA TMSPIN Kit for Soil, Bio101 Inc., USA) following the manufacturer's instructions. For pyrosequencing analysis, the V3 and V4 region of 16S rRNA gene was amplified with the primers 338F (5′-ACTCCTACGGGAGGCAGCAG-3′) and 802R (5′-TACNVGGGTATCTAATCC-3′). The PCR was carried out in a total volume of 20 μL: H_2O 13.25 μL, 10xPCR ExTaq Buffer 2.0 μL, DNA template (100 ng/μL) 0.5 μL, primer 338F (10 mmol/L) 1.0 μL, 802R (10 mmol/L) 1.0 μL, dNTP 2.0 μL, and ExTaq (5 U/mL) 0.25 μL. The DNA amplification condition used in this study was initial denaturation at 95°C for 3 min, followed by 35 cycles of 10 s at 95°C, 30 s at 58°C, and 6 sec at 72°C, followed by a final extension at 72°C for 7 min. The PCR products were purified and end-repaired, A-tailed, PE-adapter ligated, and then utilized for pyrosequencing on the 454 Genome Sequencer FLX platform [8].

The unique tags (nonredundant tags) were obtained and aligned against the 16S rRNA database using the BLASTN algorithm. The raw sequences obtained from 454 pyrosequencing were optimized. The redundant tags were deleted by Mothur v.1.11.0 [9]. Sequences with similarities greater than

97% were grouped in one OTU. Using the MEGA5.0 program, the 60 bp representative sequences were aligned by the ClustalW with default settings, and a phylogenetic analysis was performed based on the neighbor-joining method [9].

3. Results and Discussion

3.1. Characterization and Visualization of the Drinking Water Biofilms Matrix. DWDSs are engineered environments which are subject to frequent, variable disturbances caused by many factors including long residence times due to dead ends and low flow rates, and the latter are associated with loss of disinfectant residual and generating higher levels of biofilm growth. Attachment is required for biofilms formation, and bacteria interact with pipe wall surface through adhesions including polysaccharides and surface proteins, with initial contact often mediated by active motility. The formation of a biofilm is the result of successional development into a mature community, which may require several years before steady state is achieved. For example, it was found that the successional development of a model DW biofilm during a 3-year period was an orderly process resulting in a stable, well-defined community [10]. In order to observe and characterize a real DWDSs biofilm, CLSM and SEM were applied in this study. SEM analysis of the PVC slice revealed different features of biofilms morphology in different fields of the PVC pipe surface. Possible EPS was present on the PVC slice in one field (Figures 1(a) and 1(b)). Sparse populations of mainly rod-shaped bacteria were observed in another field (Figure 1(c)). There were also globular-shaped bacteria (Figure 1(d)). Using Zen 2008 software, the "range" value showed the thickness of the biofilm. CLSM 3D-image results suggested that after three months' growth the biofilm was about 20 μm thick. CLSM results also revealed different distributions of attached cells (Figure 1(e)), extracellular protein (Figure 1(f)), α-polysaccharide (Figure 1(g)), and β-polysaccharide (Figure 1(h)).

During sampling, it was found that there were some yellow iron filings in the biofilm A3, suggesting that the Fe in the stainless steel pipe was released. In order to obtain the elements contents of corroded biofilm A3, XRF was used. Figure 2 was the typical spot scan result of biofilm A3. It showed that K, Ca, Fe, Cu, and Zn were present in biofilm A3, suggesting that this pipe was corroded and metal elements were released which might affect the water quality in the DWDSs. Our study enabled the concurrent visualization and evaluation of the biofilm growth as well as EPS matrix (extracellular proteins and polysaccharide).

3.2. Diversity of Microbial Communities in the Tap Biofilms. Pyrosequencing is a powerful tool to investigate microorganisms community [11]. Compared with conventional cloning and sequencing methods, pyrosequencing can obtain more sequences and OTUs. In this study, 8 biofilms samples were successfully high-throughput pyrosequenced among the 12 samples. To assess the sequencing depth and the species richness, a rare faction curve was constructed for each sample. Alpha diversity measurement for the samples (Table 2) suggested variations in species richness (Chao1) and species evenness (Simpson index) among different biofilms samples. Higher species richness of a given sample might present a lower species diversity resulting from a lower evenness of the sample. PcoA results indicated that the biofilms samples obtained from different tap materials showed quite different clusters. Biofilms formed on PVC had a more simple microbial community compared with those formed on cast iron and stainless steel. This result was consistent with another study which conducted with 16S rRNA genes sequence [12]. These results indicated that PVC was a more ideal material compared with the other materials as fewer bacteria attached on it.

3.3. Composition of Microbial Community. DWDSs biofilms are considered to be complex, dynamic microbial assemblages with extensive phenotypic diversity supporting adaptation to different hydraulic and chemical surface conditions [3, 13–15]. As a result, biofilms formed on different materials might have different community structures. The phylogenetic analysis based on the 16S rRNA V3-V4 region sequences from the biofilms samples was showed in Figure 3. The points in this figure were dispersive. It suggested that distinct bacterial communities were detected in these biofilms from different tap materials and different ages. Many factors could influence the bacterial communities including pipe age and pipe material. However, some interesting information could be found. For example, A8 and A9 (biofilms formed on cast iron) located in one region, while A1 and A3 (biofilms formed on stainless steel) located in another region. This result suggested that the pipe materials might be an important factor for the bacterial communities of the biofilms. In addition, biofilms A2 formed on PVC had relatively simple bacterial community structure, with Betaproteobacteria (54.09%) and Alphaproteobacteria (38.24%) as its main community composition (Figure 4). It was quite different from the biofilms formed on cast iron and stainless steel.

The bacterial communities of the samples in both class and species were shown in Figure 4. A high variability of the bacterial core communities of the biofilms was found in this study. Taxonomic analysis revealed that proteobacteria was the common and predominant group in all biofilms samples. These results were broadly consistent with other biofilms studies [7, 16]. Besides, Actinobacteria was the second largest bacterial group in the samples A2, A8, A9, and A10. Some important bacteria should be paid attention to. For example, Sphingomonadales was found in all samples. This might be due to the resistance to chlorine of Sphingomonadales. In addition, Nitrospiraceae and Thiotrichales were found in this study, suggesting the occurrence of nitrification and sulfur transformation.

3.4. Potential Pathogen and Corrosive Microorganisms Occurrence. Opportunistic pathogens in drinking water systems are an emerging health concern. In this study, some waterborne opportunistic pathogens were found in the biofilms

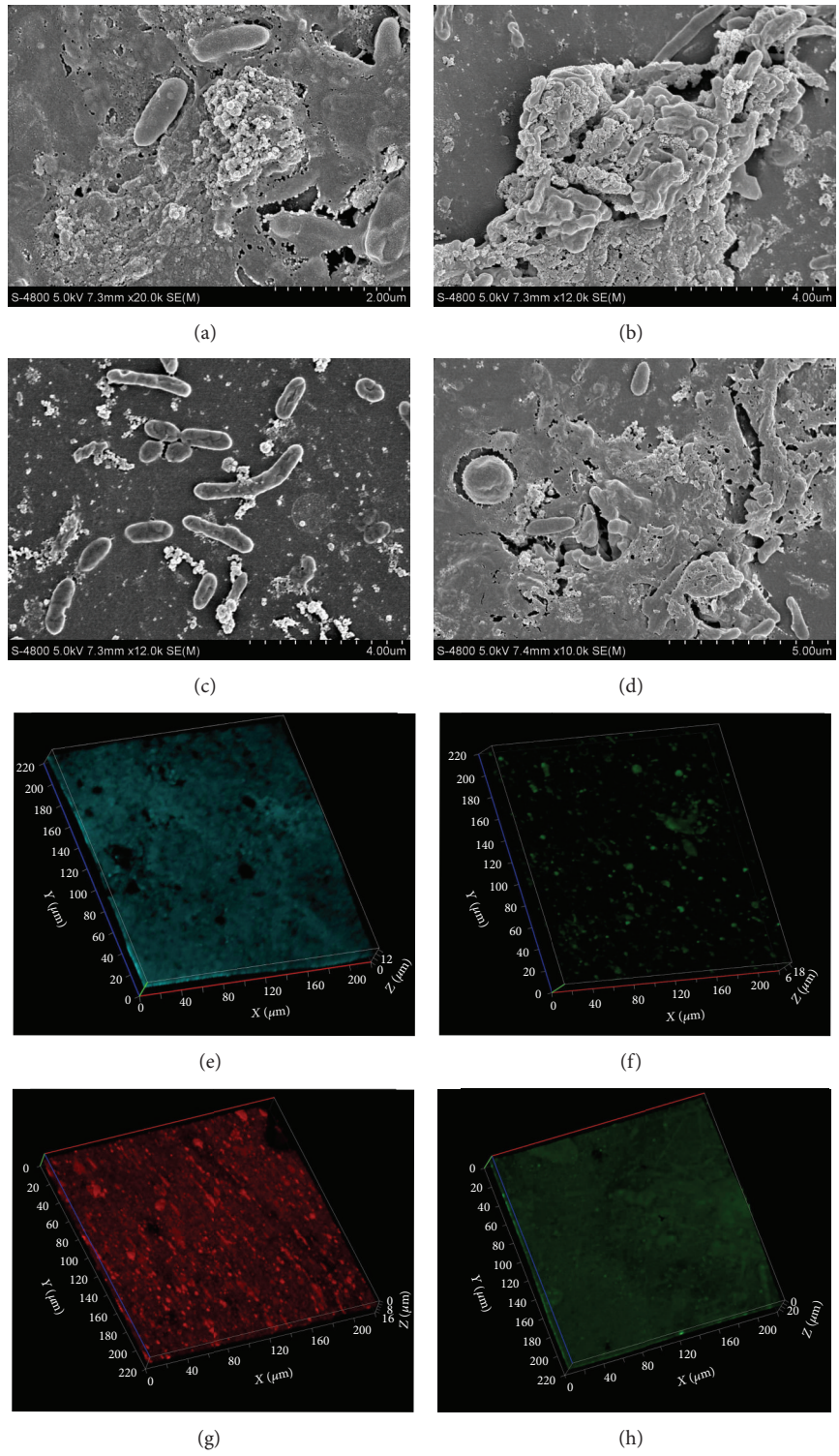

Figure 1: Visualization of the drinking water biofilms matrix on the PVC slice after three months growth. SEM images of extracellular matrix material (a, b) and rod-shaped bacteria (c) and globular-shaped bacteria (d), CLSM 3D-image of staining biofilms on the surface of the PVC slice after three months growth, DAPI for attach cells (e), FITC for extracellular protein (f), Con-A for α-polysaccharide (g), and CW for β-polysaccharide (h).

Table 2: Comparison of phylotype coverage and diversity estimators of the microbial community structure employing the 454 pyrosequencing analysis.

Tap material	Samples	Reads	OTUs	ACE	Chao 1	Shannon	Simpson
PVC	A2	10,804	81	129	139	3.64	0.862
Stainless steel	A1	9,826	186	298	292	4.63	0.898
	A3	36,655	146	294	276	3.93	0.888
	A7	14,605	114	204	202	4.08	0.896
	A10	9,826	351	478	481	5.37	0.927
Cast iron	A5	13,660	106	182	192	3.27	0.831
	A8	13,214	217	383	340	4.43	0.921
	A9	27,517	152	250	256	4.46	0.916

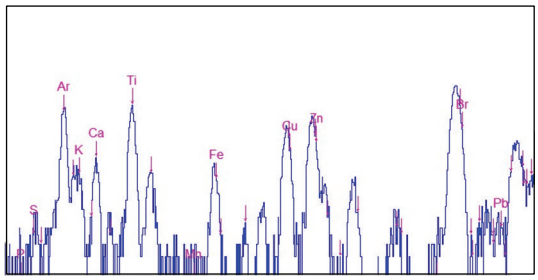

Figure 2: Typical XRF spectra in biofilm A3 from drinking water distribution stainless steel pipe wall. The Ar peak was from the air, while Ti and Br peak were artefact caused by 3M tape for fixing sample.

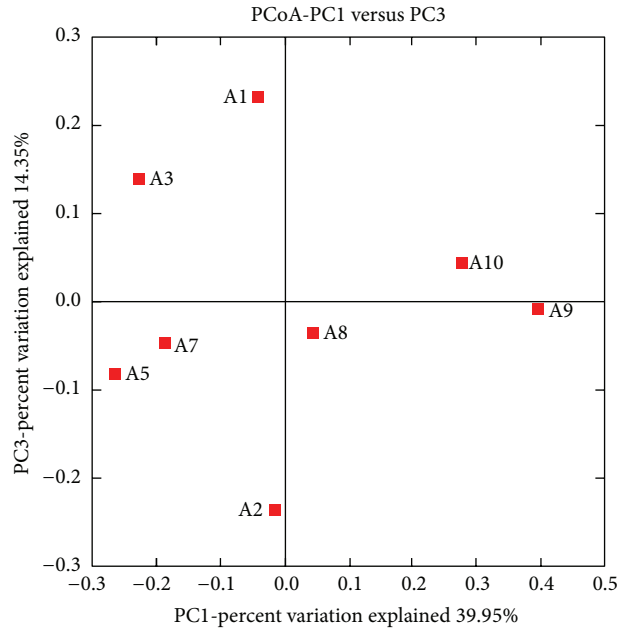

Figure 3: Phylogenetic analysis based on the 16S rRNA V3-V4 region sequences from the biofilms samples.

samples. They were members of species Legionellales, Enterobacteriales, Chromatiales, Pseudomonadales, and Enterococcaceae, although there were differences in numbers for each sample. Abundance of some potential corrosive microorganisms and pathogens in genus level in different bacterial communities was listed in Table 3. These pathogen bacteria in the biofilms may be the risk to human health and lead to clinical and outbreak cases. In previous studies, it was found that environmental pathogens such as *Legionella pneumophila* and *Mycobacterium avium* have been shown to be associated with DW biofilms [1, 17, 18]. Our taxonomic findings are consistent with these studies. In some studies, it was found that Mycobacteria were found to be the predominant bacterial genera in DWDSs because they were generally resistant to disinfectants due to their complex cell wall [3, 18–20]. However, it was not detected in this study.

As corrosion was found in the biofilm A3 and XRF result showed high Fe, Cu, and Pb contents in the biofilms sample, the bacterial community information was further analyzed to understand the possible roles of microorganisms in iron corrosion. Thiotrichales (sulfur oxiding bacteria) was found in A1 biofilm sample form on stainless steel. In addition, potential iron reducing bacteria (Bacillales, Clostridiales, and Pseudomonadales) were found in some samples (Table 3). It was reported that IRB might generate Fe_3O_4 in anaerobic conditions, leading to corrosion in DWDSs. As a key impact factor to corrosion, the sulfate contents in the drinking water of this city are usually low according to the general survey. For example, survey data in 2012 showed that there were among the 102 samples, only 2 samples had the sulfate contents higher than 30 mg/L. So in this study, fewer corrosive microorganisms were found in this city, compared with another study which was conducted on the biofilms with higher sulfate contents in water [21]. Nevertheless, these corrosive microorganisms might contribute to corrosion of drinking water pipes. It should be noticed that the genus members within the genera *Bacillus* and *Clostridium* could affect iron corrosion and modify the corrosion products [22].

4. Conclusions

In this study, combined use of SEM, CLSM, and XRF was successfully conducted for the characterization and visualization of the drinking water biofilms matrix. EPS and

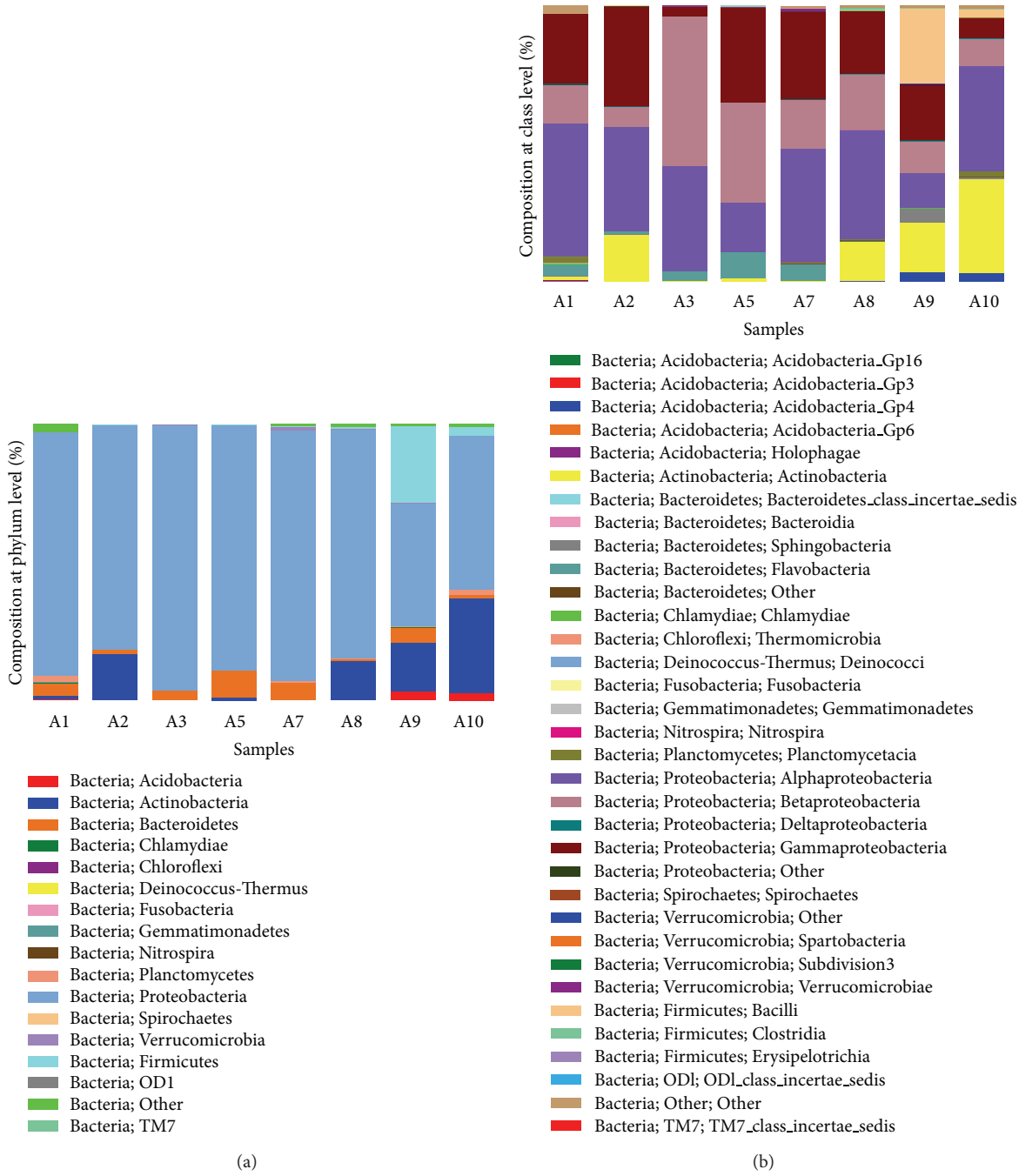

Figure 4: Proportional composition of microbes in the biofilms samples on different materials and from different ages at the phylum level (a) and class level (b). The information of each biofilm sample was listed in Table 1.

bacteria (mainly rod-shaped and coccoid) were observed in the biofilms. Four hundred fifty-four pyrosequencing used to characterize bacterial diversity in these biofilms samples suggested that there were differences in the bacterial community composition between different biofilms samples formed on different tap materials with different ages. Proteobacteria (mostly Alpha-, Beta-, and Gamma-) predominated in the biofilms samples. Some potential pathogens (members of species Legionellales, Enterobacteriales, Chromatiales, and Pseudomonadales) were found in the biofilms samples. There were also some potential corrosive microorganisms (Thiotrichales, Bacillales, Clostridiales, and Pseudomonadales). In order to prevent biofilms formation, PVC might be a more ideal material compared with the others. This work might add some new insights into microbial community and its influential factors in DWDSs.

Table 3: Abundance of some potential pathogen and corrosive microorganisms in genus level in different bacterial communities (count).

	genera	PVC	stainless steel				cast iron		
		A2	A1	A3	A7	A10	A5	A8	A9
Pathogen	*Escherichia_Shigella*	1	0	1	0	0	0	1	0
	Legionella	0	4	5	0	7	0	4	4
	Pseudomonas	13	27	70	39	444	66	429	1219
	Enterococcus	0	0	0	0	0	0	2	0
SOB	*Thiobacillus*	0	7	0	0	0	0	0	0
IRB	*Bacillus*	0	0	2	1	382	0	1	1826
	Clostridium_XlVa	0	0	0	0	0	4	0	0
	Clostridium_XVIII	0	0	0	0	0	0	1	0
	Pseudomonas	13	27	70	39	444	66	429	1219

SOB: sulfur oxidizing bacteria; IRB: iron reducing bacteria.

Conflict of Interests

The authors declare that there is no conflict of interests regarding the publication of this paper.

Acknowledgments

This work was supported by National High-Tech Research and Development (2012AA062607), the National Natural Science Foundation of China (31300109 and 51278482), Fujian Provincial Natural Science Foundation (2013J05087), and the Science and Technology Project of Xiamen (3502Z20132013).

References

[1] F. Emtiazi, T. Schwartz, S. M. Marten, P. Krolla-Sidenstein, and U. Obst, "Investigation of natural biofilms formed during the production of drinking water from surface water embankment filtration," *Water Research*, vol. 38, no. 5, pp. 1197–1206, 2004.

[2] M. Tachikawa, M. Tezuka, M. Morita, K. Isogai, and S. Okada, "Evaluation of some halogen biocides using a microbial biofilm system," *Water Research*, vol. 39, no. 17, pp. 4126–4132, 2005.

[3] D. Berry, C. W. Xi, and L. Raskin, "Microbial ecology of drinking water distribution systems," *Current Opinion in Biotechnology*, vol. 17, no. 3, pp. 297–302, 2006.

[4] M. W. LeChevallier, W. Schulz, and R. G. Lee, "Bacterial nutrients in drinking water," *Applied and Environmental Microbiology*, vol. 57, no. 3, pp. 857–862, 1991.

[5] C. M. Buswell, Y. M. Herlihy, L. M. Lawrence et al., "Extended survival and persistence of *Campylobacter* spp. in water and aquatic biofilms and their detection by immunofluorescent-antibody and -rRNA staining," *Applied and Environmental Microbiology*, vol. 64, no. 2, pp. 733–741, 1998.

[6] J. M. Regan, G. W. Harrington, and D. R. Noguera, "Ammonia- and nitrite-oxidizing bacterial communities in a pilot-scale chloraminated drinking water distribution system," *Applied and Environmental Microbiology*, vol. 68, no. 1, pp. 73–81, 2002.

[7] P.-Y. Hong, C. Hwang, F. Ling, G. L. Andersen, M. W. LeChevallier, and W.-T. Liu, "Pyrosequencing analysis of bacterial biofilm communities in water meters of a drinking water distribution system," *Applied and Environmental Microbiology*, vol. 76, no. 16, pp. 5631–5635, 2010.

[8] P. D. Schloss, S. L. Westcott, T. Ryabin et al., "Introducing mothur: open-source, platform-independent, community-supported software for describing and comparing microbial communities," *Applied and Environmental Microbiology*, vol. 75, no. 23, pp. 7537–7541, 2009.

[9] K. Tamura, D. Peterson, N. Peterson, G. Stecher, M. Nei, and S. Kumar, "MEGA5: molecular evolutionary genetics analysis using maximum likelihood, evolutionary distance, and maximum parsimony methods," *Molecular Biology and Evolution*, vol. 28, no. 10, pp. 2731–2739, 2011.

[10] A. C. Martiny, T. M. Jørgensen, H.-J. Albrechtsen, E. Arvin, and S. Molin, "Long-term succession of structure and diversity of a biofilm formed in a model drinking water distribution system," *Applied and Environmental Microbiology*, vol. 69, no. 11, pp. 6899–6907, 2003.

[11] A. Gobet, S. I. Böer, S. M. Huse et al., "Diversity and dynamics of rare and of resident bacterial populations in coastal sands," *ISME Journal*, vol. 6, no. 3, pp. 542–553, 2012.

[12] W. F. Lin, Z. S. Yu, X. Chen, R. Liu, and H. Zhang, "Molecular characterization of natural biofilms from household taps with different materials: PVC, stainless steel, and cast iron in drinking water distribution system," *Applied Microbiology and Biotechnology*, vol. 97, no. 18, pp. 8393–8401, 2013.

[13] P. Deines, R. Sekar, H. S. Jensen et al., "MUWS (Microbiology in Urban Water Systems)—an interdisciplinary approach to study microbial communities in urban water systems," in *Integrating Water Systems*, pp. 397–403, 2014.

[14] R. S. Roeder, J. Lenz, P. Tarne, J. Gebel, M. Exner, and U. Szewzyk, "Long-term effects of disinfectants on the community composition of drinking water biofilms," *International Journal of Hygiene and Environmental Health*, vol. 213, no. 3, pp. 183–189, 2010.

[15] I. Douterelo, R. L. Sharpe, and J. B. Boxall, "Influence of hydraulic regimes on bacterial community structure and composition in an experimental drinking water distribution system," *Water Research*, vol. 47, no. 2, pp. 503–516, 2013.

[16] R. P. Revetta, V. Gomez-Alvarez, T. L. Gerke, C. Curioso, J. W. S. Domingo, and N. J. Ashbolt, "Establishment and early succession of bacterial communities in monochloramine-treated drinking water biofilms," *FEMS Microbiology Ecology*, vol. 86, no. 3, pp. 404–414, 2013.

[17] J. O. Falkinham, M. D. Iseman, P. de Haas, and D. van Soolingen, "*Mycobacterium avium* in a shower linked to pulmonary

disease," *Journal of Water and Health*, vol. 6, no. 2, pp. 209–213, 2008.

[18] R. Liu, Z. Yu, H. Zhang, M. Yang, B. Shi, and X. Liu, "Diversity of bacteria and mycobacteria in biofilms of two urban drinking water distribution systems," *Canadian Journal of Microbiology*, vol. 58, no. 3, pp. 261–270, 2012.

[19] L. C. Simões, M. Simões, and M. J. Vieira, "Influence of the diversity of bacterial isolates from drinking water on resistance of biofilms to disinfection," *Applied and Environmental Microbiology*, vol. 76, no. 19, pp. 6673–6679, 2010.

[20] R. Liu, Z. Yu, H. Guo, M. Liu, H. Zhang, and M. Yang, "Pyrosequencing analysis of eukaryotic and bacterial communities in faucet biofilms," *Science of the Total Environment*, vol. 435-436, pp. 124–131, 2012.

[21] H. F. Sun, B. Y. Shi, Y. H. Bai, and D. Wang, "Bacterial community of biofilms developed under different water supply conditions in a distribution system," *Science of the Total Environment*, vol. 472, pp. 99–107, 2014.

[22] J. E. Kostka, D. D. Dalton, H. Skelton, S. Dollhopf, and J. W. Stucki, "Growth of iron (III)-reducing bacteria on clay minerals as the sole electron acceptor and comparison of growth yields on a variety of oxidized iron forms," *Applied and Environmental Microbiology*, vol. 68, no. 12, pp. 6256–6262, 2002.

Hindawi Publishing Corporation
BioMed Research International
Volume 2015, Article ID 242856, 11 pages
http://dx.doi.org/10.1155/2015/242856

Research Article

Diverse Reductive Dehalogenases Are Associated with Clostridiales-Enriched Microcosms Dechlorinating 1,2-Dichloroethane

Giuseppe Merlino,[1,2] Annalisa Balloi,[1] Massimo Marzorati,[1,3] Francesca Mapelli,[1] Aurora Rizzi,[1] Davide Lavazza,[1] Francesca de Ferra,[4] Giovanna Carpani,[4] and Daniele Daffonchio[1,2]

[1]*Department of Food, Environmental and Nutritional Sciences (DeFENS), University of Milan, 20133 Milan, Italy*
[2]*Biological and Environmental Sciences and Engineering Division, King Abdullah University of Science and Technology, Thuwal 23955-6900, Saudi Arabia*
[3]*Laboratory for Microbial Ecology and Technology (LabMET), Ghent University, 9000 Ghent, Belgium*
[4]*Research Center for Non-Conventional Energy, Istituto Eni Donegani, Environmental Technologies, 20097 San Donato Milanese, Italy*

Correspondence should be addressed to Daniele Daffonchio; daniele.daffonchio@unimi.it

Received 8 November 2014; Accepted 6 March 2015

Academic Editor: Ameur Cherif

The achievement of successful biostimulation of active microbiomes for the cleanup of a polluted site is strictly dependent on the knowledge of the key microorganisms equipped with the relevant catabolic genes responsible for the degradation process. In this work, we present the characterization of the bacterial community developed in anaerobic microcosms after biostimulation with the electron donor lactate of groundwater polluted with 1,2-dichloroethane (1,2-DCA). Through a multilevel analysis, we have assessed (i) the structural analysis of the bacterial community; (ii) the identification of putative dehalorespiring bacteria; (iii) the characterization of functional genes encoding for putative 1,2-DCA reductive dehalogenases (RDs). Following the biostimulation treatment, the structure of the bacterial community underwent a notable change of the main phylotypes, with the enrichment of representatives of the order *Clostridiales*. Through PCR targeting conserved regions within known RD genes, four novel variants of RDs previously associated with the reductive dechlorination of 1,2-DCA were identified in the metagenome of the Clostridiales-dominated bacterial community.

1. Introduction

Chlorinated compounds are among the major global environmental contaminants [1]. A large number of compounds of this class of chemicals have been produced in big quantities for several applications in industry and agriculture such as biocides, flame retardants, solvents, and intermediates for the production of polymers (e.g., PVC) [1, 2]. Their widespread diffusion and use resulted in the massive release in the environment, with consequent concerns for human health due to the persistence, tendency to bioaccumulate, and proven toxicity [2, 3]. Due to the physicochemical properties, most halogenated compounds are recalcitrant to aerobic dehalogenation and tend to accumulate in anoxic ecosystems (e.g., soils and groundwater aquifers). For this reason, many of the research efforts of the last decades, aimed at defining efficient remediation approaches, were focused on the investigation of anaerobic degrading potential of microbial cultures enriched/isolated from typical anoxic environments. Chlorinated solvents in these conditions can undergo biologically mediated degradation through either oxidative, fermentative, or reductive processes [4]. Particular interest has been focused on the third kind of biodegradation process, since several studies have highlighted the high dechlorinating

performances of pure and mixed microbial cultures through reductive dehalogenation [5–10]. The peculiarity of this process is that the chlorinated molecule is the terminal electron acceptor of the membrane-bound electron transport chain coupled to the generation of energy in the form of ATP [4].

Among the wide variety of chlorinated solvents, 1,2-dichloroethane (1,2-DCA) is considered one of the major pollutants, being one of the most widespread contaminating groundwater worldwide and being classified as a possible human carcinogenic agent by many environmental agencies [2]. 1,2-DCA can undergo either partial or complete detoxification in anoxic conditions through three different mechanisms: dichloroelimination, reductive hydrogenolysis, and dehydrochlorination [5]. Among these, only the first mechanism leads to the production of the harmless end-product ethylene, while the other two generate molecules whose toxicity is even higher than 1,2-DCA, in particular the carcinogenic vinyl chloride (VC). Key enzymes involved in this anaerobic dehalogenating metabolism are the reductive dehalogenases (RDs), a class of cobalamin-dependent oxygen-sensitive enzymes, usually associated with the membranes and capable of replacing halogen atoms with hydrogen ones from the carbon backbone of the molecules [4, 11]. Different studies have unveiled details about structure and function of some enzymes belonging to this class [12–14]. Only recently, novel RDs sequences were correlated with 1,2-DCA dechlorination to ethene in a 1,2-DCA dehalogenating enrichment culture containing a *Dehalobacter* sp. WL (rdhA1, rdhA2, and rdhA3) [15] and *in situ* in the upper water layer of a double layer aquifer contaminated by 1,2-DCA (RD54) [16]. The enrichment culture setup from the upper layer of the aquifer (culture 6VS) contained both *Dehalobacter* and *Desulfitobacterium* spp. In addition to the two just cited representatives of the phylum Firmicutes, only few other bacterial strains have been identified so far as capable of detoxifying 1,2-DCA to ethylene via dichloroelimination. Papers [17, 18] were the first to report the ability of two *Chloroflexi* representatives, respectively, *Dehalococcoides ethenogenes* strain 195 and *Dehalococcoides* sp. strain BAV1 to grow on 1,2-DCA as electron acceptor producing ethylene as the main end product. A peculiarity of the species of this genus is their capability to grow exclusively on chlorinated compounds as electron acceptor. Other representatives of the phylum Chloroflexi with the ability to grow on 1,2-DCA described recently are two strains of the genus *Dehalogenimonas*: *D. lykanthroporepellens* [19] and *D. alkenigignens* [20], both characterized by the ability to degrade high concentration of 1,2-DCA up to 8.7 mM [21].

In the present work, the dechlorinating bacterial microbiome in the lower layer of the same aquifer investigated by [16] has been characterized in terms of structure and functionality, before and after the supplement with lactate. We have investigated (i) the response of the indigenous microbial community to lactate treatment, (ii) the key microbial dehalogenating bacteria, and (iii) the RDs involved in the dehalogenation process.

2. Materials and Methods

2.1. Preparation of Enrichment Cultures. Evaluation of biodegradation of 1,2-DCA was carried out in anaerobic microcosms set-up with groundwater collected from the lower layer (from 14 m to 40 m deep) of an aquifer previously studied in northern Italy [7, 9, 16], heavily polluted exclusively by 1,2-DCA more than 30 years ago. Concentration of the contaminant in the lower aquifer was about $197 \pm 23\,mg\,L^{-1}$ and it was maintained the same during preparation of anaerobic cultures. The other chlorinated ethane and ethene were not detected. Thirty mL triplicate microcosms were assembled in 50 mL vials under an atmosphere of 80% N_2, 15% CO_2, and 5% H_2 in the anaerobic glove-box Simplicity 888 (Plas-Labs, USA). Culturing medium consisted of a 1 : 200 dilution of a trace elements solution ($12.8\,g\,L^{-1}$ nitrilotriacetic acid, $1.35\,g\,L^{-1}$ $FeCl_3{\cdot}6\ H_2O$, $0.1\,g\,L^{-1}$ $MnCl_2{\cdot}4\ H_2O$, $0.024\,g\,L^{-1}$ $CoCl_2{\cdot}6\ H_2O$, $0.1\,g\,L^{-1}$ $CaCl_2{\cdot}2\ H_2O$, $0.1\,g\,L^{-1}$ $ZnCl_2$, $0.025\,g\,L^{-1}$ $CuCl_2{\cdot}2\ H_2O$, $0.01\,g\,L^{-1}$ H_3BO_3, $0.024\,g\,L^{-1}$ $Na_2MoO_4{\cdot}2\ H_2O$, $1\,g\,L^{-1}$ NaCl, $0.12\,g\,L^{-1}$ $NiCl_2{\cdot}6\ H_2O$, and $0.026\,g\,L^{-1}$ $Na_2SeO_3{\cdot}5\ H_2O$), a supplementary salt solution ($43\,mg\,L^{-1}$ NH_4Cl, $0.5\,g\,L^{-1}$ KH_2PO_4, $0.2\,g\,L^{-1}$ $MgCl_2{\cdot}6\ H_2O$, and $0.01\,g\,L^{-1}$ $CaCl_2{\cdot}2\ H_2O$), 0.05% (w/v) yeast extract, 0.5 mM 4-(2-hydroxyethyl) piperazine-1-ethanesulfonic acid/NaOH (Hepes/NaOH) solution pH 7.0, cysteine 1 mM, and vitamin B_{12} $50\,mg\,L^{-1}$. Lactate at final concentration of 5 mM was used as the only carbon source and electron donor [22]. Control microcosms were prepared by incubating parallel vials containing the same culturing medium with filter-sterilized groundwater samples. All microcosms were sealed with teflon-faced septa and aluminum crimp seals and statically incubated in the dark at 23°C.

Concentration of 1,2-DCA and of its possible degradation products, ethane and VC, was evaluated by the injection of 500 μL samples of headspace of the microcosms in a Gas Chromatograph/Flame Ionization Detector (GC/FID) Agilent 7694 equipped with a DB624 column (J&W Scientific, Folsom, CA). The temperature of the oven and of the detector was set at 80 and 200°C, respectively. 1,2-DCA limit of detection was $1.0\,\mu g\,L^{-1}$.

2.2. Genomic DNA Isolation. Groundwater and microcosm samples, respectively, 30 and 1.5 mL (samples withdrawn from replicate cultures were pooled together for a total final volume of 4.5 mL), were filtered using Sterivex filters (Millipore, Milan, Italy). Total genomic DNA was extracted from the filtered bacterial cells by incubating the filter with 2 mL of a lysis solution containing $1\,mg\,mL^{-1}$ lysozyme, 1% (w/v) sodium dodecyl sulphate, and $0.5\,mg\,mL^{-1}$ proteinase K and purified as previously described by Murray et al. [23].

2.3. PCR Amplification of Bacterial and Archaeal 16S rRNA and RD Genes. Bacterial *16S rRNA* gene was amplified from the groundwater metagenome using universal primers 27f and 1492r [24] with the following reaction concentrations in a final volume of 50 μL: 1X PCR buffer, 1.5 mM $MgCl_2$, 0.12 mM

dNTPs, 0.3 μM of each primer, and 1 U of Taq polymerase. Thermal protocol used was the following: initial denaturation at 94°C for 5 minutes, followed by 5 cycles consisting of denaturation at 94°C for 1 minute, annealing at 50°C for 1 minute, and extension at 72°C for 2 minutes and subsequently by 30 cycles consisting of denaturation at 94°C for 1 minute, annealing at 55°C for 1 minute, and extension at 72°C for 2 minutes. A final extension at 72°C for 10 minutes was performed.

PCR with specific primers for Archaea was attempted in order to investigate the *16S rRNA* diversity of this group of prokaryotes. A first step was carried out using universal archaeal forward primers 21f and 1492r, using the same reaction mix and thermal protocol presented elsewhere [25]. Since the first PCR step did not give any amplicon, a second round of PCR using primers PARCH 340F and 934R was attempted, as previously described by Cytryn et al. [26]. However, also this second amplification attempt did not result in any PCR product.

A 2000 bp region of the reductive dehalogenase gene cluster previously identified by Marzorati and colleagues [16] was amplified using primers PceAFor1 (5′-ACGT GCA ATT ATT ATT AAG G-3′) and DcaBRev (5′-TGG TAT TCA CGC TCC GA-3′), in order to construct a gene library of the functional genes encoding for the RD specific for 1,2-DCA degradation. The reaction mix was prepared as follows: 1X PCR buffer, 1.5 mM $MgCl_2$, 0.2 mM dNTPs, 0.6 μM of each primer, and 1 U of Taq polymerase in a final volume of 25 μL. The thermal consisted of an initial denaturation at 94°C for 3 minutes, followed by 31 cycles of denaturation at 94°C for 30 seconds, annealing at 54°C for 1 minute, extension at 72°C for 2 minutes, and subsequently a final extension at 72°C for 7 minutes.

2.4. 16S rRNA and RD Genes Libraries. Cloning reactions were performed with pGEM cloning kit (pGEM-T Easy Vector Systems, Promega, Milan, Italy) following the instructions of the manufacturer. Sixty ng of PCR product was used for each cloning reaction, maintaining a molar ratio insert : vector of 3 : 1. A PCR assay was performed on white positive colonies to amplify the insert using primers T7 (3′-CTA ATA CGA CTC ACT ATA GGG-5′) and SP6 (3′-ATT TAG GTG ACA CTA TAG AAT A-5′). PCR products were purified with QIAquick PCR Purification Kit (Qiagen, Milan, Italy) according to the manufacturer's instructions.

2.5. 16S rRNA Gene Phylogenetic and RDs Diversity Analyses. Clones from bacterial *16S rRNA* and RD genes libraries were sequenced, respectively, with primers 27F and PceAFor1, using the ABI Prism BigDye terminator cycle sequencing kit (Applied Biosystems, Milan, Italy) and an ABI 310 automated sequencer (Applied Biosystems). Sequences were edited with software Chromas Lite version 2.01. Sequences of the *16S rRNA* bacterial libraries were checked for chimeric PCR products using DECIPHER online software tool [27] and nonchimeric sequences were then used to define operational taxonomic units (OTUs) at 99% of similarity (OTU99) using DOTUR [28]. Shannon diversity index (H') was calculated using software PAST version 3.02 [29]. The sequences of the OTU representatives were analysed using the Basic Local Alignment Search Tool (BLAST) of the online GenBank database [30] and by the CLASSIFIER Match Tool version 2.6 of Ribosomal Database Project II (RDP II) [31]. Pareto-Lorenz distribution curves (PL curves) [32, 33] were constructed based on the *16S rRNA* gene clone library results, in order to graphically evaluate the community organization (Co) of the bacterial consortia as described elsewhere [34].

Identification of the closest relative match for the RDs libraries was carried out comparing the sequences with BLAST. Sequences of functional gene libraries were used to construct neighbour-joining phylogenetic tree, with bootstrap of 1000 repetitions, and compute the evolutionary distances through Kimura's two-parameter model using software MEGA version 5 [35]. Alignment of amino acids sequences of the functional genes deducted from the nucleotide sequences of the RDs libraries was carried as described elsewhere [36] in order to identify characteristic amino acid residues conserved in all RDs.

2.6. Nucleotide Sequence Accession Numbers. Nucleotide sequences of all clones identified in this study were deposited in the EMBL nucleotide sequence database (GenBank/EMBL/DDBJ) under the accession numbers FM210335, FM204948 to FM204979 for bacterial *16S rRNA* genes, and FM204931 to FM204934 for RDs sequences.

3. Results and Discussion

3.1. Structure and Diversity of the Bacterial Community before and after the Biostimulation. A triplicate series of anaerobic microcosms with a concentration of 1,2-DCA of 197 ± 23 mg L^{-1} was set up using groundwater from the lower layer of a double aquifer contaminated by 1,2-DCA analogously to the experiments previously run for the upper layer of the same aquifer system [9]. Following the addition of 5 mM lactate, all the microcosms readily degraded 1,2-DCA in 15 days, with an average dechlorination rate of 13.1 ± 1.9 mg L^{-1} day^{-1}. Ethane accumulated as the only end product while the toxic intermediate VC was always below the detection limit, suggesting that degradation of 1,2-DCA occurred only via dichloroelimination [22]. The analogous biostimulation treatment with groundwater from the upper layer [9] gave considerably higher degradation rate of 69.4 ± 2.2 mg L^{-1} day^{-1}. It can be speculated that this almost-four times statistically significant difference (as determined by Student's t-test with $P < 0.000001$) between the two layers was possibly due to differences in the enriched dechlorinating species.

The bacterial diversity of the community before (t_0) and after (t_1) the biostimulation treatment was evaluated by establishing *16S rRNA* gene clone libraries. Differently from what was observed previously on the upper layer of the aquifer [9], PCR with specific primers for Archaea did not result in any amplicon either before or after lactate amendment, even after a second round of PCR using nested

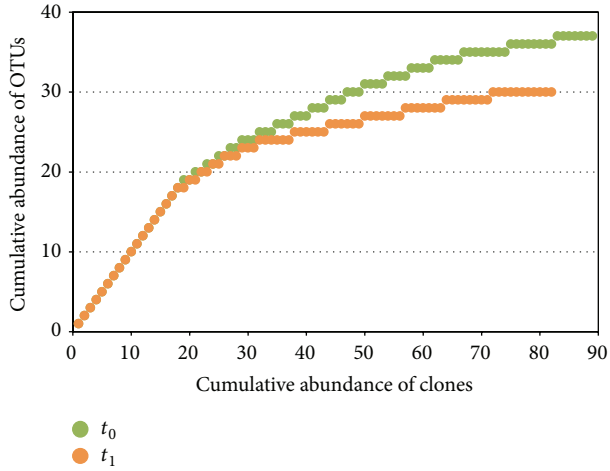

Figure 1: Rarefaction curves calculated for the bacterial *16S rRNA* gene clone libraries, before (t_0) and after (t_1) the biostimulation treatment with lactate.

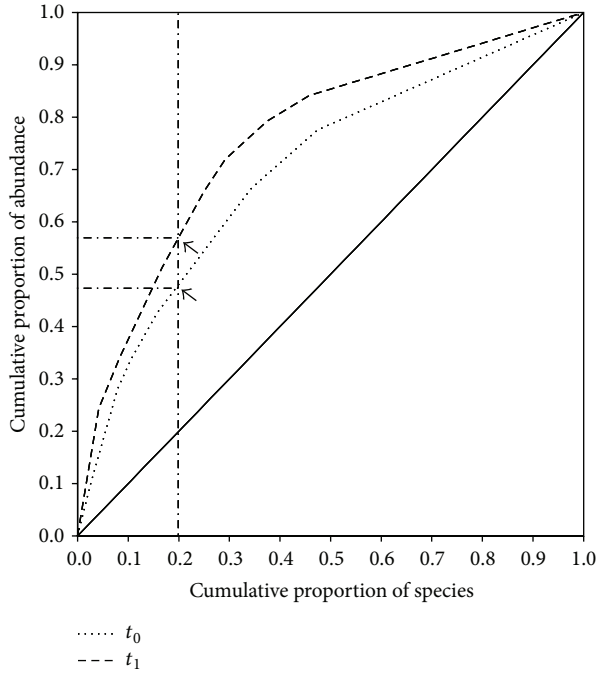

Figure 2: Pareto-Lorenz distribution curves representation of the community organization (Co) of the microbial communities before (t_0, dotted line) and after (t_1, dashed line) the treatment with lactate. The continuous line represents the perfect evenness. Black arrows indicate the OTU cumulative proportion of abundances corresponding to an OTU cumulative proportion of 20%.

primers. This suggests that in the lower aquifer Archaea are not implicated in the dechlorination process.

The bacterial libraries were made of 91 clones each. Chimera check allowed excluding 6.0% of all the sequences obtained, lowering the number of clones to 89 and 82 for t_0 and t_1, respectively. Good coverage of the dominant OTUs was confirmed with rarefaction analysis of the clone libraries (Figure 1). The diversity of the bacterial communities was evaluated by means of two parameters: (i) Shannon index (H'), which allowed describing the species richness, and (ii) evenness index, used to describe the relative abundance among species within the communities. Shannon index, which accounts for both abundance and evenness of the species present, was 3.33 in the lower aquifer with respect to 1.91 in the upper one, indicating that the lower aquifer hosted greater species diversity than the upper one before the treatment. At t_1 after lactate amendment the Shannon index in the lower aquifer decreased (2.88 versus 3.33), while in the upper aquifer it remained almost unchanged (1.81 versus 1.91). The small H' variation in the lower aquifer suggests that relatively limited changes in the biodiversity of the bacterial community occurred after the biostimulation treatment.

The PL curves, used as a graphical estimator of the Co [32, 33], confirmed the little bacterial diversity change in the lower aquifer, in response to the biostimulation treatment (Figure 2). Co curves at t_0 showed a situation where 20% of the OTUs represented about 48% of the total abundance of clones. After the lactate treatment, this proportion grew to 58%, indicating that both communities were characterized by a relatively moderate organization. It can be speculated that the bacterial community of the lower aquifer was characterized by a slight dominance both before and after the biostimulation treatment and sudden changes in the environmental conditions, as those determined by the supplement of lactate, would change the dominant species but would not influence the overall Co and evenness structure of the community.

The 171 clones obtained in the two libraries were grouped in 60 distinct OTUs. A summary of the representatives of each OTU identified through BLAST and CLASSIFIER is presented in Table 1, together with the number of clones of each OTU occurring before and after the biostimulation treatment. Thirty-eight of the 60 OTUs were detected before the lactate amendment and 24 after it, with only two OTUs detected both at t_0 and at t_1, respectively, affiliated to uncultured Clostridiales and to *Sulfuricurvum* sp. The bacterial community at t_0 was characterized by a wider diversity, with dominating sequences belonging to Proteobacteria phylum (Table 1, Figure 3): in order of abundance δ- (38 clones describing 15 OTUs), β- (26 clones describing 11 OTUs), and ε-Proteobacteria (15 clones describing 4 OTUs). Within the δ-Proteobacteria, all the sequences were closely related to genus *Geobacter* (97–100% identity), the majority of which were affiliated to uncultured *Geobacter* sp. and *Geobacter thiogenes* (15 clones each). Species of the genus *Geobacter* were commonly found in freshwater sediments and subsurface environments [37]. Previously, de Wever and colleagues [38] described the ability of *Geobacter thiogenes* to dechlorinate trichloroacetic acid. Another representative of the *Geobacter* clade, *G. lovleyi* (6 clones), a known tetrachloroethene-dechlorinating bacterium [39], was also identified. Within the β- and ε-Proteobacteria groups, the most represented phylotypes were closely related to *Hydrogenophaga taeniospiralis* (11 clones) and *Sulfuricurvum kujiense* (10 clones). These two genera are environmental

Table 1: Summary of the OTU representatives, identified in the 16S rRNA gene libraries.

OTU	Clones		Basic Local Alignment Search Tool-GenBank			CLASSIFIER Match Tool-Ribosomal Database Project II		
	t_0	t_1	Closest described relative	Acc. n°	% identity	Phylogenetic group	Closest classified relative	% certainty[A]
1	3	0	*Geobacter thiogenes*	NR_028775	98.96	Deltaproteobacteria	*Geobacter*	100
2	3	0	*Geobacter thiogenes*	NR_028775	98.78	Deltaproteobacteria	*Geobacter*	100
3	8	0	*Geobacter thiogenes*	NR_028775	99.09	Deltaproteobacteria	*Geobacter*	100
4	3	0	Unc. bacterium	AM410013	97.34	Deltaproteobacteria	*Geobacter*	100
5	1	0	Unc. *Geobacter* sp.	FM204959	98.63	Deltaproteobacteria	*Geobacter*	100
6	1	0	Unc. *Geobacter* sp.	EU266833	98.62	Deltaproteobacteria	*Geobacter*	100
7	3	0	Unc. *Geobacter* sp.	AY752765	98.56	Deltaproteobacteria	*Geobacter*	100
8	1	0	Unc. *Geobacter* sp.	AY752765	98.42	Deltaproteobacteria	*Geobacter*	100
9	1	0	Unc. *Dehalobacter* sp.	HM748813	99.43	Clostridia	*Acetobacterium*	100
10	4	0	Unc. *Sulfurimonas* sp.	KF851122	98.34	Epsilonproteobacteria	*Sulfuricurvum*	100
11	4	0	*Ferribacterium* sp. *7A-631*	KF441656	99.75	Betaproteobacteria	*Ferribacterium*	93
12	1	0	Unc. Gallionellaceae bacterium	EU266776	96.48	Proteobacteria	Betaproteobacteria	100
13	1	0	Unc. Rhodocyclaceae bacterium	JQ279024	98.83	Betaproteobacteria	Rhodocyclaceae	98
14	1	0	Unc. Rhodocyclaceae bacterium	HQ003471	97.64	Betaproteobacteria	Rhodocyclaceae	100
15	0	1	*Acinetobacter baumannii*	KJ958271	99.60	Gammaproteobacteria	*Acinetobacter*	100
16	0	1	*Pseudomonas putida*	GU396283	98.97	Gammaproteobacteria	*Pseudomonas*	100
17	0	7	Unc. *Bacteroides* sp.	AB529592	99.44	Bacteroidia	*Parabacteroides*	99
18	0	1	Unc. Bacteroidetes bacterium	FJ535139	98.31	Bacteroidia	*Parabacteroides*	100
19	0	1	Unc. *Bacteroides* sp.	JQ624314	99.75	Bacteroidia	*Parabacteroides*	100
20	0	1	Unc. Bacteroidetes bacterium	DQ676360	98.97	Bacteroidia	Porphyromonadaceae	99
21	0	1	Unc. *Bacteroides* sp.	FM204969	99.88	Bacteroidia	*Parabacteroides*	99
22	0	1	Unc. *Acidaminobacter* sp.	HM217344	98.61	Clostridia	Clostridiales Incertae Sedis XII	91
23	0	6	Unc. *Acidaminobacter* sp.	HM217344	98.78	Clostridia	Clostridiales	100
24	0	5	Unc. *Acidaminobacter* sp.	HM217344	99.46	Clostridia	Clostridiales Incertae Sedis XII	80
25	2	0	Unc. *Hydrogenophaga* sp.	HM124825	99.67	Betaproteobacteria	*Hydrogenophaga*	100
26	3	0	*Hydrogenophaga taeniospiralis*	AY771764	98.02	Betaproteobacteria	*Hydrogenophaga*	100
27	0	7	*Malikia spinosa*	NR_040904	99.86	Betaproteobacteria	*Malikia*	100
28	1	0	Unc. *Hydrogenophaga* sp.	DQ413154	98.70	Betaproteobacteria	*Hydrogenophaga*	100
29	1	0	Unc. Elusimicrobia bacterium	GU236016	94.55	Elusimicrobia	*Elusimicrobium*	98
30	0	2	*Hydrogenophaga taeniospiralis*	AY771764	98.75	Betaproteobacteria	*Hydrogenophaga*	95
31	8	0	*Hydrogenophaga taeniospiralis*	AY771764	99.06	Betaproteobacteria	*Hydrogenophaga*	98
32	0	6	*Malikia spinosa*	NR_040904	99.73	Betaproteobacteria	*Malikia*	88
33	1	0	Unc. *Acidovorax* sp.	AM084039	99.04	Betaproteobacteria	Comamonadaceae	100
34	3	1	Unc. *Dechloromonas* sp.	JN679130	98.95	Betaproteobacteria	Rhodocyclaceae	100
35	1	0	Unc. *Gallionella* sp.	FJ391502	98.72	Proteobacteria	Betaproteobacteria	100
36	0	2	*Vogesella indigofera*	NR_040800	99.60	Betaproteobacteria	*Vogesella*	100
37	0	1	*Shewanella putrefaciens*	JN019028	99.87	Gammaproteobacteria	*Shewanella*	100
38	9	0	*Sulfuricurvum kujiense*	CP002355	99.22	Epsilonproteobacteria	*Sulfuricurvum*	100
39	1	0	Unc. *Arcobacter* sp.	JQ861849	97.96	Epsilonproteobacteria	*Arcobacter*	93
40	2	0	*Geobacter metallireducens*	NR_075011	98.31	Deltaproteobacteria	*Geobacter*	100

Table 1: Continued.

OTU	Clones		Basic Local Alignment Search Tool-GenBank			CLASSIFIER Match Tool-Ribosomal Database Project II		
	t_0	t_1	Closest described relative	Acc. n°	% identity	Phylogenetic group	Closest classified relative	% certainty[A]
41	3	0	Unc. *Geobacter* sp.	EU266817	99.76	Deltaproteobacteria	*Geobacter*	100
42	2	0	Unc. *Geobacter* sp.	EU266841	99.16	Deltaproteobacteria	*Geobacter*	100
43	5	0	*Geobacter lovleyi*	NR_074979	99.03	Deltaproteobacteria	*Geobacter*	100
44	1	0	*Geobacter thiogenes*	NR_028775	97.48	Deltaproteobacteria	*Geobacter*	100
45	1	1	Unc. Firmicutes bacterium	HQ003641	98.70	Clostridia	Clostridiales Incertae Sedis XII	100
46	0	20	Unc. Firmicutes bacterium	HQ003641	99.45	Clostridia	*Acidaminobacter*	86
47	0	1	Unc. *Clostridium* sp.	FM204998	100.0	Clostridia	*Clostridium XlVa*	100
48	0	3	*Acetobacterium malicum*	NR_026326	99.53	Clostridia	*Acetobacterium*	100
49	1	0	Unc. bacterium	AB759668	95.24	Bacteria	Firmicutes	100
50	2	0	Unc. rumen bacterium	AB615047	94.24	Lentisphaerae	*Victivallis*	97
51	2	0	Unc. *Cytophaga* sp.	EU809766	99.35	Lentisphaerae	*Victivallis*	97
52	1	0	Denitrifying bacterium	FJ802233	98.54	Ignavibacteria	*Ignavibacterium*	91
53	0	8	Unc. *Bacteroides* sp.	FJ862827	99.18	Bacteroidia	*Parabacteroides*	100
54	0	3	*Macellibacteroides fermentans*	NR_117913	99.08	Bacteroidia	*Parabacteroides*	99
55	0	1	Unc. Bacteroidetes bacterium	FJ535139	94.64	Bacteroidia	Porphyromonadaceae	88
56	0	1	Unc. Bacteroidetes bacterium	DQ676360	99.30	Bacteroidia	Bacteroidales	99
57	1	0	Unc. *Prolixibacter* sp.	JQ723616	97.85	Bacteria	Bacteroidetes	100
58	1	0	Unc. *Geobacter* sp.	JQ086897	98.72	Deltaproteobacteria	*Geobacter*	100
59	1	0	*Geobacter lovleyi*	NR_074979	99.37	Deltaproteobacteria	*Geobacter*	100
60	1	0	*Sulfuricurvum kujiense*	NR_074398	99.29	Epsilonproteobacteria	*Sulfuricurvum*	100

[A] Confidence threshold of the RDPII CLASSIFIER Tool is 80%.

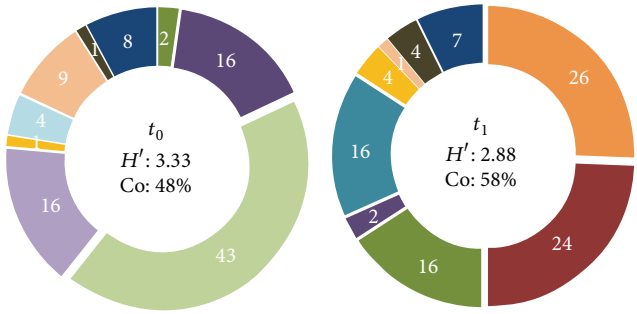

(a)

Genus	t_0	t_0 (%)	t_1	t_1 (%)
Parabacteroides	0	0.00	21	25.61
Acidaminobacter	0	0.00	20	24.39
Unc. *Clostridiales* sp.	2	2.25	13	15.85
Hydrogenophaga	14	15.73	2	2.44
Malikia	0	0.00	13	15.85
Geobacter	38	42.70	0	0.00
Sulfuricurvum	14	15.73	0	0.00
Acetobacterium	1	1.12	3	3.66
Ferribacterium	4	4.49	0	0.00
Unc. *Betaproteobacteria* sp.	8	8.99	1	1.22
Bacteroides	1	1.12	3	3.66
Others	7	7.87	6	7.32
Total clones	**89**		**82**	

(b)

FIGURE 3: (a) Pie charts illustrating the percentages of clones, identified in the bacterial communities at t_0 and at t_1, grouped in phylotypes at genus level; H': Shannon Index and Co: community organization (evenness index); (b) table showing the abundance and the percentages of clones grouped in phylotypes at genus level.

microorganisms typically detected in contaminated freshwater ecosystems [40]. For instance, *H. pseudoflava* was identified by Liang and colleagues [41] in a TCE-degrading consortium enriched from TCE-contaminated aquifer sediments and groundwater. A psychrotrophic *H. pseudoflava* strain IA3-A was isolated from polychlorinated biphenyls-contaminated soil and grew on biphenyl as sole carbon and energy source [42]. Both genera, *Hydrogenophaga* and *Sulfuricurvum*, were recently enriched and associated with NO_3^--reduction in a membrane biofilm reactor inoculated with wastewater sludge and treating perchlorate [43].

The biostimulation with lactate determined a remarkable change of the diversity within the bacterial community. A lower diversity (24 OTUs) was observed and phylotypes related to Firmicutes, Bacteroidetes, and β-Proteobacteria, not detected at t_0, became dominant; that is, representatives of genera *Acidaminobacter* (20 clones), *Parabacteroides* (21 clones), and *Malikia* (13 clones) were strongly enriched (Table 1, Figure 3). Conversely, *Geobacter*, *Hydrogenophaga*, and *Sulfuricurvum*, the phylotypes dominating the consortium before the treatment, were not detected in the library after the treatment. A similar shift of diversity was previously observed in the upper layer microcosms [9]. However, while in the upper layer of the aquifer phylotypes of known 1,2-DCA dehalogenating genera of the Clostridiales (*Desulfitobacterium* and *Dehalobacter*) were enriched after the biostimulation with lactate, none of the genera enriched in microcosms from the lower layer has been so far associated with reductive dechlorination of 1,2-DCA. Among the phylotypes enriched in the lower layer microcosms, the only characterized representative of genus *Acidaminobacter*, *A. hydrogenoformans*, has been described as a fermentative species whose growth is enhanced by cocultivation with a hydrogen-consuming partner; for example, in our study, it could be a microbe able to couple the H_2 consumption with 1,2-DCA reductive dechlorination [44]. Interestingly, another phylotype enriched at t_1 was related to an uncultured Clostridiales bacterium (12 clones) and, noteworthily, the only reductive dehalogenases specific for 1,2-DCA identified so far were previously associated only with 2 genera belonging to Clostridiales order: *Desulfitobacterium* [16] and *Dehalobacter* [15]. Taken together, these data indicate that in the lower aquifer the lactate amendment enriched different phylogenetically distant taxa previously not associated with 1,2-DCA dechlorination, suggesting that novel reductive dechlorinators may mediate such a process.

3.2. Reductive Dehalogenase Gene Libraries. The reductive dehalogenase diversity in the lower aquifer was investigated in response to lactate biostimulation to evaluate whether reductive dehalogenating functional redundancy could be associated with the diversity pattern depicted by the *16S rRNA* gene libraries. In previous works, a complete sequence of one RD gene cluster specifically adapted to 1,2-DCA was obtained from microcosms of the upper layer of the aquifer [16]. Three genes (*dcaB*, *dcaC*, and *dcaT*) of the identified RD cluster presented high nucleotide identity (above 98%) with the RDs specific for chlorinated alkenes, but the gene coding for the main catalytic subunit of the reductive dehalogenase (*dcaA*) presented only 94% and 90% nucleotide and amino acid identities. The sequence differences were associated with dechlorination of 1,2-DCA since *Desulfitobacterium dichloroeliminans* strain DCA1, capable of dechlorinating 1,2-DCA but not chlorinated ethene, showed the same amino acid signatures in the two sole RDs identified in the genome [16].

Using the same RD-targeting PCR approach of Marzorati et al. [16], a total of 17 clones were obtained after the treatment, representing four different RDs. Figure 4 shows their phylogenetic relationship with known RDs. The RD sequences found in the lower aquifer layer were grouped in one cluster together with those previously identified in the upper aquifer layer [9]. The percentage of similarity among the newly identified RDs was between 100 and 99% and shared 99% nt identity with WL rdhA1, one of the three RDs identified by Grostern and Edwards [15], in a 1,2-DCA degrading coculture where the main representative was *Dehalobacter* sp. WL. It has been previously shown that the 53% of the total amino acid diversity of *dcaA* RDs (RD-54

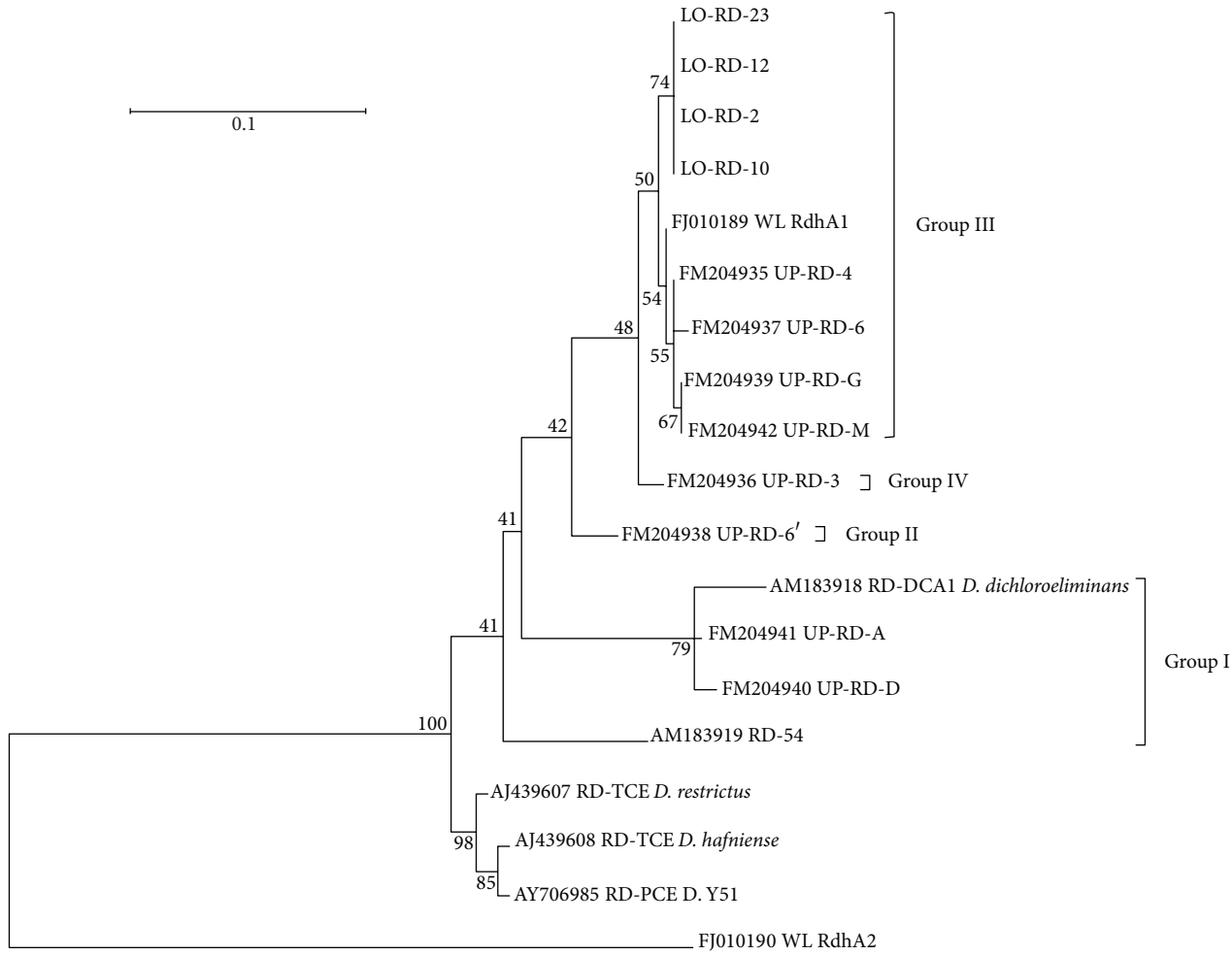

Figure 4: Neighbour-joining tree with branch length to assess the relationship between DcaA of the new RDs identified in the lower aquifer (LO-RD-X) and those previously characterized from the upper aquifer (RD-54 [16] and UP-RD-X [9]) and from *D. dichloroeliminans* strain DCA1 (RD-DCA1 [16]). Other A subunits of PceA of *Dehalobacter restrictus* strain DSMZ 9455T (RD-TCE *D. restrictus*: AJ439607), *Desulfitobacterium hafniense* strain TCE1 (RD-TCE *D. hafniense*: AJ439608), *Desulfitobacterium* sp. strain Y51 (RD-PCE D. Y51: AY706985), WL rdhA1 (FJ010189), and WL rdhA2 (FJ010190) are also reported. The numbers at each branch point represent percentage of bootstrap calculated from 1000 replicate trees. The scale bar represents the sequence divergence.

and RD-DCA1) with respect to *pceA* RDs specific for tetrachloroethene (PCE; RDs from *Dehalobacter restrictus* strain DSMZ 9455T, *Desulfitobacterium* sp. strain Y51, and *Desulfitobacterium hafniense* strain PCE-S) [12, 45, 46] was mainly localized in two small regions (blocks A and B, Figure 5) that represent only 19% (104 amino acids over 551) of the total *dcaA* residues. These two regions of hypervariability were proposed to be involved in the recognition of 1,2-DCA or in general in the substrate specificity of RDs [16]. The alignment of the RDs identified in the lower aquifer layer with the above-indicated homologs was possible to identify the two mentioned hypervariable regions overlapping with blocks A and B (Figure 5). The alignment permitted identifying amino acids specifically associated with (i) PceA of the PCE-RDs (black residues in a light grey background); (ii) DcaA of group I, specific for WL rdhA1 and for the reductive dehalogenases enriched from the lower aquifer layer (white residues in a light grey background); (iii) DcaA of group II proposed to be specific for 1,2-DCA RDs from *Desulfitobacterium* (black residues in a dark grey background); (iv) all the RDs within groups I and II but not conserved in the PCE-specific RDs (white residues in a black background).

4. Conclusions

By comparing the diversity of bacteria and RDs in the two aquifer layers following biostimulation with lactate, it can be argued that the RDs linked to 1,2-DCA reductive dechlorination, despite being diverse, are structurally conserved. However, they can be associated with different bacterial carriers selected by the environmental conditions of the specific

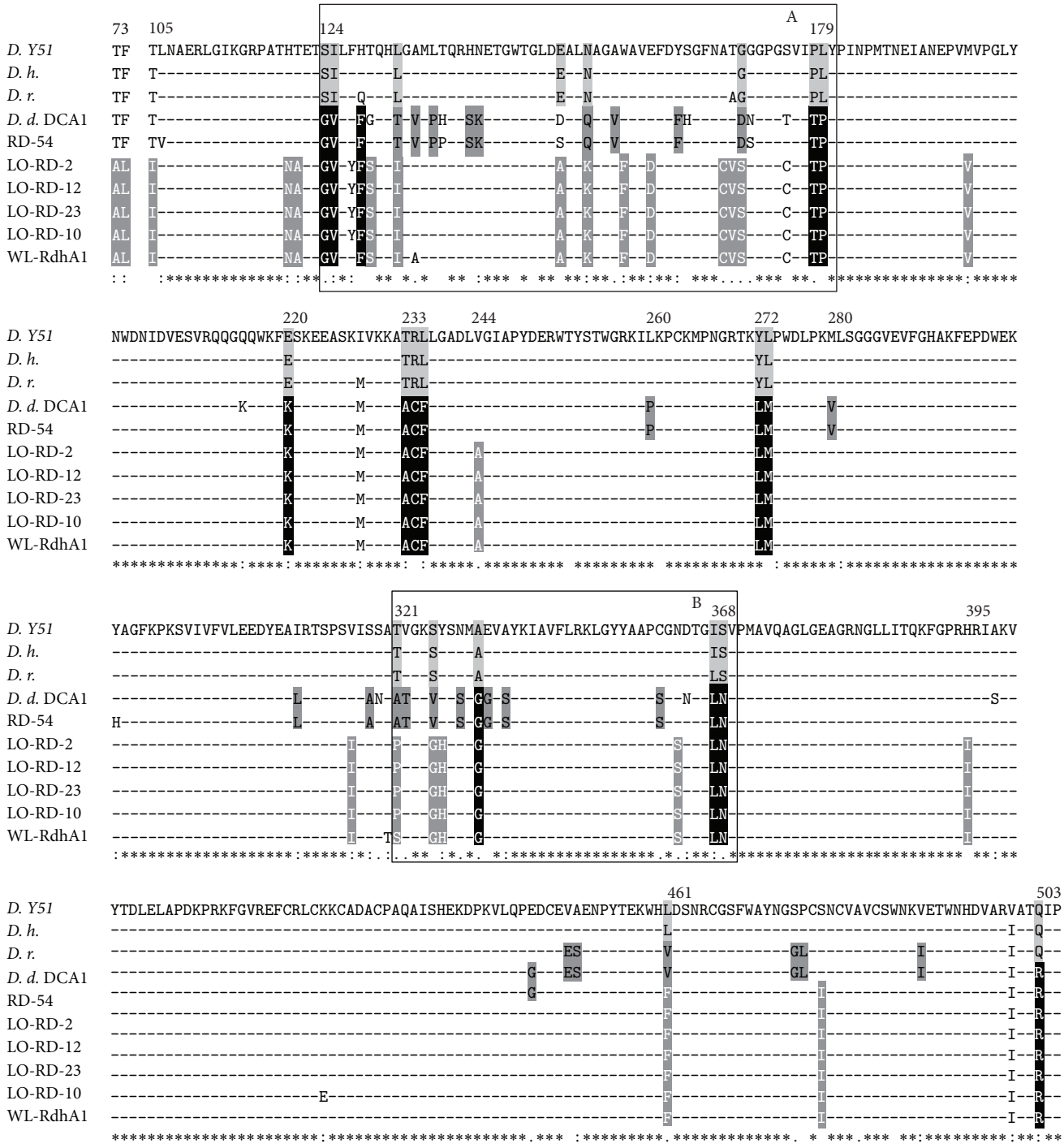

Figure 5: Amino acid alignment of the DcaA proteins of the new identified RDs, with those previously identified in the groundwater (RD-54: AM183919) and in *D. dichloroeliminans* strain DCA1 (*D. d.* DCA1: AM183918), with PceA of *Desulfitobacterium* sp. strain Y51 (*D.* Y51: AY706985), *D. hafniense* strain TCE1 (*D. h.*: AJ439608), and *D. restrictus* strain DSMZ 9455T (*D. r.*: AJ439607) and with the WL rdhA1 (FJ010189). Black line (blocks A and B) rectangles indicate two amino acid stretches where 53% of the total amino acid diversity resides between DcaA and PceA [16]. Within blocks A and B of the selected RDs sequences, as well in other smaller regions of the DcaA subunit, it was possible to identify amino acids specific for (i) PceA of the PCE-RDs (black residues in a light gray background), (ii) DcaA of group I, specific for WL rdhA1 and for the reductive dehalogenases identified in the low aquifer after the lactate treatment (white residues in a light gray background), (iii) those of group II proposed to be specific for 1,2-DCA RDs from *Desulfitobacterium* (black residues in a dark gray background), (iv) and finally those common to all the RDs within groups I and II but not conserved in the PCE-specific RDs (white residues in a black background). Asterisks, colons, and dots below the alignment indicate an identical position in all the proteins, a position with a conservative substitution, and a position with a semiconservative substitution, respectively.

aquifer, indicating their plasticity to adapt to different cellular scaffolds and machineries.

Conflict of Interests

The authors declare that there is no conflict of interests regarding the publication of this paper.

Acknowledgments

The research was supported by a grant from EniTecnologie as part of the project Genomica Ambientale per la Degradazione di Solventi Clorurati. Francesca Mapelli was supported by Università degli Studi di Milano, DeFENS, European Social Found (FSE), and Regione Lombardia (contract "Dote Ricerca").

References

[1] R. Stringer and P. Johnston, "Chlorine and the environment: an overview of the chlorine industry," *Environmental Science and Pollution Research*, vol. 8, no. 2, p. 146, 2001.

[2] A. M. Ruder, "Potential health effects of occupational chlorinated solvent exposure," *Annals of the New York Academy of Sciences*, vol. 1076, pp. 207–227, 2006.

[3] K. Hughes, M. E. Meek, and I. Caldwell, "1,2-Dichloroethane: evaluation of risks to health from environmental exposure in Canada," *Journal of Environmental Science and Health*, vol. 12, no. 2, pp. 293–303, 1994.

[4] H. Smidt and W. M. de Vos, "Anaerobic microbial dehalogenation," *Annual Review of Microbiology*, vol. 58, pp. 43–73, 2004.

[5] J. A. Field and R. Sierra-Alvarez, "Biodegradability of chlorinated solvents and related chlorinated aliphatic compounds," *Reviews in Environmental Science and Bio/Technology*, vol. 3, no. 3, pp. 185–254, 2004.

[6] T. W. Macbeth, D. E. Cummings, S. Spring, L. M. Petzke, and K. S. Sorenson Jr., "Molecular characterization of a dechlorinating community resulting from in situ biostimulation in a trichloroethene-contaminated deep, fractured basalt aquifer and comparison to a derivative laboratory culture," *Applied and Environmental Microbiology*, vol. 70, no. 12, pp. 7329–7341, 2004.

[7] M. Marzorati, S. Borin, L. Brusetti et al., "Response of 1,2-dichloroethane-adapted microbial communities to *ex-situ* biostimulation of polluted groundwater," *Biodegradation*, vol. 17, no. 2, pp. 41–56, 2006.

[8] S. K. Hirschorn, A. Grostern, G. Lacrampe-Couloume et al., "Quantification of biotransformation of chlorinated hydrocarbons in a biostimulation study: Added value via stable carbon isotope analysis," *Journal of Contaminant Hydrology*, vol. 94, no. 3-4, pp. 249–260, 2007.

[9] M. Marzorati, A. Balloi, F. de Ferra et al., "Bacterial diversity and reductive dehalogenase redundancy in a 1,2-dichloroethane-degrading bacterial consortium enriched from a contaminated aquifer," *Microbial Cell Factories*, vol. 9, article 12, 2010.

[10] A. Arjoon, A. O. Olaniran, and B. Pillay, "Enhanced 1,2-dichloroethane degradation in heavy metal co-contaminated wastewater undergoing biostimulation and bioaugmentation," *Chemosphere*, vol. 93, no. 9, pp. 1826–1834, 2013.

[11] C. Holliger, G. Wohlfarth, and G. Diekert, "Reductive dechlorination in the energy metabolism of anaerobic bacteria," *FEMS Microbiology Reviews*, vol. 22, no. 5, pp. 383–398, 1999.

[12] J. Maillard, W. Schumacher, F. Vazquez, C. Regeard, W. R. Hagen, and C. Holliger, "Characterization of the corrinoid iron-sulfur protein tetrachloroethene reductive dehalogenase of *Dehalobacter restrictus*," *Applied and Environmental Microbiology*, vol. 69, no. 8, pp. 4628–4638, 2003.

[13] B. A. van de Pas, H. Smidt, W. R. Hagen et al., "Purification and molecular characterization of ortho-chlorophenol reductive dehalogenase, a key enzyme of halorespiration in *Desulfitobacterium dehalogenans*," *Journal of Biological Chemistry*, vol. 274, no. 29, pp. 20287–20292, 1999.

[14] A. Neumann, A. Siebert, T. Trescher, S. Reinhardt, G. Wohlfarth, and G. Diekert, "Tetrachloroethene reductive dehalogenase of *Dehalospirillum multivorans*: substrate specificity of the native enzyme and its corrinoid cofactor," *Archives of Microbiology*, vol. 177, no. 5, pp. 420–426, 2002.

[15] A. Grostern and E. A. Edwards, "A characterization of a *Dehalobacter* coculture that dechlorinates 1,2-dichloroethane to ethene and identification of the putative reductive dehalogenase gene," *Applied and Environmental Microbiology*, vol. 75, no. 9, pp. 2684–2693, 2009.

[16] M. Marzorati, F. de Ferra, H. van Raemdonck et al., "A novel reductive dehalogenase, identified in a contaminated groundwater enrichment culture and in *Desulfitobacterium dichloroeliminans* strain DCA1, is linked to dehalogenation of 1,2-dichloroethane," *Applied and Environmental Microbiology*, vol. 73, no. 9, pp. 2990–2999, 2007.

[17] X. Maymó-Gatell, T. Anguish, and S. H. Zinder, "Reductive dechlorination of chlorinated ethenes and 1,2-dichloroethane by 'Dehalococcoides ethenogenes' 195," *Applied and Environmental Microbiology*, vol. 65, no. 7, pp. 3108–3113, 1999.

[18] J. He, K. M. Ritalahti, K.-U. Yang, S. S. Koenigsberg, and F. E. Löffler, "Detoxification of vinyl chloride to ethene coupled to growth of an anaerobic bacterium," *Nature*, vol. 424, no. 6944, pp. 62–65, 2003.

[19] W. M. Moe, J. Yan, M. F. Nobre, M. S. da Costa, and F. A. Rainey, "*Dehalogenimonas lykanthroporepellens* gen. nov., sp. nov., a reductively dehalogenating bacterium isolated from chlorinated solvent-contaminated groundwater," *International Journal of Systematic and Evolutionary Microbiology*, vol. 59, no. 11, pp. 2692–2697, 2009.

[20] K. S. Bowman, M. F. Nobre, M. S. da Costa, F. A. Rainey, and W. M. Moe, "*Dehalogenimonas alkenigignens* sp. nov., a chlorinated-alkane-dehalogenating bacterium isolated from groundwater," *International Journal of Systematic and Evolutionary Microbiology*, vol. 63, no. 4, pp. 1492–1498, 2013.

[21] A. D. Maness, K. S. Bowman, J. Yan, F. A. Rainey, and W. M. Moe, "*Dehalogenimonas* spp. can reductively dehalogenate high concentrations of 1,2-dichloroethane, 1,2-dichloropropane, and 1,1,2-trichloroethane," *AMB Express*, vol. 2, no. 1, pp. 54–70, 2012.

[22] S. De Wildeman, G. Diekert, H. van Langenhove, and W. Verstraete, "Stereoselective microbial dehalorespiration with vicinal dichlorinated alkanes," *Applied and Environmental Microbiology*, vol. 69, no. 9, pp. 5643–5647, 2003.

[23] A. E. Murray, C. M. Preston, R. Massana et al., "Seasonal and spatial variability of bacterial and archaeal assemblages in the coastal waters near Anvers Island, Antarctica," *Applied and Environmental Microbiology*, vol. 64, no. 7, pp. 2585–2595, 1998.

[24] D. Wen, Y. Bai, Q. Shi et al., "Bacterial diversity in the polluted water of the Dianchi Lakeshore in China," *Annals of Microbiology*, vol. 62, no. 2, pp. 715–723, 2012.

[25] P. W. J. J. van der Wielen, H. Bolhuis, S. Borin et al., "The enigma of prokaryotic life in deep hypersaline anoxic basins," *Science*, vol. 307, no. 5706, pp. 121–123, 2005.

[26] E. Cytryn, D. Minz, R. S. Oremland, and Y. Cohen, "Distribution and diversity of archaea corresponding to the limnological cycle of a hypersaline stratified lake (Solar Lake, Sinai, Egypt)," *Applied and Environmental Microbiology*, vol. 66, no. 8, pp. 3269–3276, 2000.

[27] E. S. Wright, L. S. Yilmaz, and D. R. Noguera, "DECIPHER, a search-based approach to chimera identification for 16S rRNA sequences," *Applied and Environmental Microbiology*, vol. 78, no. 3, pp. 717–725, 2012.

[28] P. D. Schloss, S. L. Westcott, T. Ryabin et al., "Introducing mothur: open-source, platform-independent, community-supported software for describing and comparing microbial communities," *Applied and Environmental Microbiology*, vol. 75, no. 23, pp. 7537–7541, 2009.

[29] Ø. Hammer, D. A. T. Harper, and P. D. Ryan, "PAST: paleontological statistics software package for education and data analysis," *Palaeontologia Electronica*, vol. 4, no. 1, 9 pages, 2001.

[30] S. F. Altschul, W. Gish, W. Miller, E. W. Myers, and D. J. Lipman, "Basic local alignment search tool," *Journal of Molecular Biology*, vol. 215, no. 3, pp. 403–410, 1990.

[31] Q. Wang, G. M. Garrity, J. M. Tiedje, and J. R. Cole, "Naïve Bayesian classifier for rapid assignment of rRNA sequences into the new bacterial taxonomy," *Applied and Environmental Microbiology*, vol. 73, no. 16, pp. 5261–5267, 2007.

[32] M. O. Lorenz, "Methods of measuring concentration of wealth," *Journal of the American Statistical Association*, vol. 9, pp. 209–219, 1905.

[33] M. Marzorati, L. Wittebolle, N. Boon, D. Daffonchio, and W. Verstraete, "How to get more out of molecular fingerprints: practical tools for microbial ecology," *Environmental Microbiology*, vol. 10, no. 6, pp. 1571–1581, 2008.

[34] G. Merlino, A. Rizzi, A. Schievano et al., "Microbial community structure and dynamics in two-stage vs single-stage thermophilic anaerobic digestion of mixed swine slurry and market bio-waste," *Water Research*, vol. 47, no. 6, pp. 1983–1995, 2013.

[35] K. Tamura, D. Peterson, N. Peterson, G. Stecher, M. Nei, and S. Kumar, "MEGA5: molecular evolutionary genetics analysis using maximum likelihood, evolutionary distance, and maximum parsimony methods," *Molecular Biology and Evolution*, vol. 28, no. 10, pp. 2731–2739, 2011.

[36] C. Regeard, J. Maillard, and C. Holliger, "Development of degenerate and specific PCR primers for the detection and isolation of known and putative chloroethene reductive dehalogenase genes," *Journal of Microbiological Methods*, vol. 56, no. 1, pp. 107–118, 2004.

[37] D. R. Lovley, D. E. Holmes, and K. P. Nevin, "Dissimilatory Fe(III) and Mn(IV) reduction," *Advances in Microbial Physiology*, vol. 49, pp. 219–286, 2004.

[38] H. de Wever, J. R. Cole, M. R. Fettig, D. A. Hogan, and J. M. Tiedje, "Reductive dehalogenation of trichloroacetic acid by *Trichlorobacter thiogenes* gen. nov., sp. nov.," *Applied and Environmental Microbiology*, vol. 66, no. 6, pp. 2297–2301, 2000.

[39] Y. Sung, K. E. Fletcher, K. M. Ritalahti et al., "*Geobacter lovleyi* sp. nov. strain SZ, a novel metal-reducing and tetrachloroethene-dechlorinating bacterium," *Applied and Environmental Microbiology*, vol. 72, no. 4, pp. 2775–2782, 2006.

[40] Y. Kodama and K. Watanabe, "*Sulfuricurvum kujiense* gen. nov., sp. nov., a facultatively anaerobic, chemolithoautotrophic, sulfur-oxidizing bacterium isolated from an underground crude-oil storage cavity," *International Journal of Systematic and Evolutionary Microbiology*, vol. 54, no. 6, pp. 2297–2300, 2004.

[41] S. H. Liang, J. K. Liu, K. H. Lee, Y. C. Kuo, and C. M. Kao, "Use of specific gene analysis to assess the effectiveness of surfactant-enhanced trichloroethylene cometabolism," *Journal of Hazardous Materials*, vol. 198, pp. 323–330, 2011.

[42] A. J. Lambo and T. R. Patel, "Isolation and characterization of a biphenyl-utilizing psychrotrophic bacterium, *Hydrogenophaga taeniospiralis* IA3-A, that cometabolize dichlorobiphenyls and polychlorinated biphenyl congeners in Aroclor 1221," *Journal of Basic Microbiology*, vol. 46, no. 2, pp. 94–107, 2006.

[43] H.-P. Zhao, S. van Ginkel, Y. Tang, D.-W. Kang, B. Rittmann, and R. Krajmalnik-Brown, "Interactions between perchlorate and nitrate reductions in the biofilm of a hydrogen-based membrane biofilm reactor," *Environmental Science & Technology*, vol. 45, no. 23, pp. 10155–10162, 2011.

[44] T. Narihiro, S. Kaiya, H. Futamata, and A. Hiraishi, "Removal of polychlorinated dioxins by semi-aerobic fed-batch composting with biostimulation of '*Dehalococcoides*'," *Journal of Bioscience and Bioengineering*, vol. 109, no. 3, pp. 249–256, 2010.

[45] A. Suyama, M. Yamashita, S. Yoshino, and K. Furukawa, "Molecular characterization of the *PceA* reductive dehalogenase of *Desulfitobacterium* sp. strain Y51," *Journal of Bacteriology*, vol. 184, no. 13, pp. 3419–3425, 2002.

[46] J. Maillard, C. Regeard, and C. Holliger, "Isolation and characterization of Tn-Dha1, a transposon containing the tetrachloroethene reductive dehalogenase of *Desulfitobacterium hafniense* strain TCE1," *Environmental Microbiology*, vol. 7, no. 1, pp. 107–117, 2005.

Hindawi Publishing Corporation
BioMed Research International
Volume 2015, Article ID 304523, 11 pages
http://dx.doi.org/10.1155/2015/304523

Research Article

Expression of Heterologous Cellulases in *Thermotoga* sp. Strain RQ2

Hui Xu, Dongmei Han, and Zhaohui Xu

Department of Biological Sciences, Bowling Green State University, Bowling Green, OH 43403, USA

Correspondence should be addressed to Zhaohui Xu; zxu@bgsu.edu

Received 19 September 2014; Revised 21 January 2015; Accepted 6 February 2015

Academic Editor: George Tsiamis

The ability of *Thermotoga* spp. to degrade cellulose is limited due to a lack of exoglucanases. To address this deficiency, cellulase genes Csac_1076 (*celA*) and Csac_1078 (*celB*) from *Caldicellulosiruptor saccharolyticus* were cloned into *T.* sp. strain RQ2 for heterologous overexpression. Coding regions of Csac_1076 and Csac_1078 were fused to the signal peptide of TM1840 (*amyA*) and TM0070 (*xynB*), resulting in three chimeric enzymes, namely, TM1840-Csac_1078, TM0070-Csac_1078, and TM0070-Csac_1076, which were carried by *Thermotoga-E. coli* shuttle vectors pHX02, pHX04, and pHX07, respectively. All three recombinant enzymes were successfully expressed in *E. coli* DH5α and *T.* sp. strain RQ2, rendering the hosts with increased endo- and/or exoglucanase activities. In *E. coli*, the recombinant enzymes were mainly bound to the bacterial cells, whereas in *T.* sp. strain RQ2, about half of the enzyme activities were observed in the culture supernatants. However, the cellulase activities were lost in *T.* sp. strain RQ2 after three consecutive transfers. Nevertheless, this is the first time heterologous genes bigger than 1 kb (up to 5.3 kb in this study) have ever been expressed in *Thermotoga*, demonstrating the feasibility of using engineered *Thermotoga* spp. for efficient cellulose utilization.

1. Introduction

Due to rising global energy demands, developing renewable forms of energy, such as solar, hydro-, and bioenergy, has become increasingly important. Traditionally, bioenergy is generated by fermenting the glucose derived from starch. Starch alone, however, accounts for too small a fraction of biomass to sustain a positive energy balance. The need to replace fossil fuels demands that cellulose, the most common and renewable organic material on Earth [1], must not be overlooked. Cellulose is a linear polymer of D-glucose units linked by 1,4-β-D-glycosidic bonds. It becomes useful as a food and energy source once it is broken down into soluble cellobiose (β-1,4 glucose dimer) and glucose, a process called hydrolysis because a water molecule is incorporated for each dissociated glycosidic bond. Effective hydrolysis of cellulose requires the cooperation of three enzymes, namely, endo-1,4-β-glucanase (EC 3.2.1.4), exo-1,4-β-glucanase (also called cellobiohydrolase) (EC 3.2.1.91), and β-glucosidase (EC 3.2.1.21) [2–5]. Endoglucanase randomly breaks down the β-1,4 linkages in the regions of low crystallinity, exoglucanase removes cellobiose units from the nonreducing ends of cellulose chains, and β-glucosidase converts cellobiose into glucose. In general, exoglucanases degrade cellulose more efficiently than endoglucanases.

Hyperthermophilic bacteria *Thermotoga* are attractive candidates for the production of biohydrogen and thermostable enzymes. Surveying of *Thermotoga* genomes in the CAZy database (http://www.cazy.org/) revealed dozens of carbohydrate-active enzymes, the molecular foundation that allows *Thermotoga* strains growing on a wide range of carbon sources such as glucose, xylose, semicellulose, starch, and carboxymethyl cellulose (CMC) [6–9]. Nevertheless, the apparent absence of exoglucanases suggests the limited ability of these organisms to use cellulose as their main carbon and energy source. Up to date, there are only two reports describing low levels of exoglucanase activities in *Thermotoga* [2, 4], a phenomenon probably caused by nonspecific reactions of endoglucanases [10–12].

Table 1: Number of predicted carbohydrate-active enzymes in *Thermotoga* genomes*.

Family categories	*T.* sp. strain RQ2	*T. maritima* MSB8	*T. neapolitana* DSM 4359	*T. petrophila* RKU-1	*T. naphthophila* RKU-10	*T. lettingae* TMO	*T. thermarum* DSM 5069
Glycoside Hydrolase family	52	49	49	50	40	36	32
Glycosyltransferase family	20	22	21	17	19	20	13
Polysaccharide Lyase family	1	1	0	1	0	1	0
Carbohydrate Esterase family	5	5	3	5	4	5	2
Carbohydrate-binding module family	20	17	17	15	15	4	8
Total	98	94	90	88	78	66	55

*Data collected from http://www.cazy.org/ on August 7, 2014.

This study aimed at introducing heterologous exoglucanase activities into *Thermotoga* by genetic engineering. *T.* sp. strain RQ2 was selected as the host strain, because its genome encodes the largest repertoire of carbohydrate-active enzymes among all published *Thermotoga* genomes (Table 1). Moreover, *T.* sp. strain RQ2 has recently been discovered to be naturally transformable, making the transformation procedure straightforward [13]. The selection of candidate cellulases was focused on *Caldicellulosiruptor saccharolyticus*, a Gram-positive anaerobe growing optimally at 70°C and can use cellulose as a sole carbon source [14]. Csac_1076 (CelA) [15, 16] and Csac_1078 (CelB) [17, 18] of *C. saccharolyticus* DSM 8903 have been experimentally characterized as multidomain proteins with both endo- and exoglucanase activities and are suitable candidates to be introduced into *T.* sp. strain RQ2. However, *Caldicellulosiruptor* are Gram-positives and *Thermotoga* are Gram-negatives; CelA and CelB are unlikely to be secreted properly in *T.* sp. strain RQ2. The *Thermotoga* host would not benefit much from the heterologous cellulases unless the enzymes can be secreted to the extracellular environment. Signal peptides with a *Thermotoga* origin would be required to guide the transportation of foreign proteins in *T.* sp. strain RQ2. A literature search revealed that *T. maritima* TM1840 (amylase A, AmyA) [19–21] and TM0070 (xylanase B, XynB) [20] have been experimentally confirmed to be secretive proteins. The former is anchored on the "toga" part with catalytic domain facing outward, and the latter is secreted into the environment after the cleavage of its signal peptide. Therefore, the promoter regions and the signal peptide sequences of TM1840 (*amyA*) [19–21] and TM0070 (*xynB*) [20] were chosen to control the expression and transportation of the *Caldicellulosiruptor* cellulases in *T.* sp. strain RQ2.

2. Materials and Methods

2.1. Strains and Cultivation Conditions. The bacterial strains and vectors used in this study are summarized in Table 2. All *E. coli* strains were cultivated in Luria-Bertani (LB) medium (1% tryptone, 1% NaCl, 0.5% yeast extract) at 37°C. *Thermotoga* strains were cultivated at 77°C, 125 rpm in SVO medium [22]. SVO plates were made with 0.25% (w/v) gelrite [23]. *Thermotoga* plates were put into Vacu-Quik Jars (Almore International Inc., Portland, OR, USA) filled with 96 : 4 N_2-H_2 and 4 g palladium catalyst (to remove oxygen) and incubated at 77°C for 48 h. When needed, ampicillin was supplemented into LB medium to a final concentration of 100 μg mL^{-1}, and kanamycin was added into liquid SVO medium and SVO plates to a final concentration of 150 and 250 μg mL^{-1}, respectively.

2.2. Construction of Vectors. All vectors were constructed by following standard cloning methods and verified by restrictive digestions. Primers used in this study are summarized in Table 3. The *Thermotoga-E. coli* shuttle vector pDH10 was used as the parent vector. Inverse PCR was performed with pDH10 [23] using primers *DBs F* and *DBs R*, and the amplicon was digested with *Bsa*I followed by self-ligation to give rise to pDH26. With the same approach, pDH27 was generated based on pDH26 using primers *DNd F* and *DNd R*, and pHX01 was created from pDH27 using primers *DLZ F* and *DLZ R*. Compared to pDH10, pHX01 is 342 bp shorter and is free of the *Bsa*I and *Nde*I recognition sites, which makes it a better cloning vector than pDH10. Based on pHX01, intermediate vectors pHX02.1, pHX04.1, and pHX07.1 were constructed. Vector pHX02.1 carries the promoter and signal peptide region of *TM1840* (*amyA*), which was inserted immediately upstream of the Ap^r gene (Figure 1(a)); primers *AmP F* and *Amp R* were used to amplify the desired region from *T. maritima* chromosome, and the amplicon was digested with *Not*I and *Sac*I. Vectors pHX04.1 and pHX07.1 both carry the promoter and signal peptide region of TM0070 (*xynB*), but one has the insert upstream of the Ap^r gene (Figure 1(b)) and the other has it downstream of the *ori* region (Figure 1(c)). Because the two insertions sites were recognized by different restriction enzymes, primers *XyBPB F* and *XyBPB R* were used to amplify the insert for pHX04.1, and the amplicon was digested with *Not*I and *Sac*I; primers *XyBPA F* and *XyBPA R* were used to prepare the insert for pHX07.1, and the amplicon was digested by *Xho*I and *Pst*I. As a result, a *Bsa*I site was

Table 2: Strains and vectors used in this study.

Strain or plasmid	Description	Reference
E. coli		
DH5α	F$^-$ *endA1 hsdR17* (rk$^-$, mk$^+$) *supE44 thi-1* λ^- *recA1 gyrA96 relA1 deoR* Δ(*lacZYA-argF*)-U169ϕ80d*lacZ*ΔM15	[24]
Thermotoga		
T. sp. strain RQ2	Isolated from geothermally heated sea sediment, Ribeira Quente, São Miguel, Azores.	[25]
T. maritima MSB8	The first type strain of *Thermotoga,* isolated from geothermally heated sea sediments, Porto di Levante, Vulcano, Italy.	[25]
Caldicellulosiruptor		
C. saccharolyticus DSM 8903	Isolated from wood in the flow of geothermal spring, Taupo, New Zealand.	[14]
Plasmids		
pDH10	*Thermotoga-E. coli* shuttle vector; Ap^r, Kan^r*	[23]
pDH26	pDH10-derived, with *Bsa*I site erased; Ap^r, Kan^r	This study
pDH27	pDH26-derived, with *Nde*I site erased; Ap^r, Kan^r	This study
pHX01	pDH27-derived, having *lacZ* residual sequence removed; Ap^r, Kan^r	This study
pHX02.1	Promoter and signal peptide region of TM1840 (*amyA*) were inserted into the *Not*I-*Sac*I sites of pHX01; Ap^r, Kan^r	This study
pHX02	Coding region (without the signal peptide) of Csac_1078 (*celB*) was inserted into *Bsa*I-*Sac*I sites of pHX02.1; Ap^r, Kan^r	This study
pHX04.1	Promoter and signal peptide region of TM0070 (*xynB*) were inserted into the *Not*I-*Sac*I sites of pHX01; Ap^r, Kan^r	This study
pHX04	Coding region (without the signal peptide) of Csac_1078 (*celB*) was inserted into the *Bsa*I-*Sac*I sites of pHX04.1; Ap^r, Kan^r	This study
pHX07.1	Promoter and signal peptide region of TM0070 (*xynB*) were inserted into the *Xho*I-*Pst*I sites of pHX01; Ap^r, Kan^r	This study
pHX07	Coding region (without the signal peptide) of Csac_1076 (*celA*) was inserted into the *Bsa*I-*Pst*I sites of pHX07.1; Ap^r, Kan^r	This study

* Ap: ampicillin; Kan: kanamycin.

introduced immediately after the signal peptide sequence in each vector to facilitate the insertion of the coding regions of the *C. saccharolyticus* cellulases.

Once the regulation and transportation regions were in place, the cellulases genes from *C. saccharolyticus* were inserted into pHX02.1, pHX04.1, and pHX07.1 to give rise to pHX02, pHX04, and pHX07, respectively (Figure 1). The total DNA of *C. saccharolyticus* DSM 8903 was used as the template. Primers *CelB F* and *CelB R* were used to amplify Csac_1078 (*celB*), and the amplicon was digested with *Bsa*I and *Sac*I. Primers *CelA F* and *CelA R* were used to amplify Csac_1076 (*celA*), and the amplicon was digested with *Bbs*I and *Pst*I.

The transformation of *E. coli* was done with standard calcium chloride method, and the transformation of *Thermotoga* was done by natural transformation, as described previously [13]. The DNA substrates used to transform *Thermotoga* were *in vitro* methylated by methylase M. *Tne*DI [26, 27].

2.3. Detection of Endoglucanase Activity with CMC Plates. Endoglucanase activities were evaluated using Congo red assays [28]. For preliminary screening, *E. coli* transformants were inoculated on CMC plates (1% NaCl, 0.5% yeast extract, 0.2% CMC, 1.5% agar) and incubated at 37°C for overnight. The plates were then kept at 77°C for 8 h, stained with 0.1% Congo red (dissolved in water) at room temperature for 15 min, and washed with 1 M NaCl until clear halos showed up. After that, the plates were rinsed with 1 M HCl, which changed the background color into blue, providing a better contrast for the halos. To test liquid cultures, 40 μL of each normalized overnight culture was directly loaded onto CMC plates. To minimize the sizes of the loading spots, the liquid cultures were loaded through 8 times with 5 μL in each loading. The next round of loading only happened when the liquid from the previous loading had been completely absorbed. To localize the expression of the recombinant proteins, supernatants were collected from 1 mL of normalized overnight culture by centrifugation. Meanwhile, the cells were washed once with fresh medium and resuspended in 1 mL of the same medium.

2.4. Detection of Endoglucanase Activities with Zymogram. Native polyacrylamide gel electrophoresis was modified from a previous report [29]. SDS (sodium dodecyl sulfate) was omitted from the gel (10%, w/v), but CMC was added to a final concentration of 0.08% (w/v). Protein samples were prepared in the absence of SDS, reducing agents, and the heat treatment. After electrophoresis, gels were rinsed with

Table 3: Nucleotide sequences of primers used in this study.

Primer	Sequence and restriction sites
DBs F	5′ATCATGGGTCTCGCGGTATCATTGCAGCACTGGGGCCAGATGGTAAGC3′ (*Bsa*I)
DBs R	5′ATCGTCGGTCTCTACCGCGGGAACCACGCTCACCGGCTCCAGATTTATCAGC3′ (*Bsa*I)
DNd F	5′ATCGTCGGTCTCTATATGCATGTGCACCAAACCACTTTGAGTACGTTCCCG3′ (*Bsa*I)
DNd R	5′ATCGTCGGTCTCCATATATTATTTAGAGGACCTTATATTCCCCAAGATTGG3′ (*Bsa*I)
DLZ F	5′GTCTGACTAGTGCAACGCATGCGAGGTTCTAGAGATTAGGGTGATGGTTCACGTAGTGG3′ (*Sph*I)
DLZ R	5′GACACGCATGCCGACGGCCAGTGAATTGTAATACGAC3′ (*Sph*I)
AmP F	5′CGAGGAACGAAGCGGCCGCGGACACCTCCTTTAGATTACAAAGAGTTTAC3′ (*Not*I)
AmP R	5′GACTTAGAGCTCGATGACGGTCTCACTGGGCTAGTACCATCTGTGTTTGTGCTGTTTG3′ (*Sac*I, *Bsa*I)
XyBPB F	5′CGAGGAACGAAGCGGCCGCGAAAACTCACCTCCCTTGATTGTATG3′ (*Not*I)
XyBPB R	5′GACTTAGAGCTCGATGACGGTCTCACTGGAGAGCTGAAAACTGGAACACATCCCAAC3′ (*Sac*I, *Bsa*I)
XyBPA F	5′CGAGGACTCGAGGAAAACTCACCTCCCTTGATTGTATG3′ (*Xho*I)
XyBPA R	5′GATTAGCTGCAGGATGACGGTCTCAATGGAGAGCTGAAAACTGGAACACATCCCAAC3′ (*Pst*I, *Bsa*I)
CelB F	5′GACGACGGTCTCACCAGACTGGAGTATTCCAAGTTTATG3′ (*Bsa*I)
CelB R	5′GGCGCGGAGCTCTCATCAGTGATGGTGATGGTGATGTTTTGAAGCTGGAACTGGCTCAGGCTCATTATTG3′ (*Sac*I)
CelA F	5′GACTACGAAGACATCCATGGCAGGAGGCTAGGGCTGGTTC3′ (*Bbs*I)
CelA R	5′GGCGCGCTGCAGTCATCAGTGATGGTGATGGTGATGTTGATTACCGAACAGAATTTCATATGTTG3′ (*Pst*I)
CelBV F	5′AGACGCGATGGGACATATCTATCCGGTATGG3′
CelBV R	5′GAAGCTGGAACTGGCTCAGGCTCATTATTG3′

deionized water for 3 times prior to immersion in 0.25 M Tris-HCl (pH 6.8) for 8 h at 77°C. Following the enzymatic reaction, gels were visualized with Congo red, as detailed above.

2.5. Detection of Exoglucanase Activity. MUC (4-methylumbelliferyl β-D-cellobioside) agar was used to detect exoglucanase activity [17, 30]. Under the hydrolysis of exoglucanase, MUC is converted to cellobiose and MU (4-methylumbelliferone), which shows fluorescence under ultraviolet light. Forty microliters of normalized overnight culture of each *Thermotoga* transformant was spotted on MUC plates, incubated at 77°C for 8 h, and examined under UV light. The formation of fluorescent halos surrounding the loading spots indicates the activity of exoglucanase.

3. Results and Discussion

3.1. Expression and Localization of the Chimeric Enzymes in E. coli. In the endoglucanase activity screening experiment, all tested DH5α/pHX02 (Figure 2), DH5α/pHX04, and DH5α/pHX07 strains showed clear halos surrounding the overnight colonies, indicating functional expression of the recombinant cellulases in *E. coli*. To determine the localizations of the recombinant cellulases, cultures were normalized and supernatants and cell suspensions were tested separately. Because pHX07 and pHX04 share the same localization signal, experiments were carried out with just pHX04 and pHX02 transformants. On CMC plates, the pHX04 transformant demonstrated a higher endoglucanase activity than the transformants of pHX02 (Figure 3). For both constructs, most of the endoglucanase activity was associated with the cell suspensions (Figure 3). This is not surprising for pHX02, because its fusion protein is designed to be anchored on the outer membrane of a Gram-negative host. As for pHX04, since its fusion protein is meant to be released into the medium, these data suggest that the signal peptide of TM0070 (XynB) is not functional in *E. coli,* even though its promoter is.

3.2. Detection of Endoglucanase Activities in Thermotoga. As our main purpose is to express the recombinant cellulases in

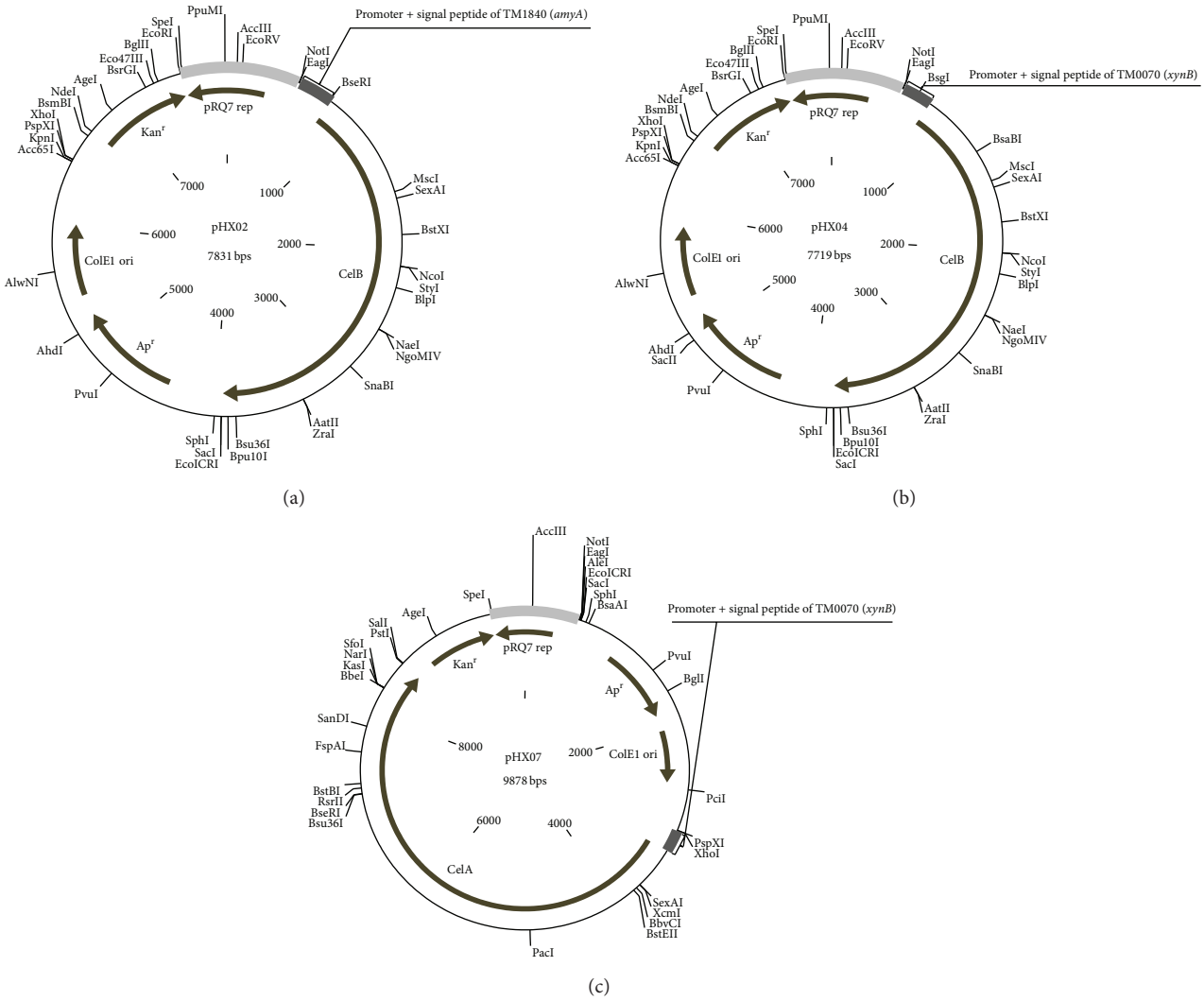

Figure 1: Maps of the expression vectors pHX02 (a), pHX04 (b), and pHX07 (c). Gray region represents sequence of pRQ7. Unique restriction sites are shown.

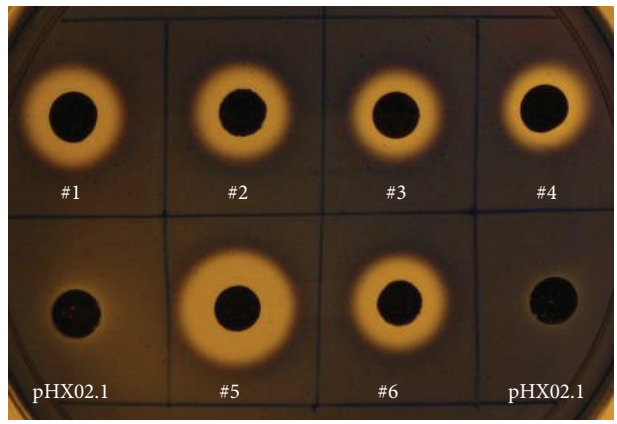

Figure 2: Detection of endoglucanase activities in *E. coli* DH5α transformants (showing DH5α/pHX02 as an example). #1–#6, DH5α/pHX02 transformants; DH5α/pHX02.1, negative control.

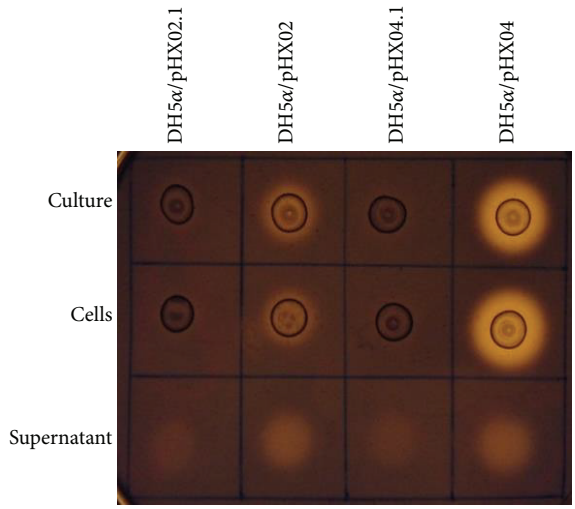

Figure 3: Localization of recombinant enzymes in *E. coli* DH5α transformants. DH5α/pHX02.1 and DH5α/pHX04.1 were used as negative controls.

Thermotoga, we next transformed these 3 expression vectors into *T.* sp. strain RQ2. Eleven *T.* sp. strain RQ2/pHX02, eleven RQ2/pHX04, and eight RQ2/pHX07 transformants were isolated and tested with Congo red assays. Wild type *T.* sp. strain RQ2 and *C. saccharolyticus* DSM 8903 were used as the negative and positive controls. Almost all transformants showed enhanced endoglucanase activities compared with the wild type strain (Figure 4), indicating the successful transformation and expression of the recombinant enzymes. Next we set out to validate the transformants with PCR and restriction digestions.

3.3. Validating Thermotoga Transformants. Three RQ2/pHX02 transformants (#2, #3, and #4) and three RQ2/pHX04 transformants (#3, #4, and #5) were picked up from SVO plates and grown overnight in liquid SVO medium with 150 μg kanamycin mL^{-1}. Plasmid extracts were prepared and used as the templates to amplify the exoglucanase domain of recombinant *celB* gene with primers *celBV F* and *celBV R*. One RQ2/pHX02 isolate (#4) and two RQ2/pHX04 isolates (#4 and #5) showed bands with the expected size (in addition to some nonspecific bands) (Figure 5). The positive bands from RQ2/pHX02 #4 and RQ2/pHX04 #5 were gel-purified, reamplified using the same primers, and digested with *Hae*III (Figure 6). Both amplicons developed the expected digestion profile, demonstrating the authenticity of the two transformants, which were then selected to be further characterized in later studies. The attempts to amplify either exo- or endoglucanase domain from the pHX07 transformants failed. Since pHX07 carries the *celA* gene, instead of the *celB* as found in pHX02 and pHX04, further optimization of PCR conditions and/or primer selections may eventually allow one to validate the transformants of this vector. Nevertheless, pHX07 #2 was selected for further studies, because it at least displayed strong endoglucanase activity on CMC plates.

3.4. Detection of the Exoglucanase Activity in Thermotoga. The exoglucanase activity of the *Thermotoga* transformants was tested with MUC plates (Figure 7). Compared to the host strain, RQ2/pHX02 and RQ2/pHX04 demonstrated greatly enhanced exoglucanase activities, as bright fluorescent light emitted under UV light from the spots where their overnight cultures were loaded. This suggests that the exoglucanase domain of *Caldicellulosiruptor* CelB was successfully expressed and fully functional in *T.* sp. strain RQ2. However, the fluorescence level displayed by RQ2/pHX07 was at about the same level to the wild type strain. Because the recombinant enzymes carried by pHX04 and pHX07 share the same promoter and signal peptide, the low level of exoglucanase activity presented by RQ2/pHX07 indicates the exodomain of *Caldicellulosiruptor* CelA was either lost (which echoes the PCR results above) or not functional in *T.* sp. strain RQ2.

3.5. Localization of the Recombinant Cellulases in Thermotoga. Localization of the recombinant enzymes was carried with *T.* sp. strain RQ2/pHX02 #4, pHX04 #5, and pHX07 #2 by comparing the endoglucanase activity in supernatants versus cell suspensions. Unlike what happened in *E. coli* where the majority of the activity was associated with cell suspensions, the *Thermotoga* transformants had about half of the endoglucanase activity found in supernatants (Figure 8(a)). The endoglucanase activity in the supernatants was double-checked with native polyacrylamide gels followed by Congo red assay. All supernatants showed brighter bands than the wild type strain, indicating enhanced cellulases activities (Figure 8(b)). No protein bands were detectable in the supernatants by Coomassie brilliant blue staining. The cell suspensions retained the other half of the enzymatic activities, probably because of the cytoplasmic proproteins of the chimeric enzymes (Figure 8(a)).

3.6. Stabilities of the Recombinant Strains. Stabilities of the *E. coli* and *T.* sp. strain RQ2 recombinant strains were tested

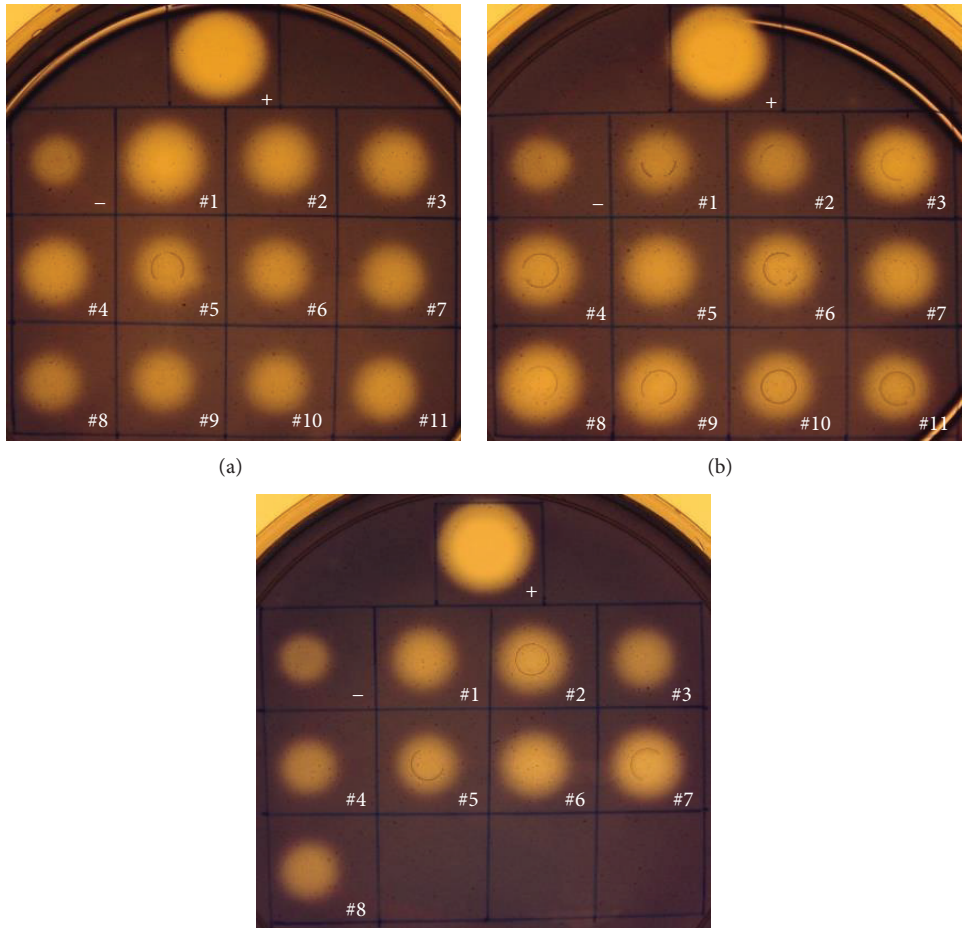

Figure 4: Screening of endoglucanase activities in *Thermotoga* transformants RQ2/pHX02 (a), RQ2/pHX04 (b), and RQ2/pHX07 (c). +, *C. saccharolyticus* DSM 8903, positive control; –, *T.* sp. strain RQ2, negative control.

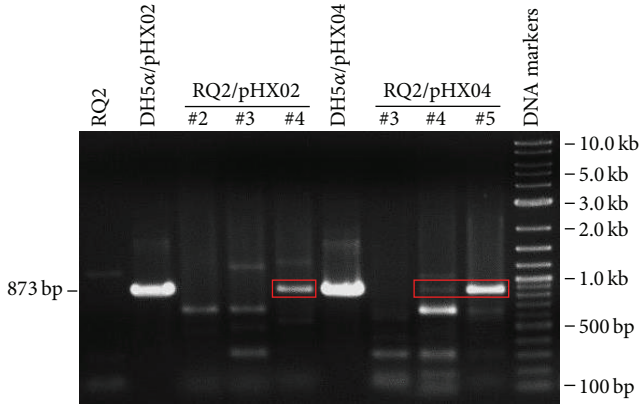

Figure 5: Amplification of the exoglucanase domain in *T.* sp. strain RQ2 transformants.

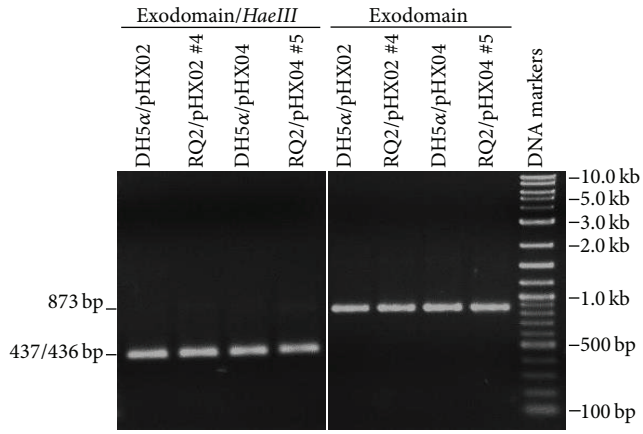

Figure 6: Restriction digestion of PCR products of the exoglucanase domain of *T.* sp. strain RQ2 transformants.

by consecutively transferring corresponding cultures under the selection of antibiotics. After four transfers, all shuttle vectors were readily detected in the *E. coli* transformants (Figure 9(a)). The endo- and exodomains of *celA* and *celB* were also successfully amplified from the plasmid DNA extracts (data not shown). Congo red assays with DH5α/pHX02 showed that the enzyme was as active as before

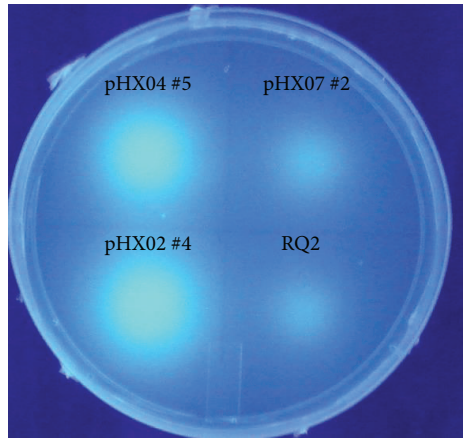

Figure 7: Detection of exoglucanase activities in *T.* sp. strain RQ2 transformants. RQ2, wild type strain, used as the negative control.

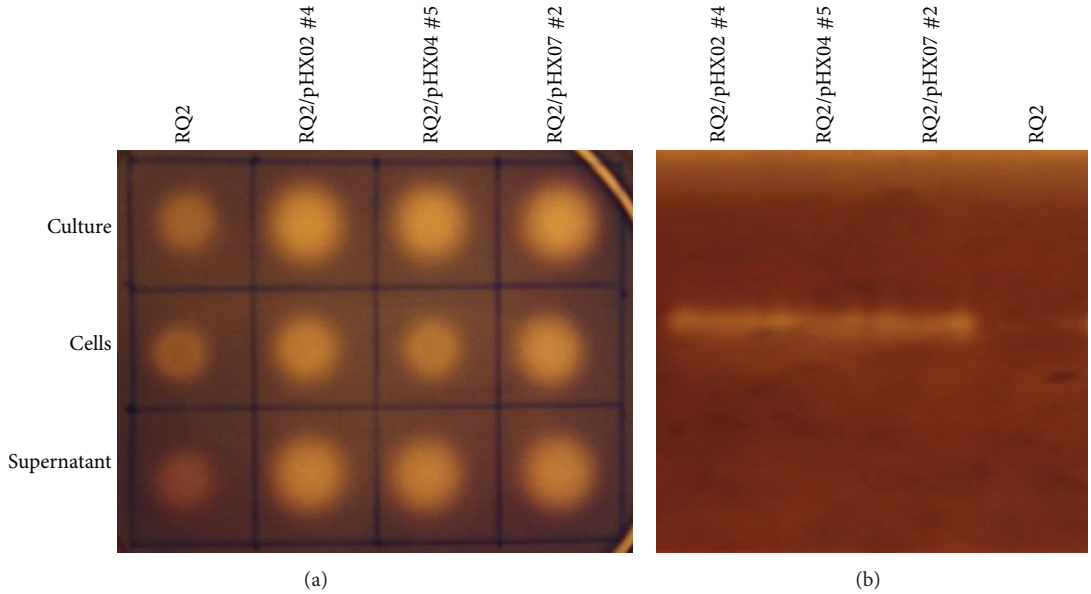

Figure 8: Localization of recombinant proteins in *T.* sp. strain RQ2 transformants. (a) CMC plate; (b) zymogram of the supernatants. *T.* sp. strain RQ2 was used as the negative control.

and the expression level of the enzyme was not affected by the inclusion of 0.25% starch in the medium [21, 25] (Figure 9(b)). These results indicate that, in *E. coli* DH5α, the constructed vectors are stably maintained and the enzymes are constitutively expressed.

Unfortunately, in *T.* sp. strain RQ2, the vectors seemed to be gradually lost, as indicated by decreasing enzyme activities with each transfer. After the 3rd transfer, the activities of both endo- (Figure 10) and exoglucanase (data not shown) were at the same level as the negative control. Trying to induce the cultures with 0.25% starch or 0.25% xylose [21, 25, 31] did not result in improved expression of the enzymes, suggesting the diminishing of enzyme activities was a result of loss of genes rather than a lack of expression. Our previous study demonstrated that the *Thermotoga-E. coli* shuttle vector pDH10 is stably maintained in both *E. coli* and *Thermotoga* [23]. However, the vectors constructed in this study, which are derived from pDH10, were only stable in *E. coli*, but not in *Thermotoga*. This might be due to different genetics of the *Thermotoga* hosts. In the previous study, *T.* sp. strain RQ7 and *T. maritima* were used, and in this study, the host was *T.* sp. strain RQ2. Cryptic miniplasmids pRQ7 and pMC24 have been found in *T.* sp. strain RQ7 and *T. maritima* [32, 33], but no natural plasmids have ever been seen in *T.* sp. strain RQ2. Plasmids pRQ7 and pMC24 are only 846 bp in length and encode just one apparent protein, which seems to play a role in plasmid replication but lacks the site-specific nuclease activity typical to a fully functional replication protein [34]. It is possible that the genomes of *T.* sp. strain RQ7 and *T. maritima* encode gene(s) essential to the replication of pRQ7-like plasmids, allowing the survival of pRQ7/pMC24-based vectors, whereas *T.* sp. strain RQ2 may lack such gene(s). As about half of the *Thermotoga* genomes encode uncharacterized proteins, finding such gene(s) requires thorough

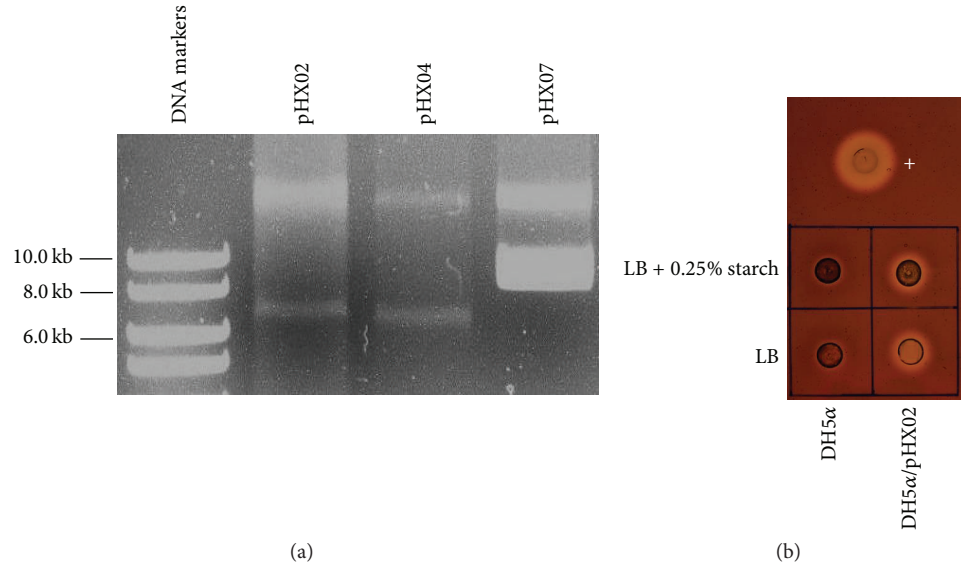

Figure 9: Stabilities of the *E. coli* recombinant strains. The bacterial cultures were transferred for four consecutive times with 100 μg mL^{-1} ampicillin and were subject to plasmid extraction (a) and Congo red plate assays (showing DH5α/pHX02 as an example) (b). Samples used for plate assays were prepared from normalized cultures. +, *C. saccharolyticus* DSM 8903; LB, Luria-Bertani broth.

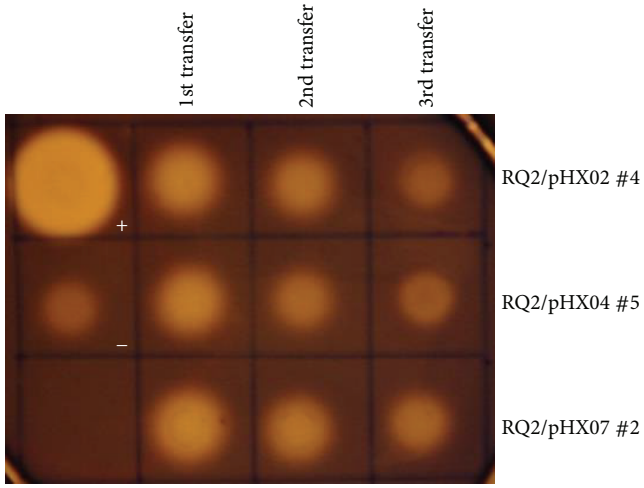

Figure 10: Stabilities of the *T.* sp. strain RQ2 recombinant strains. The bacterial cultures were transferred for three consecutive times with 150 μg mL^{-1} kanamycin. Samples used for plate assays were prepared from normalized cultures. +, *C. saccharolyticus* DSM 8903, –, *T.* sp. strain RQ2.

functional genomics studies and will be the future direction of our work.

4. Conclusions

This work demonstrated that it is possible to functionally express large heterologous proteins in *Thermotoga*. Transformed with the recombinant *Caldicellulosiruptor* cellulases, *T.* sp. strain RQ2 displayed increased endoglucanase activity with the expression of all three engineered enzymes, namely, TM1840 (AmyA)-Csac_1078 (CelB), TM0070 (XynB)-Csac_1078 (CelB), and TM0070 (XynB)-Csac_1076 (CelA). Exoglucanase activity was also improved significantly in *T.* sp. strain RQ2 transformants expressing the chimeric enzymes TM1840 (AmyA)-Csac_1078 (CelB) and TM0070 (XynB)-Csac_1078 (CelB). However, the *Thermotoga* transformants lost their recombinant genes after three consecutive transfers. This study represents an important milestone in the effort of using *Thermotoga* to produce biohydrogen directly from cellulosic biomass. Future studies should be focused on improving the stability of the transformants.

Conflict of Interests

The authors declare that they have no competing interests.

Acknowledgments

This work was supported by the BGSU Commercialization Catalyst Award, the Building Strength Award, and the Katzner Award.

References

[1] T. Wang, X. Liu, Q. Yu et al., "Directed evolution for engineering pH profile of endoglucanase III from *Trichoderma reesei*," *Biomolecular Engineering*, vol. 22, no. 1–3, pp. 89–94, 2005.

[2] K. Bronnenmeier, A. Kern, W. Liebl, and W. L. Staudenbauer, "Purification of *Thermotoga maritima* enzymes for the degradation of cellulosic materials," *Applied and Environmental Microbiology*, vol. 61, no. 4, pp. 1399–1407, 1995.

[3] J. I. Park, M. S. Kent, S. Datta et al., "Enzymatic hydrolysis of cellulose by the cellobiohydrolase domain of CelB from the

hyperthermophilic bacterium *Caldicellulosiruptor saccharolyticus*," *Bioresource Technology*, vol. 102, no. 10, pp. 5988–5994, 2011.

[4] L. D. Ruttersmith and R. M. Daniel, "Thermostable cellobiohydrolase from the thermophilic eubacterium *Thermotoga* sp. strain FjSS3-B.1: purification and properties," *Biochemical Journal*, vol. 277, no. 3, pp. 887–890, 1991.

[5] H. Wang, F. Squina, F. Segato et al., "High-temperature enzymatic breakdown of cellulose," *Applied and Environmental Microbiology*, vol. 77, no. 15, pp. 5199–5206, 2011.

[6] M. Balk, J. Weijma, and A. J. M. Stams, "*Thermotoga lettingae* sp. nov., a novel thermophilic, methanol-degrading bacterium isolated from a thermophilic anaerobic reactor," *International Journal of Systematic and Evolutionary Microbiology*, vol. 52, no. 4, pp. 1361–1368, 2002.

[7] S. Belkin, C. O. Wirsen, and H. W. Jannasch, "A new sulfur-reducing, extremely thermophilic eubacterium from a submarine thermal vent," *Applied and Environmental Microbiology*, vol. 51, no. 6, pp. 1180–1185, 1986.

[8] C. Jeanthon, A.-L. Reysenbach, S. L'Haridon et al., "*Thermotoga subterranea* sp. nov., a new thermophilic bacterium isolated from a continental oil reservoir," *Archives of Microbiology*, vol. 164, no. 2, pp. 91–97, 1995.

[9] G. Ravot, M. Magot, M.-L. Fardeau et al., "*Thermotoga elfii* sp. nov., a novel thermophilic bacterium from an African oil-producing well," *International Journal of Systematic Bacteriology*, vol. 45, no. 2, pp. 308–314, 1995.

[10] J.-D. Bok, D. A. Yernool, and D. E. Eveleigh, "Purification, characterization, and molecular analysis of thermostable cellulases CelA and CelB from *Thermotoga neapolitana*," *Applied and Environmental Microbiology*, vol. 64, no. 12, pp. 4774–4781, 1998.

[11] T. T. Teeri, "Crystalline cellulose degradation: new insight into the function of cellobiohydrolases," *Trends in Biotechnology*, vol. 15, no. 5, pp. 160–167, 1997.

[12] P. Tomme, R. A. J. Warren, and N. R. Gilkes, "Cellulose hydrolysis by bacteria and fungi," *Advances in Microbial Physiology*, vol. 37, pp. 1–81, 1995.

[13] D. Han, H. Xu, R. Puranik, and Z. Xu, "Natural transformation of *Thermotoga* sp. strain RQ7," *BMC Biotechnology*, vol. 14, no. 1, article 39, 2014.

[14] F. A. Rainey, A. M. Donnison, P. H. Janssen et al., "Description of *Caldicellulosiruptor saccharolyticus* gen. nov., sp. nov: an obligately anaerobic, extremely thermophilic, cellulolytic bacterium," *FEMS Microbiology Letters*, vol. 120, no. 3, pp. 263–266, 1994.

[15] V. S. J. Te'O, D. J. Saul, and P. L. Bergquist, "*celA*, Another gene coding for a multidomain cellulase from the extreme thermophile *Caldocellum saccharolyticum*," *Applied Microbiology and Biotechnology*, vol. 43, no. 2, pp. 291–296, 1995.

[16] V. Zverlov, S. Mahr, K. Riedel, and K. Bronnenmeier, "Properties and gene structure of a bifunctional cellulolytic enzyme (CelA) from the extreme thermophile '*Anaerocellum thermophilum*' with separate glycosyl hydrolase family 9 and 48 catalytic domains," *Microbiology*, vol. 144, no. 2, pp. 457–465, 1998.

[17] D. J. Saul, L. C. Williams, R. A. Grayling, L. W. Chamley, D. R. Love, and P. L. Bergquist, "*celB*, a gene coding for a bifunctional cellulase from the extreme thermophile '*Caldocellum saccharolyticum*'," *Applied and Environmental Microbiology*, vol. 56, no. 10, pp. 3117–3124, 1990.

[18] A. L. VanFossen, I. Ozdemir, S. L. Zelin, and R. M. Kelly, "Glycoside hydrolase inventory drives plant polysaccharide deconstruction by the extremely thermophilic bacterium *Caldicellulosiruptor saccharolyticus*," *Biotechnology and Bioengineering*, vol. 108, no. 7, pp. 1559–1569, 2011.

[19] W. Liebl, I. Stemplinger, and P. Ruile, "Properties and gene structure of the *Thermotoga maritima* α-amylase amyA, a putative lipoprotein of a hyperthermophilic bacterium," *Journal of Bacteriology*, vol. 179, no. 3, pp. 941–948, 1997.

[20] W. Liebl, C. Winterhalter, W. Baumeister, M. Armbrecht, and M. Valdez, "Xylanase attachment to the cell wall of the hyperthermophilic bacterium *Thermotoga maritima*," *Journal of Bacteriology*, vol. 190, no. 4, pp. 1350–1358, 2008.

[21] J. Schumann, A. Wrba, R. Jaenicke, and K. O. Stetter, "Topographical and enzymatic characterization of amylases from the extremely thermophilic eubacterium *Thermotoga maritima*," *FEBS Letters*, vol. 282, no. 1, pp. 122–126, 1991.

[22] S. A. van Ooteghem, S. K. Beer, and P. C. Yue, "Hydrogen production by the thermophilic bacterium *Thermotoga neapolitana*," *Applied Biochemistry and Biotechnology*, vol. 98–100, pp. 177–189, 2002.

[23] D. Han, S. M. Norris, and Z. Xu, "Construction and transformation of a *Thermotoga-E. coli* shuttle vector," *BMC Biotechnology*, vol. 12, article 2, 2012.

[24] S. G. N. Grant, J. Jessee, F. R. Bloom, and D. Hanahan, "Differential plasmid rescue from transgenic mouse DNAs into *Escherichia coli* methylation-restriction mutants," *Proceedings of the National Academy of Sciences of the United States of America*, vol. 87, no. 12, pp. 4645–4649, 1990.

[25] R. Huber, T. A. Langworthy, H. König et al., "*Thermotoga maritima* sp. nov. represents a new genus of unique extremely thermophilic eubacteria growing up to 90°C," *Archives of Microbiology*, vol. 144, no. 4, pp. 324–333, 1986.

[26] Z. Xu, D. Han, J. Cao, and U. Saini, "Cloning and characterization of the TneDI restriction-modification system of *Thermotoga neapolitana*," *Extremophiles*, vol. 15, no. 6, pp. 665–672, 2011.

[27] H. Xu, D. Han, and Z. Xu, "Overexpression of a lethal methylase, M.*Tne*DI, in *E. coli* BL21(DE3)," *Biotechnology Letters*, vol. 36, no. 9, pp. 1853–1859, 2014.

[28] R. M. Teather and P. J. Wood, "Use of Congo red-polysaccharide interactions in enumeration and characterization of cellulolytic bacteria from the bovine rumen," *Applied and Environmental Microbiology*, vol. 43, no. 4, pp. 777–780, 1982.

[29] K. A. Laderman, B. R. Davis, H. C. Krutzsch et al., "The purification and characterization of an extremely thermostable α- amylase from the hyperthermophilic archaebacterium *Pyrococcus furiosus*," *Journal of Biological Chemistry*, vol. 268, no. 32, pp. 24394–24401, 1993.

[30] S. J. Han, Y. J. Yoo, and H. S. Kang, "Characterization of a bifunctional cellulase and its structural gene—the *cel* gene of Bacillus sp. D04 has exo- and endoglucanase activity," *The Journal of Biological Chemistry*, vol. 270, no. 43, pp. 26012–26019, 1995.

[31] C. Winterhalter and W. Liebl, "Two extremely thermostable xylanases of the hyperthermophilic bacterium *Thermotoga maritima* MSB8," *Applied and Environmental Microbiology*, vol. 61, no. 5, pp. 1810–1815, 1995.

[32] T. Akimkina, P. Ivanov, S. Kostrov et al., "A highly conserved plasmid from the extreme thermophile *Thermotoga maritima* MC24 is a member of a family of plasmids distributed worldwide," *Plasmid*, vol. 42, no. 3, pp. 236–240, 1999.

[33] O. T. Harriott, R. Huber, K. O. Stetter, P. W. Betts, and K. M. Noll, "A cryptic miniplasmid from the hyperthermophilic bacterium *Thermotoga* sp. strain RQ7," *Journal of Bacteriology*, vol. 176, no. 9, pp. 2759–2762, 1994.

[34] J.-S. Yu and K. M. Noll, "Plasmid pRQ7 from the hyperthermophilic bacterium *Thermotoga* species strain RQ7 replicates by the rolling-circle mechanism," *Journal of Bacteriology*, vol. 179, no. 22, pp. 7161–7164, 1997.